cea

Direction des Sciences de la Matière
Département de Recherches sur la Fusion Contrôlée

Progress Report

2000 / 2001 Rapport d'activité

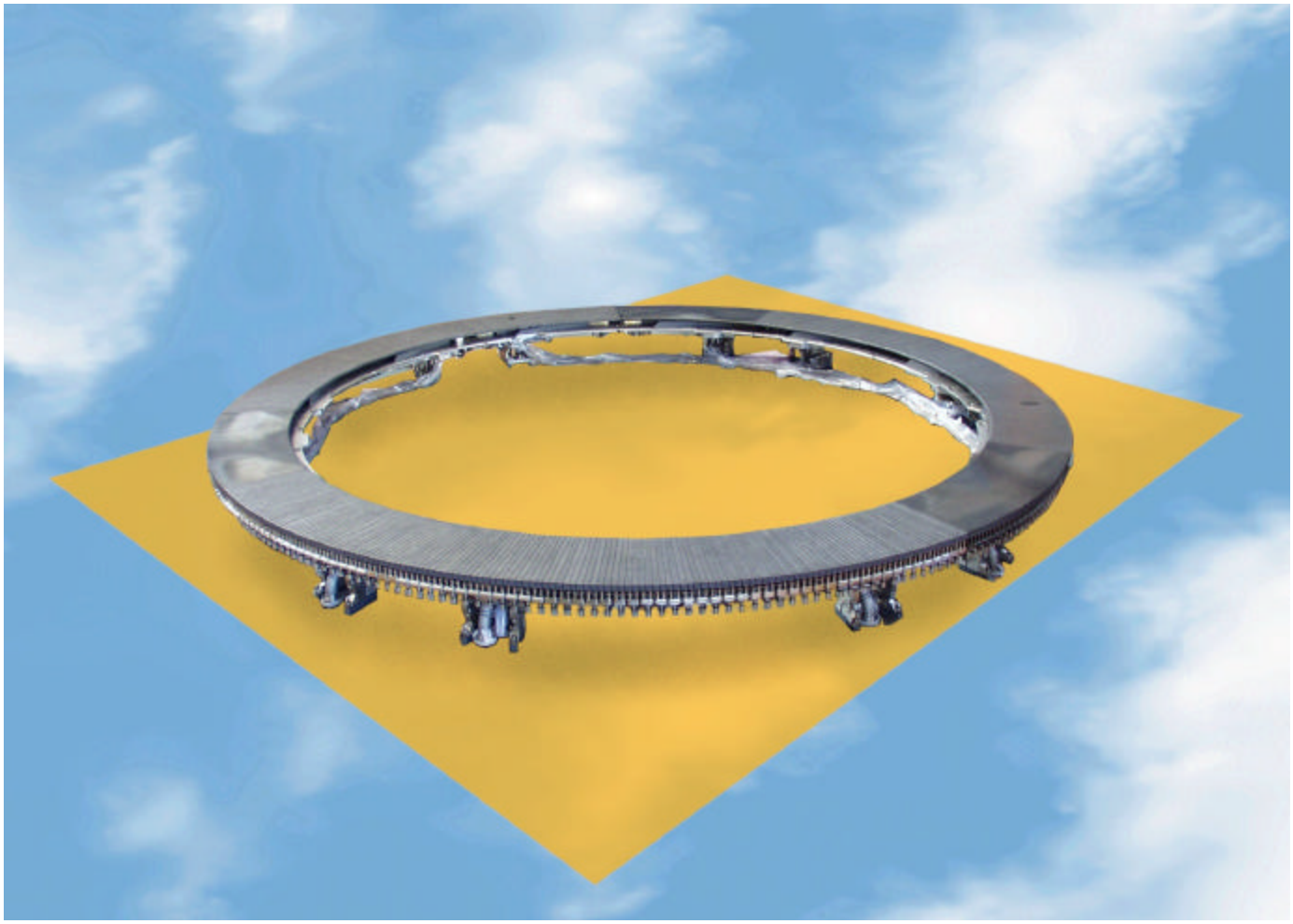

English Issue

CEA Cadarache

Association EURATOM-CEA

Progress Report

2000 / 2001 Rapport d'Activité

Illustration de couverture
Cover drawing

Vue du limiteur pompé toroïdal (LPT)
Toroïdal pumped limiter view

Commissariat à l'Energie Atomique

Direction des Sciences de la Matière
Département de Recherches sur la Fusion Contrôlée (DRFC)
Tél (0)4 42 25 70 01 - **Fax** (0)4 42 25 64 21 - **e.mail** dirdrfc@drfc.cad.cea.fr

cea Cadarache F - 13108 Saint Paul-Lez-Durance Cedex

Insertion of ITER in the Landscape, seen from the Castle of Cadarache

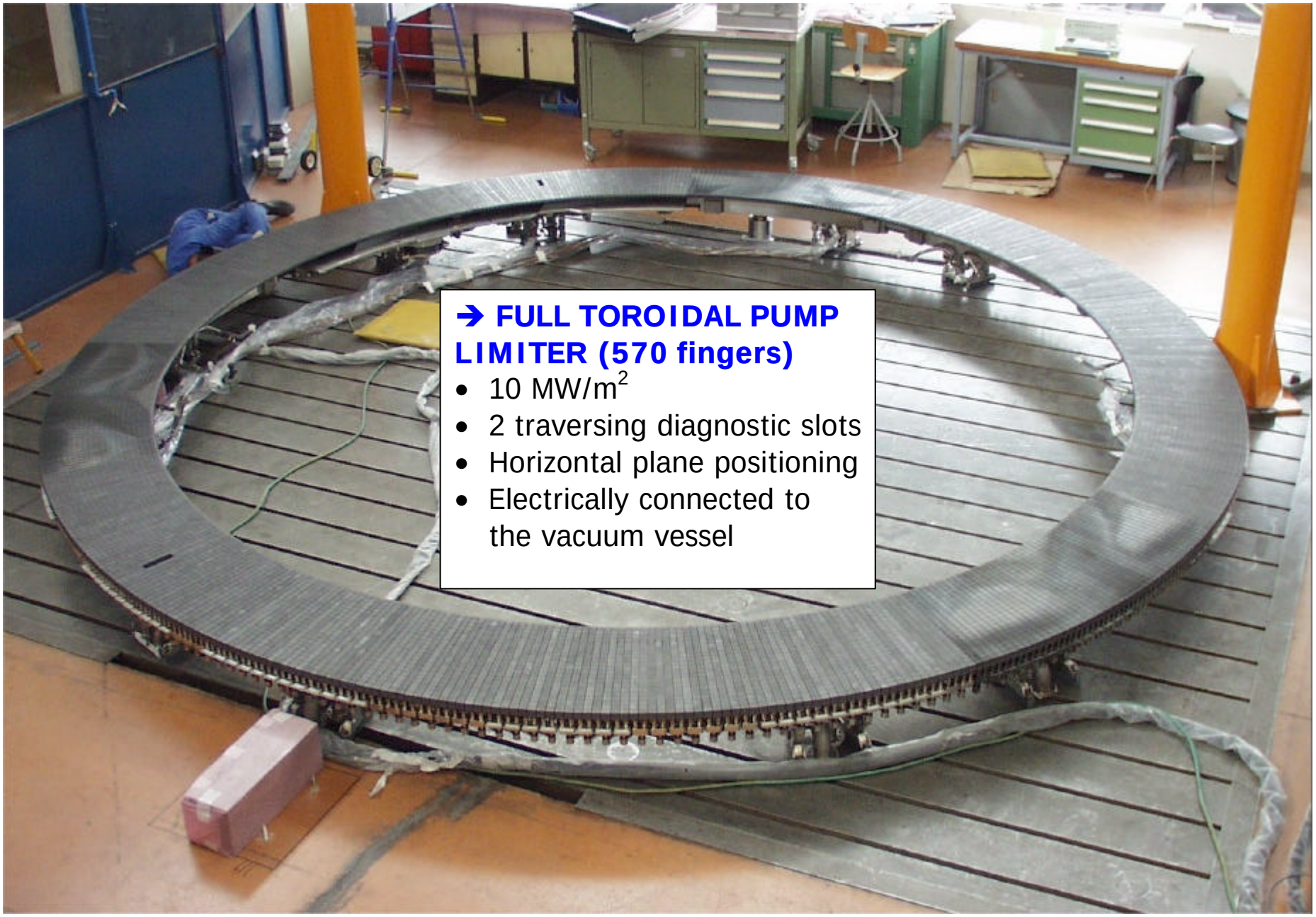
➔ FULL TOROIDAL PUMP LIMITER (570 fingers)
• 10 MW/m^2
• 2 traversing diagnostic slots
• Horizontal plane positioning
• Electrically connected to the vacuum vessel

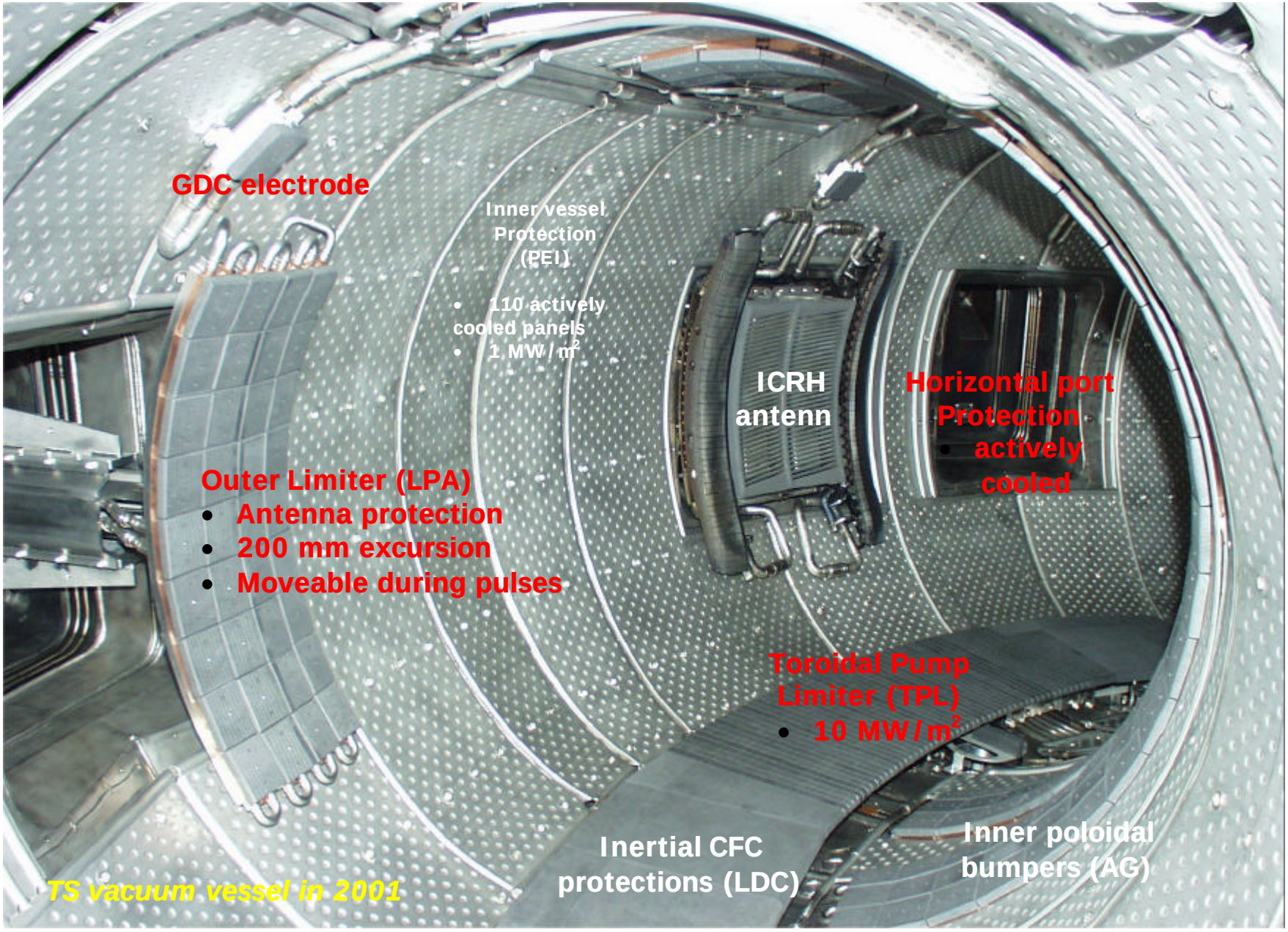
GDC electrode
Inner vessel Protection (PEI)
• 110 actively cooled panels
• 1 MW / m²
ICRH antenn
Horizontal port Protection
• actively cooled
Outer Limiter (LPA)
• Antenna protection
• 200 mm excursion
• Moveable during pulses
Toroidal Pump Limiter (TPL)
• 10 MW / m²
Inertial CFC protections (LDC)
Inner poloidal bumpers (AG)
TS vacuum vessel in 2001

FOREWORD

The 2000-2001 period has seen many facts of importance for the Euratom-CEA Association.

ITER as a start …The first outstanding fact is, of course, the positive evolution of the international ITER project situation, because of both the goodwill shown by the three partners, Japan, European Union and Russia (with the late addition of Canada), to engage in its realisation, and the French proposition to the European Union to consider the Cadarache site as the European site.

This evolution is the outcome of a favourable context, due not only to an increasing international consciousness of the necessity to develop the energy sources needed in the long term, but also to the fusion community capability to propose solutions to build a fusion reactor on the horizon of a few decades. We can point out with satisfaction the very positive impact on many deciders of the success of the research communal organisation and of the visits to our laboratories clearly showing the quality of our realisations.

At the same time as the international negotiations, a thorough work has been organised at Cadarache, within a European framework, to prepare all the documents which will be necessary in the future to allow the project effective implementation without delay: documents concerning safety and administrative licences, on- and off-site reception infrastructures, reception of the participants and their families during the construction and exploitation phases. These activities have been extremely well supported by other Cadarache departments, by the state regional administrative authorities and by the territorial communities. A strong technical team is now well operational.

Tore Supra, of course …The second outstanding fact is the installation on Tore Supra of a new generation of plasma facing components: the CIEL project. It is an essential step, which ends ten years, remarkably productive, of experimentation with the Ergodic Divertor, whose European future is now on the Textor tokamak at Jülich. Will the new Tore Supra CIEL components keep the promise to extract, at steady state, the 15MW power carried by the plasma charged particles to its border, plus 10 MW of volume radiated power? Will several hundred seconds plasmas be obtained, well over the Tore Supra record of 280MJ extracted? It is obviously too early to answer these questions, which are the object of the experimental program of the coming years.

Coherently with the achievement of the CIEL project, the Association obtained, in the spring 2000, Euratom preferential support for the CIMES project, designed to increase the power available for heating and current generation by lower hybrid frequency waves for durations compatible with the performances of the newly installed components. As in the case of CIEL, numerous progress in the mastery of the technologies necessary for these systems are expected, in particular concerning the capacity to sustain long pulses. The availability of powerful heating means and the capability to obtain long duration plasmas should then allow a major contribution to the physics of steady state tokamaks, in particular by allowing an active control of these discharges, thus prefiguring the ITER operational methods for its continuous operation.

JET, last but not least … The third outstanding fact is the continuation, within the new EFDA framework, of experiments on JET after 1999, end date of the JET Joint Undertaking. These new provisions aim at maintaining in activity the spearhead of the European program, waiting for a clarification of the ITER situation, while making it possible for the Associations to become major actors of the exploitation. It has been necessary to reform in-depth the operational method, the English Association (UKAEA) becoming the machine operator and the European associations the actors of the scientific program, driven by a central team (Closed Support Unit). This organisation has become quickly operational, in spite of some early shortcoming, and it allowed to realise four experimental campaigns in 2000 and 2001, resulting in a beautiful harvest of results. This is the result of the enthusiasm and commitment of the scientific staff of the European associations (particularly of the French Association), has been an example which was precious in the European and French decision processes of engagement towards ITER.

These two past years have therefore seen a major scientific and programmatic wealth, which must be clearly perceived by everybody inside and outside the Association. The commitment and quality of the engineers, of the physicists and of the technical and administrative staff of the Association have been essential in the success of the different actions. More than ever, it is important to demonstrate our capability to undertake in all these fields, while accentuating our capability to opening towards the other partners of the program. This attitude is certainly justified by the necessity to share the means within the international programme, but it is even more given a stimulus by the hope of receiving the ITER project on the Cadarache European site.

Jean Jacquinot
Head of the EURATOM-CEA Association on Fusion

CONTENT

I. ITER SITE

The objective of the ITER machine is to demonstrate the scientific feasibility of fusion, with extended burn and marginally controlled ignition for a duration sufficient to achieve stationary conditions on all time-scales characteristics of plasma processes and plasma-wall interactions. To do so the installation will produce 500 MW of fusion power during pulses of at least 400 seconds. The facility will also demonstrate key fusion technologies.

The ITER Engineering Design Activities (EDA) were carried out between July 1992 and July 2001 under the framework of the ITER Agreement and Protocol signed by representatives of the four Parties, the European Atomic Energy Community, Japan, the Russian Federation and the United States of America (the USA withdrew in 1999). During the EDA, the ITER Joint Central Team (JCT) elaborated a reference site design, called hereafter "generic design", including in particular a minimum set of requirements to be satisfied by any proposed site and additional assumptions.

Canada, the European Atomic Energy Community, Japan and the Russian Federation are about to start negotiations in order to select a site for the construction of ITER and to establish an ITER Legal Entity. In Europe, on 16 November 2000, the Research Council of Ministers asked the European Commission "to conduct negotiations on the establishment of an international framework allowing the ITER EDA Parties and qualified third countries to prepare jointly for the future establishment of an ITER Legal Entity for ITER construction and operation, if and when so decided."

At the European Consultative Committee on Fusion (CCE-FU) meeting on 11 July 2000, the French Delegation announced that "CEA was proposing the site of Cadarache as a possible site for ITER construction", calling on active contributions from the Euratom-Fusion Associations and on a strong involvement of European industry in the preparation of the proposal. The CCE-FU invited the EFDA Steering Committee to carry out swiftly – in close interaction with CEA and in consultation with the ITER JCT – an in-depth examination of the CEA proposal.

A European ITER Site Technical Study group (EISS group) has been established to examine ITER sites in Europe. For the Cadarache site, the EISS group was asked to:

- establish the compliance of the site with the ITER technical site requirements;
- identify key elements for the licensing procedure;
- examine site specific aspects of the ITER construction and operation costs;
- evaluate the social and infrastructure impacts of the project.

This document summarises the main conclusions of the work undertaken by the EISS group on the Cadarache site.

I.1. Technical Aspects

Cadarache satisfies all ITER site requirements. The design assumptions are satisfied, most of them with a comfortable margin, with two minor exceptions :

- the seismic level is slightly higher in Cadarache than on the generic site;
- the capability of the network to supply reactive power is lower than on the generic site.

No technical difficulty is anticipated and the extra cost with respects to these issues is limited.

Two different routes for the transportation of large and heavy components have been fully assessed.

I.1.1. Overview of CEA Cadarache

Cadarache, established in 1959, covers 1600 hectares and is the largest research centre of the French Atomic Energy Commission (CEA). It is located at the very heart of historical Provence, halfway between Aix-en-Provence and Manosque.

Cadarache is the main CEA centre for power oriented nuclear research, with experimental reactors, specialised laboratories and workshops for a total of 18 nuclear facilities. The centre provides employment for 5 000 people and it has an annual budget of 400 M€. The Euratom-CEA Association, which co-ordinates the French activity on magnetic thermonuclear fusion, is also based on the Cadarache site and it operates the supraconducting tokamak Tore Supra since 1988. In addition to several specialised laboratories and reactors, a number of general services are available on the Cadarache site, e.g. local security and radiation protection. The Cadarache research centre has all the necessary infrastructure to host a nuclear facility such as ITER.

I.1.2. ITER site layout

Following the assessment of 3 specific areas, it is proposed to locate ITER at the Northeast boundary of the Cadarache site. The layout of the buildings is in accordance with the generic site drawings, except for the cooling towers, which have been repositioned 300 m away according to the dominant winds. The office building has been rotated to improve access (figure I-1). Additional buildings and services (restaurant, medical service, etc.) are also indicated.

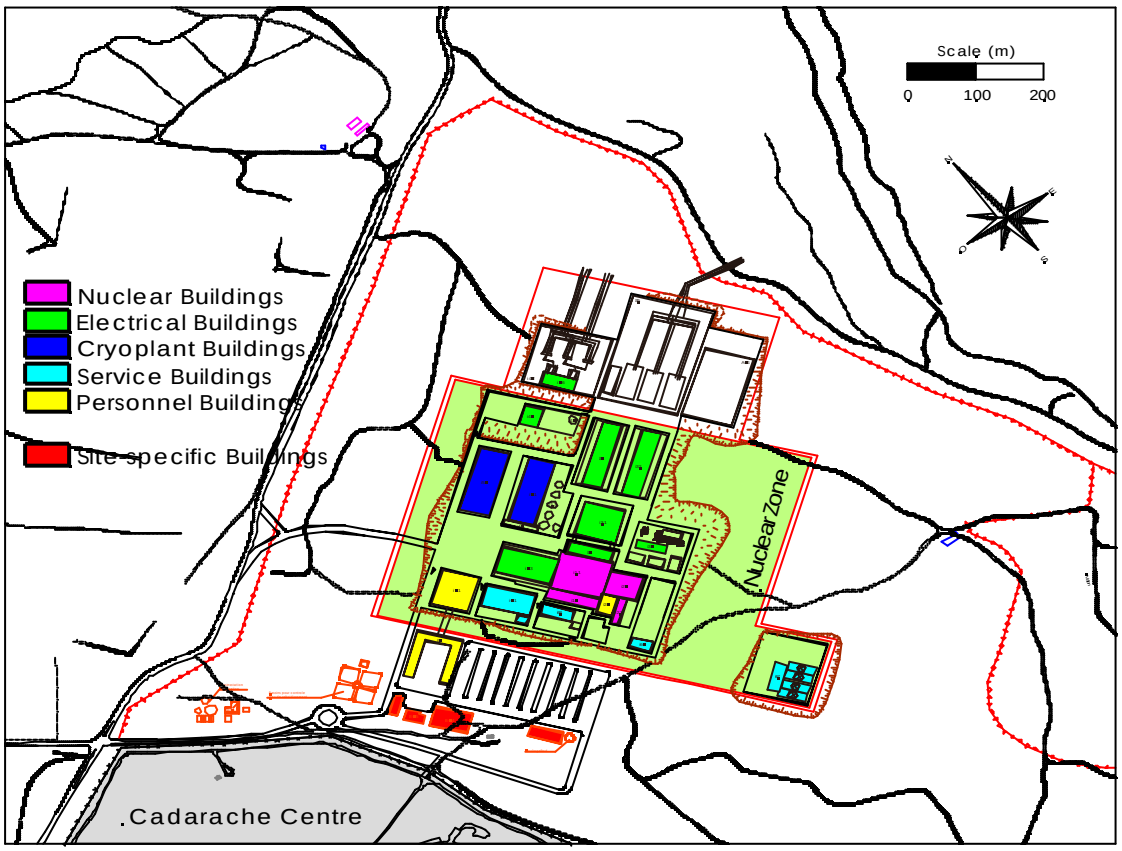

Figure I-1 : Detailed layout of the buildings

Test drillings were carried out to determine the location of the limestone substrate, which was found to be of good quality and at a maximum depth of about 10 m. A more detailed geological investigation is underway to finalise the exact location of all buildings and to determine the soil characteristics necessary for the detailed design of the foundations.

I.1.3 Seismic aspects

The ITER JCT has designed the safety-classified buildings in accordance with the ASME and the US NRC guidelines. The results should be valid for a wide range of sites with the exclusion of those with unusually soft soils. The primary scaling parameter used is the maximum ground acceleration, assumed to be 0.2 g for the generic ITER site. At Cadarache, the "Règles Fondamentales de Sûreté" require to consider the so-called "Séisme Majoré de Sécurité" (magnitude of 5.8, epicentre at 7.1 km) and the "Paléoséisme" (magnitude of 7, epicentre at 18 km), whose maximum ground acceleration

are, respectively, 0.315 g and 0.281 g. Stress analysis shows that the tokamak building, as it is now designed, is able to withstand the Cadarache seismic conditions without any major reinforcement. About 150 eigenmodes have been calculated in each of the three directions and the main modes in the horizontal directions were found in the range 3.6 – 3.7 Hz. A few weak points have been identified at the level where the superstructure is connected to the upper slab. Floor spectra have also been computed in order to assess the design of the safety related equipment inside the tokamak building (this assessment has not yet been done for the generic site).

As an alternative, the use of 400 paraseismic bearings for the ITER tokamak building has been assessed. These bearings, made with elastomer foils interleaved with stainless steel plates, are commonly used for bridge supports and in some nuclear buildings. Their use leads to a decrease in the overall acceleration on the building, and consequently on the equipment, to 0.1 g. This would result in significant savings for the building and all inner equipment but, on the other hand, an *overall* displacement of the building of roughly 75 mm (without bearings, the displacement is a few mm a ground level and 52 mm at the superstructure level) is foreseen at a frequency of 0.56 Hz. The interfaces with nearby buildings will need to be checked carefully because of this motion.

The two options (local reinforcement of the building and the use of paraseismic bearings) are feasible. No major modification with respect to the generic design is foreseen.

I.1.4. Heat sink and water supply

A consumption of 1.5 million m^3 per year has been estimated for the cooling water circuits. This is equivalent to the present total consumption of the Cadarache centre. It will therefore be necessary to install a new system. The preferred solution is to supply water by means of gravity from the EDF canal of Vinon-sur-Verdon. The investment cost for this solution is slightly higher than for other alternatives, but this is offset by the reduced cost of operation since no pumping station is required. Other new installations are foreseen at Cadarache and will also require modifications of the water supply; synergies might be obtained between the different projects.

The climate in Cadarache, warm but very dry in the summer, allows the overall dimensions of the cooling towers to be reduced, the wet bulb temperature in Cadarache being 24°C instead of 29°C as assumed by ITER. However, the relocation of the cooling towers leads to an increase in the length of pipe work by 300 m (2 pipes of 2 m diameter).

About two thirds of the water evaporates in the cooling towers. The rest will be discharged into the Durance River or the canal, after the necessary controls, making use of the current discharge outlet of the Cadarache site.

I.1.5. Electrical Power Supply

The electrical network around Cadarache is well equipped with many lines and two powerful nodes, Boutre (5 km east of the ITER site, with an interconnection at the 400 kV/225 kV level through an autotransformer) and Sainte-Tulle (8 km north of the ITER site, with an interconnection at the 225 kV/63 kV level). Moreover, Tore Supra is already supplied by a 400 kV dedicated line and the Cadarache centre by two 63 kV lines.

The generic ITER design is based on a single 400 kV line and a double 225 kV line. Several alternatives have been considered and compared by the public company RTE. In particular, the environmental impact has been considered very carefully taking into account the visual impact of 225 kV and 400 kV pylons. The reference scheme is shown figure I-2. All modifications necessary take place on CEA property.

The design assumptions for the reactive power compensation are not satisfied. The ITER static VAR compensator will have to be increased from 540 Mvar to 660 Mvar and driven as voltage regulator to reduce the voltage drop on the network within acceptable limits. This design modification will have a modest impact because there are margins in the present design. On the other hand, the design assumptions with respect to the active power are widely exceeded and 1000 MW could be delivered for 30 s instead of the assumed 500 MW. Should this point be confirmed, a scheme with only a double 400 kV line could be proposed, leading to cost savings on both site adaptation and generic design. This scheme is fully compatible with the ITER site requirements and design assumptions.

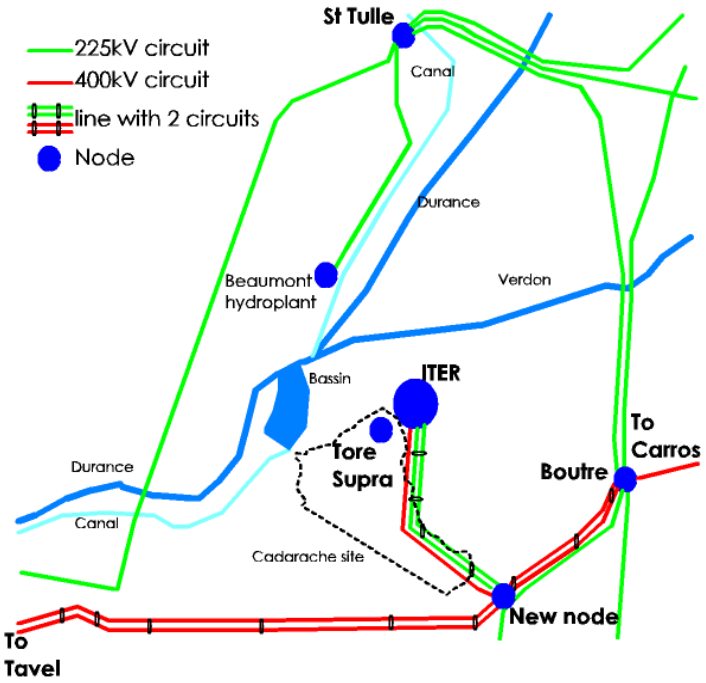

Figure I-2 : Proposed ITER High Voltage Supply Scheme

I.1.6. Transport of heavy and large components

The transport of large and heavy components to Cadarache, which is located 70 km from the nearest sea harbour, has required specific studies. A careful review of all dimensions and weights of these components has been made in close collaboration with the ITER JCT and the weight and size of the handling and protection equipment have been estimated. The public agency “Centre d’Études Techniques de l’Équipement” (CETE) has evaluated two routes:

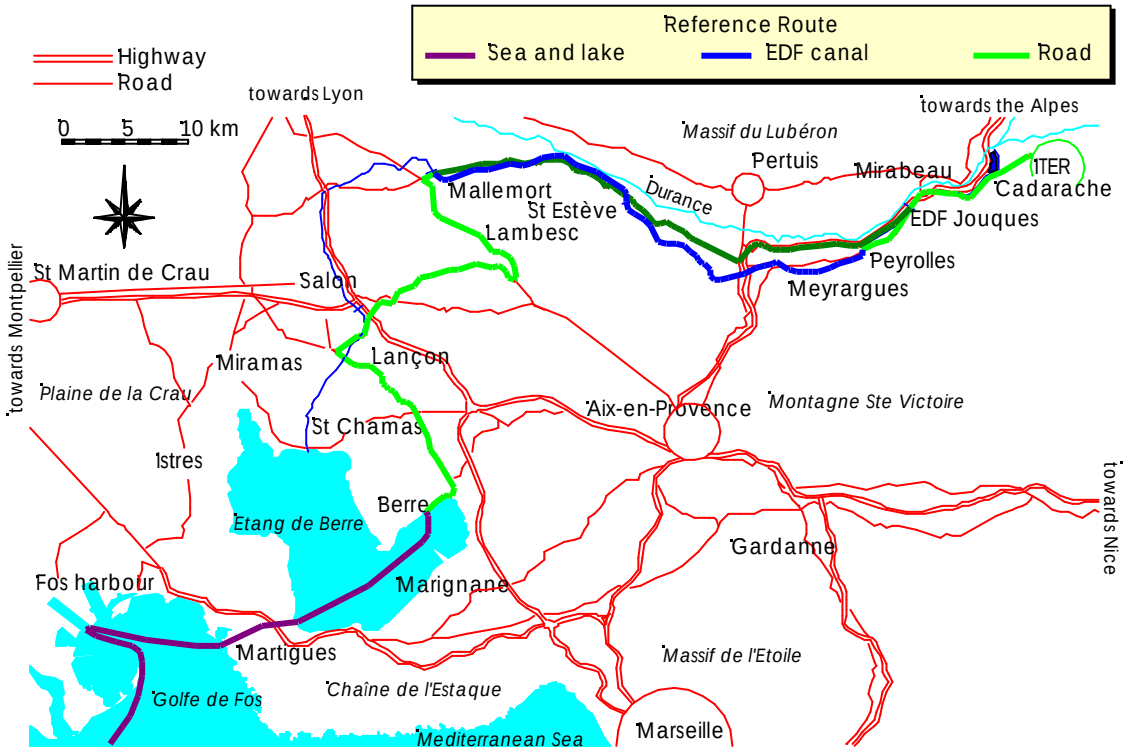

Figure I-3 : Reference routes (by road only, or combination of road and canal), from Fos harbour to Cadarache

- in a first instance, the use of an already existing itinerary for "convoi exceptionnnel" (road already qualified for "exceptional" transport) between Fos-sur-Mer (Marseille) and Cadarache. Certain sections would require technical adaptations, in particular roundabouts and bridges, but no administrative difficulty is anticipated. This first scheme requires the use of a section of EDF canal (see below);
- in a second instance, an alternative route, only by road has been assessed. It has the advantage to be faster: 3 days, compared to 10 days (no load transfers to and from the barges), but would require more technical adaptations.

In addition, the "Centre d'Ingénierie Hydraulique d'EDF" analysed the transportation on the Durance EDF canal by means of ad-hoc barges. One hydroelectric power station would be by-passed via a specifically constructed track. The use of about 40 km of the canal requires, besides the manufacture of the barges, the modification of a few bridges and the construction of specific handling equipment for loading and unloading the components on the barges.

Figure I-3 illustrates the two possible routes.

I.2. Safety and licensing

The ITER regulatory and decommissioning requirements are compatible with the French licensing regulations. CEA has started the licensing procedure in order to satisfy the ITER planning assumptions.

I.2.1 Licensing procedure

A licensing procedure is required in France for all nuclear installations. The definition of a nuclear installation, i.e. an "Installation Nucléaire de Base" (INB), is based on the inventory of radioactivity. The ITER device would be classified as an INB because of the expected tritium inventory.

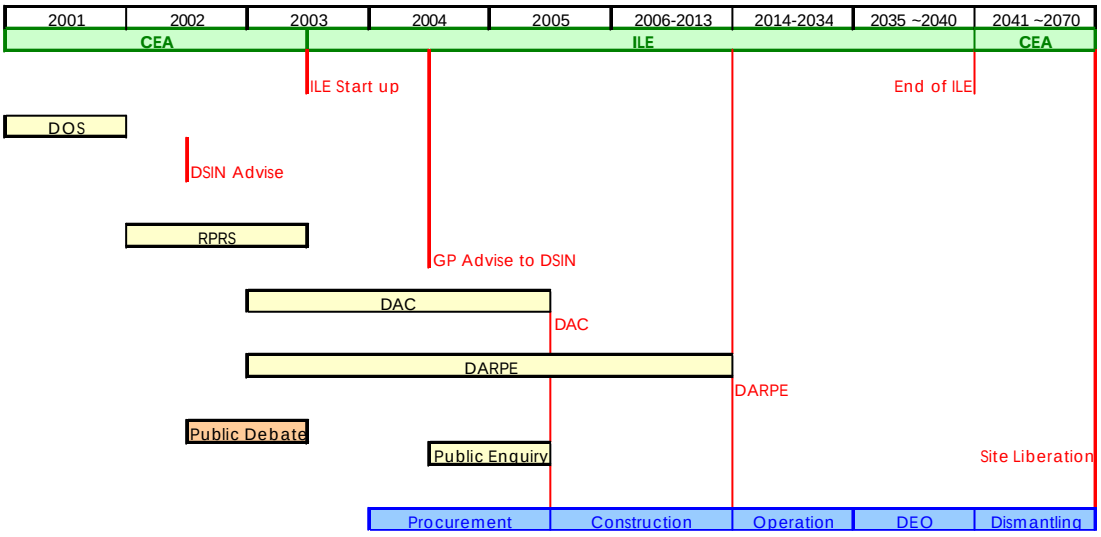

Acronym	*French meaning*	*English Translation or Meaning*
ASN	Autorité de Sûreté Nucléaire	French Safety Nuclear Authority
DAC	Demande d'Autorisation de Création	Request of Authorisation of Creation
DAC	Décret d'Autorisation de Création	Decree of Authorisation of Creation
DARPE	Demande d'Autorisation de Rejet et de Prélèvement d'Eau	Request of Authorisation for Water Release and Extraction
DARPE	Décret d'Autorisation de Rejet et de Prélèvement d'Eau	Decree of Authorisation for Water Release and Extraction
DEO	Mise à l'Arrêt Définitif (MAD)	Definitive End of Operation
DIN	Division des Installations Nucléaires	In charge of Nuclear Installation Control
DOS	Dossier d'Options de Sûreté	Description of Safety Objectives (not compulsory)
DSIN	Direction de la Sûreté des Installations Nucléaires	ASN Legal Head
GP	Groupe Permanent	Permanent Group (in charge of Request Examination)
ILE	Entité Juridique ITER	ITER Legal Entity (status to be defined)
IPSN	Institut de Protection et de Sûreté Nucléaire	ASN technical Adviser
RPRS	Rapport Préliminaire de Sûreté	Initial Safety Report (compulsory, to be borne by ILE)

Figure I-4 : Overall Licensing Process, from Today until Site Liberation

The operator of the INB is responsible for the safety and for the environmental impact of the installation from the beginning of construction to the final step of decommissioning. The current hypothesis is that the future operator will be the ITER Legal Entity, which will have to undertake the licensing process.

In order not to delay the licensing procedure, CEA and EFDA have started the first step of the licensing procedure, i.e. the preparation of the "Dossier d'Options de Sûreté", which is planned to be submitted to the French safety authorities at the end of 2001. CEA and EFDA also plan to prepare key elements of the "Rapport Préliminaire de Sûreté" which, to respect the proposed time scale, should be submitted by the ILE to the French safety authorities mid 2003.

According to French law (loi Barnier, 95/101), any new, large project or installation may be submitted to a "public debate" during its design phase. The objective is to promote a countrywide discussion on the project socio-economic and/or environmental advantages and drawbacks. CEA and EFDA are considering how and when it would be more appropriate to initiate the ITER public debate.

The last step of the licensing process would be the authorisation to build and to operate ITER, formalised by two governmental decrees: the "Décret d'Autorisation de Création", required to start the construction, and the "Décret d'Autorisation de Rejets et de Prélèvements d'Eau", required to start operations. A Public Enquiry would also be held at this stage. It is a consultation process among the local communities around the proposed site on the external effects resulting from the construction and operation of the plant.

Licensing of ITER would finally require an agreement with the safety authority clearly stating that CEA would take care of decommissioning and waste management after the ITER Definitive End of Operation (DEO).

The time scale of the complete process is shown in figure I-4. Since the preliminary safety report must be submitted to the safety authority by the ITER Legal Entity (ILE), its establishment is on the critical path and should be completed by mid-2003, to allow the construction of the buildings by mid-2005. Assuming 1 year to complete the call for tender for the long-lead items (buildings, superconducting strand and vacuum vessel), their technical specifications should also be ready mid 2003. This time-scale is consistent with groundbreaking mid 2004.

I.2.2. Effluents and releases

To be granted a license, the design target for the effluents and releases should be defined so as to minimise their effects. The analysis shows that, for all foreseeable accidents, the release level will be about two orders of magnitude below the one for which any countermeasure or food restriction is needed for the population outside the site fence (less than 10 mSv).

The environmental impact related to the gases and airborne particulates effluents and liquid releases is being assessed. Preliminary results indicate that they are well below internationally accepted levels. In fact, the preliminary evaluation of doses to the public from atmospheric release is less than 10 µSv per year *at the end of life of ITER*. Concerning the tritium concentration in water, expectations in terms of doses are also very low (less than 0.1 µSv per year). ITER effluents and release are well below the current legal limits for all effluents (1 mSv). A detailed study will allow checking whether a further reduction of the releases to the Durance can be achieved.

ITER effluents and releases can be accommodated within the present Cadarache site authorisations.

I.2.3 Waste management and dismantling

The waste inventory expected during the operation phase and during dismantling has been established following the current French classification, which considers four levels for wastes:

- Very low level waste (TFA: "très faible activité"): activity lower than 10^4 or 10^5 Bq/kg, depending on the half-life, but for which trace-ability is mandatory;
- A-type waste: activity lower than 10^6 or 10^9 Bq/kg, depending on the half-life, which can be disposed of in the "Centre de l'Aube" repository;
- B-type waste: all waste that cannot be classified as TFA or A type;

- C-type waste: from fission fuel cycle (ITER does not produce any C-type waste).

It has been foreseen to minimise the B-type wastes volume and weight. Well-known technologies will allow the sorting to be performed.

The analysis of several scenarios shows that the amount of B-type waste does not vary significantly over time, whilst the amount of A-type and TFA-type wastes vary, as shown in Table I-1. The total amount of waste is currently estimated at 30 000 t. Consequently, after the disassembly of the in–vessel components, the decommissioning process should be mainly driven by considering workers occupational doses and economic aspects.

	Phases	Masses (tons)			
		TFA	A-Type	B-Type	*Total*
Hypothesis 1	All wastes at shutdown	10577	19492	3502	*33570*
	Total of hypothesis 1	**10577**	**19492**	**3502**	***33570***
Hypothesis 2	Part at shutdown	10577	9970	3114	*23660*
	Part after 30 years	4924	1		*4925*
	Part at 50 years or detritiation simulation		387		*387*
	Part at 100 years or CWS decontamination simulation	4598			*4598*
	Total of hypothesis 2	**20099**	**10358**	**3114**	***33570***

Table I-1 : Breakdown of waste at shutdown or after decay

Different methods of disposal are proposed for the different types of waste depending on the disposal foreseen. The reference scenario currently favours the local disposal and the temporary storage on the ITER site before the final deposit in a permanent storage facility.

I.2.4. Tritium management

After an initial phase of operations with hydrogen and deuterium, ITER will operate during 10 years with a deuterium-tritium mixture. 15 kg of tritium will be supplied from off-site sources so that tritium transport, inventory tracking and accountancy have to be done according to French and international regulations.

A container for the transport of 25 g of tritium is already qualified internationally. Alternatively, a container with a larger capacity could be extrapolated from an existing cask and qualified.

A specific accountability procedure would have to be defined and implemented for non-proliferation reasons. Detailed studies on the uncertainties in the measurement processes are in progress. A periodic check of the tritium inventory might have to be done to minimise the uncertainties due to administrative limits on the total tritium inventory allowed in the torus (ITER has proposed 700 g in the vacuum vessel, and a total of 3 kg on site).

I.3. Socio-economic aspects

The Provence Alpes Côte d'Azur region has all the necessary resources and infrastructure to respond to the industrial, social and cultural needs of ITER.

Cadarache is located near the city of Aix-en-Provence (distance 35 km, 137,000 inhabitants) and the towns of Manosque (15 km, 20,000) and Pertuis (25 km, 18,000), where the majority of the people currently working on site live. Marseille, the largest harbour of the Mediterranean and second largest city in France, is 70 km away.

Local and regional authorities have expressed their strong support for ITER in Cadarache and they are actively involved in the on-going studies.

European industry would greatly benefit from the ITER construction. This would be particularly true if ITER were to be hosted in Cadarache.

A team of international fusion experts is already working at Cadarache. This presence, together with specific facilities to be set up in the nearest villages, would ease the integration of the ITER international personnel.

Either the expansion of existing, nearby international schools, or the establishment of a new European / international school, as it was done for JET, are being considered for the education of the children of foreign ITER personnel.

Last but not least, the exceptional climate, the great variety in sport and relaxation activities and the quality of Provencal life constitute an “art de vivre” that should be attractive to the best fusion specialists in the world.

I.4. Cost evaluation

The preliminary cost evaluation of the additional infrastructure required to host ITER, based on the ITER site requirements and assumptions, amounts to about 100 M€. This total includes transport, site preparation (excavation, access, etc.), electrical and water supplies, building adaptation and site services (wastes processing and storage are not included).

II. TORE SUPRA PROGRAM : EVOLUTION

II.1. The CIEL project

The CIEL project, launched in 1996, consisted in designing and fabricating new generation internal components for Tore Supra, so as to increase its performances in terms of heat and particle removal over long periods of time (25 MW of power injected continuously over times up to 1000 s with 4 Pam^3s^{-1} of particle extraction). Its main components are :

- a toroidal pumped limiter (LPT), main element of interaction with the plasma, consisting of fingers made of carbon fibre composite (CFC), able to withstand intense thermal fluxes, and assembled on a stainless steel support structure
- the internal wall protection (PEI), made of stainless steel panels covering all the internal wall of the machine, aimed at protecting the latter from plasma radiation
- the safety rings, made of 6 pairs of CFC tile rings, aimed at absorbing the energy deposited during transients (disruptions…)

In the last two years, the main Tore Supra project components have been installed, after construction which lasted one and a half years, and the machine was started up again in the fall of 2001, under a configuration of «CIEL start-up limiter » (LDC), which includes 3 LPT 30° sections, actively cooled, equipped with inertial bows, pending the complete installation of the LPT in 2002.

II.1.1. Fabrication of components

II.1.1.1. Toroidal Pumped Limiter fingers (LPT)

Fabrication problems

The fabrication of the LPT fingers has continued in 2000 and 2001. After a satisfactory fabrication start-up, the Plansee Company met up with cracking problems on the interface between the CFC tiles and the body of the copper finger, resulting in a significant rejection rate of the fabricated elements. Indeed, even a low cracking rate in the tiles (about 3% in the case of Plansee) is enough to significantly reduce production, knowing that only one defective tile can condemn the finger, which has 21 of them.

The problem was identified at the end of 1999; the beginning of 2000 was essentially devoted to the analysis of these defects. The first explanation investigated was that of the thermal treatment the fingers had been submitted to, during fabrication. However, sets of fingers fabricated with a more efficient control during the year 2001 did not show any improvement. The hypothesis presently under study focuses on the type of CFC used, which might influence the quality of the assembly procedure of the tiles on the finger body, namely the « Active Metal Casting » (AMC), developed by Plansee. Indeed, the use of a different batch of CFC, slightly less efficient from a thermo-mechanical point of view, and more porous, resulted in a lesser cracking rate, without providing any actual explanation to the problem. The collaboration between the CEA and Plansee has been very active in attempting to solve this problem, with the use, in particular, of the thermographic control facility called SATIR at the DRFC, which was used to test the fingers at different fabrication phases.

Repair procedure

A repair process has been developed by Plansee, so as to not reject the fingers including only one or two faulty tiles (machining of bad tile, welding of new tile, repair by machining and associated thermal treatment). The process was validated on a mock-up with repaired tiles, tested under high thermal flux by the DRFC in the FE200 electron beam (cf. figure II-1).

Furthermore, a contract on the repair of fingers was signed with Plansee, which should allow for a permanent stock of about forty fingers to be kept in reserve. This contract covers a period of five years for limiter maintenance.

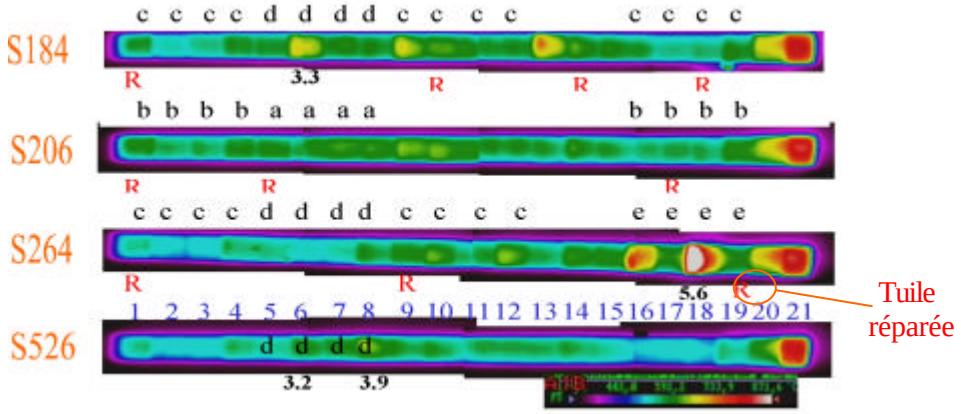

Nombre de cycles subis par tuile (5-9 MW/m²) :
a = 1500; b = 1250; c = 1000; d = 500; e = 250

Figure II-1 : Infrared view of surface temperature distribution of 4 LPT fingers under an incident thermal flux of 5 MW/m^2. The repaired tiles indicated in red do not show local heating even after many cycles.

State of progress

The contract signed with Plansee includes several types of fingers :

- standard LPT fingers (574 are required to equip the LPT, 600 have been initially ordered)
- « diagnostic » LPT fingers, with a slot in order to let the beam of some diagnostics pass (4 are required, 8 were ordered)
- « neutraliser » fingers, equipping the neutralisers under the LPT, with 4 different geometries N1 to N4 (48 are required for the 12 neutralisers, 60 have been ordered)

The delivery schedule initially set up and finally achieved is presented in figure II-2. After the fabrication problems encountered at the end of 1999 and at the beginning of 2000, the deliveries were increased during 2001. At the end of October, nearly 540 of the 600 standard fingers ordered were delivered by the Plansee Company to Tore Supra. 80%, in other terms 434 fingers, were accepted during delivery tests (leak test, SATIR thermographic test). 60 new fingers and nearly 140 repaired fingers should be delivered by the end of 2001.

At the same time, 72 « neutraliser » fingers, including type N1 fingers with complex geometry (ends in the shape of « ship hulls »), were delivered instead of the 60 ordered. 6 N1 fingers were accepted and 12 sent back for repair (6 are still required to equip the neutralisers). All the N2, N3, N4 fingers required were accepted.

Among the 12 «diagnostic » type fingers delivered instead of the 8 ordered, 9 were sent back for repair (3 have now been accepted out of the 4 required for the LPT).
In order to ensure that fabrication will be finished at the end of 2001, the CEA ensures the thermal quality control of 100% of the finger tiles by means of infrared tests on the SATIR bench. The tiles to be repaired are clearly identified on the fingers, which are then sent back to the supplier as quickly as possible. Moreover, some of the tiles have been accepted with a derogation (SATIR test result slightly under the $|\Delta T_{ref}| < 3°C$ criterion, see explanations in section VI.3.2). These fingers accepted with a derogation (about 8%) are submitted to additional optical tests, in order to make sure they do not have any cracks, and are placed in the self-shadowed zones of the limiter (tiles less charged thermally, see section II.1.3.1). This new procedure does not put into question, a priori, the global performances expected of the LPT (15 MW thermal continuously convected).

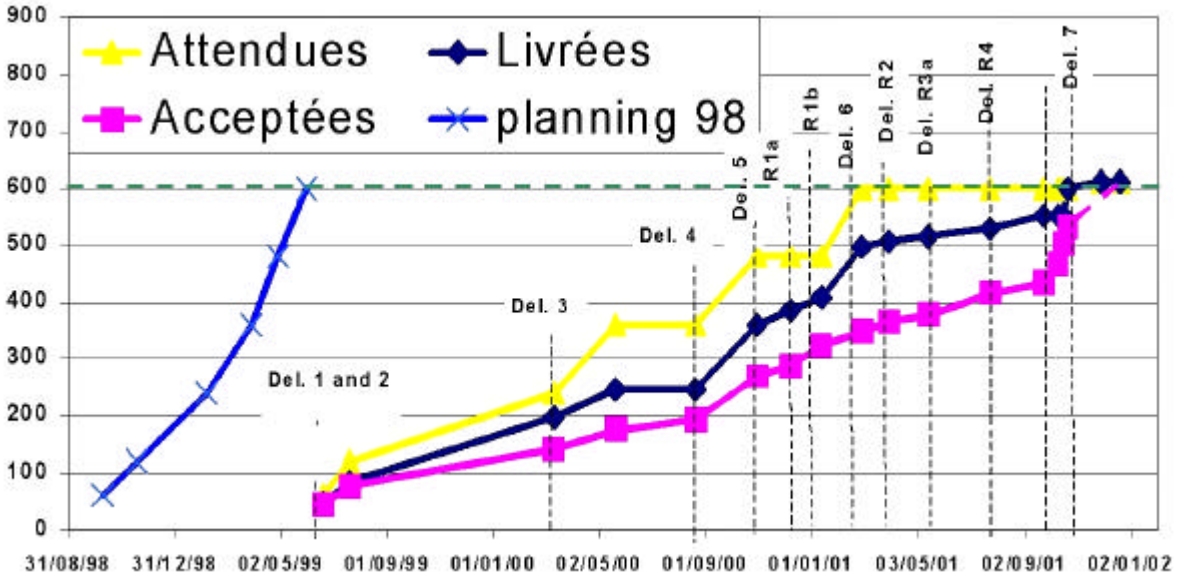

Figure II-2: delivery and acceptance of standard LPT fingers.

II.1.1.2. CIEL start-up limiter (LDC)

Because of the delay which occurred at the beginning of the year 2000 concerning the delivery and availability of fingers, an alternative solution to the LPT had to be found to restart the plasmas, scheduled for 2001. Since three sectors equipped with fingers were available out of the 12 required for the LPT, a complete study of a « CIEL start-up» limiter (LDC) was conducted during three months on the basis of the final limiter.

The LDC consists of a beam including 9 circular sectors, connecting the 3 sectors equipped with fingers and placed at 120°. The beam is designed to be semi-inertial (cooling between discharges) and is mostly placed far from the convected plasma flux. The three sectors equipped with actively cooled fingers are in contact with the plasma so as to be able to test the behaviour of the fingers under flux and experimentally validate the flux deposition estimated in the modelling (*Tokaflu* code).

The ends of the sectors equipped with fingers are protected by inertial CFC plates bolted onto the stainless steel beam sectors. The whole limiter is designed to withstand an energy of 30 to 40 MJ deposited during each discharge.

The LDC was successfully built in the second semester of 2000 (9 stainless steel sectors and associated CFC plates) then paired with the 3 LPT type sectors and installed on Tore Supra at the beginning of 2001. It was successfully experimented during the campaign on the fall of 2001 (see section II.1.3.1). This first phase in CIEL configuration evidenced design problems for the support structure columns and the insulating cuts between sectors. These defects were corrected in October or will be during the 2001-2002 winter shutdown.

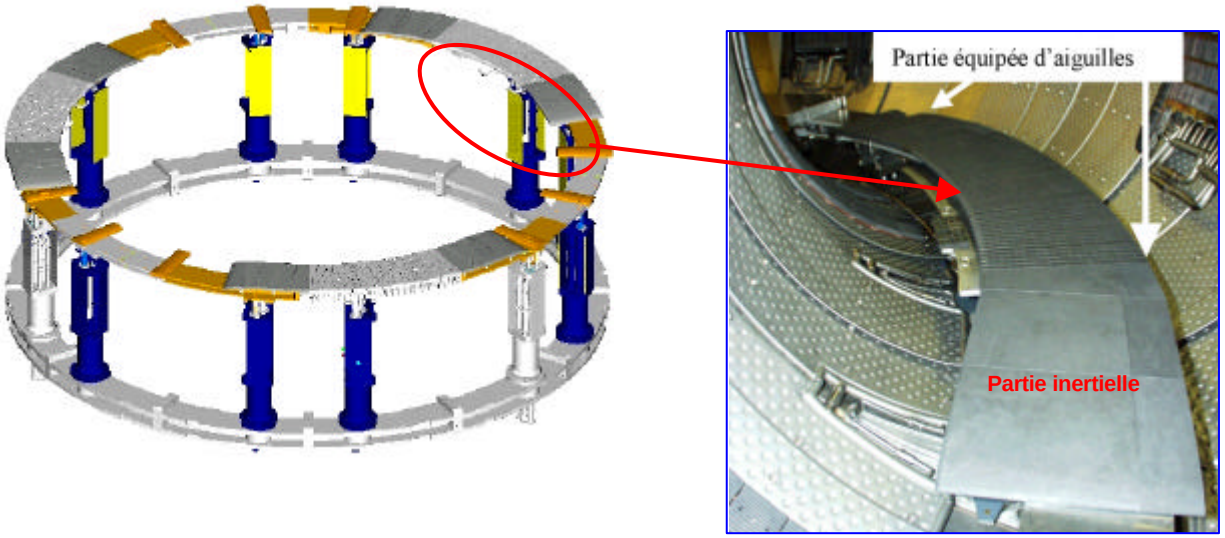

Figure II-3 : CIEL start-up limiter (schematic view of support structure and view of LDC installed on the machine)

II.1.1.3. Internal wall protection, safety rings, antenna protection limiter

The *internal wall protection* (PEI), in charge of protecting the Tore Supra vacuum chamber from the power radiated by the plasma, is made of 108 actively cooled honeycombed stainless steel panels. Except for the protections of the horizontal ports, which will be installed in 2002, all of these panels, made by the *DATE* Company, have been placed in the machine during 2000.

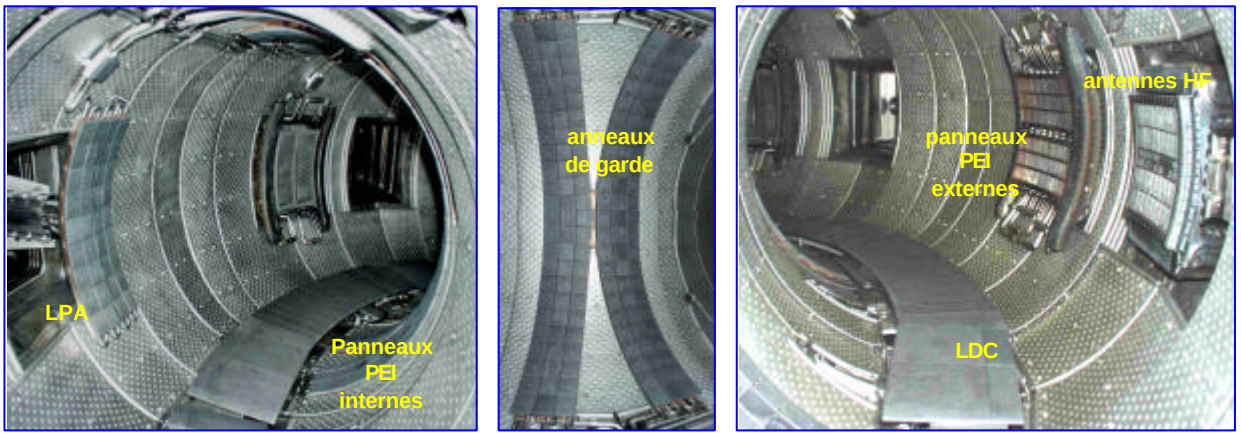

Figure II-4: Panoramic view of the PEI, safety rings, Antenna Protection Limiter (LPA), LDC and HF heating antennae, installed in Tore Supra

The *safety rings,* aimed at internally limiting the plasma during transient phases (start-up, loss of position control, disruptions), are made of thick tiles of carbon fibre composite (CFC), bolted onto an actively cooled copper alloy structure (CuCrZr). Six pairs of rings are positioned on the internal side of the machine. A problem with this fabrication (carried out by the *SICN* Company) concerned the making of square and hollow CuCrZr sections 3 m long, without any intermediate welding: the wire-drawing, done by *Swissmetall*, was in fact a European innovation in this geometry. Another difficulty to overcome was the achievement of reliable welding by electron bombardment between two CuCrZr sectors. The 12 structures were made and placed in the machine in 2000. They were placed with a radial accuracy of 0.5 mm in relation with the magnetic axis, to evenly distribute the energy deposition during disruptions.

The function of the *antenna protection limiter* (LPA) is to protect the heating system antennae from possible damage (energetic electrons, for example). It is placed on the low field side, in a horizontal port. Experience has shown that this object must be strong enough and the thermal shield (tiles) easy to replace (which consequently means that it cannot extract significant fluxes). The design of the LPA head is of the safety ring type, with 4 cooled CuCrZr tubular structures, with thick CFC bolted tiles. The LPA is placed in front of the antennae and against the plasma during the discharge start-up phase, and then, once the plasma plateau is reached, is automatically withdrawn (displacement speed of 10 cm/s). The head of the LPA, with its hydraulic displacement system, was installed in Tore Supra at the beginning of 2001.

II.1.1.4. LPT neutraliser cases

A first neutraliser case, equipped with instrumented fake inertial CFC fingers, was successfully installed in Tore Supra during the 2001 campaign. This allowed the assembly procedure of the entire machine to be tested, along with the associated diagnostics and to obtain the first results on the pumping efficiency as well as monitoring the neutraliser fingers by means of optical fibres.

The remaining neutraliser cases are being assembled (December 2001), along with the cooled neutraliser fingers delivered by Plansee and will be installed when Tore Supra starts up again in 2002 in the final CIEL configuration.

II.1.1.5. In situ diagnostics

These include :

- periscopes equipped with infrared fibres for the surveillance of the neutralisers (see paragraph II.1.1.6),
- Langmuir probes, including “pop up”,
- pressure gauges, thermocouples.

A first block of “pop up” probes was installed on the LPT with the neutraliser case during the 2001 start-up. The standard Langmuir probes are ready to be installed during the 2002 campaign on the neutraliser cases.

The barometry has been in operation since the 2001 start-up (5 instrumented ports), to estimate the pumping performances at the level of the neutraliser installed on the machine.

II.1.1.6. IR safety of neutralisation cassettes

12 periscopes equipped with 3 optical fibres ensure the infrared surveillance of the neutraliser fingers, and allow the finger surface temperature to be measured, particularly at the critical point on the attack edge. Previous studies on Tore Supra using a prototype showed measurement difficulties in the spectral domain allowed by common transparent silica optical fibres, up to 2 μm, the thermal spectrum not being that of a black body. Studies are underway to determine why there is this difference, the eroded CFC surface being a possible reason. For the 2001 campaign, a periscope including 3 fibres, one of which is a special fibre operating up to 4 μm to eliminate measurement difficulties in the infrared probe, was installed on the neutraliser case equipped with fake inertial CFC fingers. A standard optical fibre was also installed inside the fake finger, aimed at by the periscope, so as to serve as a reference to the remote fibre measurements. The first results are being analysed.

For the next campaign, all the neutralisers will be equipped with 3 fibre periscopes during the 2001-2002 shutdown, of which 1/3 of the “special” optical fibres (transparent up to 4 μm to eliminate the measurement problems in the near infrared), the remaining fibres being the usual ones (transparent up to 2 μm).

The series of 11 periscopes for the other neutraliser cases, as well as the fibres and vacuum feeds-through, are under fabrication to be delivered in January 2002.

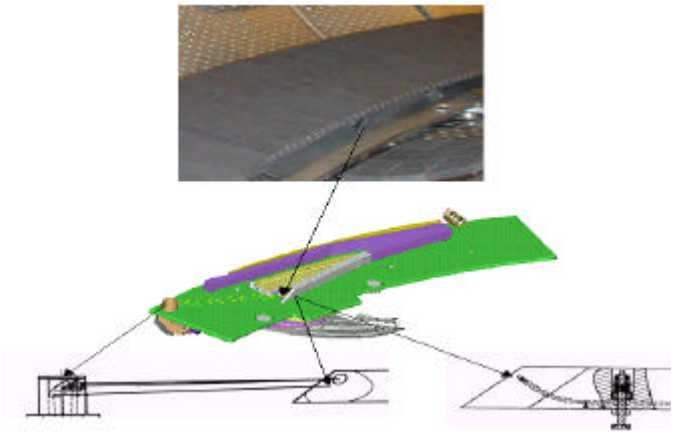

Figure II-5 : Lines of sight of infrared periscope for the surveillance of neutraliser fingers during the 2001 experimental campaign. At the top, the neutraliser case installed under the limiter in the machine, then a drawing of the cassette with its periscope, and finally the periscope and the lines of sight of the fibres, as well as the internal fibre.

II.1.1.7. Development of PCM80K cooled pump

The CIEL project, in its initial design, includes ensuring the LPT pumping by means of mechanical pumps able to remove a total flux of 4 Pam^3/s at a pressure of 0.1 to 0.15 Pa at the inlet of the pump cryostat. The principle of turbo-molecular pumping at low temperature was chosen. Based on the lessons drawn from the PCM prototype cooled at 20K and in collaboration with the Service of Low Temperatures (DRFMC/SBT CEA Grenoble), the CEA launched at the beginning of 2000 a call for tenders for the study and construction of a turbo-molecular pump prototype, cooled at a temperature of 80K by liquid nitrogen. The specifications are as follows : design of a pump which can be integrated under a lower port of the Tore Supra machine, withstanding the residual magnetic field and able to continuously remove a pumped flux of 0.4 Pam^3/s. The pump must be able to operate at both 80K and 300K and must be able to pump all the plasma impurities (D_2, H_2, He…). The contract was given to the ELETTRORAVA Company (Italy). The design studies on the pump and cryostat were conducted during 2001 (Figure II-6). The first tests made by the builder based on a V2000 VARIAN pump at ambient temperature resulted in proposing an increase of the size of the pump so as to meet the performances requested by the CEA. The materials able to work at 80K were validated. The magnetic swivels and the gaps imposed by the differential expansions, as well as the 80K exchanger, were designed. The final PCM80K project was approved in December 2001. The delivery of the prototype is scheduled for September 2002.

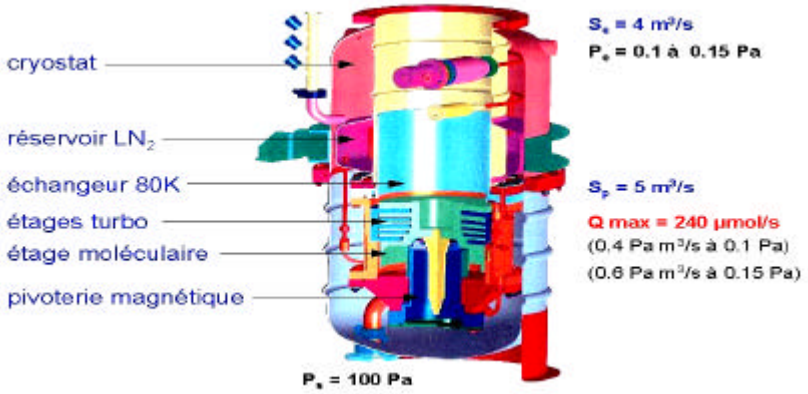

Figure II-6: Cross section view of PCM80K cryomechanical pump, for LPT pumping

II.1.1.8. Design taking into account the radiated flux

The optical diagnostics are exposed to the direct plasma radiated flux; they therefore require to be designed specifically for CIEL operation (high radiated power during long discharges). The design must integrate, on the one hand, the desired features of the object (operating mode, viewing angle, materials), of its positioning (vertical or horizontal window) and, on the other hand, the technological solutions chosen. In this context, the most fragile mechanical objects are found to be the diagnostic windows, the optical mirrors and the lenses. Some thermo-mechanical evaluations using numerical simulations (Castem 2000 calculations) were made for these elements and helped in identifying the critical points or even to define the operating limits for the power scenarios expected in the next experimental campaigns.

II.1.1.9. The Infrared Irradiation Test Facility (IRIFA)

The evaluation by thermo-mechanical calculations of the optical elements is difficult (see § II.1.1.8). Consequently, it has been decided to test the assembly behaviour in a real situation (high thermal gradients) on the InfraRed Irradiation Facility, of the Reactor Studies Department of Cadarache (DER). The facility, which includes an electrical resistance made of carbon and used as a radiation source (up to 1 MW/m^2), has been adapted to meet our needs. The optical elements to be tested must have an absorbing deposit, covering the useful range of the radiating source spectrum. It is to be noted that this type of test will also be included in the development procedure of some ITER optical elements (thermal gradients due to baking of the vacuum vessel).

A first test was conducted on a crystalline quartz window when the facility was started. This showed the difficulty of simulations (modelling of the soldering/welding, material properties), which predicted that the window would resist, when it actually cracked. The sapphire windows of the head of the infrared endoscope were then tested. They were submitted to a cycling with thermal fluxes equivalent to 20 MW radiated at the edge of the plasma without damage.

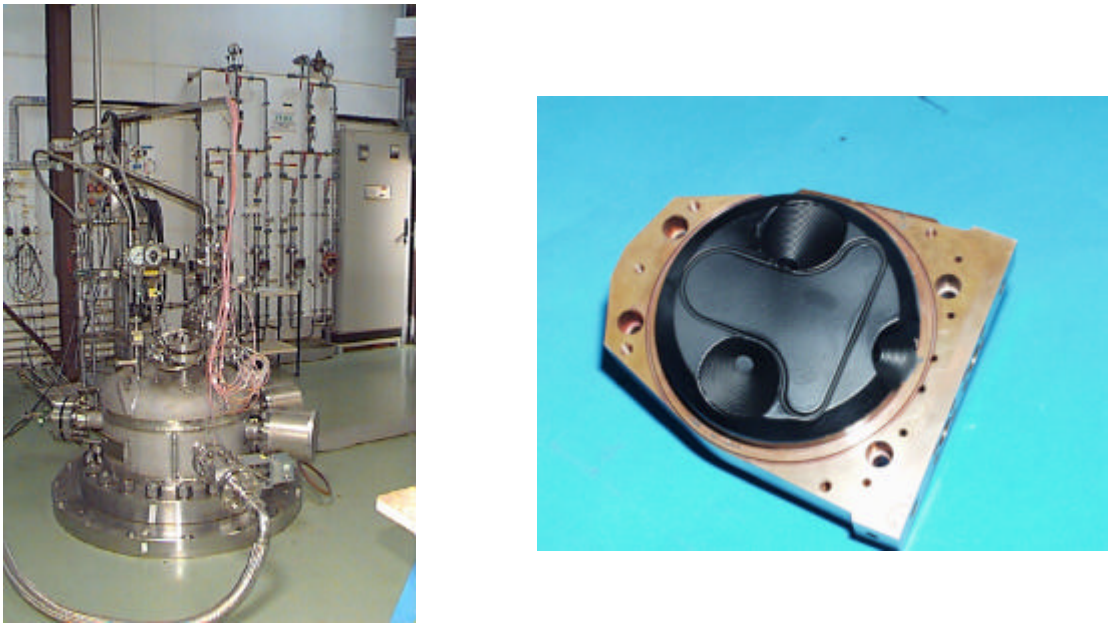

Figure II-7 : view of the IRIFA facility, on the left, and of the head of the infrared endoscope tested, equipped with three sapphire windows. The component to be tested was covered with a black deposit, so as to simulate the absorption of the radiation emitted by the plasma.

II.1.1.10. LPT infrared safety

The beginning of 2000 was devoted to achieving the detailed plans of the endoscopes and to drawing up the specifications so as to use them for international calls for tender. At the end of 2000, six contracts were signed : endoscope heads, endoscope bodies, infrared cameras and finally the system of acquisition and operation of the infrared cameras and two contracts for the optics :

- Endoscope heads. The first prototype delivered had a micro-leak, but was nevertheless used to thermally test the windows on the IRIFA facility (see Section II.1.1.9). Analyses are underway to solve the welding problems by electronic beam.
- Endoscope bodies. Concerning the mechanical part, the endoscope body prototype was delivered mid-October 2001 in Cadarache after technical difficulties during its fabrication. It is being submitted to the usual checks and will be assembled and tested in extenso. The series of 7 endoscopes should be delivered during December 2001.
- Infrared cameras. The contract to make the infrared cameras is underway and on time. The two cameras scheduled to be delivered in 2001 were delivered at the beginning of October.
- Acquisition system. The data acquisition and analysis system was successfully validated in October 2001.
- Optics : The contracts are not on schedule, which results in the optic systems only being delivered in spring 2002.

During 2002, the first of the entirely equipped endoscopes will be assembled, and will monitor 1/6 of the pumped toroidal limiter as well as one of the 5 heating antennae placed in a middle port. The aim of the 2002 campaign is to develop and validate this complex system which will be inserted in the general Tore Supra safety system. In the long term, this must ensure the safety of the toroidal pumped limiter as well as that of the 5 heating antennae.

Due to the delay in setting up the endoscopes, the old infrared cameras will be re-assembled in March 2002. A few direct views have been set up using teleobjectifs instead of the former generation endoscopes, not compatible with the new Tora Supra structure in its CIEL configuration. The aim is twofold : allow the CIEL start-up limiter to be thermally qualified and temporarily monitor the additional heating antennae, pending the arrival of the new generation endoscopes (see Section II.1.3.1).

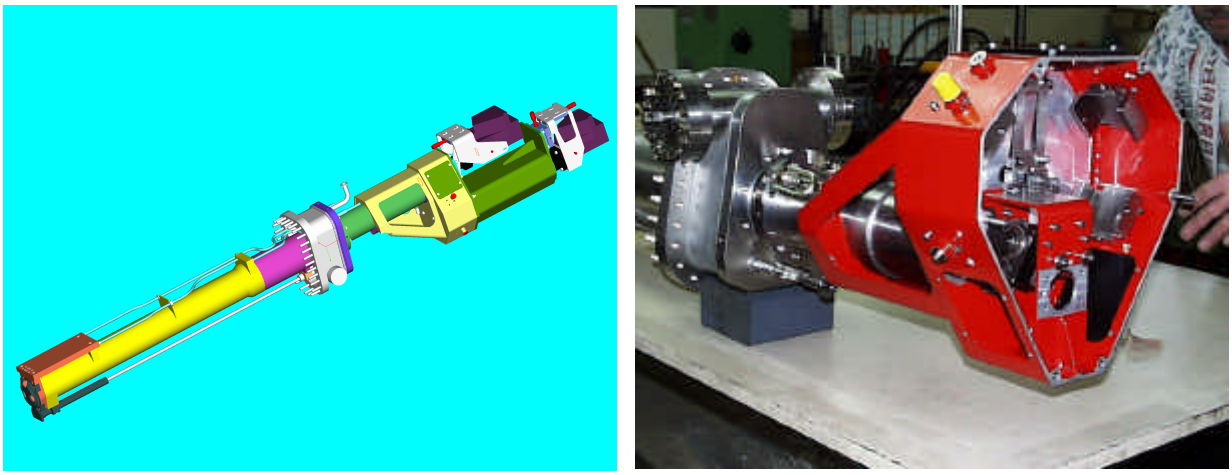

Figure II-8 : On the left, artistic view of the endoscope, equipped with two infrared cameras. On the right, body of the endoscope equipped with upper optical box, allowing the combination of two LPT views so as to be projected on a single camera.

II.1.1.11. Magnetic measurements

The new magnetic measurement diagnostic, meeting the demands of the CIEL project, is now installed on Tore Supra. A set of 415 magnetic field and flux measurement detectors is in place in the Tore Supra vacuum vessel, behind the first wall elements (figure II-9). The position of the measurements prevents any access after setting them up; some redundancy is therefore respected.

Each detector has been defined and optimised in geometry and surface for the different measurements. These detectors must also be submitted to the strains imposed by the machine vacuum and high temperatures. Particular attention has been given to their design and choice of materials used. The detectors are made of a ceramic mandrel, around which an enamelled copper wire is coiled. Four types of field measurement detectors are used (Figure II-10), to which the flux loops must be added.

The diagnostic is already operational. It is routinely used to control and calculate the plasma parameters in real time, but also for more accurate physical studies, such as MHD mode measurements.

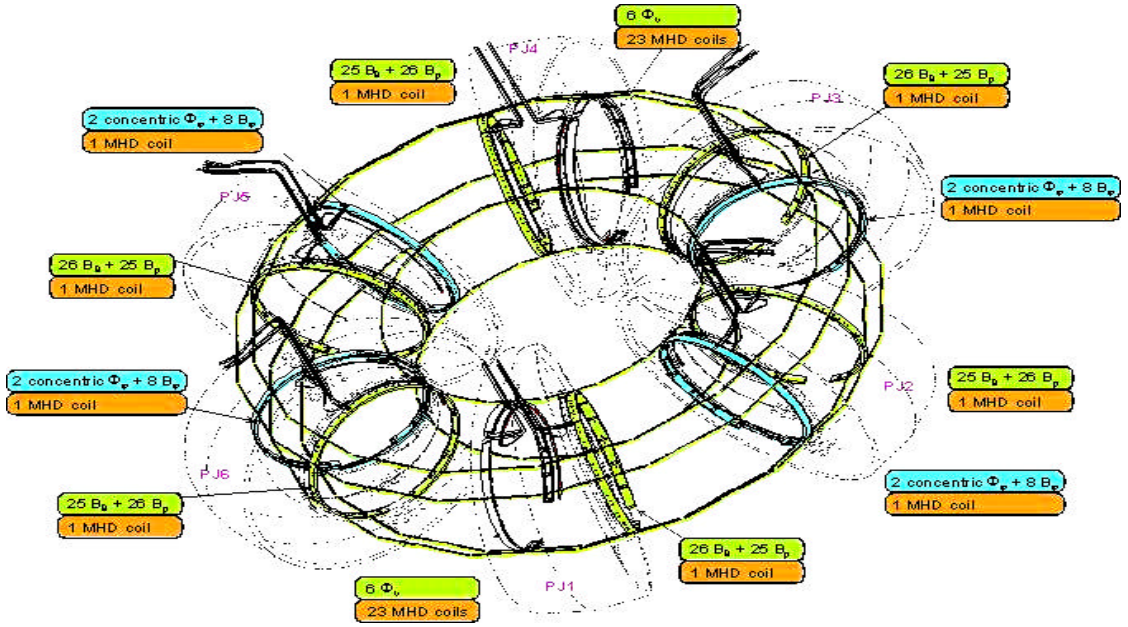

Figure II-9 : General view of new magnetic diagnostic measurement detectors.

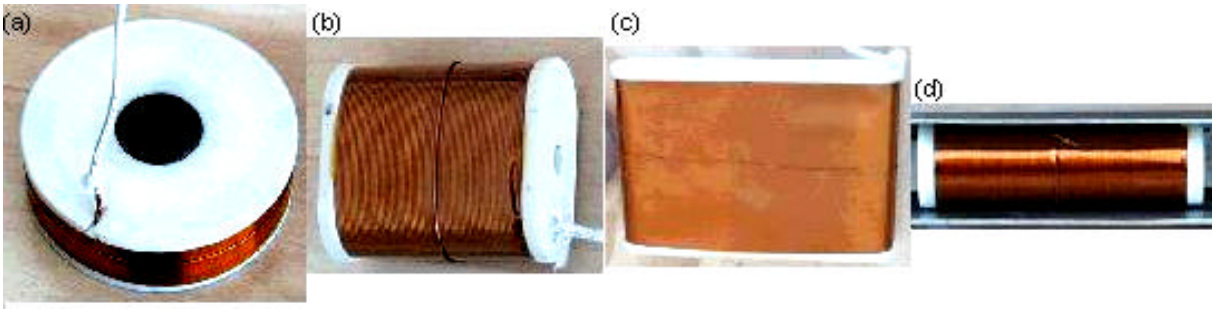

Figure II-10 : Detectors used to measure magnetic field (a) radial, (b) poloidal, (c) toroidal and (d) MHD studies (poloidal field).

II.1.2. CIEL working site

The Tore Supra working site program started at the beginning of December 1999, and ended when Tore Supra was started up again in August 2001. The initially planned schedule was respected from the beginning of the work. The plasma start-up, foreseen for July 2001, was however delayed until end of August 2001. This delay is due to a late start-up of the toroidal magnet cooling system, caused by the loss of redundancy in the 15 kV electrical supply (due to the high voltage lines being brought down by snowstorms in Cadarache in February 2001).

The construction program included the following main operations :

- stripping down the interior and exterior of the machine.
- assembly of CIEL components.
- necessary re-configuration of the machine sub-systems, on the mechanical, hydraulic, electro-technical and operating levels.
- maintenance operations necessary for start-up in 2001.
- sub-system re-qualification and plasma conditioning and start-up operations.

The first phase of the program, from December 1999 to April 2000, included the stripping down of the interior and exterior of the machine, the removal of the hydraulic networks of Loop 30 (Boucle 30) and the disconnection of the systems connected to the machine.

II.1.2.1. Assembly of LPT support structure

After a simulation of the LPT support structure assembly carried out on marble (figure II-11), the latter was dismantled to be installed under the machine. Specific tools were developed at DRFC, controlled by an official organization before being used, to install this structure in a complex environment, difficult to access. The assembly operation (figure II-11) was carried out without any incident during May and June 2000.

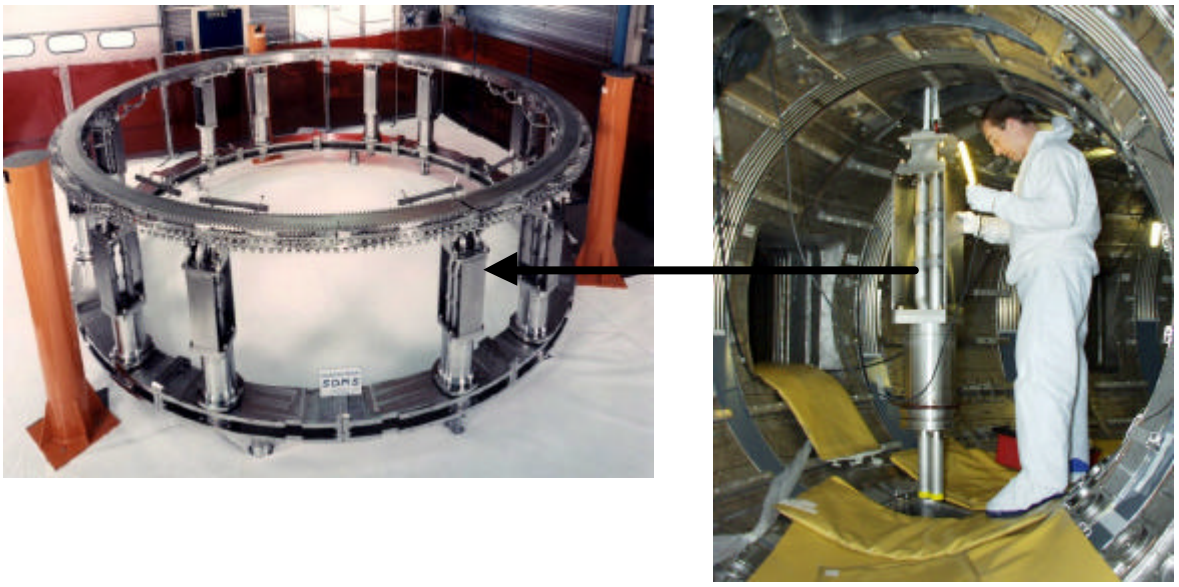

Figure II-11 : LPT support structure mounted on marble (left hand side). Introduction of a support column through a triangular port (on the right hand).

II.1.2.2. Test on installation of LPT support jacks

The 6 vertical displacement electrical jacks of the LPT ring were successfully tested in May prior to their installation in TORE SUPRA. Movement tests on a specific test bench (figure II-12) essentially focused on checking the position feedback accuracy, controlling the trajectory in simultaneous movement of the 6 jacks and associated safety systems. All these tests showed that the specifications

had been respected with a significant margin. The maximum difference between the jacks position during the simultaneous displacement of the 6 jacks is lower than 0.1 mm for a displacement speed lower than 0.5 mm/s, the absolute positioning of the cylinders being adjusted to better than 0.1 mm. In figure II-12, one of these jacks can be viewed in its final position on Tore Supra.

Figure II-12 : Test bench for the 6 jacks simultaneously; one jack assembled on the magnetic circuit

II.1.2.3. Implementation of LPT pumping

Six lower ports are equipped with a standard turbo-molecular pump of 2200l/s. These pumps are connected at the pumping line end under ports Q1B, Q2B, Q4B, Q5B, Q6A and B by means of an isolation valve

Only port Q6B is equipped with a neutraliser case, in compliance with the CIEL project. Ports Q6A and B are also equipped with mass spectrometers and pressure gauges, allowing the analysis and measurement of the pumped flux.

II.1.2.4. Assembly of Internal Wall Protection (PEI) and of safety rings

The PEI panels were all installed in the fall of 2000, except for the six middle port protections, whose fabrication was delayed. These components will be installed after the experimental campaign of 2001 when Tore Supra will be started up again in CIEL configuration.

The 12 limiter safety rings located in the inner part of the machine on the high field side and the 12 ripple upper protections in CuCrZr were also installed during this period. Each of these components was secured by TIG welding to the water supply collectors installed in the upper part of the machine. The 12 limiter safety rings were then equipped with 830 bolted CFC tiles. These were positioned with a radial accuracy of 0.5 mm with respect to the magnetic axis, in order to distribute as evenly as possible the energy deposition during disruptions.

Before starting to assemble the CIEL start-up limiter, it was necessary to check that there were no leaks in the PEI cooling circuit. The plasma chamber was thus placed under vacuum on 15 December 2000 and all the joints and vacuum welding were checked during the first two weeks of January. At the same time, all of the PEI panels were pressurised at 5 bar of helium, evidencing a single internal leak due to a fabrication fault in one of the panels. The latter was identified and repaired.

II.1.2.5. Assembly of HF heating antennae

This program was started end of 2000, while the PEI assembly operations were being finished. Four antennae equipped with lateral protections were installed, including 2 FCI heating antennae and 2 hybrid heating couplers.

II.1.2.6. Preparation and installation of CIEL Start-up Limiter (LDC)

The installation on the machine of the 12 (300 kg) sections making up the circular beam of the LDC was successfully performed in February 2001, using a specific kinematic with a suspended circular rail and handling and positioning equipment specially designed for this operation.

2.1.2.7. Installation of lateral protection of HF heating antennae and of LPA (Limiter for Antennae Protection)

The installation of lateral protections on three of the four HF antennae was carried out in January 2001, at the same time as the LDC was prepared. The lateral protections were re-assembled as such, without undergoing any modifications or adaptations during the shutdown. They were TIG soldered to the cooling collectors fed by the water loop pressurised at 30 bar.

The LPA, with its hydraulic displacement system, was installed on Tore Supra at the beginning of 2001. The limiter head, actively cooled, was also connected to the B30 network, in the same way as the lateral protections.

II.1.2.8. Leak test of all plasma facing components

Except for the middle port protections, whose installation is postponed to the winter of 2001-2002, the CIEL program for the Tore Supra vacuum chamber equipment, was finished mid-March 2001. The Tore Supra vessel was put again under vacuum in March 2001, in order to leak test the PEI cooling circuit under a helium pressure of 60 bar at ambient temperature. This verification evidenced a leak on one of the PEI panels. The latter was identified and repaired.

The global leak test of the CIEL Start-up Limiter cooling circuit was simultaneously carried out section by section (total number of sections : 12), also under a pressure of 60 bar of helium at ambient temperature. Slight leaks appeared on 2 of the 28 connecting flanges of the water circuit between columns and sections. These problems were solved, thus guaranteeing the global tightness under 60 bar of helium of all the cooling circuits of all the CIEL components, HF antennae and their lateral protections.

II.1.3. Start-up of Tore Supra under CIEL configuration

The aim of the 2001 campaign was to qualify the new components installed in the machine, especially the CIEL Start-up Limiter (LDC), made of three sections of the future LPT.

In order to achieve this, the Tore Supra program was organised around 3 action programs (AP) for 2001 : start-up, heat and particle removal, heating and transport. The program co-ordinator, along with the AP leaders (RAP), proposes an experimental program to the Tore Supra Experimental Committee. This new operation structure has also taken over a more formalised definition of the operational limits of Tore Supra, now gathered in validated files. It has also promoted European collaborations around the Tore Supra program. A two-day workshop was organised with the participation of over 40 outside collaborators, mostly from the other Associations.

II.1.3.1. LDC thermal characteristics

The infrared cameras viewing the LDC surface allowed both the qualitative and quantitative studies of the thermal deposition to be started.

Quality of fingers

The fingers react as predicted by the thermal simulations, with a satisfactory time constant (stabilisation of the surface temperature in less than 10 seconds). They were only submitted to thermal fluxes below 1 MW/m^2, which does not yet allow their ability to withstand nominal fluxes (10 MW/m^2) to be judged, nor their ageing. The results given here nevertheless give a good indication as to their fabrication quality.

The comparison of the performances obtained in Tore Supra with the SATIR non-destructive test bench data (see Section V.3.2) is in a preliminary phase. The verification on SATIR determines for each finger a temperature response difference ΔT_{ref}, which characterises the quality of the thermal transfer between the part of the finger facing the plasma and the cooling water, compared to a reference finger. It would seem that for the assembled fingers (accepted after being tested on SATIR with a $|\Delta T_{ref}| < 3°C$), there is no correlation between the relative heating of the tile on the limiter and its performance on SATIR. This result is in agreement with the observations obtained with the FE200 electron beam, where correlations are only observed at $|\Delta T_{ref}| > 3°C$, which is the limit value for the fingers to be accepted.

Characterization of thermal flux deposition and validation of model

The heat deposition is in agreement with the simulations, with its « snake-skin » pattern and the flux-deprived areas by shadow phenomena under the toroidal field coils (figure II-13). This pattern is particularly observed on the vertical surveillance CDD camera pictures, where the recycling flux has the same pattern (figure II-14). The first estimates of the heat decrease length provide a value of 10 to 12 mm, close to that observed on ALT-II, the Textor limiter having a configuration similar to that of the LDC. This value is globally confirmed by different measurement means including calorimetry (see Section II.1.3.3). The first series of plasmas validate the TOKAFLU heat deposit model, but the analysis is at a preliminary stage. The perpendicular flux is, as predicted, weaker than on the former inner wall; the quantitative aspect is under study.

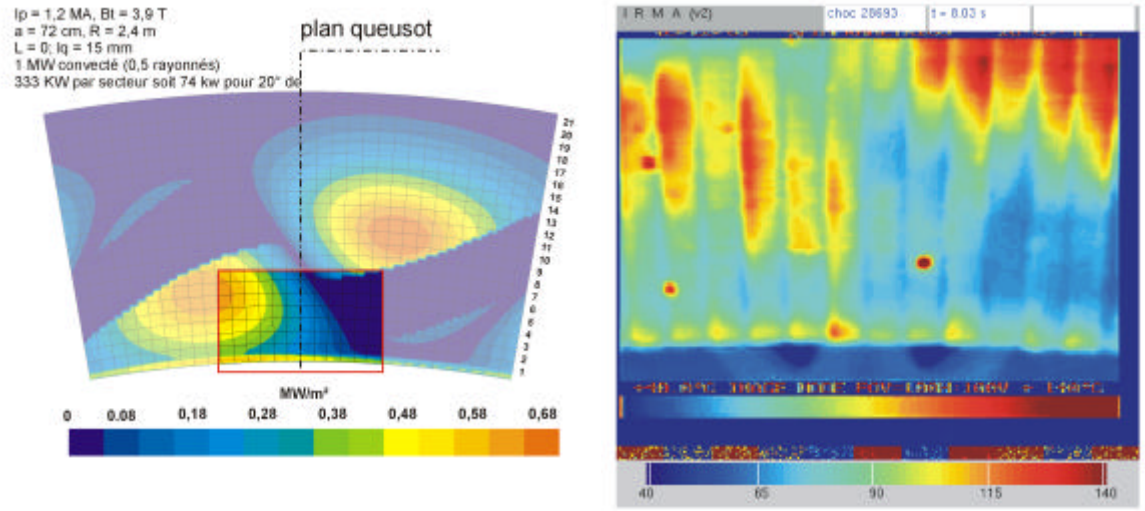

Figure II-13 : Comparison of the flux deposition calculated by TOKAFLU (on the left) and observed by infrared camera (on the right). On the left picture, the area aimed at by the camera is inside the red frame. The characteristics predicted by calculation (snake-skin pattern) can be seen. The IR picture is slightly different from the simulation because of the plasma major radius of 2.38 m for the measurement instead of 2.40 m for the calculations.

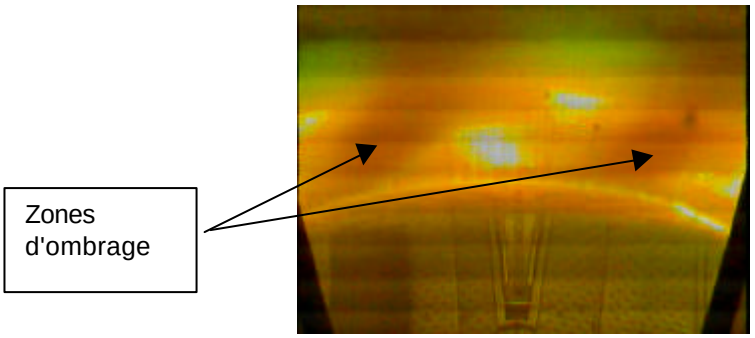

Figure II-14 : CDD picture of limiter section, illustrating the recycling pattern on the limiter. Flux deposition zones and shadowed zones can be seen near the toroidal field coils (snake-skin pattern), as predicted by modelling.

II.1.3.2. Measurement of currents in the LDC

The LPT (Toroidal Pump Limiter) was designed to be polarised to a voltage of ± 1kV with respect to the inner vessel. This voltage should allow the creation of an electric field at the edge of the plasma and thus modify the plasma flowing along the field lines. Waiting for the polarisation power supply to be installed on the final LPT, the LDC and internal chamber were connected through a resistance. Figure II-15 shows a schematic view of the localisation of the resistances (resistance R_{LPT} of 1 Ω withstanding a power of 1 kW) which connect the 6 LDC sections to the machine potential. In this configuration, the 3 final LPT sections (Q2B, Q4B and Q6B) are isolated from the intermediate sections (Q1, Q3 and Q5). When the plasma is against the LDC, a current circulates between the latter and the chamber via the resistance R_{LPT}. The circuit closes by means of the edge plasma (the SOL) ; the current essentially depends on the edge plasma density and the distance between the last closed magnetic surface and the inner safety rings.

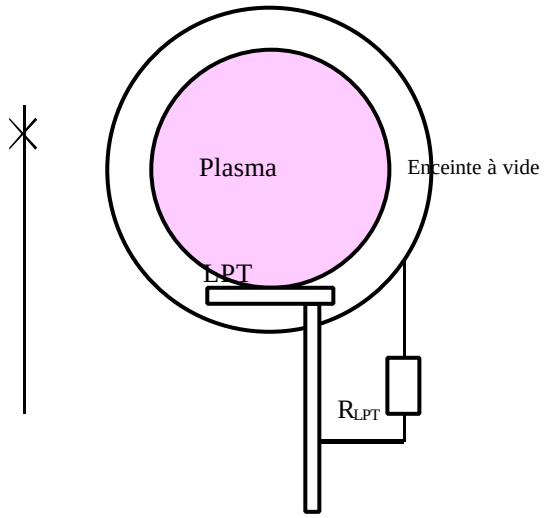

Figure II-15 : Schematic view of the connection of the 6 LDC sections to the vacuum chamber

The absolute values of the currents measured during these first experiments are as expected. Especially, the evolution of the current collected versus the distance Δ between the last closed magnetic surface and the vacuum chamber confirms the validity of the model used (figure II-16).

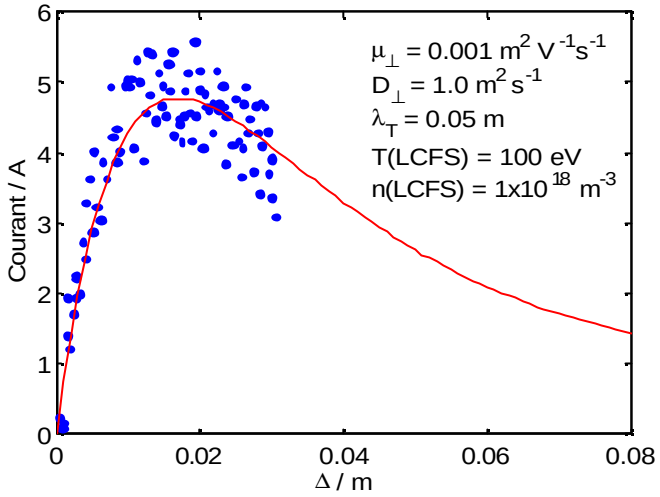

Figure II-16 : Current collected in the LDC as a function of the distance between the last closed magnetic surface and the vacuum chamber. The blue dots show experimental data, the red curve is the model result.

Moreover, the current collected, reflecting the particle flux falling on the limiter, has been shown to be a good indicator of plasma detachment. Whereas its increases normally with density, it saturates and then decreases when the plasma detaches (figure II-17). A detachment degree can be defined (DoD) as being the ratio between the current from the fit done in attached regime and the current actually measured. In the attached regime, this DoD is equal to 1, whereas it is above 1 when the plasma detaches. This can be very useful to feedback the plasma on the gas injection, allowing the plasma to be driven at high densities, close to detachment, without losing control.

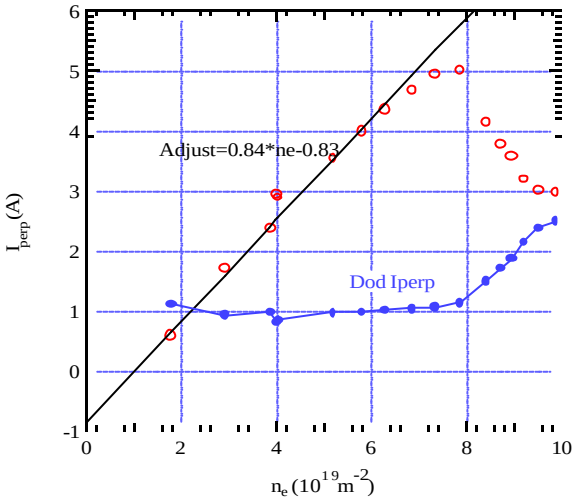

Figure II-17 : Evolution of the current collected as a function of the plasma density (red dots), which shows the increase of the current in attached regime, then the decrease when the plasma detaches. A detachment degree is deduced (blue dots), which indicates that the plasma detaches itself when its value is larger than 1.

II.1.3.3. Calorimetric analyses

The analyses carried out in 1998-1999 showed the interest in studying the ohmic regime in order to validate the calorimetric balance, so as to establish a sound basis before going on to plasmas with additional power. Within the framework of the CIEL project, the complete overhaul of both the internal components and the calorimetric diagnostic again require such validation. With the increase of the nominal flow rate of the B30 cooling loop components and despite a significant improvement of the signal to noise ratio on temperature measurements, the thermal balance of ohmic discharges in the CIEL configuration could not be analysed with sufficient accuracy. After a thermohydraulic study

followed by validation tests on the FE200 facility, it was decided to perform ohmic discharges in Tore Supra with a flow rate for the cooling loop B30 reduced by a factor of 4 (in other terms, a water speed in the LPT fingers of 2 m/s instead of 8-10 m/s in normal operation). The study and the tests demonstrated that under these conditions, the margin to critical flux is still 10 times greater than the nominal operation margin. The experimental results on Tore Supra were in agreement with the thermohydraulic calculations. Particularly, in ohmic discharges, the temperature increases measured at the LPT sections outlets reached 2,5°C. with a signal to noise ratio of about 50 (figure II-18). The time resolution of the calorimetric measurements is of about 2-3 s.

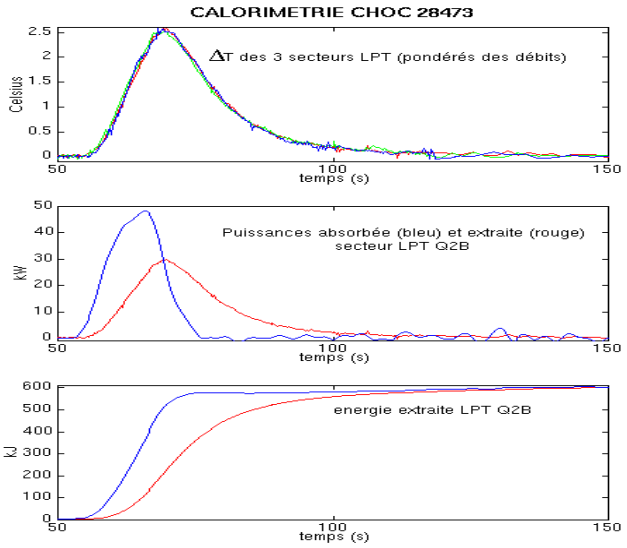

Figure II-18 : Example of calorimetric data treatment (LPT section). Top : temperature measurement; center : removed and absorbed power; bottom : removed energy calculation.

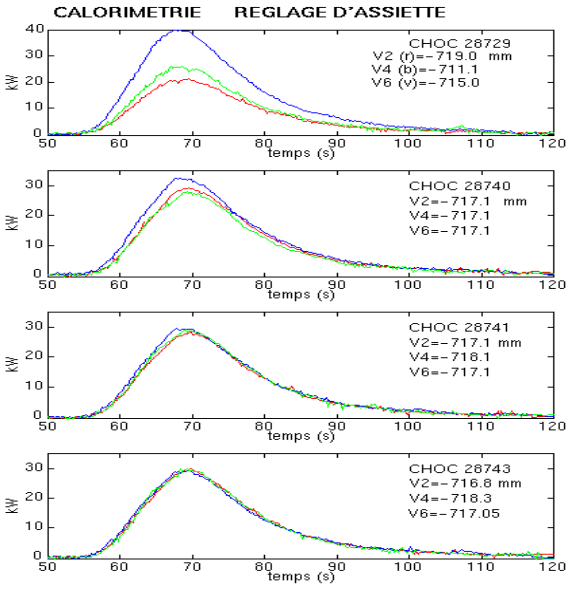

Figure II-19 : Analysis of LDC plane setting : power removed from the 3 LPT sections as a function of the jacks height.

The preliminary analyses on the experimental results, obtained with a reduced flow rate, showed that by taking into account the flux deposition on the inertial LDC sectors, calculated with TOKAFLUX, there is no difficulty in obtaining the energy balance of the ohmic discharges.

Moreover, the analysis of experiments on the LDC horizontal setting, also carried out with reduced flow rate, showed the great sensitivity of the diagnostic, detecting variations in LPT plane adjustment of about 0.2 mm (figure II-19).

Lastly, a first estimate of the decrease length using the calorimetric measurement, taking into account the radiated power, gives a value of 12 mm, in good agreement with the infrared measurements (see Section II.1.3.1).

II.1.3.4. LDC pumping performances

The neutralisation cassette installed on the machine allowed the first qualification experiments of the pumping system to be conducted. The usual behaviour of pressure is observed in the pumping line, which increases at first with plasma density (linear regime with high recycling) before saturating when the plasma starts to detach (figure II-20). It is to be noted that the neutraliser case is significantly shadowed by the inertial baffles of the LDC, which explains the low pressure observed. This will no longer be the case in the final LPT configuration in 2002. However, even in the present unfavorable configuration, a slight effect on plasma density is observed when two identical discharges are compared, with and without activated pumps.

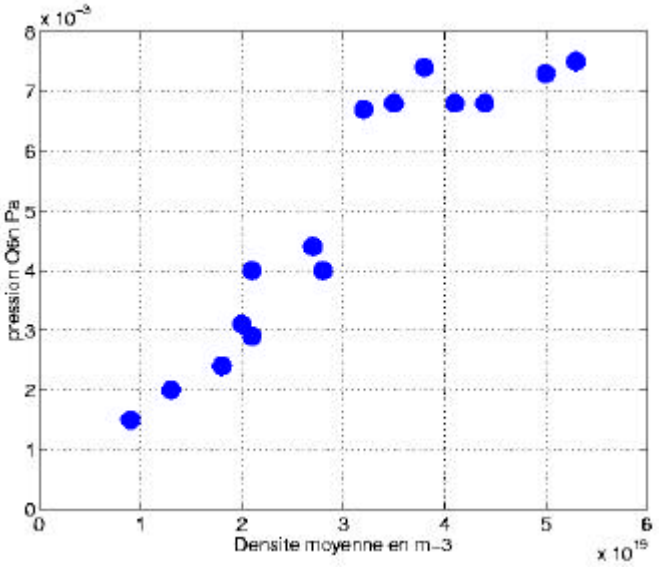

Figure II-20 : Pressure evolution in pumping line versus plasma density.

II.2. CIMES Project

II.2.1. Objectives and strategy

II.2.1.1. Scenarios

The aim of the CIMES project is to allow Tore Supra to reach discharge durations up to 1000 s, with in particular :

- heating and current generation systems able to provide a total power of 20 MW,
- a particle injection system with high performances coupled to high reliability.

These new heating and matter injection systems, combined with the recently installed CIEL components, and with the electron cyclotron frequency heating system, will enable TORE SUPRA to explore two types of discharges. The aim of the first one (A) is to carry out technological performance tests to sustain fusion technology development on long discharges. The aim of the second one (B) is to explore Advanced Tokamak discharges, again on long discharges.

In terms of fusion technology, the heating, current generation, matter injection systems and the components in contact with plasma as well as the energy and particle removal systems, are necessary to maintain the plasma over characteristic times exceeding the equilibrium times between the walls and the plasma. Demonstration of the reliability of these different components at thermal equilibrium under high heat fluxes is an important phase for ITER. Concerning physics studies, obtaining high power long discharges in Tore Supra will be a landmark in the study of physics in stationary tokamaks : the current must be non-inductive at 100%, with a large part self-generated by the bootstrap effect. The demonstration that the « advanced tokamak » can be extrapolated to the stationary regime is a fundamental question for ITER. The CIMES project will attempt to reach these stationary conditions in the plasma and study the robustness of the equilibrium versus perturbations. One of the key points will be to demonstrate that the optimised profiles can be created and maintained for times much longer than the current diffusion time. The time aimed at of 1000s is well above the characteristic times of internal plasma equilibrium and those of plasma/wall interactions. TORE SUPRA could then reach and study the energy and particle balances, thanks to extraction (CIEL) and injection (CIMES) tools.

The main characteristics of the discharges are gathered in table II-1 :

Aim	*A: Fusion technology*	*B: Advanced Tokamak Physics*
Density	~ 1.5×10^{19} m^{-3}	~ 4×10^{19} m^{-3}
q at the edge	~3	~5.5
Plasma current at 4 T	1.4 MA	0.8 MA
Bootstrap fraction	~ 20 %	~ 50 %
Profile control	Not necessary	Paramount
H factor	H~1	H~2

Table II-1 : Characteristics of typical CIMES project discharges

II.2.1.2. Contribution for ITER

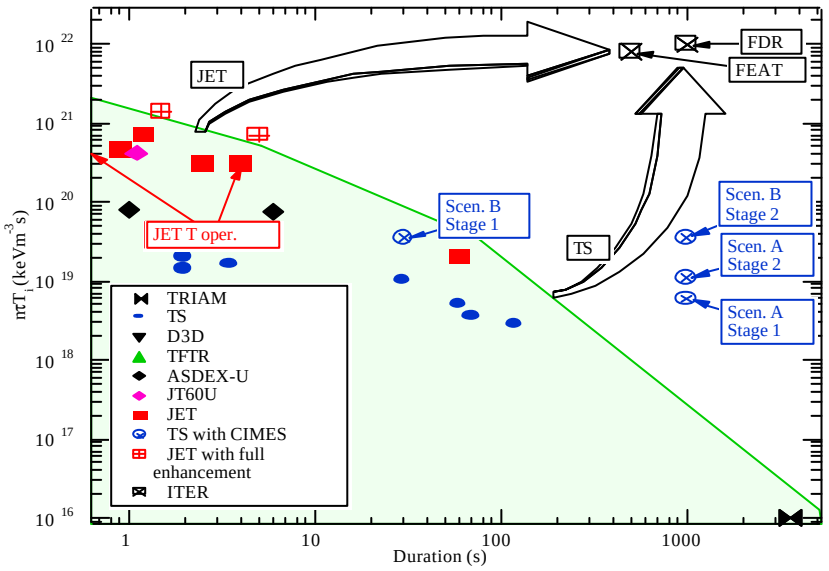

Figure II-21 : Type A and B discharges in the diagram triple product/discharge duration

In the context of fusion research machines, scenarios A and B can be placed in the triple product/time diagram (figure II-21), where the influence of the first 2 phases of the project can be seen :

It is to be noted that Tore Supra is the only machine which can provide contributions for plasma discharges of 10 to 1000 s. The necessary developments on the heating systems allow progress to be made on advanced technologies to ensure stationary power injections.

II.2.1.3. Schedule

From a technical point of view, the necessary developments cover several years, and the corresponding financial commitments are also distributed over time. To keep a certain flexibility in management and decision making, the project has been divided into three phases :

- the first phase concerns the LH system injected power, brought up to 8 MW and 1000 s,
- the second phase concerns the FCI system injected power, brought up to 9 MW and 1000 s,
- the last phase concerns the extension of the LH system to add 4 MW during 1000 s.

The first phase obtained the preferential support at the beginning of 2001; its technical content is detailed in the following chapter (II.2.2) and its planning is shown in figure II-22.

Nº	Nom de la tâche
1	Application for Preferential Support
2	**Project implementation**
3	Call for tenders ; contracts
4	700 kW prototype Klystron
5	LHCD generators upgrade with 700 kW klystrons
6	LHCD Mk2 Launcher maunfacturing
7	LHCD : 5MW for 1000 s
8	LHCD : 8 MW for 1000s
9	Pellet injector manufacturing
10	Pellet injector available

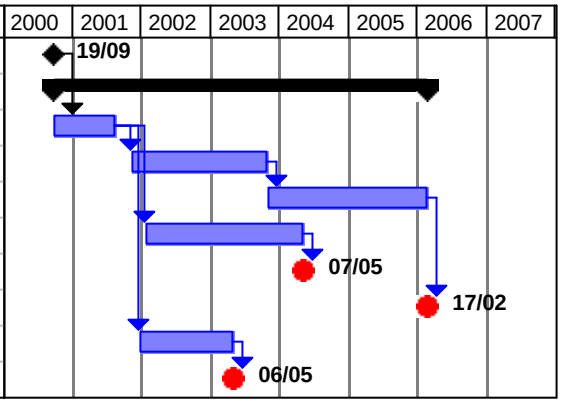

Figure II-22 : Schedule of the first phase of the CIMES project

II.2.2. Implementation and technical developments (first phase)

II.2.2.1. LH system : emitter and coupler

The LH emitter must be transformed so as to reach the required specifications : 8 MW injected in the plasma. Indeed, by taking into account the loss of the transmission lines, the average reflection coefficient of 5% and the margin necessary to be compatible with the controls and transients, the nominal initial power of the emitter, 8 MW (16 klystrons of 500 kW), is not enough. The output power will be increased by using a new klystron specially developed for this use. This new tube is an extrapolation of the current TH2103 klystron, its characteristics being given in table II-2.

It is to be noted that this new tube, by using a higher beam voltage, allows a greater output power to be obtained for a stationary wave rate (TOS) significantly less favourable. Experience on the use of current tubes allowed this new tube to be simplified so as to increase its reliability : elimination of the modulation anode and of one output window.

Klystron type	*TH 2103*	*TH 2103 C*
Frequency (GHz)	3.7	3.7
Frequency band (-1dB) (MHz)	5	5
Power (kW)	500 TOS <1.1	700 TOS < 1.4
Pulse duration (s)	60	1000
Cyclic ratio	0.25/0.35	1/6
Output	42%	>45%
Cathode voltage (kV)	60	70
Beam current (A)	20	<25
Gain (dB)	45	>50
Number of vindows	2	1
Modulation anode	Yes	No
Klystrons per antenna	8	8
Power available per antenna (MW)	4 (nominal)	5.6

Table II-2 : Characteristics of new klystrons (TH2103C) compared to current klystrons (TH1203)

It is also planned in the project to fabricate a second LH coupler of the same type as that recently installed on Tore Supra (see Chapter III.3.1.2 of progress report 1998/1999). This new type of coupler, developed to inject 4 MW at 3.7 GHz for 1000s with a conservative power density of 25 MW/m^2, was successfully tested during the 1999 experimental campaign. It benefits from new lateral protections compatible with the CIEL project parameters.

II.2.2.2. Cooling system

In addition to the evolution in the power injected by the LH system, modifications of the heating systems cooling loops are necessary. The loops concerned, B50 and B60, are those which ensure cooling of the high frequency power sources, ECRH, LHCD and ICRH. The modifications mainly concern one pump and water storage capacities, to be able to store the energy dissipated during the plasmas. The operation of these loops is pulsed : the energy is therefore removed between plasmas by means of a heat exchanger, which operates with a lower flow rate.

II.2.2.3. IR antennae surveillance system

The LH and ICRH antennae are placed in the immediate vicinity of the plasma. The coupling properties impose small distances between the last closed magnetic surface and the antennae structure surface. For an optimised and safe use, a surveillance system with infrared cameras will be installed. This is an extension of the system planned to check the surface of the toroidal floor limiter of the CIEL project. The CIEL endoscopes will indeed be equipped with additional specific optical views aimed at each of the 5 antennae (3 FCI and 2 LH). An appropriate treatment by infrared camera and digitalisation card will take into account the surface temperature of the antennae in the plasma control loops. In case of a local temperature increase in an antenna, the controls will be able to react on the power injected by this antenna and/or on the plasma parameters (shape and position of the plasma).

II.2.2.4. Quasi-continuous pellet injector

In order to control the density over times of about 1000s, a pellet injector will be specially developed for Tore Supra. It is based on a prototype developed by PELIN in Saint Petersburg. The required performances are a rate of up to 600 m/s, a frequency of 10 Hz, and D_2 pellets of 1.6 to 2.2 mm. The total injection capacity is 10 000 pellets per plasma, with a reliability of more than 98%. The injection guide tubes will be improved to allow injection on the high field side, near the equatorial plane and 38° above it.

II.3. Heating systems

The developments described below, concerning the heating systems, are those not included in the CIMES project.

II.3.1. LH

II.3.1.1. Emitter

The years 2000/2001 were marked by finalising the change to an industrial programmable automatic system for the second half of the facility. This includes a modification of the graphs of one of the hybrid Tore Supra couplers as well as a complete re-cabling of its control command part. A first modification had been made for half the facility in 1998-1999. Preliminary tests were made to check these modifications. These were completed by tests on loads to finally be validated by the operation campaign in 2001.

For the klystrons themselves, three tubes coming from the Varennes Tokamak were installed and tested on the emitter. For two of them re-conditioning is necessary and is underway in the Thales Electron Devices Laboratory.

A complete re-distribution of klystrons was made in order that the best tubes be used to feed the new generation C3 coupler, installed on the machine since 1999. After this re-distribution, HF power shots on an adapted charge load enabled to define the limits in power and in time of the 16 klystrons. Thus, the power available at the sources is of about 3 MW for the former generation C2 coupler and 3.3 MW for the C3 coupler. Five klystrons provide a power of less than 400 kW and are therefore outside nominal limits. Beam focusing adjustments and outlet cavity tuning will be necessary to improve the output of those tubes which are limited either on loads or on plasma.

Thus, all the control command system of the emitter, the safety systems of each tube and the electrotechnique associated to the anode modulator were checked. The tube reference curves were defined and validated both on the Panorama supervision software and on the VME data acquisition program.

Tore Supra experimental campaign

A very good behaviour of the emitter was observed both on the control command level and on the level of comparison between the power emitted by the tubes and their calibration on adapted loads. The maximum power injected on C3 was 2.53 MW, for 3.0 MW requested (#29186), that on C2 of 1.76 MW, for 2.1 MW requested (#29183). The maximum lower hybrid energy injected was obtained for discharge #29364 (23.2 MJ on C3 and 10.7 MJ on C2).

II.3.1.2. Couplers and measurement systems

During the 2000 – 2001 shutdown, the following actions were carried out on antenna C3 :

- the HF windows were repaired. Indeed, a very large number of arcs occurred during the 1999 conditioning campaign. Inspection of the windows has shown many traces on the beryllium oxide part. After cleaning, the titanium anti-multipactor flash (which had not been done before) was performed,
- the antenna protections, which were distant 3 mm from the wave guides, were placed at 1.5 mm,
- the antenna was turned around so that the radiated spectrum be compatible with the new direction of the plasma current,
- the antenna support were changed.

During the 2001 experimental campaign, the effect of different modifications was studied :

- very few arcs were observed during the conditioning periods on the C3 coupler. A power of 300 kW per tube was obtained on vacuum very quickly. The repair of the windows as well as improving their baking was very positive,
- the coupling observed in 1999 on the modules close to the protections was not efficient. The power reflection coefficients were above 15% and could reach 30%. In 2001, the coupling was greatly improved since, on average, the same reflection coefficients are lower than 10%. The C3 antenna has a coupling sensitivity dependence on shadowing, plasma shape, and antenna position, greater than antenna C2. There are several explanations :
    - the poloidal extension of the antenna is greater by 50 %,
    - the only self-adaptation effect in the C3 coupler is linked to its multi-junction. There is no hybrid junction with a short circuit on the equilibrium port which partly reflects the power at the plasma as in antenna C2.

  Antenna movements were made to check that the antenna was protected from the convective flux. This was the case. The present protections position thus seems more appropriate to work with a good coupling and to be compatible with long impulsions,
- the decrease in loop voltage is in agreement with the level of injected power, electron density and radiated spectrum. Thus, the antenna orientation is validated,
- in 1999, the antenna support vibrated while the antenna was moved. This was not observed this year. The change of the supports was positive. Displacement tests at greater speeds should be carried out to make sure that the support structure is compatible with rapid movement.

Hybrid test bench

On the Cadarache lower hybrid test bench, a module including graphite wave-guides covered with copper and made by JAERI was tested on long impulsions at high power. This module, which is in graphite with high thermal conductivity, is coated with copper on the surface to reduce the HF losses and is actively cooled. It has been successfully tested up to a power density of 125 MW/m^2 (Erf = 5.1 kV/cm) over times exceeding 600 seconds (Figure II-23) for which the module thermal equilibrium is practically obtained and the walls de-gassing is nearly stationary.

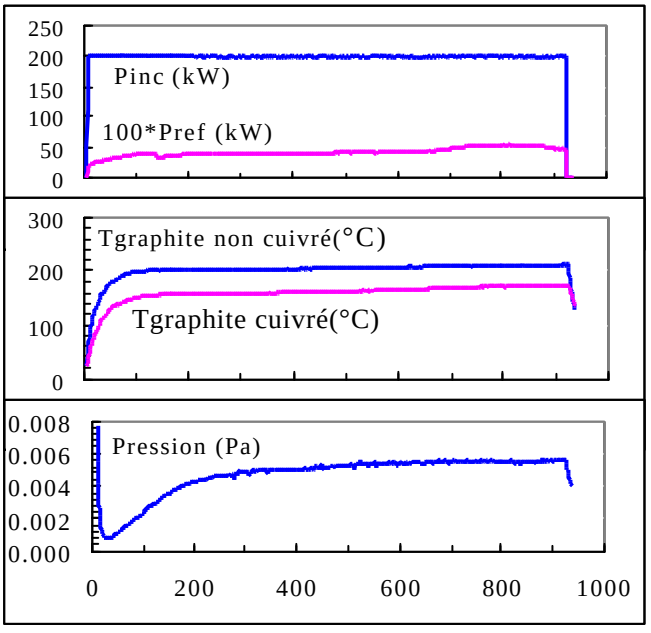

Figure II-23 : Test under power of coppered graphite module (P=100MW/m^2, E_{rf}=4.5 kV/cm)

II.3.2. FCI

II.3.2.1. Generators

In order to optimise the operating conditions of the tetrodes of the high power stage, and consequently the RF power delivered to the plasma, modifications were made to better supply each tube independently in high voltage (up to now the HT supply was shared by two tubes) : reconfiguration of an available HT supply, development of a new regulation module. The actual tests, planned on one of the 3 modules, will be carried out as soon as the new fast protection system for the tubes against HT supply is delivered (thyristors short-circuiter developed by CEA).

In order to solve the reliability problems observed in the preceding years on the capacitance de-coupling the anode of the high power stage (breakdowns, progressively leading to the destruction of the component), the Thales Electron Devices company was contacted and asked to develop a prototype capacitance with an improved behaviour under voltage, to be used in the validation tests of spring 2002.

II.3.2.2. Antenna and measurement systems

Because of the CIEL evolution in the use of the machine ports, the power injection of port Q4 was transferred to port Q2 : the ports were modified, and the power and cable transmission lines moved. In view of the availability of only 2 pairs of new generation lateral antenna protections, and after difficulties in the delivery of limiter fingers by the Plansee company, only 2 of the 3 FCI antennae were re-installed (in ports Q1 and Q2), with the usual leak and voltage behaviour tests. Moreover, the Q1 antenna was first entirely renovated (feeds-through and new tuning capacitances).

Within the framework of the corrective measures taken for the hot spots problems observed in the corners of the antennae during previous campaigns, the modification previously made on the lower right hand corner of the antennae was also made on the three other corners. In order to obtain local physical data, particularly particle density, necessary to validate the formation mechanism of these hot spots, two Langmuir triple probes were designed and installed in the upper and lower right hand corners of the Q1 antenna. The electronics devoted to supply and measurement of these probes was installed and cabled to render the signal treatment operational for the campaign at the end of 2001.

The prolonged shutdown period was also used to analyse the accuracy of the RF power measurements, because of the differences between a priori redundant measurements, up to 20%, observed during previous experimental campaigns. A thorough investigation showed a certain number of sources of errors on the power measurement couplers and allowed the calibration process to be made more reliable. A re-calibration of all the RF power couplers was then made.

In order to remedy to the diaphony problems between antenna power measurements (especially in scenarios with low absorption per passage) likely to switch on the security system using the reflected power, a new power measurement system was developed and successfully implemented during the short experimental campaign of 2001. Based on a synchronous detection principle, it allows the discrimination between antenna power measurements by using a slight difference in their frequencies (lower than 0.5%). Moreover, it solves the reliability problems of the previous detectors and includes an automatic verification procedure for the calibration of measurements before each discharge.

The change of the acquisition and piloting systems to « all VME » led to significant modifications on electronic cabling and programming, which were successfully tested during the 2001 campaign. This will help the implementation of several feedback controls (for example, power modulation with respect to a given physical quantity, or limitation of the current in the tuning capacitances over long periods of time) for future campaigns. Moreover, a new piloting system for the conditioning mode was also elaborated (piloting by API, parametering and VME acquisition).

A conceptual design activity for a new generation of FCI antennae (4MW, 1000 s) has been started, essentially focused, for the time being, on the geometry of the front face and on the electrical configuration of the resonant circuit.

II.3.3. FCE

The first gyrotron of a series, after factory acceptance trials during the summer of 1999, was delivered to Cadarache for long impulsion tests on a 210 s load. A power of about 300 kW for a 111 s pulse was obtained. This power is the maximum value that the gyrotron can provide at the nominal operating parameters. The length of the impulsion is limited by strong degassing inside the gyrotron, reaching 100 µA and activating the associated security. It is also observed that after a significant number of conditioning shots, the pressure inside the tube only starts to increase after 60 s; a strong duration limit has apparently been reached. A power close to 10 kW, deposited in the mirror box, was measured by calorimetry. Thermo-mechanical calculations for this component with the Castem 2000 code showed that such a power deposited on certain parts of this component allows reaching the temperature increase and times constant measured at the outlet of the cooling circuit. The calculation also shows that this localized power deposition leads to a surface temperature of 500 °C, which is roughly the gyrotron baking temperature, thus possibly entailing significant degassing. The gyrotron was also connected to a 5 s load, to check if the ˜10% reflection of the 210 s load was not a limiting factor for the gyrotron performances. During this series of tests, parasite oscillations appeared for some operating regimes; they could lead to residual deformations in the cavity-injector set, thus explaining a degradation of the gyrotron performances in terms of output power. The same oscillations can also explain the power deposited in the mirror box.

Substantial modifications in the gyrotron design thus became necessary. A project for a study contract with TED (Thales Electron Devices, ex TTE) and EPFL was signed so as to define the modifications to be made to the gyrotrons in order to suppress these parasite oscillations and to improve their performances. The aim now is to obtain a power of 400 kW for a pulse duration of 600 s. An addendum to the contract on the gyrotron series fabrication between the CEA and TED was also re-drafted so as to define new performances, fabrication deadlines and tests and the costs of the gyrotrons to be produced in the future. This contract and this addendum will be examined at the beginning of February 2002 by the CCM. In the best of cases, the second series gyrotron will not be delivered to Cadarache before end of March 2003.

The first series gyrotron was accepted by the CEA at the end of 2001 with the performances it had achieved. This gyrotron, as well as the prototype gyrotron, were used for FCE experiments on TS during a campaign at the end of 2001, and will also be largely used during the 2002 campaigns.

The on line tests on a prototype diamond window were made during October 2000. The maximum strain to which the window was submitted was a power of 300 kW during 111 s. The through-window losses were of 1.4 kW ; this value, even though low in absolute terms, corresponds to 40 or 50 times the value theoretically expected. The diamond disk will thus be tested again to determine how much of the loss coefficient (tan δ) degradation can be attributed to the diamond brazing.

II.4. Diagnostics

With the LPT forbidding the use of the lower vertical ports, the CIEL project led to a re-installation of many diagnostics. A list of priorities was established to ensure the availability at start-up of the diagnostics necessary to obtain the plasmas. This operation was conducted successfully with the help of all involved, and there were many operational diagnostics at start-up. Meanwhile, the shutdown was used to start changing over to the VME standard for the acquisition and control command of the different systems. In the following paragraphs, only the diagnostics which, even though they are not included in the preferential support, were considerably improved are described.

II.4.1. IR thermography of LPT neutralisers

The safety of the LPT neutraliser cases is insured by thermography with infrared fibres. The preliminary projects of 1999 showed difficulties in making this measurement in the near infrared in the presence of a strong interaction of the plasma with the wall (the spectra do not follow the black body law). However, since the near infrared is much easier to diagnose with optical fibres than the average infrared around 4 µm, we wanted to know if nevertheless this spectral range could be used for safety measurements around 1000°C. Experiments at the University of Marseille, with low energy electrons, and at Le Creusot, with high energy electrons, did not reproduce these difficulties, at least for the bombardment of carbon reinforced with carbon fibres. However, the bombardment of pyrolythic graphites by low energy electrons seems to show a comparable effect. For the 2001 experimental campaign, a ZrF_4 fibre (transparent up to 4 µm) was installed in parallel to fibres transparent only in the near infrared; the emission in the near and average infrared can therefore compared, after transmission in the optical fibres. The first measurements (figure II-24) seem to show that the temperatures estimated from the near infrared are clearly higher than those estimated from the average infrared. This confirms the results of the preliminary projects and could justify the use of fibres for the average infrared. However, this is only a first conclusion, since temperatures of up to 1000°C have not been reached and that the origin of this additional radiation is not clear yet.

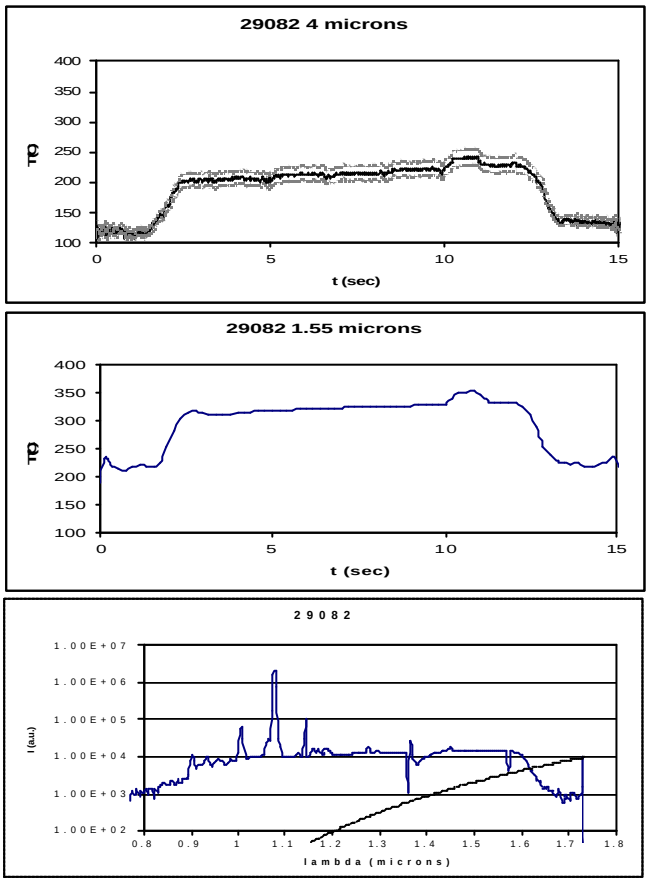

Figure II-24 : First measurements with ZrF_4 fibres between 3 and 4 µm (top), to compare with measurements at 1.6 µm (middle). The spectrum between 0.9 and 1.6 µm is in the lower part, the dashed line indicates the emission of a black body at 300K.

II.4.2. X-mode reflectometry: density profile measurement

After the installation in 1998 of a reflectometre in the frequency band 50-75 GHz, allowing the measurement of the density profile at the edge of the plasma at 3 T, a second reflectometre, sweeping the 75-110 GHz band, is now operational and allows the edge measurement of 4 T plasmas or up to the centre of the 3T plasmas (figure II-25). The two reflectometres are simultaneously frequency swept in 20 µs. The diagnostic control has evolved towards a VME system. The diagnostic is installed much closer to the torus, because of the new position taken by the Thompson scattering diagnostic. However, the antennae are placed further away from the plasma, at 1.2 m (instead of 60 cm).

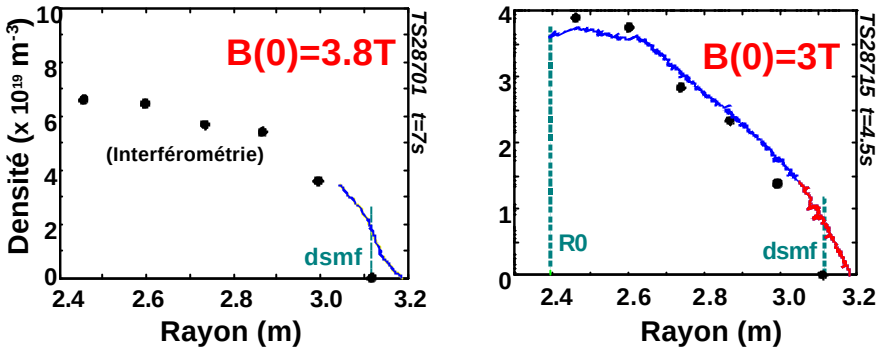

Figure II-25 : Density profiles for plasmas at 3 T and 3.8 T, measured by 50-75 GHz reflectrometry (red) and 75-110 GHz reflectometry (blue) and by interferometry.

II.4.3. Calorimetry

Within the framework of the CIEL project, the multiplication of B30 networks outside the machine would have enabled a complete calorimetric instrumentation to be set up for the measurement of the thermal energy removed from each internal component. This however, would have led to high costs. Thus, each circuit was equipped with temperature detectors, even though the flow rate measurement is not thorough.

The Tore Supra calorimetric diagnostic was completely overhauled during the shutdown. The changes, aimed at improving the measurement accuracy, concerned the following :

- temperature detectors. The K type thermocouples previously used were replaced with Pt probes, providing a greater accuracy and stability. However, their response time is longer (1 s instead of 0.5 s). 150 detectors of this type were installed on the different circuits of the B30 cooling loop.
- flow rate meters. The flow rate meters used on the refrigeration loops of Tore Supra were exclusively deprimogenous devices connected to pressure transmitters. This principle was maintained for pipes with a diameter >100 mm. For smaller diameter circuits, Vortex type flow rate meters, which have many advantages, including greater accuracy (1%), have been used. 57 networks are equipped with flow rate meters.
- temperature converters already installed, of analogical type, were replaced by more recent and efficient devices. In 2000, significant efforts were made in product research and on temperature converter tests. The converter selected has an accuracy of ± 0.15°C and a resolution of less than 0.02°C.
- the 4-20 mA current transmission lines between the converter and the acquisition system, a potential source of noise, were replaced by multiplexed numerical connections (optical fibres), using the TAXI protocol with the VME format. The optical fibre connections allowed the DCALOR acquisition unit to be installed in the electronics gallery.
- the DCALOR acquisition diagnostic is now on the VME standard, for which a continuous acquisition program has been developed. This program allows calorimetric measurements to be acquired 24 hours a day. The TS data reading tasks have also been modified so as to integrate this new type of data.

- for the refrigeration system, the implementation of the B30 inlet temperature regulation has been set up by means of a derivation towards the heat exchanger of part of the exiting flux.

All these systems were successfully tested when Tore Supra was started up again (figure II-26).

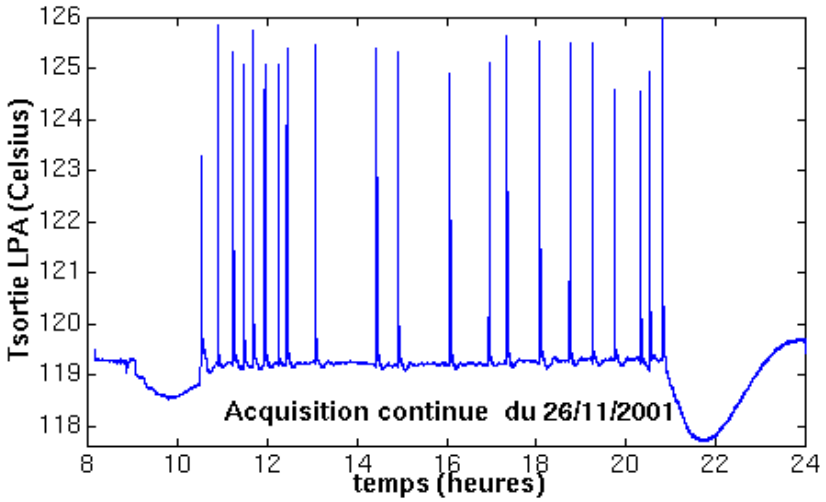

Figure II-26 : Example of continuous acquisition. The constancy of the base temperature level is ensured by the temperature regulation system of the B30 loop.

The first results on calorimetry, which are very satisfactory, are described in II.1.3.3.

II.4.4. Interfero-polarimetry

During the shutdown, the diagnostic was moved from port Q2B to Q3A. In order to take into account the geometry of the new limiter, the orientation of the 5 chords going through the plasma was modified. Three chords were placed at an oblique angle on the high field side, in front of the limiter, and two chords go through a slit in the limiter. This involved entirely re-designing the mirror support boxes which are located on either side of the vacuum vessel, designing new small dimension welded windows, and re-designing the polarimetry calibration plate. All the mirror boxes were placed on a new concrete slab to eliminate vibrations. A new liquid helium supply system for the cryostats was designed and installed. For improved access, the two infrared lasers were moved outside the torus hall; the site of the lasers was entirely re-designed. The infrared beam transport boxes towards the tokamak were designed and installed. The laser and cryogenic sub-system control commands were changed to API. The control command of the new rotating grating motors and for the new polarimetry calibration system were also developed. The three measurement and acquisition boards were entirely re-designed. Acquisition is now on VME. All of these changes were done over 21 months and the interferometry diagnostic started up at the same time as the first plasmas in September 2001. The polarimetry part is under testing.

With the aim to improving the spatial resolution of the diagnostic, additional horizontal lines of sight were studied (figure II-27). They would use retro-reflector mirrors placed on the PEI. A special PEI panel was made as well as mirror prototypes and the necessary port flange. At the same time, the transport of the infrared beams from the tokamak to the detectors was studied. The windows were designed and all of the 150 mirrors required were positioned in space. Their design, depending on the size of the infrared beams, is underway.

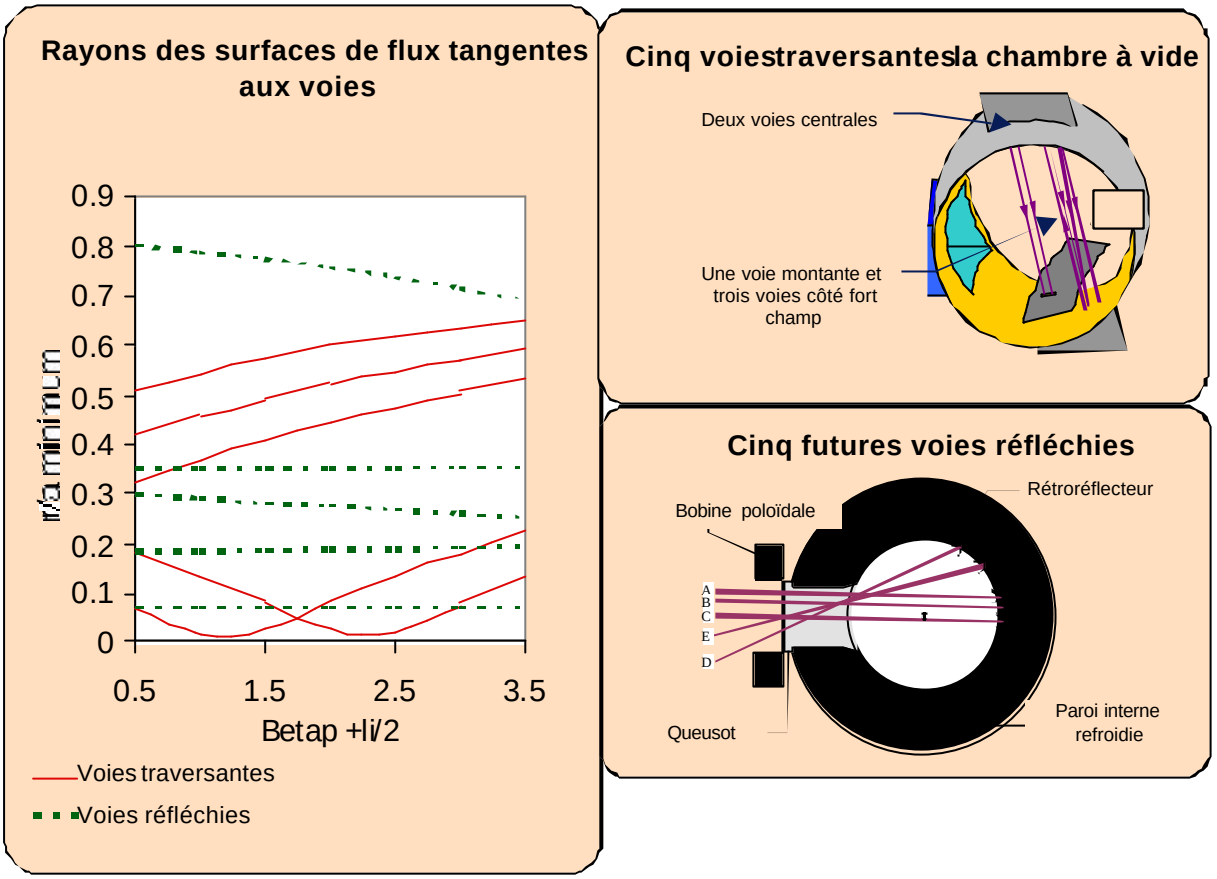

Figure II-27 : Improvement of spatial resolution of interfero-polarimetry using horizontal chords.

II.4.5. Diagnostic neutral beam

The Pagode source was modified (magnetic confinement, cathodes) until obtention of a homogeneous source, with a proton rate of 80%, and a current density allowing the extraction of 40 A ions. In parallel, the injector energy recuperation system was changed, by replacing the electrostatic retention of the neutralising plasma with a magnetic retention, thus considerably simplifying the injector and its environment.

At the end of 2000, beams were obtained on the BEL test bench, up to the nominal rate of the injector (70 keV, 40 A in H_2), the power of the neutrals (H^0) on the target being of 450 kW, and the beam divergence of 0.65°. A quick week end campaign also allowed the testing of the injector in D_2 ; in two days, 90 keV, 30 A, 700 kW of neutrals on the target were reached, for a divergence of 0.55°. Figure II-28 shows the comparison between calculations and retrieved current measurements, by assuming 80% of protons in the source.

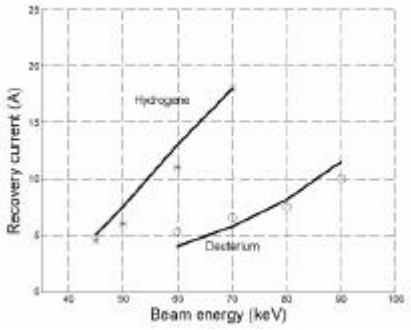

Figure II-28 : Comparison between calculation (line) and measurements (dots) of the retrieved current by assuming 80% of protons in the source (results obtained on the BEL).

The year 2001 was devoted to installing the injector on Tore Supra. The first shots in the plasma, within the framework of the start-up phase of fall 2001, occurred at 50 keV in H_2 ; for the moment, the injector adjustments are still ongoing, as high voltage parasites prevent to increase the power.

gas	*E (keV)*	*Iht (A)*	*Irec (A)*	*Pt (kW)*
H2	50	20	5.5	288
H2	60	27	11.5	373
H2	70	35	18	450
D2	70	22	6	520
D2	80	27	7.5	625
D2	90	32	10	710

Table II-3 – Experimental results on the BEL in H_2 and D_2 : E : energy of beam; Iht : extracted ion current; Irec : recuperation ion current; Pt : power of neutrals measured on the target.

II.4.6. Motional Stark Effect (MSE) and Charge Exchange Spectroscopy (CXS)

A project review, done at the beginning of 2000, showed that the complete study and then the achievement of the cooled version of the common optical part of the MSE and CXS diagnostics for CIEL led to time frames too long. Thus, it was decided to go towards a non-cooled temporary version, with a simpler design and allowing the start-up of the diagnostic for the 2002 campaign. The optical calculations aimed at determining the number and shape of the lenses were made with an optician external to the DRFC. This led to launching the end of study contract and the fabrication contract at the end of November 2001. The opto-mechanical part located on the machine should be delivered around mid-February 2002 and assembled just before the torus is closed, so as to make the alignments and calibrations of the two diagnostics. Nine lines of sight are planned. Each line has a CXS fibre (in the equatorial plane) and 3+3 MSE fibres, vertically stacked in a sort of «comb ». To measure the CVI profile with the filter spectrometer, 8 additional fibres of the PCS-600 type are foreseen. An additional hole in each comb «tooth » will allow their installation on the equatorial plane. The material supply aimed at equipping 5 MSE lines of sight has started. The first measurement tests should start as soon as plasma start-up occurs.

II.4.7. Speckle interferometry

For the CIEL plasma durations, the erosion of the CFC (Carbon Fibre Composite) covering the LPT can be significant. Simulations give an erosion rate of about one micron per discharge, with large error bars due to the uncertainty on the re-deposited fraction and localization of the deposit. A new method, based on Speckle interferometry, to measure an erosion of the limiter surface between 0.1 and 10 µm, with 10 nm resolution, is proposed. A laser beam reflected on the limiter surface interferes with a reference beam on a CCD camera. The position of the reference beam mirror can be adjusted, so as to obtain several images by changing the phase. The displacements of the surface in the direction of the beam, due to erosion or to re-deposition, modify the interference fringes. The principle of the Speckle interferometer is that of a Michelson interferometer, in which one of the mirrors is replaced by the surface to be studied.

The first Speckle interferometry experiments on carbon-carbon composite samples were carried out to test the feasibility of this technique on this type of material. The beam of a YAG laser (532 nm) was directed onto a CFC (N11) tile, identical to those used on the LPT, soldered on a copper support. Three pictures were recorded with a phase difference of $2\pi/3$ between them. A force applied to the sample induces a slight displacement perpendicular to the surface plane. Three new pictures with the same phase difference are then recorded. The analysis of the interference fringes obtained by comparison of the interferograms allows the measurement, at all points of the picture, of displacements of less than one micron (figure II-29).

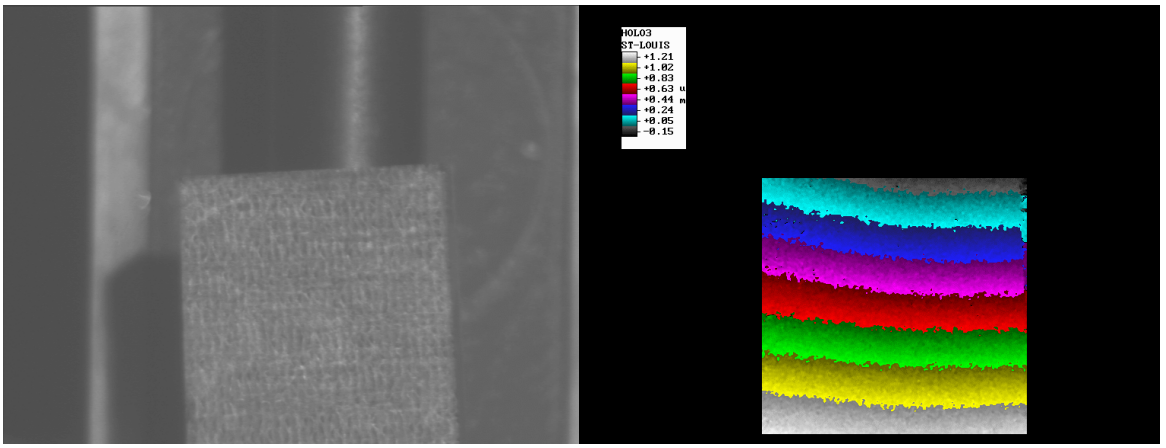

Figure II-29 : CCD image of a CFC sample (a) and displacements deduced from Speckle interferometry (b)

However, because of the limiter vibrations, this technique is not directly applicable to Tore Supra. It is necessary to have a second laser to cancel global displacements of the observed surface. The choice of the wavelength of the second laser must be such that the synthetic wavelength, $\Lambda = \lambda_1\lambda_2/(\lambda_1-\lambda_2)\cos\theta$, be of the order of magnitude of the erosion to be measured. By using two wavelengths, it is possible not only to measure a relative displacement but to also measure the shape of the object. A two wavelengths assembly with a tuneable laser and several cameras (figure II-30) was selected and is under development, to be validated in the laboratory.

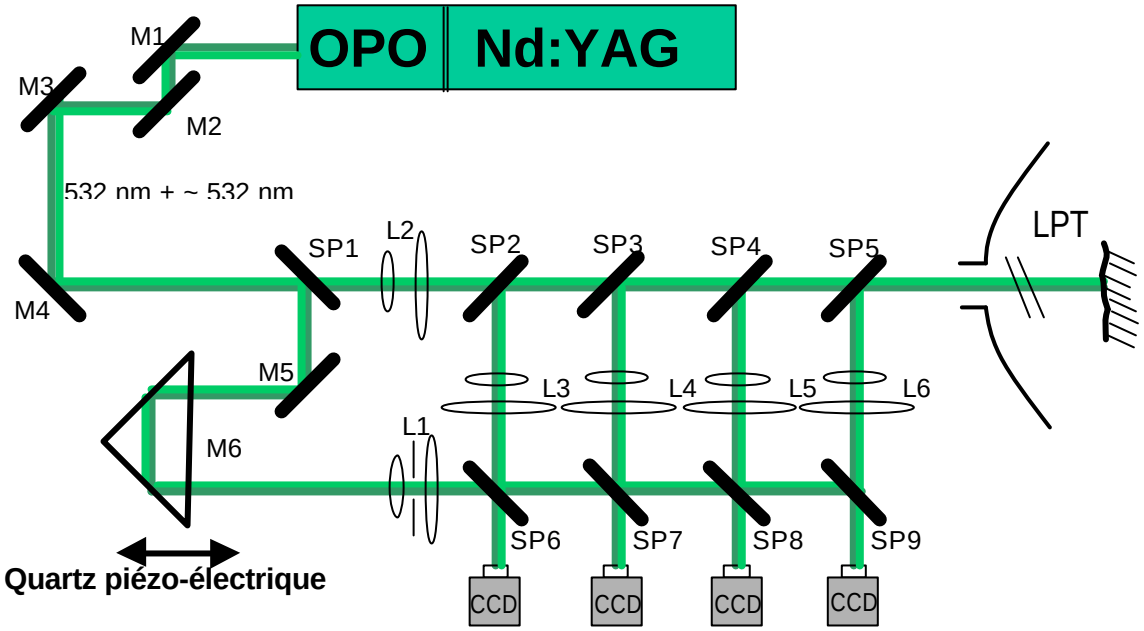

Figure II-30 : Speckle interferometry diagnostic principle on Tore Supra.

The development of this diagnostic, which is of paramount importance for ITER, benefits from a preferential support from EFDA.

II.4.8. Bolometry

For the CIEL-LDC start-up, 5 cameras each with 8 bolometres were re-installed on Tore Supra : 2 on the equatorial port Q2Am, and 3 on the upper port Q4Bh, with one viewing the LPT in the small field mode. The viewing angles and aperture of the cameras were modified to obtain the optimum coverage of the plasma (figure II-31–top left). The acquisition and control command of the diagnostic are now integrated in an autonomous VME unit.

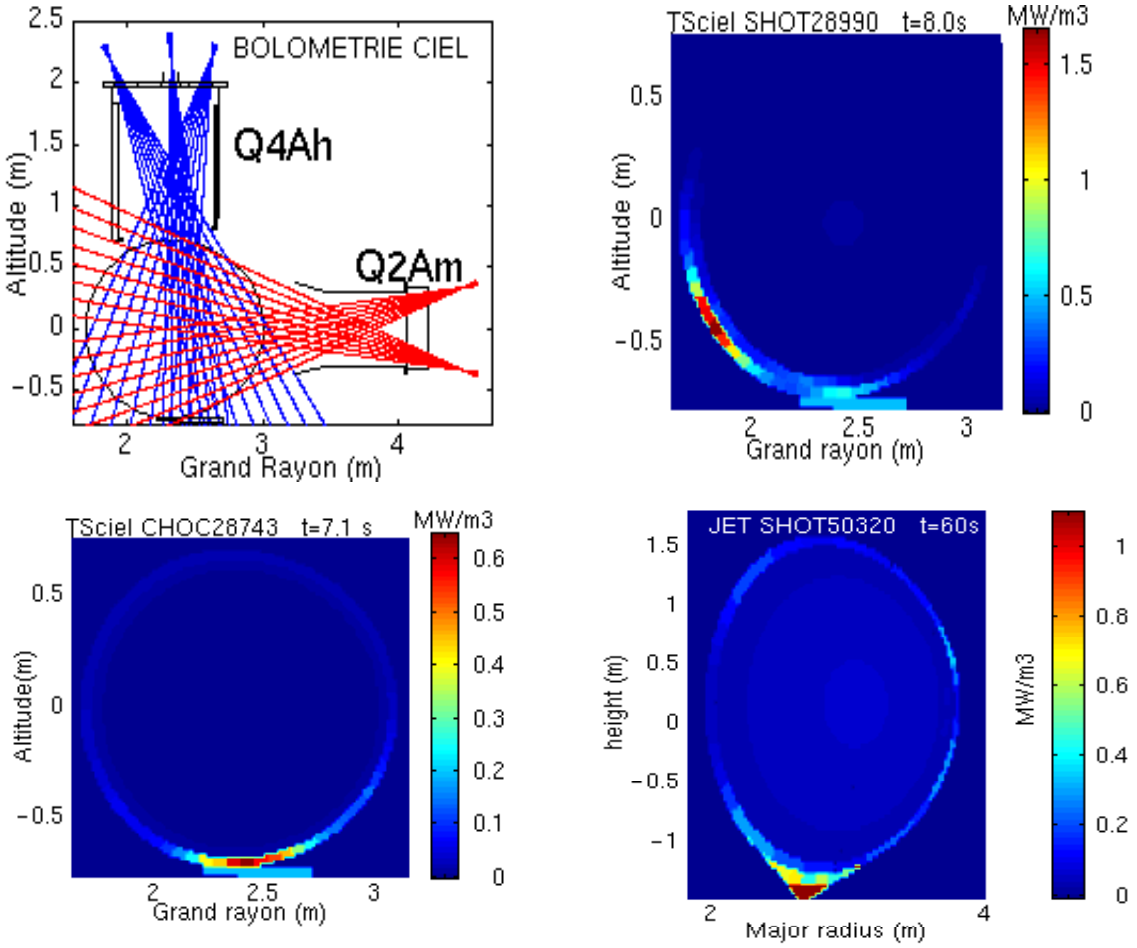

Figure II-31 : Bolometric cameras views (hg) and tomographic reconstructions of Tore Supra (hd and bg) and JET (bd).

The tomography program was changed to allow the treatment of plasma geometries with any ellipticity and triangularity parameters. Particularly, it has been possible, with this program, to reconstruct the emissivity of the main JET plasma (figure II-31-bottom right), showing a high emissivity localised near the X point. Compared to those calculated on JET, the emissivities obtained with this program are inherently positive and show a much greater regularity (entropy). On Tore Supra, even though the horizontal and vertical profiles come from different toroidal sections, but fortunately symmetrical compared to the LDC (upper part of left bow of sections 2 and 4), tomographic reconstructions are possible and provide extremely contrasted images. In particular, it appears that, for attached plasmas, the radiation near the LDC (figure II-31-bottom left) is roughly 4 times more peaked than it was near the PPI. Figure II-31 (bottom left) is characteristic of an attached plasma limited by the LDC, and figure II-38 (top right) is characteristic of a thermal instability of the “MARFE ” type. Figure II-32 shows an example of convergence between the measured and reconstructed profiles.

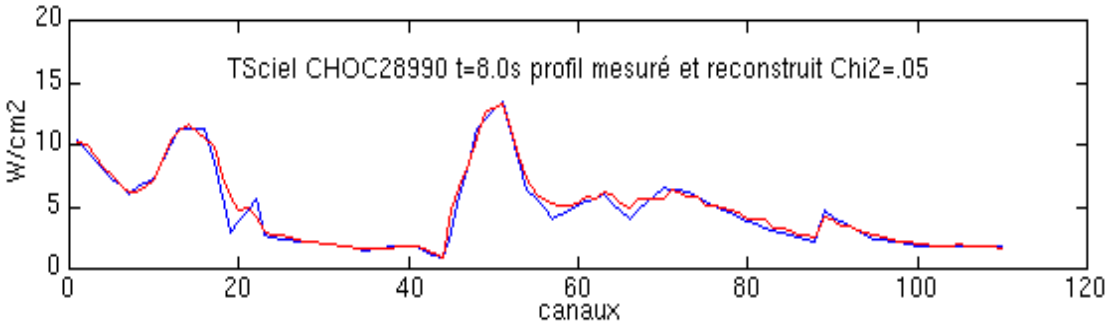

Figure II-32 : Measured (blue) and reconstructed (red) profiles

Because of the toroidal inhomogeneity in the temporary LDC configuration and of the geographic position of the bolometric views, in the close neighbourhood of an LPT section (a high recycling area), the hypothesis of the toroidal symmetry of the radiation is not verified and leads to a significant increase in the estimation of the radiated power obtained from bolometric measurements. The calorimetric analysis of the energy removed from the PEI shows that the bolometric estimation of the radiated power is too large by a factor of 1.3 to 1.4. Consequently, this corrective factor is applied to bolometric measurements. This toroidal symmetry problem should disappear with the complete achievement of the LPT.

II.4.9. Langmuir probes

In CIEL, there will be three types of probes. On the front face of the LPT, there will be 6 sets of 4 pop-up probes. They are made of small graphite pins hidden under the fingers, and periodically inserted in the plasma by the action of an electrical current going through a flexible sheet, on which the probes are placed. This current being perpendicular to the magnetic forces lines, the Lorentz force makes the probes move. These probes will provide the density, temperature and potential of the plasma in contact with the LPT. These measurements are necessary to characterise the particle and energy deposition on the LPT. A first set of pop-up probes was installed on the LDC for the campaign at the end of 2001.

Four sets of 3 standard probes will be installed in the LPT notches. These probes will provide the same physical quantities as the pop-up ones, but in the plasma flowing towards the neutralization plates. These measurements are needed to model the throat pumping characteristics.

Two mobile probe carriers will be installed in the upper ports. They can be equipped with different probe heads: Mach probes to measure the density, temperature, potential and toroidal speed of the plasma ; Gundestrup probes to additionally measure the poloidal speed of the plasma ; delayed field probes to measure the ion speed distribution ; and, in collaboration with the Moscow Physics Institute, sample carrier probes to expose CFC samples to controlled plasma doses. A probe has already been placed on Tore Supra for the 2001 campaign, and regularly provided the radial profiles of the plasma parameters ; it covers a range of 46 cm in 200 ms.

II.4.10. ECE

The superheterodyne radiometer, the wave-guides and the antenna equipped with a window identical to that of the middle port, were installed on a mobile support so as to be movable ; this allows the calibration with a black body from the laboratory, located outside the vacuum chamber, without affecting the operation of the machine. An electronic commutation in mode O/X prevents hysteresis effects from the former technological solution (electro-mechanical millimetric switch). The achievement of identical plasmas with different magnetic fields also allowed the relative accuracy to be improved between the different radiometer channels.

The radio frequency band of the X mode has been extended. It now ranges from 94 to 126 GHz; this allows the center to be aimed at for magnetic fields of 2 T. A study on radial resolution (ECE relativistic

and instrumental) resulted in a proposal to implement 32 channels. The technical specifications for the change over to VME and to 32 channels have been drawn up.

To each angular pulsation ω of the ECE spectrum correspond a non relativistic radial position R_{nr} (ECE resonance cold model), and a position R_{max}, shifted towards the strong magnetic field side, from which the radiation maximum originates (ECE resonance relativistic model). Relativistic numerical simulations show that $T_{rad}(R_{max}) = T_e(R)$, where $T_e(R)$ is the temperature profile and T_{rad} the radiative temperature (figure II-33a). The radial relativistic shift can be defined as the difference $(R_{max} - R_{nr})$. This shift is now included in the data treatment by using an analytical formulation; this is, for example, very useful in the study of internal transport barriers (ITB). This procedure has been validated by numerical simulations (figure II-33b).

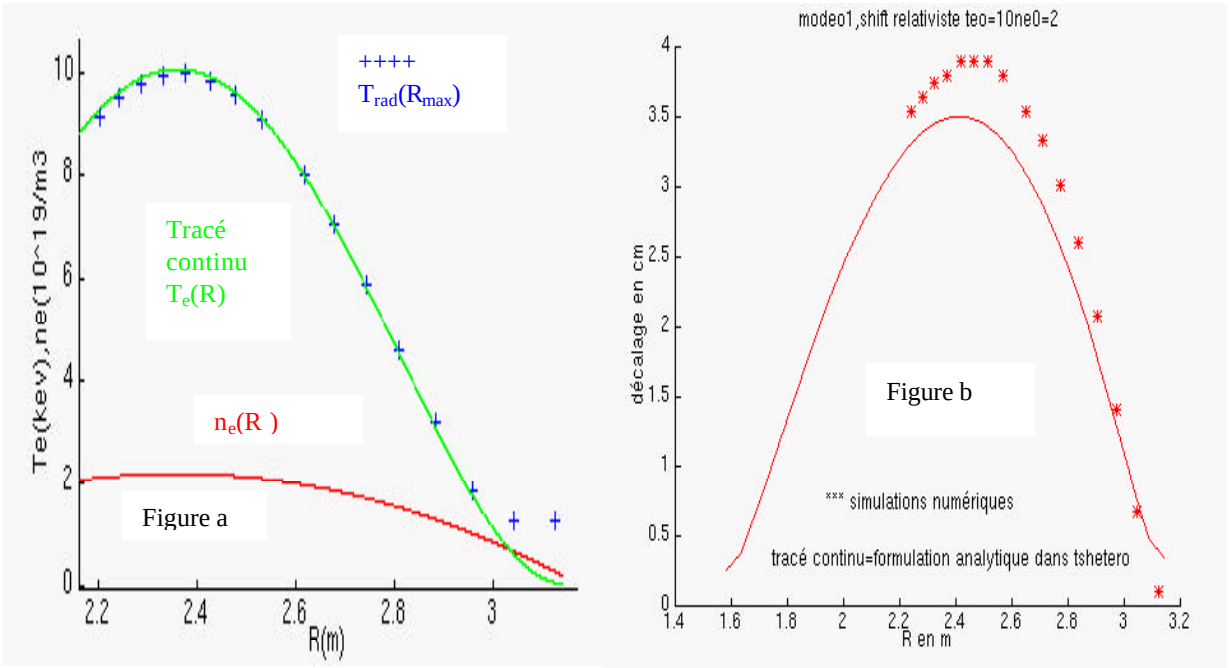

Figure II-33 : (a) numerical simulation of the T_e profile; (b) relativistic radial shift (numerical simulation and analytical formulation)

II.4.11. Thomson scattering

The Thompson scattering diagnostic has been completely changed. The initial system, designed at the beginning of Tore Supra experimentation, included three different sub-sets :

- 12 spectrometers (3 analogical channels each),
- 1 YAG laser,
- a MULTIBUS/CAMAC mixed architecture pilot and acquisition system.

The pilot and acquisition systems were entirely changed to VME, both for the materials and programs. The only remnants of the former configuration are the spectrometers and the YAG laser. New Lecroy 1182 numerisation cards, in VME format, were selected. The command (laser diode, YAG laser, spectrometers) as well as the final acquisition of the diagnostic were successfully implemented and tested prior to the first Tore Supra plasma at the end of 2001.

A programming « by object » was used to make these software parts. This methodology considerably simplified the piloting and acquisition codes while making them more reliable and easier to modify. The measurements made by the diagnostic were extended to the plasma light outside the time window of the YAG laser. The aim is to accurately measure the fluctuations of the raw signals during a plasma discharge. This work allowed us to be operational for the beginning of the 2001 campaign (Figure II-34).

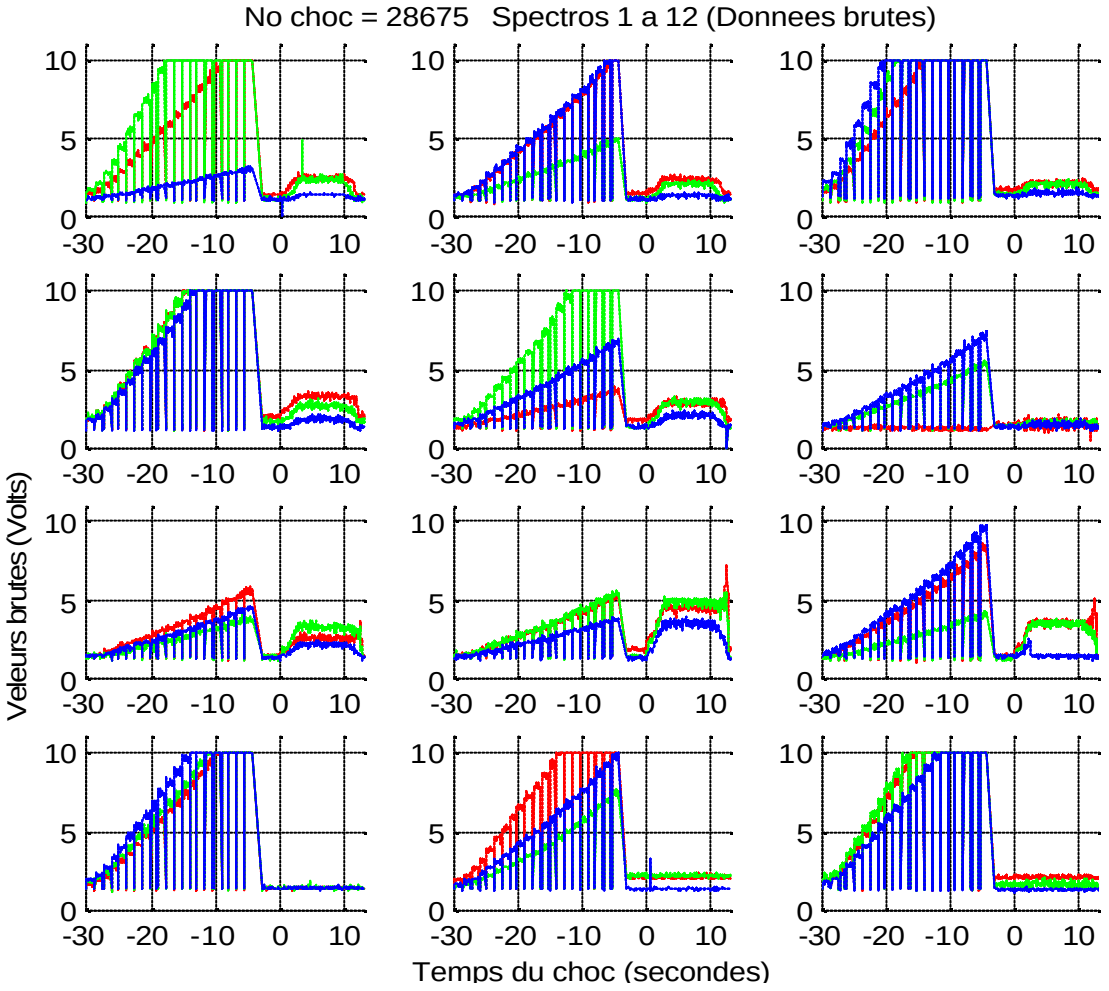

Figure II-34 : Thomson scattering raw data

III. TORE SUPRA – PHYSICS STUDIES

III.1. The Ergodic Divertor

After the last ergodic divertor experimental campaign in 1999, the past two years have been used to synthesise the results obtained with this configuration during the last ten years of experiments.

III.1.1. Configuration aspects

III.1.1.1. Connection lengths in ergodic divertor configuration

The current in the ergodic divertor coils creates a magnetic perturbation, which destroys the flux surfaces close to the wall. Two distinct regions can be identified : the first in contact with the wall elements (laminar zone) in which parallel transport is classic, and a second, degraded confinement, region onwards (the ergodic layer) where radial transport is increased. To characterise the transport in the two regions, a calculation of the magnetic connection lengths must be used (figure III-1). The MASTOC code calculates the transformation of a poloidal mesh, passing in front of a divertor module, following the magnetic force lines. The transformation map thus generated is then used to calculate the magnetic lines trajectories by iteration. The interpolation algorithm on the mesh is based on magnetic flux conservation.

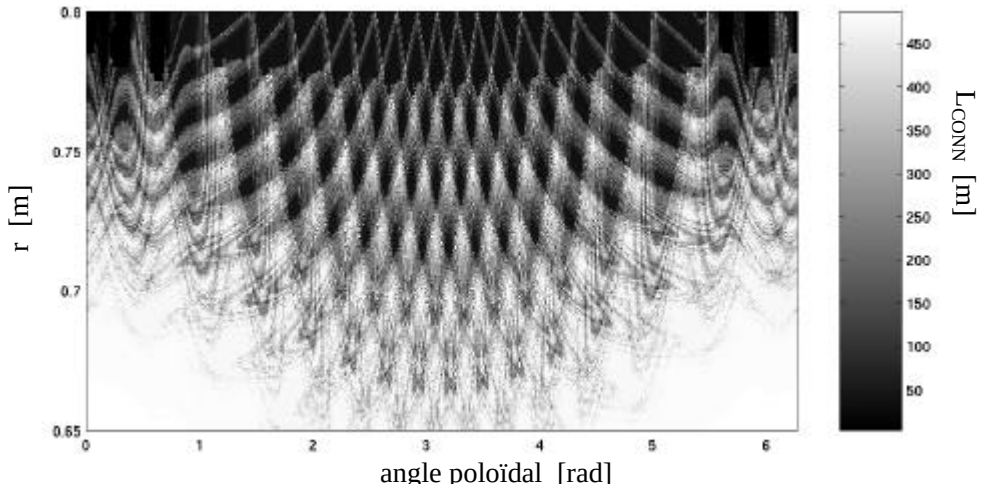

Figure III-1: Connection length in the poloidal plane for a divertor current I_{DE}=40kA. The black zones are connected to the wall elements, in particular to the divertor neutralisers.

III.1.1.2. Plasma flow, consequences on impurity screening

The ability to quickly calculate the magnetic line trajectories with the method described above allows many applications. For example, a Monte Carlo 3D fluid code has been developed to calculate the ion flux in the laminar zone taking into account shading by the divertor modules. This calculation has demonstrated the existence of a fast flow layer, corresponding to the 3D convolution of the divertor pre-sheath, having a radial thickness of 3-4 cm.

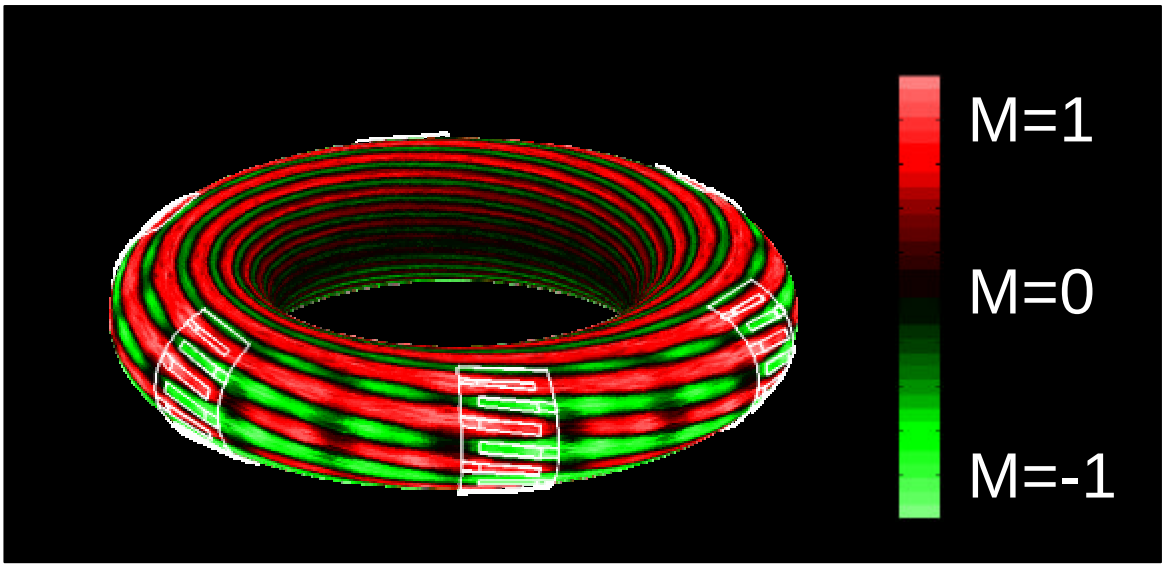

Figure III-2: Simulation of the ion flux flow in terms of Mach numbers in the ergodic divertor configuration

These flows exert a friction force on the impurities coming from the first wall by sweeping them to the divertor, thus protecting the central plasma. A test particle code, calculating the entrainment of ionised impurities in the deuterium flow, does indeed show that the fraction of screened impurities considerably increases if they are ionised in the fast flow region, since the ions are swept to the neutralisers. Figure III-3 presents the impurity fraction which penetrates through the edge plasma with (I_{ED} = 40 kA) and without (I_{ED} = 0 kA) divertor, and the screening improvement versus ionisation length.

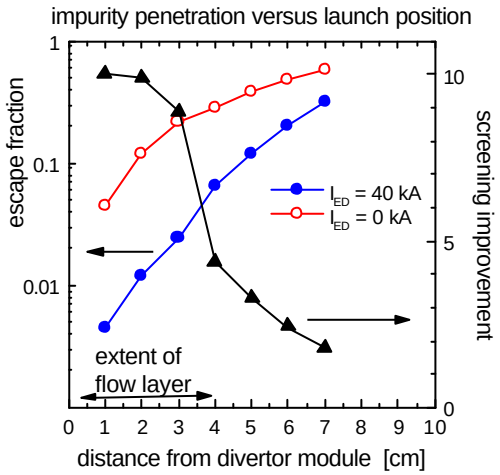

Figure III-3: Penetration probability of impurities with (I_{ED} = 40 kA, full circles) and without (I_{ED} = 0 kA, empty circles) divertor as a function of the distance to the divertor module. The screening improvement, defined as the ratio of penetration probabilities with and without divertor, is also represented (triangles).

III.1.1.3. Plasma flow in front of neutralisers, existence of an inverse flux zone

An extension of the ED-COLL code was developed to give a local image of the flux distribution around a wall element introduced in the edge plasma. Using density and temperature profiles at the surface of the object studied, the code calculates in a coherent way, over a dozen centimetres inside the plasma, the density, ionisation source, potential and electrical field distributions. The Mach number distribution,

in both the parallel and perpendicular directions, mainly depending on the ionisation source distribution and the field line connection length, are also obtained. The considered atomic physics reactions and the isothermal field line hypothesis limit the validity domain of the model to relatively hot edge plasmas (temperatures higher than 10 eV).

The main result of this study is the characterisation of the plasma circulation in front of the ergodic divertor neutralisers. Thus : (a) the poloidal rotation follows the trigonometric direction (the plasma current and the magnetic field being outwards), (b) the parallel speed is alternately positive and negative, the variation in Mach number can reach $\approx \pm 1$ over a distance similar to that separating two successive neutralisers in the poloidal direction and (c) in all the regions with a high poloidal gradient of the parallel flux, a radial speed appears, alternately inwards and outwards, in order to ensure the poloidal flux continuity.

Lastly, the calculations have shown the possibility of having a slightly inverse flux zone above the neutraliser (figure III-4). They show a zone where the field lines are directly connected to the neutraliser, « zone down », and a zone where the field lines are connected further away, « zone up ». As predicted, in the « zone down » the calculated Mach number remains positive (as a rule « positive » means that the speed is directed to the wall) and generally rather high, $M \geq +0.1$. In the « zone up » the connection lengths can be very different, depending on the magnetic configuration considered. In many cases, the Mach number calculated in the « zone up » is low, $|M|<1$. Calculations show that it is possible to obtain an inverse flux above the neutralisation plates as long as the field lines in this area are connected far enough (at least several dozen meters) or the plasma parameters are favourable (high recycling).

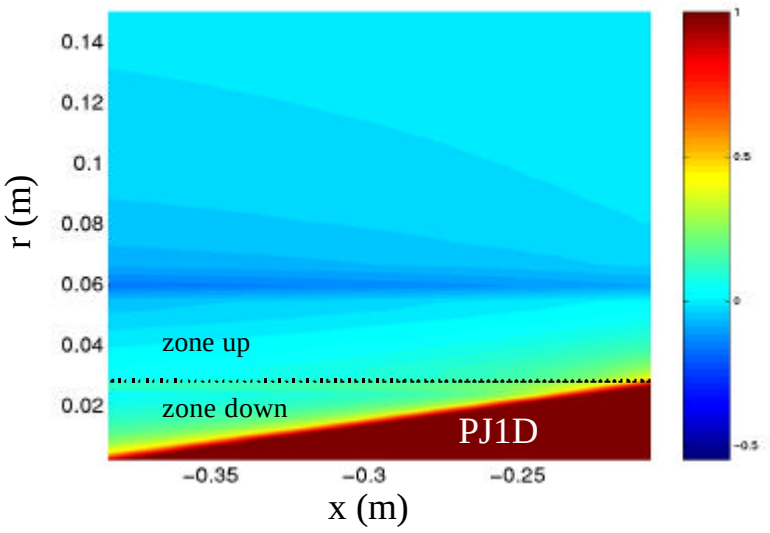

Figure III-4 : Distribution of Mach number above the neutraliser in the case where the field lines in the « zone up » are connected to another neutraliser (x represents the toroidal direction).

III.1.1.4. Intrinsic transport barrier

Tore Supra experimental measurements have shown the existence of transport barriers in the presence of ergodic magnetic fields. MHD stability analyses indicate that the barrier is present in all plasmas with ergodic divertor (DE). This barrier acts near the separatrix, so that it compensates for the low confinement in the ergodic region and maintains the temperature profile inside the plasma : the profile with DE (empty circles) is similar to the profile obtained in limiter configuration (full circles) in figure III-5a, whereas it is flatter in the ergodic region. This implies an increase in the temperature gradient at the separatrix.

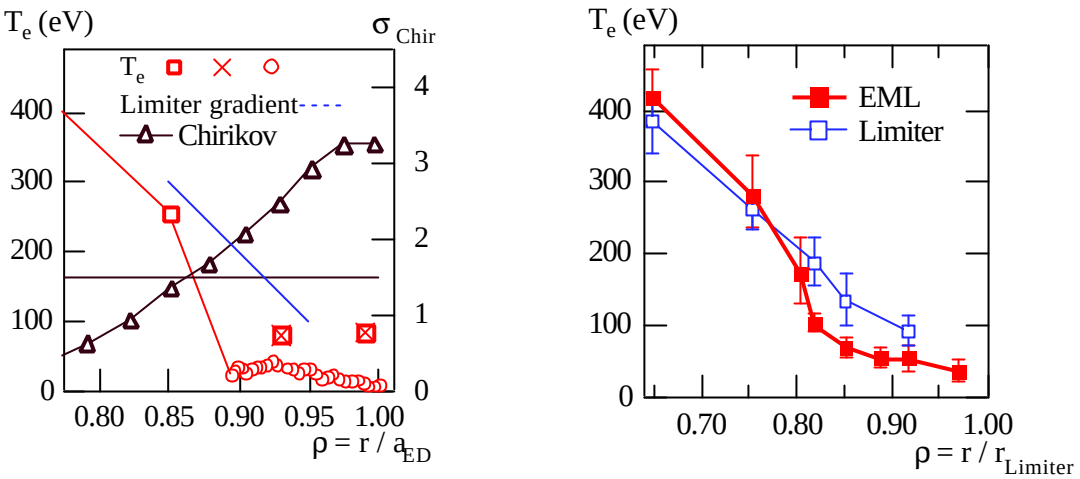

Figure III-5: (a) Tore Supra electron profiles in the presence of ergodic divertor (empty circles) and without divertor (full circles) obtained during two series of shocks with a small change in toroidal field; (b) comparison of calculated (ERGOT code) and measured profiles.

The non-linear ERGOT code was developed for a 3D description of thermal transport in the ergodic magnetic field. The effects of edge impurity radiation can be taken into account in the code. The flattening of the T_e profile is due to the effective radial diffusivity, which appears in the chaotic field lines. Numerical simulations reproduce the experimental data (figure III-5b).

Earlier work showed that Monte Carlo type simulations, taking into account ergodic transport and abnormal transport processes, can reproduce this behaviour. This was confirmed, as shown in figure III-6, and developed : the results of the numerical simulation can be analytically reproduced.

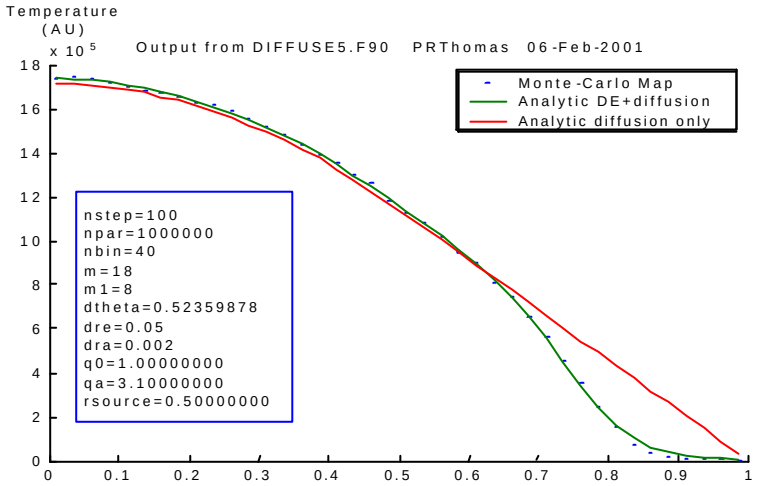

Figure III-6 : Electron temperature profile obtained with Monte Carlo simulation (dots) and analytical calculation (green curve). The red curve shows the analytical result for the case without ergodic divertor.

III.1.1.5. Axisymmetrical divertor and ergodic divertor : comparison

The 10 years Tore Supra experimentation with the ergodic divertor (DE) being over, an evaluation of this program is underway. A ceremony marking the end of the DE program was organised on 15 December 2000 in the presence of R. Aymar and A. Samain. A retrospective of the results obtained was presented, as well as a comparison between the DE and axisymmetrical divertors (DA).

It is essential to note that, concerning the plasma in the area of the divertor, the ergodic and axisymmetrical divertors have a very similar behaviour. Both configurations have shown to be

compatible with high recycling and detachment regimes, where the plasma temperature is reduced and the neutral density is high in front of the neutraliser. These plasma states allow both systems to meet some of the fundamental requirements of divertors : reduction of the power density on the neutralisers to an acceptable level, decrease of the plasma temperature to a value low enough to eliminate physical sputtering, and efficient pumping.

The most significant differences between the DE and DA are in the existence of an H-mode for the latter and the presence of a plasma screen against impurities for the former. If it were not for the negative secondary effects, the H-mode would give the DA an advantage compared to all the devices in charge of managing plasma-wall interaction. This is the main reason why it was chosen for ITER. However, the H-mode brings with it the ELMs (edge plasma instabilities which make the design of neutralisers difficult and sometimes impossible) and a narrow SOL (which offers less impurity screening). On the other hand, the edge zone in the DE configuration forms a cold plasma blanket which protects both the central plasma from the impurity sources and the first wall from energetic neutrals. If it could be demonstrated that the DE is compatible with an improved confinement mode, the advantage of the DA would be eliminated. However, one could think that the additional technical complexity of the DE would favour the DA. Work is ongoing to see if this is a real advantage or not.

In summary, both concepts have some advantages, and it is clear that neither is completely satisfactory. For this reason, the approach taken is that of a clever combination of both configurations in order to use all their respective advantages, particularly in controlling ELMs : this is now being studied. (see III.1.4)

III.1.2. Particle flux control

III.1.2.1. Control of gas injection on plasma edge electron temperature

The determination of the density threshold beyond which plasma detachment occurs and leads to a disruption is a very difficult parameter to measure. The limit temperatures before detachment, measured at the plasma edge with Langmuir probes, are however quasi independent from plasma scenarios. When studying the control of highly radiating plasma in the presence of the ergodic divertor, gas injection feedback control mechanisms were developed and used with the real time measurements produced by these probes. When the plasma reaches detachment, the filling efficiency increases drastically and the control loop becomes unstable. A detachment criterion was determined to allow the gas injection to be managed in real time and to keep the plasma at the threshold of high-density detachment and high radiated power.

These techniques have been used on Tore Supra in studies of density regimes with the DE, of power coupling (ICRH) at high density and of experiments with high radiated power induced by impurity injection.

III.1.2.2. Deuterium recycling

A spectroscopic study of the Dα (6561 Å) emission spectral line has been conducted to further the knowledge on the interaction processes between deuterium and the wall. This was done in different experimental conditions to better understand the physical phenomena influencing Dα (electron temperature and density, status of the wall…). A nearby spectral line coming from ionised helium was firstly showed not to contribute to the signal. The spectral analysis was made taking into account the degeneration suppression of the atomic levels due to the Zeeman effect, the Doppler width and the incidence angle between the lines of sight and the magnetic field. This analysis shows that at least two different temperature populations (cold at T~1,4-2,5 eV and hot at T~5-30 eV) coexist near the neutraliser. This study was extended to measure the atomic and molecular deuterium densities (AMDM method). In order to achieve this, a collisional-radiative model was used taking into account the most significant molecular reactions and the «cold » and «hot » Dα brightness measurements. The results show the significant contribution of molecules (n_{D2} ~ 0.5 n_D), irrespective of the edge parameters. The results were then compared to the numerical simulations of the multi-1D ED-COLL and 3D Monte-Carlo BBQ codes, the edge parameters (n_e, T_e) being constrained by the measurements of a Langmuir probe located on the surface of the neutraliser. The comparison (figure III-7) shows a good agreement in view of the approximations characterising these different determinations.

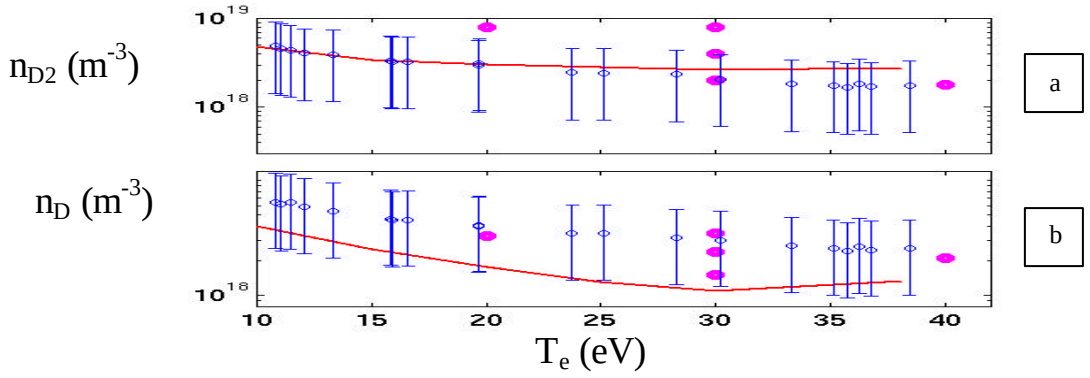

Figure III-7 : Dependence on edge temperature of atomic (a) and molecular (b) deuterium densities. AMDM method with (n_e, T_e) measured by a Langmuir probe located at the surface of the neutraliser (empty circles); ED-COLL simulation (continuous line); BBQ simulation (full circles)

III.1.2.3. Screening efficiency, impurity control

A new analysis of particle screening confirmed that the penetration of impurity or deuterium ions in the plasma centre was controlled by the parameter Δ/λ_i, where Δ represents the effective length of the ergodic zone, and λ_i the ionisation length of neutrals : the contamination of the central plasma is lower when the ionisation length of the neutrals is shorter than the ergodic zone width. For both the impurities and deuterium, a screening factor can be measured, $f = (N_{pl}/\tau)/\Phi$, where N_{pl} is the number of particles in the plasma, τ their lifetime, and Φ the edge incident flux. Figure III-8 represents this screening factor measured for deuterium, carbon and oxygen, as a function of Δ/λ_i. Moreover, nitrogen injection experiments in which the position of the impurity source varied, showed that the effective width Δ is an average value in the complex 3D structure of the ergodic zone. Indeed, to obtain a given contamination of the central plasma, a nitrogen injection three times greater is required when the injection valve is located in the ergodic divertor neutralisers.

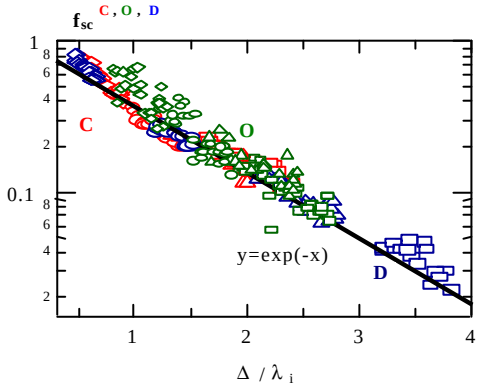

Figure III-8: Screening factor determined experimentally as a function of the control parameter Δ_{erg}^{eff}/l_i for deuterium, carbon and oxygen. The ionisation length of the neutrals is calculated using the electron densities and temperatures on the neutralisers. A hypothesis is made on the energy of the neutral particles : $0.1\times T_e^{div}$ for deuterium, $0.5\times T_e^{div}$ for carbon and $0.05\times T_e^{div}$ for oxygen.

III.1.2.4. Carbon production and propagation.

A tool was developed to study the production and propagation of carbon impurities near the neutraliser. It is based on the coupling of the BBQ (carbon propagation) and ED-COLL (deuterium recycling) codes, the self-coherence of the base plasma being ensured by the calculation of the Mach number distribution, in the approximation of an isothermal laminar pre-sheet. It has been used to characterise the predominant processes in the production of carbon and plasma contamination in different edge regimes.

Concerning the production of carbon impurities, it appears that if the chemical erosion process is dominant at low electronic temperatures, the hydrocarbon molecules, which come from it, have an average free length which is much too short to significantly move them away from the neutraliser. Their re-deposition rate is therefore near 1. At higher temperatures, the main contributions come from physical sputtering ($D^+ \rightarrow C$) and self-sputtering ($C^{n+} \rightarrow C$), this latter process taking on more importance as the plasma temperature increases (figure III-9).

The propagation of carbon ions is greatly influenced by the base plasma flux, because of the parallel electric field and of the D^+/C^{n+} friction. In the region where the field lines are directly connected to the neutraliser, the plasma flux is directed towards the neutralisation plate, with a parallel Mach number close to 1 (see figure III-4). The carbon ions are then quickly pushed to the wall. Inversely, in the region where the field lines are not connected, the parallel Mach number is nearly nil. The ions can then freely propagate along the field lines and possibly contaminate the central plasma.

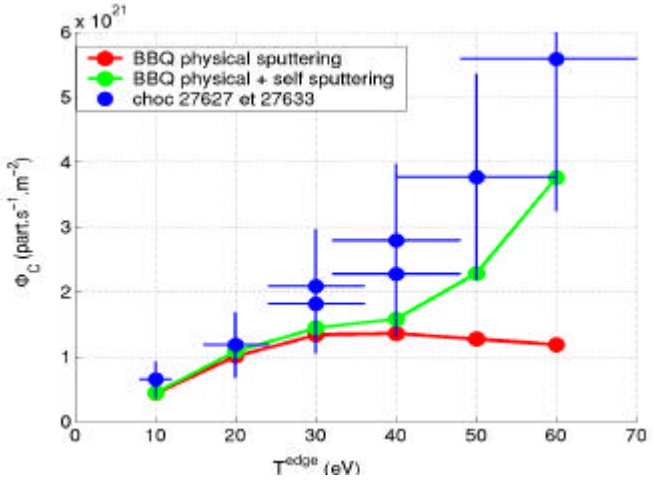

Figure III-9: Carbon flux extracted from a neutralisation plate. The blue points are the measurements, the two lines the results of BBQ simulations without (red curve) and with (green curve) self-sputtering

III.1.2.5. Neutral carbon temperature

A preliminary study was conducted on two series of neutral carbon spectra to evaluate a possible characterisation of the atomic temperature at the plasma edge, using visible spectra observed parallel to one neutraliser. The study was made by using a spectral line profile code, which takes into account the Doppler effect, the fine structure and the Zeeman effect, by using a non-perturbing exact method. It is to be noted that all the radiative transitions must be calculated at the same time so that the intensity ratios between doublets be correct.

The two discharges analysed for this preliminary study involved increasing density ramps (and thus a decreasing electron temperature). In both cases, the magnetic filed deduced from the spectra shows that the emission did really occur in the immediate vicinity of the neutraliser. The neutral carbon temperature is estimated to be at 12 eV in one case, at 5.2 eV in the other (higher density ramp, lower electron temperature than in the first case). In both cases the neutral carbon temperature is constant during the discharge, although the electron temperature decreases ; the atom temperature is always lower than the electron temperature.

The coherence of the theoretical results gives hope as to continuing the study on carbon ions to determine an ion temperature from spectra of the different ions further away from the neutraliser.

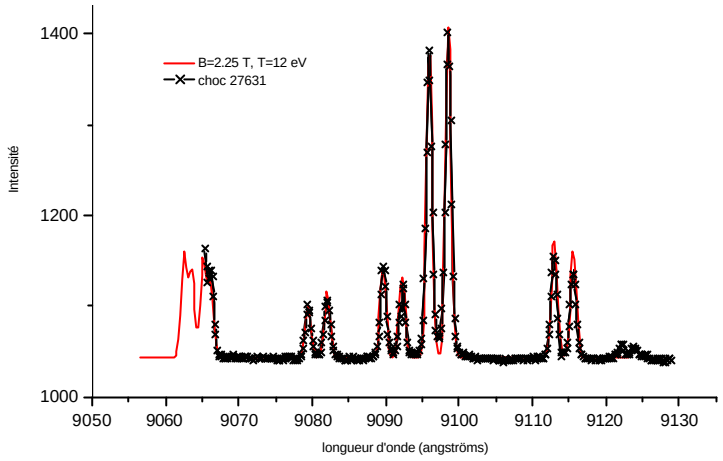

Figure III-10: Comparison of simulated (red line) and experimental (cross) spectra, used to deduce the magnetic field at the emission region and the temperature of the emitting species.

III.1.2.6. Structure of oxygen and neon peripheral spectral line radial profiles

The radial emission profiles of the peripheral spectral lines of the impurities measured with the DDUO (duochromator) diagnostic show a composed structure when the middle limiter is placed in front of the ergodic divertor. In addition to the peripheral expected peak (due to the emission of the peripheral layer of ions), a central peak, interpreted as being due to the local interaction of the plasma with this limiter, is observed. These profiles were simulated by combining the BBQ code for the central asymmetrical part and the MIST code for the peripheral symmetrical part (figure III-11). The decay time of these two peaks gives a view of the transport in the transition area between the ergodic zone and the confined plasma.

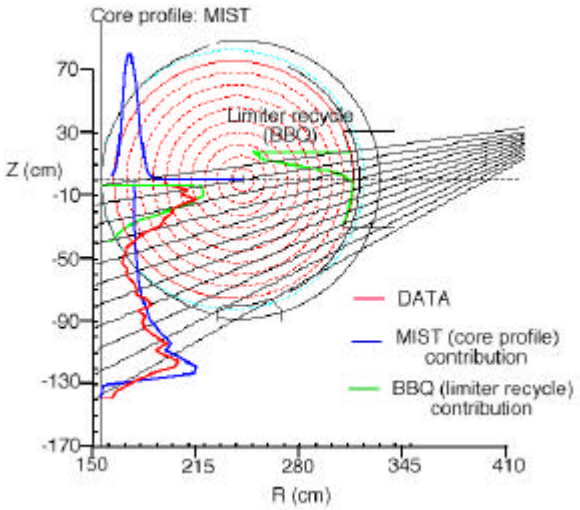

Figure III-11: Modelling principle, showing the duochromator diagnosis lines of sight, the experimental data (in red) and the profile simulated by the MIST code for the central part (in blue) and BBQ for the peripheral part (in green)

Other modulations, whose number varies with the safety factor value, are observed when the distance between the inner wall and the plasma last closed magnetic surface is less than 6 cm. Since they are also seen on the emission of $\Delta n=0$ transitions (excitation rate independent from T_e in the range concerned), they cannot be due to the temperature modulations characteristic of the ergodic zone. Another explanation must therefore be found. A good possibility is charge exchange with neutral deuterium, whose entering flux is modulated by the effect of the ergodic divertor on the electron temperature profile. The modulations can be qualitatively simulated by using the BBQ impurity

transport code. Figure III-12 shows the simulated profiles for three densities of neutral deuterium. For N_{D0}=0, there is no charge exchange effect and the simulations do not reflect the modulations experimentally observed. For N_{D0}?0, charge exchange intervenes, the modulations appear and are qualitatively comparable to the measurements.

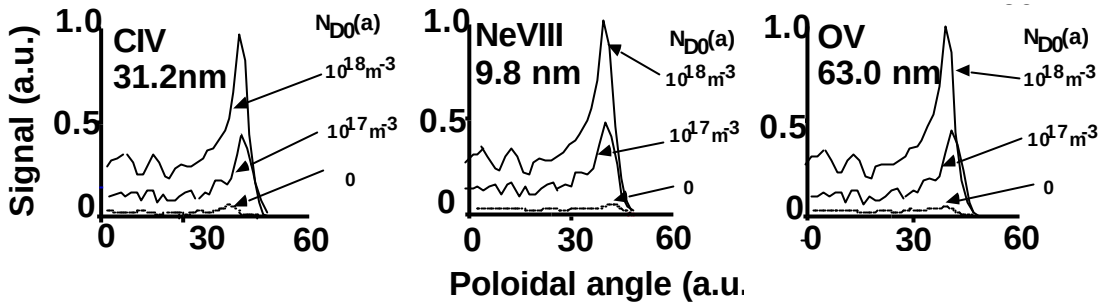

Figure III-12: Simulation of poloidal profiles of carbon, neon, and oxygen spectral lines for three values of the neutral deuterium densities.

III.1.2.7. Carbon and neon screening

A study on the screening of carbon and neon impurities by the DE was conducted using edge radiation (in situ optical fibres in front of a neutraliser) and central radiation (SIR and Z_{eff} diagnostics). These brightness profiles in front of the neutraliser have been interpreted in terms of impurity penetration, and are qualitatively in agreement with the results of the simulations made using a relatively simple 2D code and the 3D Monte Carlo code. This data, as well as that on confined plasma, allow the evolution to be found, as a function of the electron temperature on the neutraliser T_e^{edge}, of C and Ne densities at the edge and in the centre of the plasma (figure III-13). For carbon, a decrease in the central density is observed at high density and low temperature T_e^{edge}, which is coherent with the fact that the edge flux and the penetration probability decrease in these plasma conditions. However, the central neon density is constant whatever the density regime ; the behaviour of Ne in the core is thus de-coupled from that of the edge. This difference in behaviour can be explained by the complex production mode of carbon and a deeper penetration for neon than carbon.

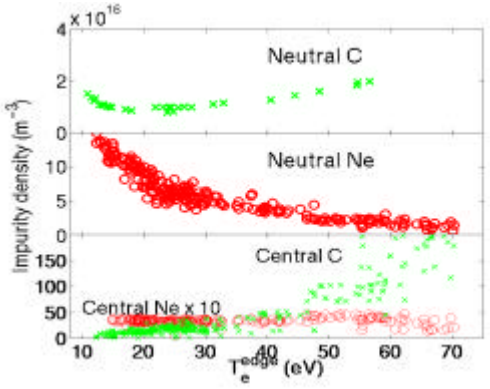

Figure III-13 : Peripheral densities of C (top) and Ne (centre) and corresponding central densities (bottom) versus electron temperature on neutraliser.

III.1.2.8. Carbon and neon transport

Besides the ion temperature profiles and the plasma rotation speed, an important outcome of measurements with an energetic neutral particle beam is the impurity profiles and their transport coefficients.

The modulated neutral beam source allowed the carbon and neon profiles to be measured simultaneously during discharges with neon injection. The spectral lines produced by charge exchange between the beam neutrals and the impurities (CXS) are visible on three spectrometers : a) XUV spectrometer, b) high resolution visible spectrometer and c) low resolution filter spectrometer. This helped to determine the C/O/Ne density ratio in the centre of the discharge, as well as the profiles of completely ionised carbon and neon (figure III-14). By using the effective plasma charge (Z_{eff}), the radiated power (bolometry) as well as the electron density and temperature profiles, the transport coefficients can be obtained with a 1D code which simulates the profiles of C^{6+} and Ne^{10+}. Contrary to the discharges without DE, the diffusion coefficient increases by a factor of 5 at the plasma edge, in the ergodic zone where radial transport is greatly increased.

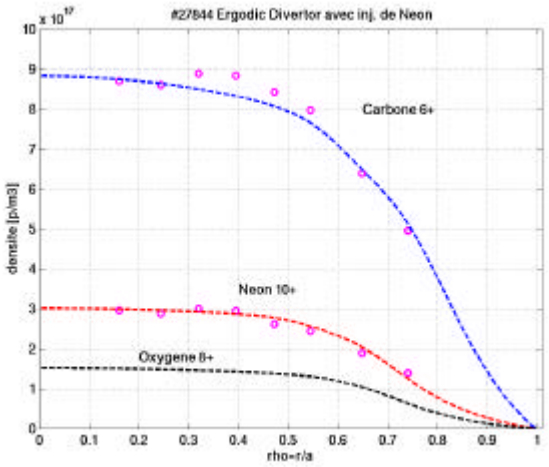

Figure III-14 : Impurity profiles measured by CXS for a discharge with neon injection

III.1.3. Heat flux control

The characterisation of the heat flux control capability with the ergodic divertor has essentially focused on the effects of plasma density, type of gas injected (helium or deuterium), the presence of impurities and the injected power into the plasma. The first results of these experiments clearly show the low heat flux values falling on the neutralisers compared to «limiter » mode plasmas (a factor of 5, typically, at low density). The parallel thermal flux ($Q_{//} \alpha \gamma n_e T_e^{3/2}$) on the neutralisers decreases when the plasma density increases, as a consequence of an increase in the radiated power associated to a very significant drop in electron temperature in the edge plasma.

Moreover, the effect of a large power leads to a uniform energy deposition on the neutralisers. Powers of 8-9 MW were injected in the plasma, resulting in values of $Q_{//}$ of about 20 MWm^{-2}, very much below the heat flux deposition limits (~100 MWm^{-2} in terms of $Q_{//}$, which is reduced on the wall by an angle of incidence as grazing as possible). Figure III-15 shows the evolution of $Q_{//}$ versus the total injected power. An extrapolation based on the results obtained suggests, by taking into account the limitation of the critical fluxes on the neutralisers and by assuming a reasonable radiated power fraction (60%), a maximum power injection of 50 MW in Tore Supra, i.e., a power density of 2MW per m^3 of plasma.

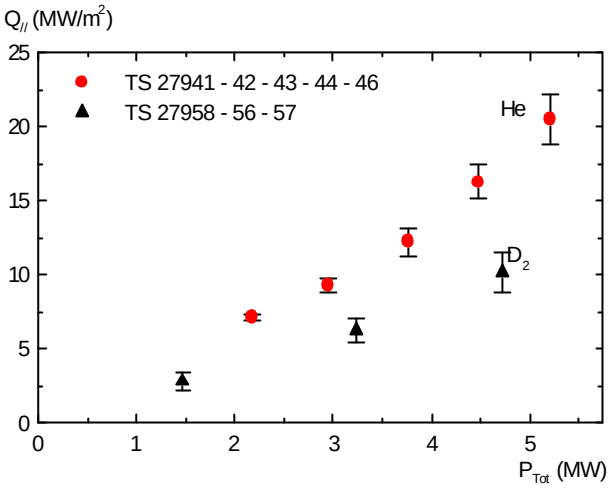

Figure III-15: Average thermal flux along the field lines as a function of total power for a series of plasmas with helium and deuterium (average values calculated during the power plateau)

The correlation between the fluxes given by infrared thermography and the Langmuir probe measurements permitted to study the experimental values of the heat transmission factor in the sheath, γ. For deuterium and helium discharges in ohmic regime, $\gamma \sim 7$ increasing with the injected power, probably indicating an increase of the ion temperature. Figure III-16 shows the evolution of the transmission factor as a function of total injected power.

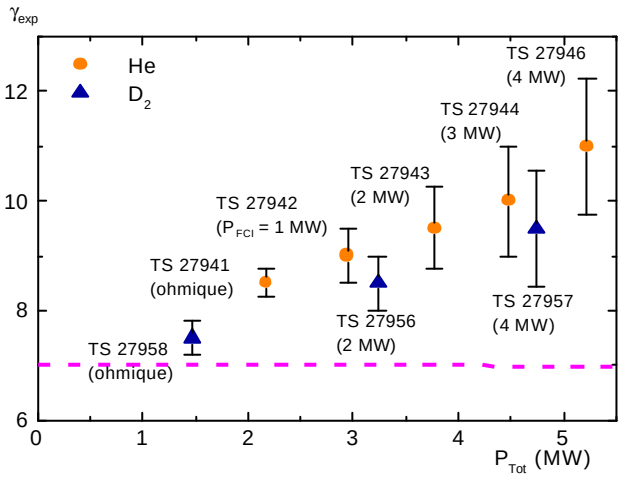

Figure III-16 : Experimental evolution of the transmission factor through the sheath, γ , as a function of total power for He and D_2 plasmas.

These experiments have also allowed the study of « detached regimes », when $Q_{//}$ becomes very low and the power from the plasma is dissipated in its periphery as radiation. A detachment criterion (DoD) based on the variation of $Q_{//}$ on the neutralisers derived from the infrared (IR) signals was developed. A very good correlation with the DoD from the Langmuir probes is obtained. The IR DoD, however, prevents the difficulties lined to the choice of the zone. Figure III-17 represents the evolution of the DoD IR as a function of the electron temperature. At the beginning of the detachment, the decrease of $Q_{//}$ is clear and occurs for a threshold value of $Q_{//}$, $Q_{//threshold}$. This value increases with the injected power, but detachment always occurs for an electron temperature of about 10-12 eV, independently of the experimental conditions. The knowledge of $Q_{//threshold}$ and/or electron temperature is used to qualify the detachment, allowing to feedback control the main plasma parameters (gas injection, power) in order to keep the latter in a stationary state.

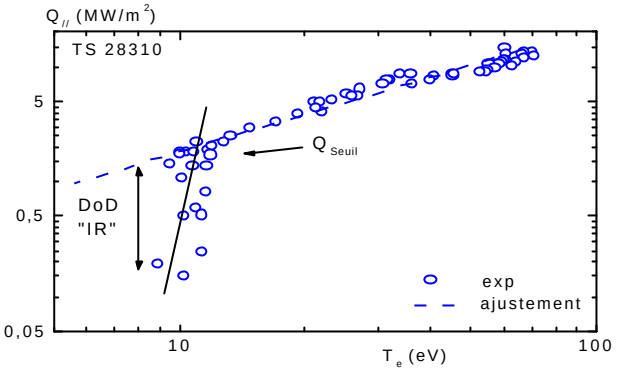

Figure III-17 : Evolution of parallel thermal flux as a function of edge electron temperature for a plasma which detaches itself. The infrared measurement is made along a neutraliser.

The flexibility of the infrared thermography diagnostic results in an optimal choice of the zone exposed to the flux and a space and time analysis on the local detachment to be made, over a surface which corresponds respectively to about 5 mm^2 and/or 50 cm^2. It can be directly applied to Tore Supra for the CIEL project, but also to JET and of course ITER.

III.1.3.1. Radiation efficiency

Different impurity mixtures (C, O, Cl, N, Ne, Ar) were tested for their ability to reduce the heat flux on the neutralisation plates, without however excessively diluting the central plasma (in ITER, the effective plasma charge, Z_{eff}, must be lower than 1.6). For a given mixture, the electron density and temperature in the divertor volume control the radiation efficiency (ratio of total radiated power, P_{rad}, to the dilution generated by impurities (Z_{eff}-1)). Figure III-18 shows the radiation efficiency of the mixture of intrinsic impurities C/O/Cl, as a function of T_e^{div}, for two values of n_e^{div} corresponding to different injected powers (greater injected power for higher n_e^{div}). For T_e^{div} >15 eV, carbon is the dominant impurity. The radiation efficiency increases with the power injected because of the reduced penetration of the carbon neutrals and of the higher radiation due to the high density n_e^{div}. For T_e^{div} <15 eV, carbon production is very low, the oxygen contribution, and sometimes chlorine, becomes significant and considerably complicates the analysis on radiation efficiency.

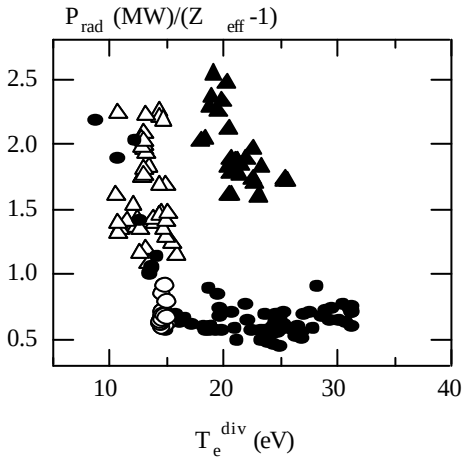

Figure III-18 : Radiation efficiency as a function of electron temperature on neutralisation plates. Circles: $n_e^{div} = 0.5\times10^{19}\,m^{-3}$. *Triangles:* $n_e^{div} = 1.5\times10^{19}\,m^{-3}$. *Open symbols (full) : C/O/Cl (C/O) mixture.*

The impurity injection experiments show that nitrogen is the most adapted species to reduce the heat flux on the neutralisation plates (Figure III-19) : as the intrinsic C/O mixture, nitrogen only produces a small contamination of the central plasma for a strong reduction of the parallel heat flux ($Q_{//}^{min}$ =2.5 MW/m^2), and has the additional advantage of being controllable (since it is purposely injected). The low dilution observed in the case of nitrogen (Z_{eff} - 1 ≅ 1.5) can be explained by the fact that the N neutrals ionise and radiate in the ergodic zone. In the case of neon, on the contrary, the neutrals are ionised in the confined plasma, therefore contaminating the core. For argon, neutrals ionise in the ergodic zone, but the Ar ions producing the radiation have greater charges and are found in the confined plasma : in these conditions, a high radiation necessarily goes along with a high dilution, which is observed in figure III-19.

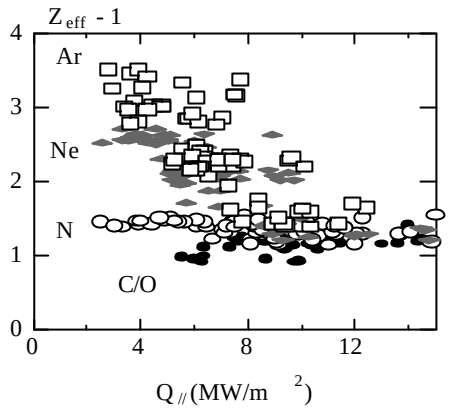

Figure III-19 : Central plasma dilution as a function of parallel heat flux on the neutralisers. P_{tot} = 5MW. Full circles : intrinsic C/O mixture. Open circles : nitrogen injection. Diamonds : neon injection. Squares : argon injection

III.1.3.2. Radiation analysis

The radiated power for each element can be calculated by using the atomic coefficients of the ADAS database. By using the impurity profiles determined by CXS (see III.1.2), we find, for the discharge analysed, whose total radiation is 1.17 MW : Prad-C/Prad-O/Prad-Ne = 0.5/0.18/0.49 (MW). Figure III-20 clearly shows that the neon radiation comes from a large volume at the plasma edge whereas the radiation of light intrinsic impurities, C and O, is limited to the edge.

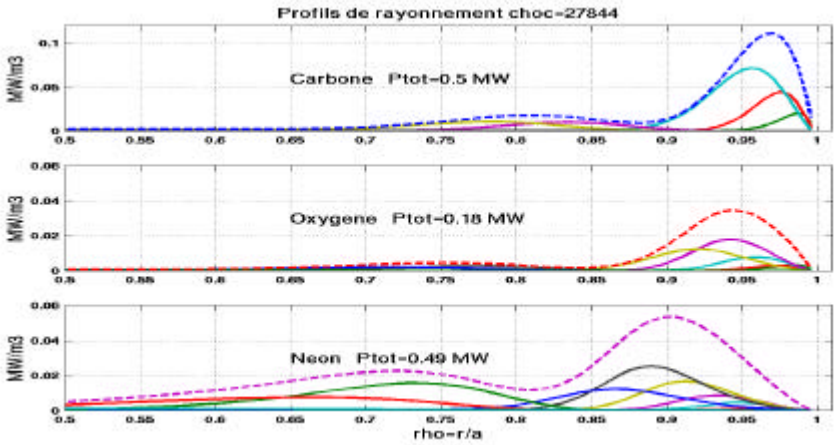

Figure III-20 : Calculation of the radiated power as a function of plasma radius. Neon, whose concentration is 1/3 the carbon concentration, efficiently radiates in a large volume in the plasma edge and therefore decreases the convective heat flux on the neutralisers.

Moreover, a characterisation study on the ion species participating in the radiation was carried out using the analysis on the bolometry and UV spectroscopy measurement coherence. The time evolution of the radiated power measured by bolometry was correctly reproduced by a linear combination of the brightnesses of the spectral lines from a small number of ions, OV, CIV, and CIII. This analysis was done over several series of discharges, which had been made for the study of density regimes. It shows that, when the electron temperature on the neutralisers decrease from 60 eV to ≅ 10 eV, the oxygen contribution to the total radiation increases : it typically goes from 10 to 40%, the rest being due to the carbon in the discharges analysed. At the same time, when the temperature on the neutralisers decreases, the carbon radiation distribution between CIII and CIV ions significantly changes to the benefit of CIII ions.

III.1.4. Extrapolation of ergodic divertor to a future machine

The reference scenario for ITER is based on an H mode with type I ELMs (Edge Localised Modes), instabilities which regularly expel from the edge plasma significant heat and particles fluxes. These phenomena limit the lifetime of the internal plasma facing components. Therefore, the aim is to control and reduce these ELM effects. Preliminary experimental results on the JFT2-M and COMPASS machines have shown that an ergodisation of the edge plasma allows the energetic content of the ELMs to be reduced without excessively perturbing the confinement. The principle is to affect the perpendicular transport in an optimal way so as to prevent, in particular, the stiffening of the pressure profile leading to type 1 ELMs. In a magnetic configuration with an X point, of the axisymmetrical divertor type, there is, near the separatrix, a region with a high shear of the safety factor, which makes ergodisation easy. There thus is a synergetic effect in the AD/ED coupling.

Preliminary studies on the magnetic configuration with a DA/DE coupling for ITER have been carried out. Ergodic divertor coils rather similar to those of Tore Supra (six toroidal modules, seven poloidal bars), with a current of 100 kA, allow the ergodisation of :

~ 10 cm inside the separatrix, if the coils are located behind the shielding.
~ 2 cm inside the separatrix, for coils behind the vacuum chamber (figure III-21).

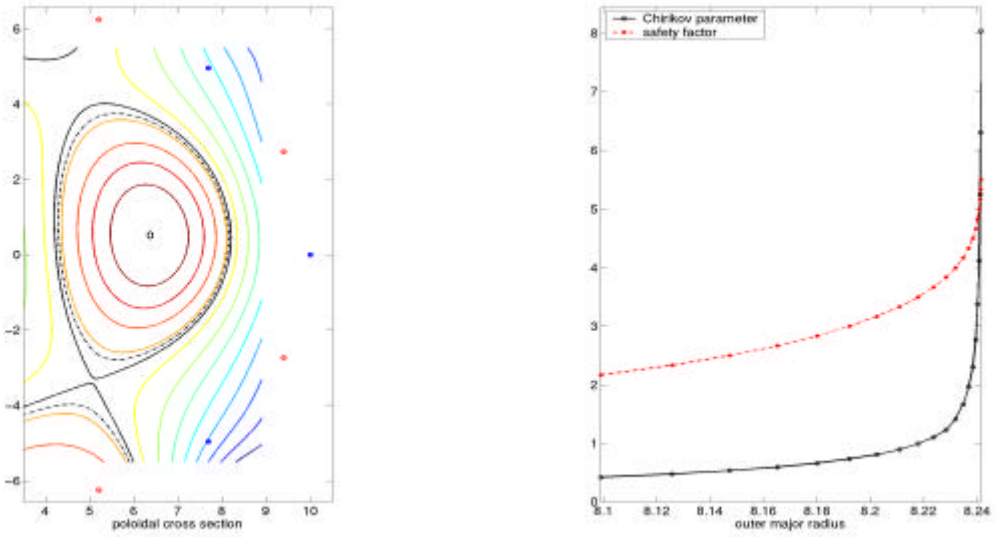

Figure III-21 : Ergodic divertor/axisymmetrical divertor coupling for ITER with coils outside the vacuum chamber (ergodic divertor current 100 kA). On the left, magnetic surfaces in a poloidal cross section view ; on the right, Chirikov parameter, characterising the magnetic configuration, and safety factor. The perturbed zone (Chirikov parameter higher than 1) extends over 2 cm at the plasma edge.

In a first approximation, the AD/ED coupling on ITER therefore appears to be feasible and interesting form a physical point of view. The technical implementation will however be difficult.

In order to validate the concept on an existing machine, the implementation of an ergodic divertor was studied for JET and DIII-D. In both cases, for a current in the ED coil of ~100 kA, a region of about 10 cm can be ergodised. For JET, the coils would be located inside the vacuum chamber (which makes their installation difficult), and outside for the DIII-D. A design study is underway for ASDEX Upgrade.

III.2. Edge plasma physics

III.2.1. Polarisation experiments

III.2.1.1. LPT polarisation

The LPT was designed to be polarised with a voltage of ±1 kV with respect to the internal chamber. The resulting electric field at the edge of the plasma should allow the plasma flow to be changed along the field lines and the particle pumping to be improved and thus the density controlled. The experiments conducted on the TEXTOR tokamak (Juelich - Germany), whose ALT II limiter geometry is very similar to that of the LPT and is equipped with a polarisation system, enabled us to validate the model developed in order to estimate the effects of an electric field in the edge plasma.

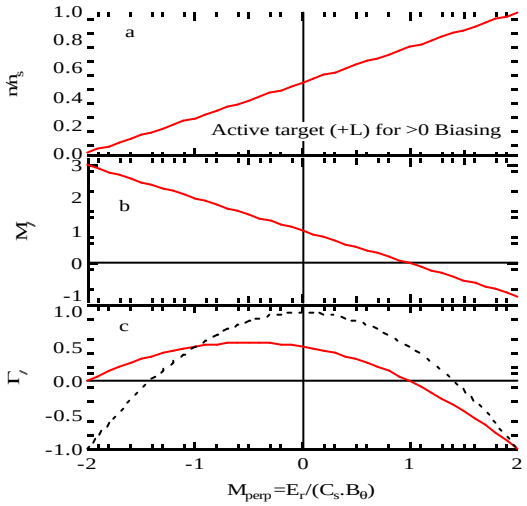

Figure III-22: Evolution of plasma density, parallel Mach number, $M_{//}$, and parallel particle flux, $G_{//}$, on the neutralisation plate as functions of the perpendicular Mach number, $M_\wedge$, characteristic of the applied electric field. The dotted line corresponds to the flux collected when pumping is active on both limiter sides (- L and +L).

III.2.1.2. Experiments on CASTOR (Prague)

The density, parallel and perpendicular Mach number and floating potential radial profiles were measured with a mobile Mach probe and a « rake » probe for two configurations of positive polarity : (1) polarisation of the plasma with insertion of an electrode inside the separatrix, and (2) polarisation of the separatrix. This second mode is interesting since by polarising the edge plasma, the electric field and central plasma confinement are modified. The Mach number was calculated using a 2D kinetic model. A good correlation between the profile of the electric field and the poloidal Mach number was found (figure III-23). In CASTOR, with a configuration very similar to that in CIEL, the polarisation of the edge plasma results in modifications of the electric field in the central plasma, a significant reduction of turbulence on both sides of the separatrix, and an improvement in the global confinement.

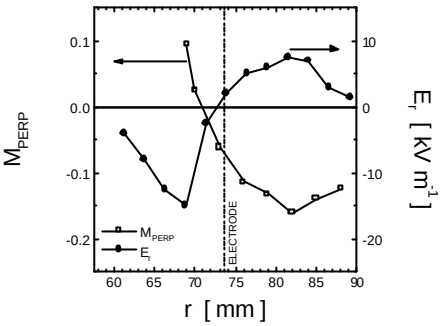

Figure III-23 : Radial profiles of the perpendicular Mach number and of the radial electric field during polarisation of the separatrix at +150 V with respect to ground.

The second experiment consisted in exploring the floating potential profile in front of the lower hybrid grill in order to detect the signature of electrons accelerated by the high $N_{//}$ components of the spectrum. A small Langmuir probe allowed a very fine measurement of the profile (figure III-24). No polarisation effect on the measured profiles was evidenced. Such measurements will allow a thorough study to be conducted on the possible mechanisms of fast electron generation.

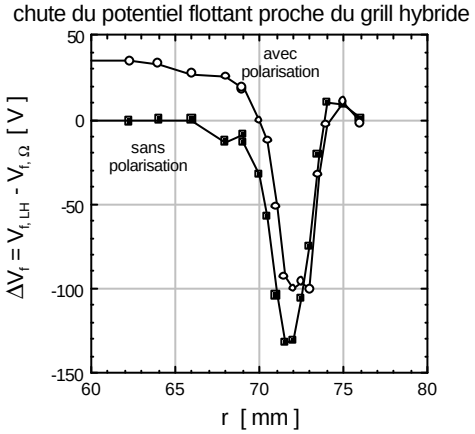

Figure III-24 : Difference in local floating potentials with and without hybrid heating. The squares are without polarisation, the circles are with polarisation

III.2.1.3. Experiments on TEXTOR (Jülich)

The Tore Supra Gundestrup probe was installed on TEXTOR, where new experiments were made to characterise the physics of toroidal limiter polarisation. It provided density, temperature, floating potential, and parallel and perpendicular Mach number measurements at the top of the torus. Moreover, a « rake » probe measured the profile of the floating potential at the equatorial plane. Most of the measurements were made in positive polarisation configuration with the magnetic field in its normal direction (figure III-25). It was noted that, in perfect agreement with the model developed at DRFC, the positive polarisation does not generate any effect on the edge plasma since the drop in potential occurs in the wall sheath (negative with respect to the limiter), and not through the flux surface. However, in negative polarisation, as noted in December 1999, significant modifications occur in the edge plasma.

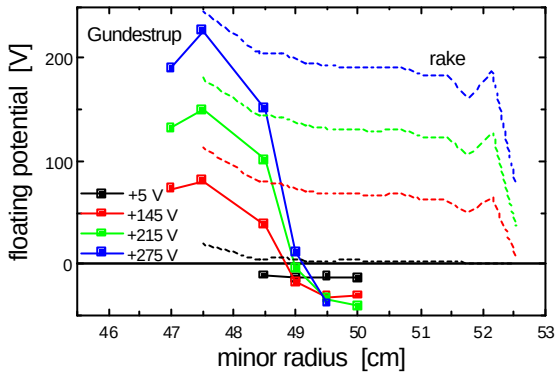

Figure III-25 : Radial profile of floating potential at top of torus, measured by a Gundestrup probe, and on equatorial plane, measured by a rake probe. The Gundestrup probe was placed behind a poloidal limiter (r=49 cm), which explains the sharp drop towards the machine ground in that region.

A new series of experiments on the effects of an electric field applied between the limiter and the internal tokamak walls was made on TEXTOR, but this time in the configuration where the plasma current, I_p, and the magnetic field, B_T, were inverted compared to the standard configuration, during which a negative polarisation showed a very clear decrease in the collection of particle in the ALT-II toroidal pumped limiter throats. This decrease is attributed to the reduction of the parallel flux in the SOL, a consequence of the imposed electric field. By inverting I_p and B_T, the idea was to create an inverse effect, i.e., an increase in the parallel flux collected in the ALT-II throat. Figure III-26 shows the evolution of the apparent particle confinement time, (τ^*_p) which also characterises the pumping efficiency. In this figure, it is clear that maximum pumping is obtained for a negative polarisation of 75 V (τ^*_p decreases), associated to a large λ_n increase.

Measurements of the parallel, $M_{//}$, and perpendicular, M_{perp}, Mach numbers also show a clear dependence on the polarisation voltage (figure III-27). As with the evolution of τ^*_p and λ_n, a decrease in M_{perp} is observed for a voltage of –75 V before returning to a value close to zero. On the other hand, a continuous variation of $M_{//}$ as a function of voltage is observed. These measurements were made with the Gundestrup probe located in the equatorial plane on the low field side, close to the limiter particle collection throats. In so far as there is no significant increase of τ^*_p, which would indicate a loss in density control associated to a lower particle collection, this drop on the lower field side is therefore compensated for by a greater increase in the collection on the high filed side.

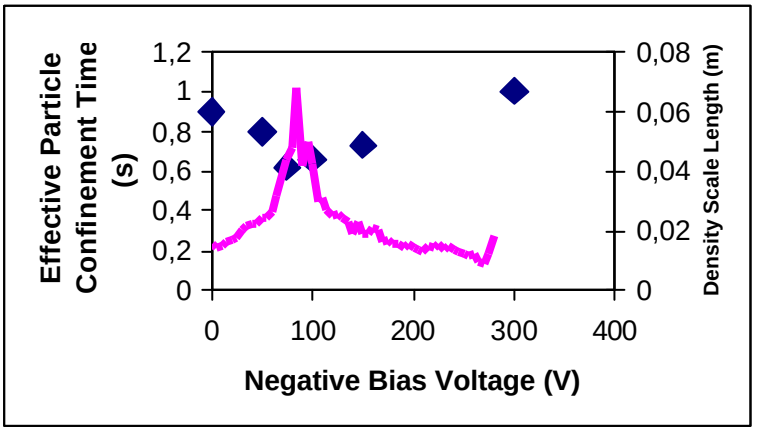

Figure III-26 : Evolution of apparent confinement time of particles (t^*_p) and of density decrease length in SOL as functions of biasing voltage

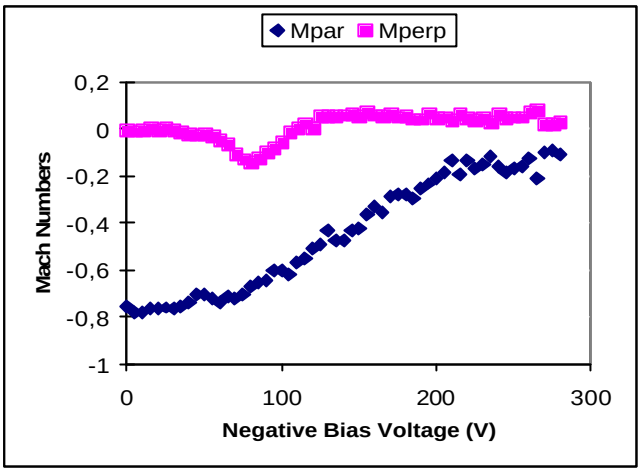

Figure III-27 : Evolution of $M_{//}$ and M_{perp} as functions of polarisation voltage

The analysis of these results is still underway, but all the experiments made on TEXTOR have shown that the application of an electric field in the SOL would significantly change the particle flux at the plasma edge.

III.2.2. Modelling of pellet injection

The study of pellet ablation and homogenisation of the ablated material was jointly conducted with the Consorzio RFX group (Padova, Italy). The starting point was a comparison of the signals of the two interferometers installed on the Reversed Field Pinch RFX, one located on the injection plane, the other 120° away in the toroidal direction. For each pellet injected, the first interferometer measures a very large density peak, since the measurement cord crosses the ablation cloud. Its analysis allowed the size of the cloud and its inner density to be measured; the density is more than one order of magnitude lower than what is measured in tokamaks. Simulations made with a NGPS ablation code showed that this low density was the cause of the greater ablation rate (by about a factor of 3) measured in RFPs. The other characteristic of the increase in plasma density, this time measured by the two interferometers, is the absence of very dense structures propagating over long distances parallel to the magnetic field. This absence demonstrates that the distance required for the homogenisation of the ablated material is short in RFX (typically 4 m within the centre of the discharge, versus about 30 m in Tore Supra). This difference was interpreted as being due to the differences in magnetic topology and transport properties characteristic of both configurations. Finally, it was possible to describe within the same theoretical framework both the pellet ablation and the homogenisation of ablated material processes in RFPs and tokamaks, and this in spite of extremely different experimental signatures.

Moreover, modelling of the pellet ablation in the presence of large additional powers was developed. Up to now, nearly all modelling for the plasma-pellet interaction assumed a Maxwellian plasma target. This approximation was justified by the complex physics involved (mainly the electrostatic sheath), which is easier to describe in this context. This approach had led to building a model validated on the entire IPADBASE (many experiments in different machines), but unfortunately limited to ohmic discharges or with little additional heat. In the last year, this model was extended to plasmas characterised by arbitrary ion and electron distribution functions, thus enabling it to be used to analyse pellet injection experiments in plasmas with large FCI heating or current generation. To do this, it has been necessary to introduce the geometrical effects due to the large size of the Larmor radius of suprathermal ions and the mass heating of the pellet, as well as the electrostriction for fast electrons (typically, for E > 100-200 keV). The use of this code now requires the explicit knowledge of the electron and ion distribution functions; interfaces have therefore been built to couple it to the FIDO (calculation of ion distribution), KOLTRA and DELPHINE (calculation of electron distribution) codes.

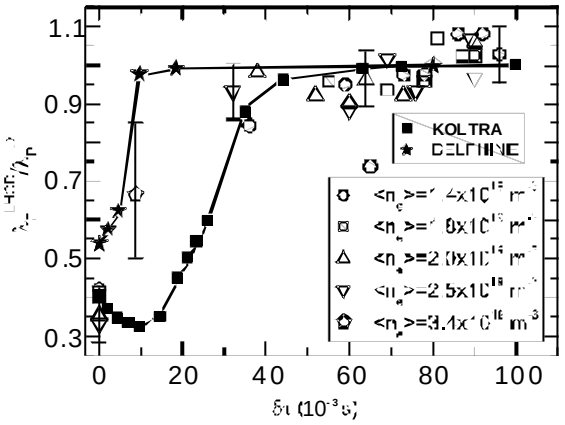

Figure III-28 : Reduction of pellet penetration compared to ohmic plasmas, l_p^{LHCD}/l_p^{W}, as a function of the time separating the shutdown of hybrid power from the pellet injection, dt, for discharges with current generation (modulated hybrid power).

These predictions were successfully compared to the available data. An example is given in figure III-28, where the reduction of the pellet penetration compared to ohmic conditions ($\lambda_p^{LHCD}/\lambda_\pi^{\Omega}$) is shown as a function of the time interval $\delta\tau$ separating the hybrid power shutdown from the pellet injection, during discharges with current generation (modulated hybrid power). The different symbols correspond to different average density plasmas, the two curves to the model predictions for the electron distribution functions calculated with the KOLTRA and DELPHINE codes.

III.2.3. Supersonic injection

A supersonic gas injection was developed for the start-up of Tore Supra in 2001. At the same time, a modelling effort was made to evaluate the performances of this new system, whose aim is to be an intermediate system between pellet injection, efficient but complex, and the usual gas injection, easy to implement but not very efficient.

The interaction between the plasma and the supersonic jet is complex. To start with, two approaches were studied, corresponding to the two following extreme cases :

- The cloud is “transparent” for the plasma. There is no collective behaviour of the cloud, and the injection can be simulated with the 3D Eirene neutral transport code, which individually follows the neutral particles generated from the injection point into a fixed plasma,

- The cloud is «opaque » for the plasma; it is sufficiently dense to stop ions and electrons. The cloud then has a collective behaviour, and one can hope to benefit from pellet type drift effects when injecting on the high field side. A liquid jet model, where plasma cooling is taken into account to estimate the jet penetration, was adapted to describe this situation. Figure III-29 represents the ionisation source feeding the plasma, calculated by the Eirene code in the two cases of a usual and supersonic gas injection. It is clear that there is no gain in penetration depth (indeed, the ionisation source mostly comes from the dissociation of molecules, having a short average free path). However, supersonic injection has a lower (and thus better) beam divergence, concentrating the particles in a cloud of reduced size and thus more dense. One can then hope to reach sufficient pressure conditions in the cloud to observe drift phenomena.

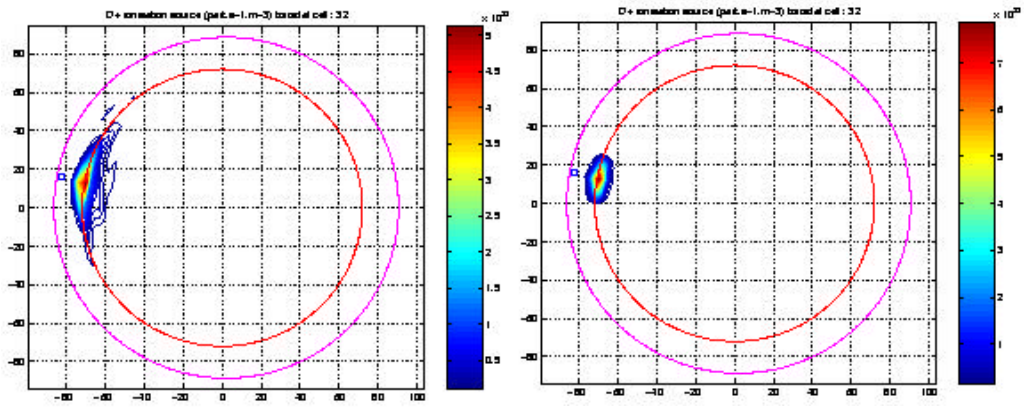

Figure III-29 : Comparison of ionisation source in the poloidal injection plane for the same quantity of particles injected in the case of the usual gas injection (on the left) and of a supersonic jet (on the right), calculated with the Eirene code.

At the other end, the first calculations made with the liquid jet model resulted in penetrations of 10 to 20 cm inside the last closed magnetic surface, depending on the plasma conditions and jet characteristics. However, this calculation very optimistically assumes that the ions and electrons are stopped by the cloud. An estimation of the cloud line density necessary to stop the plasma shows that this assumption can only be verified in the SOL and in the plasma very near the edge. With the experimental pulsed supersonic injection system installed on Tore Supra, able to typically inject 0.5 Pam^3 in 10 ms, the first estimations show that liquid jet type propagation conditions can only be marginally reached. A drift phenomenon is therefore not very likely. The results would be improved with shorter injection times (2 to 4 ms were obtained in the laboratory).

The first experimental results on plasma, obtained during the 2001 campaign, are shown in figure III-30. The filling efficiency is estimated to be over 30%, which is higher than that obtained with the usual gas injection (≅ 15 %). These results are being analysed.

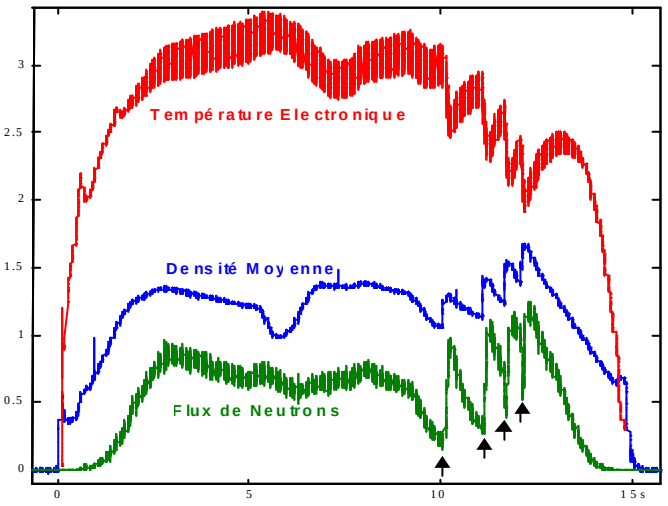

Figure III-30 : Use of supersonic injection during in a Tore Supra plasma. Variation of electron temperature, average density and neutron flux. The arrows indicate the 4 injection times.

III.2.4. Characterisation of chemical erosion

During plasma/wall interactions, the carbon plasma facing components (CFP) are subjected to significant erosion, which limits their lifetime, generates dust and induces tritium retention in the co-

deposited layers. Whereas physical erosion and bombardment induced sublimation can be controlled (by remaining under the energy and surface temperature thresholds), chemical erosion, which leads to the formation of volatile molecules (CH_4, C_2H_X, C_3H_Y) will be the predominant mechanism. The chemical erosion rate, defined as the ratio between the carbon emitted by the wall and the incident hydrogen ion flux, depends both on the material surface temperature (T_s), on the energy of the particles hitting the wall (E_i) and on the incident flux (ϕ). Previous studies, conducted on JET, TEXTOR, JT-60, have shown a dependence of the chemical erosion rate on the incident flux of the type $\phi^{-\alpha}$, with α varying between 0.06 and 1.25. These differences, resulting in significant uncertainties on the lifetime of CFPs, led to this study on Tore Supra. By considering CH_4 as the main impurity, an erosion rate variation in $\phi^{-0.23}$ was found (figure III-31). Heavier hydrocarbons, such as C_2H_X and C_3H_Y, were also considered. The contribution of these hydrocarbons to the carbon production is not negligible (figure III-32). Indeed, at low flux, the contribution of C_2H_X is equivalent to that of CH_4, and that of C_3H_Y corresponds to 50% of the value of CH_4.

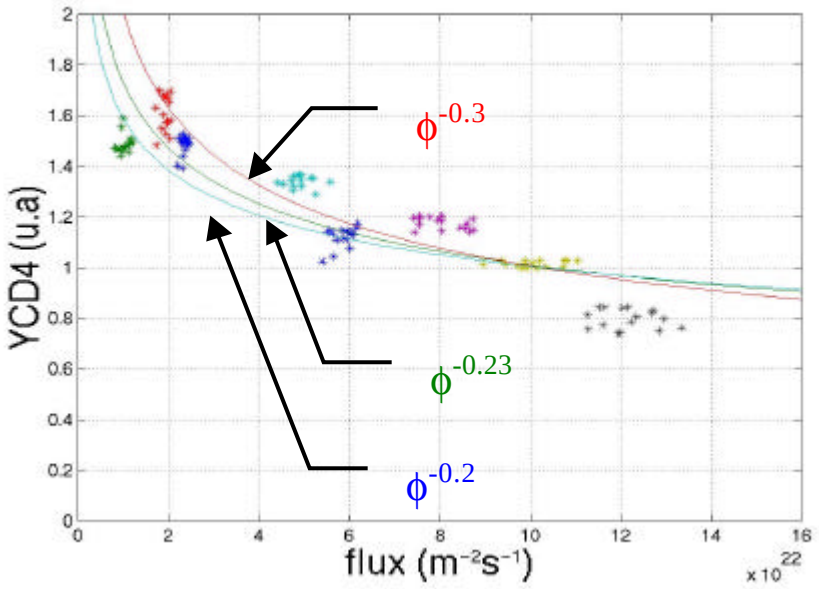

Figure III-31 : Variation of emission rate of CD_4 as a function of incident ion flux

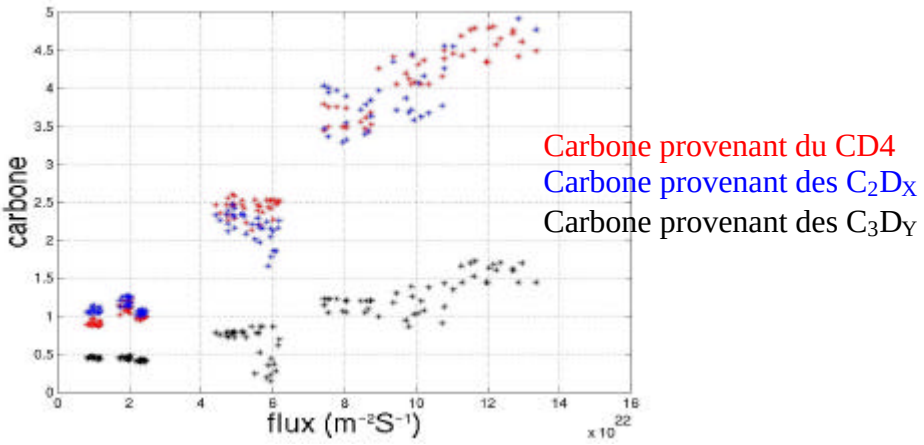

Figure III-32 : Carbon from molecules (CD_4, C_2D_X, C_3D_Y) as a function of incident ion flux

III.2.5. HF conditioning

Cleaning discharges are regularly made in tokamaks to reduce the concentration of light impurities such as oxygen and to control particle recycling, mainly by making luminescent discharges in hydrogen (or deuterium) and in helium. Nevertheless, because of the intense and permanent magnetic field, this type of conditioning cannot be made in the next machines, such as W7X or ITER.

Discharges created by ion cyclotron frequency waves were tested on Tore Supra and on TEXTOR and showed the potential of this technique. To compare performances, electron frequency (ECR) and ion frequency (ICR) conditioning discharges were alternatively made in TEXTOR in collaboration with Tore Supra.

Preliminary results indicate that for similar conditions (helium pressure P = 5.10^{-2} Pa, magnetic field B_T=2 T) and for injected powers of 200 kW, the plasma parameters are very different for the two frequencies (f_{ICRF} = 32.5 MHz, f_{ECRF} = 110 GHz). The density in a plasma created by ECR is higher (2.5 10^{18} m^{-3}) and is localised along the trajectory of the microwave beam. In ICR discharges, the density is lower (0.5 10^{18} m^{-3}) and the plasma fills the vacuum chamber homogeneously. The conditioning efficiency of both techniques, when compared in terms of hydrogen production, shows that ICR discharges are 20 times more efficient than ECR discharges.

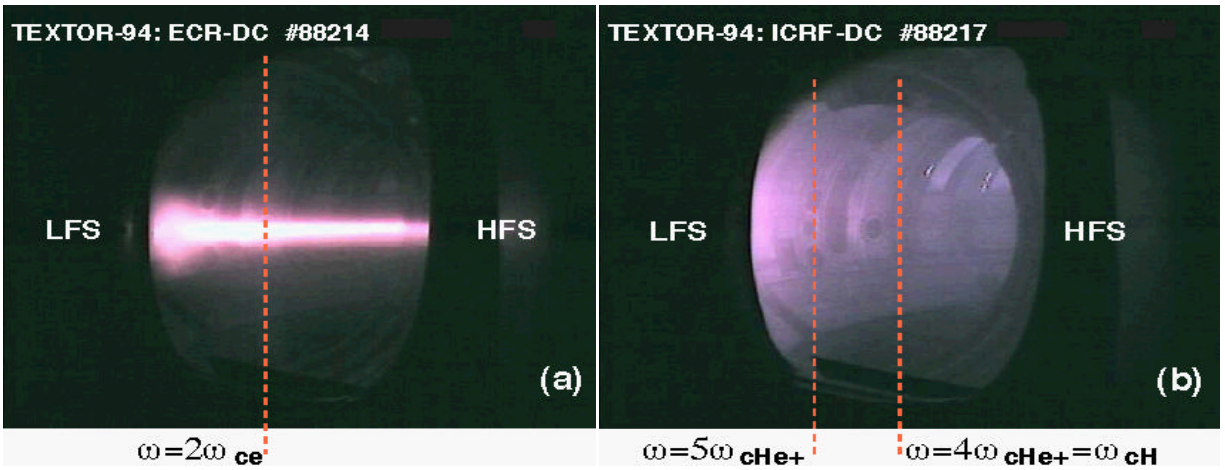

Figure III-33 : Tangential view with CCD camera during an ECR discharge (a) and an ICR discharge (b).

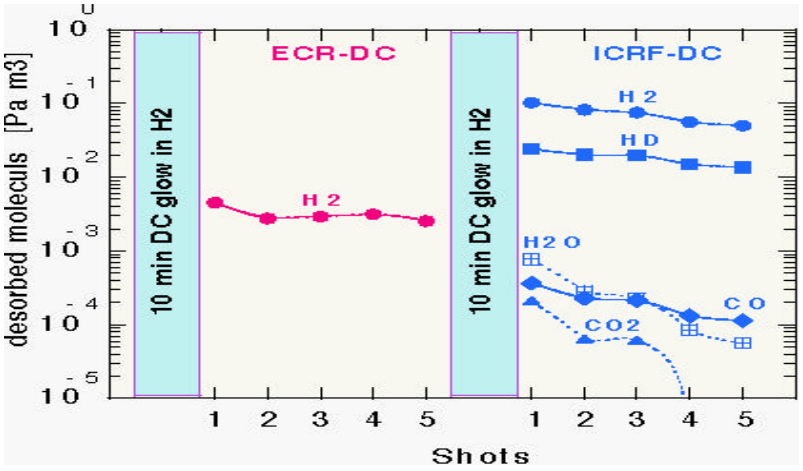

Figure III-34 : Comparison of conditioning efficiency of ECR and ICR discharges in terms of hydrogen and H_2O, CO and CO_2 molecules production.

III.3. Heating and current generation

III.3.1. Ion heating with ion cyclotron frequency waves (FCI)

On the path to ignition in a reactor, it is important to control the electron temperature so that it does not increase too rapidly, which would lead, at low density, to a deterioration of the efficiency of the energy redistribution process between the different species. In order to prevent this, a significant fraction of the heating must go to thermal ions (ion heating). Heating by ion cyclotron frequency waves (FCI) can produce significant fractions of ion heating. The minority heating scenario, using Helium 3 as the minority ion species, was used on Tore Supra: a tail of suprathermal ions, not too energetic and very collisional, is favourable to redistribute the energy to the thermal ions and to low ion loss rates induced by the magnetic ripple. Predictions of the ion losses due to the magnetic ripple in the CIEL configuration, resulting in a comparison of minority heating D(H) and D(3He), were conducted (III.3.2.3). Moreover, a scenario using a small percentage of ^{3}He, aimed at maintaining significant ion heating, was developed for ITER (III.3.1.2). Another possibility to produce a tail of not too energetic suprathermal ions is to increase the fraction of minority ions: this study was conducted on Tore Supra in deuterium plasma with minority hydrogen (III.3.1.1). Lastly, different exploratory scenarios of ion heating based on mode conversion of the FCI wave have been defined for Tore Supra (III.3.1.1).

III.3.1.1. Development of scenarios for ion heating in TS

There are several different possibilities of heating a minority ion species at the fundamental cyclotron ion harmonic to achieve ion heating using the ion cyclotron frequency wave (FCI). It is in particular possible to use a Bernstein wave produced by mode conversion from the FCI wave launched from the tokamak low field side.

Bernstein wave heating at the ion cyclotron harmonic 3/2

The scenario consists in creating an ion Bernstein wave by mode conversion in a plasma with two ion species (H and ^{4}He). Any other ion cyclotron resonance layer (1^{4}He on the high field side and 1H on the low field side) is excluded from the plasma so as to prevent parasitic power absorption. A competition is thus created between, on the one hand, the direct absorption of the fast wave (Fast Wave Electron Heating) and the absorption of the Bernstein wave by electrons, and on the other hand, the non-linear absorption on helium ions of the Bernstein wave at the helium cyclotron harmonic 3/2.

The plasma chosen is an H-^{4}He mixture (H-D is also possible). The reference discharge is TS#26445 (figure III-35), with an adapted plasma composition.

The $\omega=3/2\omega_{4He}$ layer is placed near the plasma centre. The required relative ion concentrations to localise the mode conversion layer near this 3/2 layer are approximately $n_H/n_{4He}=2$, i.e. $n_H/n_e=50\%$ and $n_{4He}/n_e=25\%$. An analysis with a ray-tracing code shows that the absorption of the Bernstein wave (IBW) by the electrons is low in these conditions. This experiment was transposed and performed on the ASDEX-Upgrade tokamak, in a deuterium/hydrogen plasma, within the framework of our collaboration with the Euratom –Max Planck Institut für Plasmaphysik Association. The analysis is still in its preliminary stages, but there are indications of ion heating when the mode conversion layer is actually close to the deuterium 3/2 cyclotron harmonic (figure III-36).

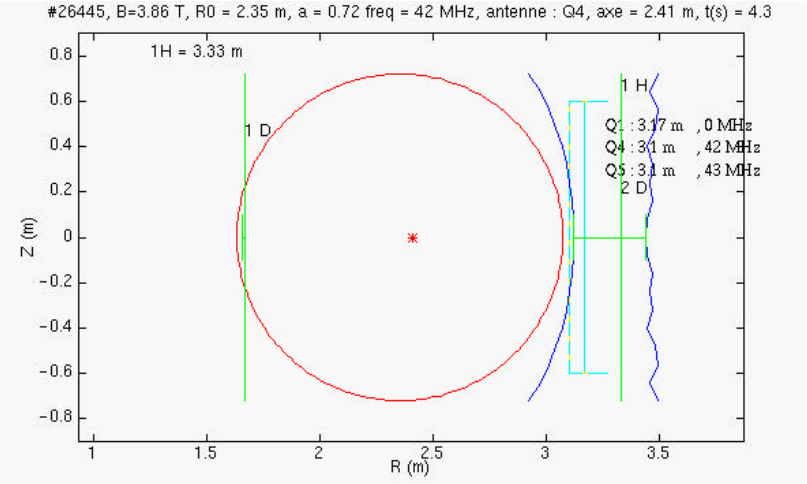

Figure III-35: Position of 1D and 1H ion cyclotron resonance in a poloidal cross section of Tore Supra. The magnetic field is B_T=3.7T and the ion cyclotron frequency of the fast magnetosonic wave is f_{FCI}=42 MHz.

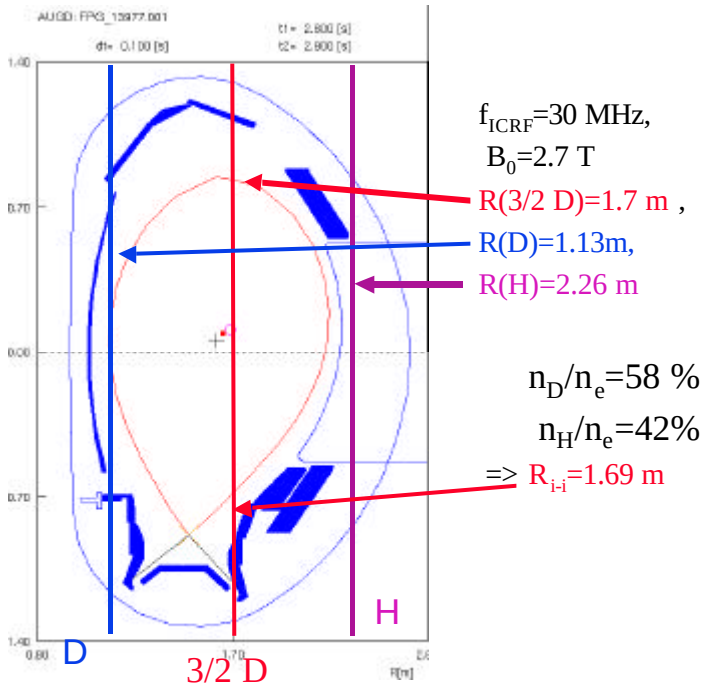

Figure III-36 : Position of 1D, 3/2D and 1H ion cyclotron resonance layers in a poloidal cross section of ASDEX Upgrade.

If the 3/2 ion cyclotron harmonic is not close enough, electron heating by direct coupling of the FCI wave (Fast Wave Electron Heating) and of the Bernstein wave is observed. The localisation of the power deposition by mode conversion, deduced by modulating the FCI power, indeed varies with the composition of the H/D mixture (figure III-37).

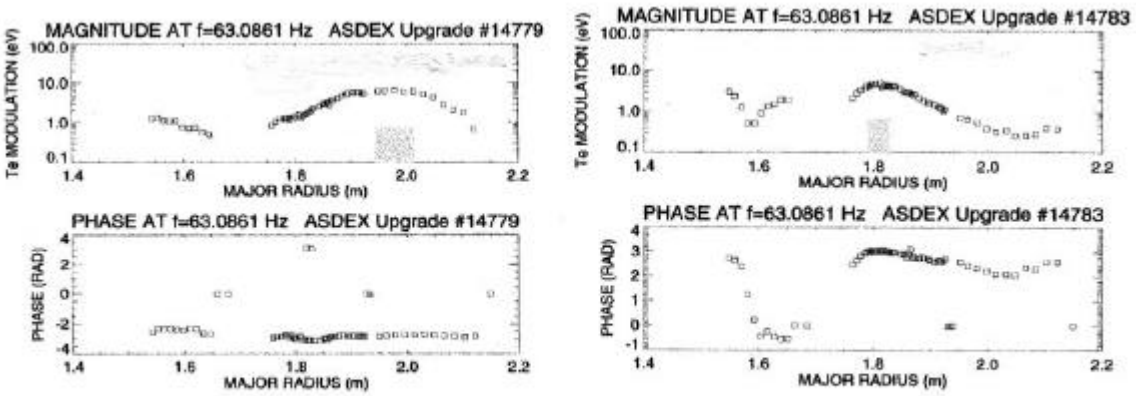

Figure III-37: AUG # 14779, power deposition on electrons outside the magnetic axis for $n_H/(n_H+n_D)$~80%, AUG#14783, power deposition on electrons closer to the centre for $n_H/(n_H+n_D)$~40%.

Ion heating with a Bernstein wave at the second ion cyclotron harmonic

This scenario consists in creating an ion Bernstein wave by mode conversion in a plasma with two ion species (H and ^{3}He). A competition is created between, on the one hand, direct absorption of the fast wave by the electrons (Fast Wave Electron Heating) and absorption of the Bernstein wave by the electrons, and, on the other hand, absorption of the Bernstein wave on the ions of a third minority species (Boron), whose second cyclotron harmonic coincides with the mode conversion layer. This experiment (already performed on the T-11M tokamak) is shown in figure III-38.

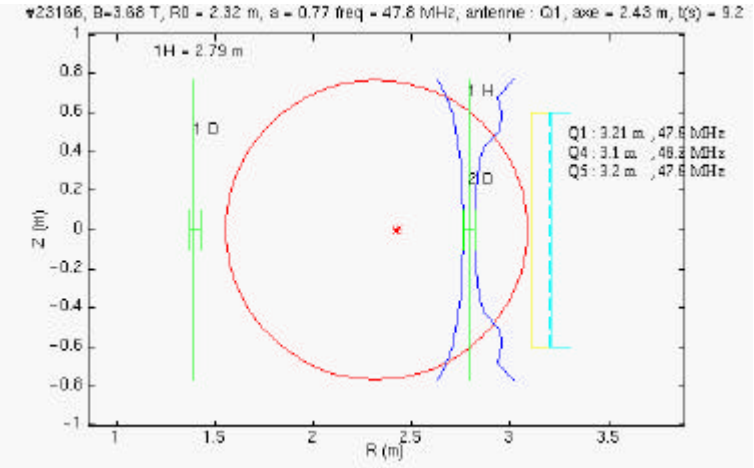

Figure III-38 : Reference shock TS #23166, B_T=3.6 T, f_{ICR}=48 MHz, ^{3}He and H plasma, n_H/n_e~25%, n_{3He}/n_e~37% (n_H/n_{3He}~65%), B_{11}^{+5}>0.1% at the centre (need for boronisation between shocks), $w=2w_c$(B) at +9.3 cm from the centre, $w=w_c$(H) at +34 cm, $w=w_c(^3$He) at -56 cm, S=0 (hybrid ion resonance H-^{3}He) at +10 cm, $S=N_{//}^2$ (mode conversion layer) at +13 cm

Ion heating with high minority concentration in Tore Supra

It is also possible to modify the power fraction absorbed by the electrons and the ions of the thermal plasma component during FCI heating, by varying the resonant ion concentration. Experimentally, an increase in the energy content of thermal ions was observed on Tore Supra for a high concentration of the minority species, in other terms, when the power fraction transferred to the ions through collisions is high. Figure III-39 shows two discharges in Tore Supra : discharge #21044 has a rather high minority concentration, whereas discharge #23967 has a low concentration.

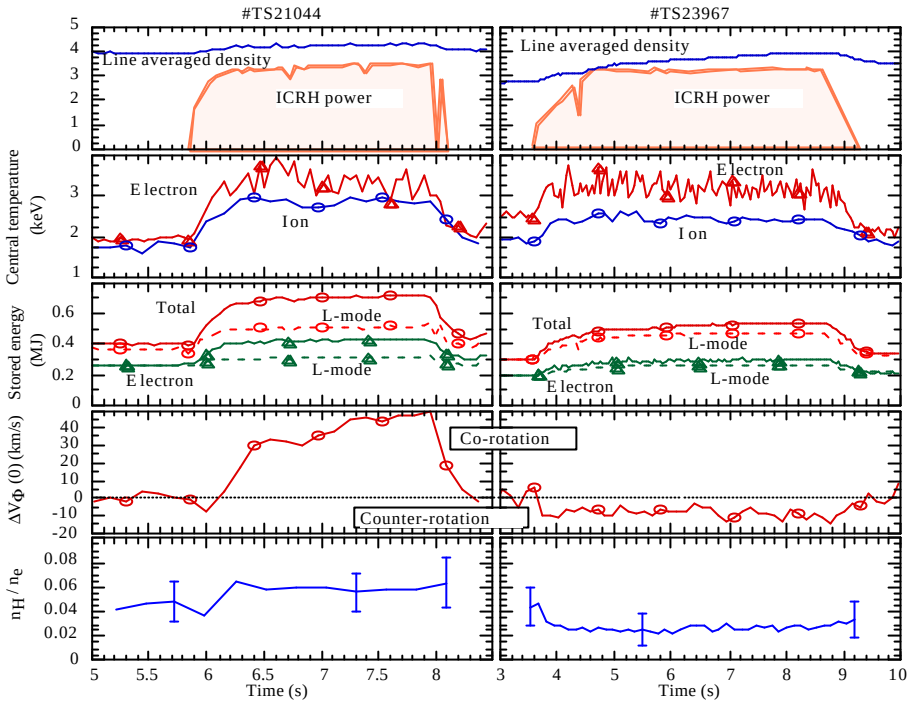

Figure III-39 : Time traces of: a/ line average density and FCI power, b/ electron and ion temperatures, c/ electron and total energies stored and L mode predictions, d/ toroidal rotation speed, and e/ minority fraction

III.3.1.2. Development of ion heating scenarios for ITER

To predict the efficiency of heating scenarios in an ITER-EDA type configuration, the PION code was used, in an attempt to evaluate ion heating in different heating scenarios. The two scenarios studied were that of the second tritium harmonic ($2\omega_{cT}$) and the heating in minority ^{3}He. The geometry studied was that of ITER-EDA (characterised by the data in Table 5.2).

R_0	a	B_0	f	κ
8.14 m	2.41 m	5.68 T	≈57 MHz	1.7

Table III-1 : ITER parameters used in simulations

Second tritium harmonic

The simulations were made in a configuration which was optimised for ion heating: 70% of tritium was used so as to reduce the power per particle and to limit the development of the suprathermal ion tail. Moreover, a polychromatic heating was used, with different frequencies, which allowed for a better power distribution in the plasma. 70% of the power was injected at 54 MHz, which corresponds to a resonance slightly shifted from the magnetic axis (r/a=0.2), whereas 30% of the power was injected at 57 MHz, corresponding to a resonance on the axis. To optimise ion heating, a toroidal spectrum at low $k_{//}$ was used, with a phasing at 90°.

Based on the assumption $T_i=T_e$, many simulations were carried out, at different temperatures and densities, which provided a complete image of the power absorbed by the ions in a reactor, in very different situations (figure III-40).

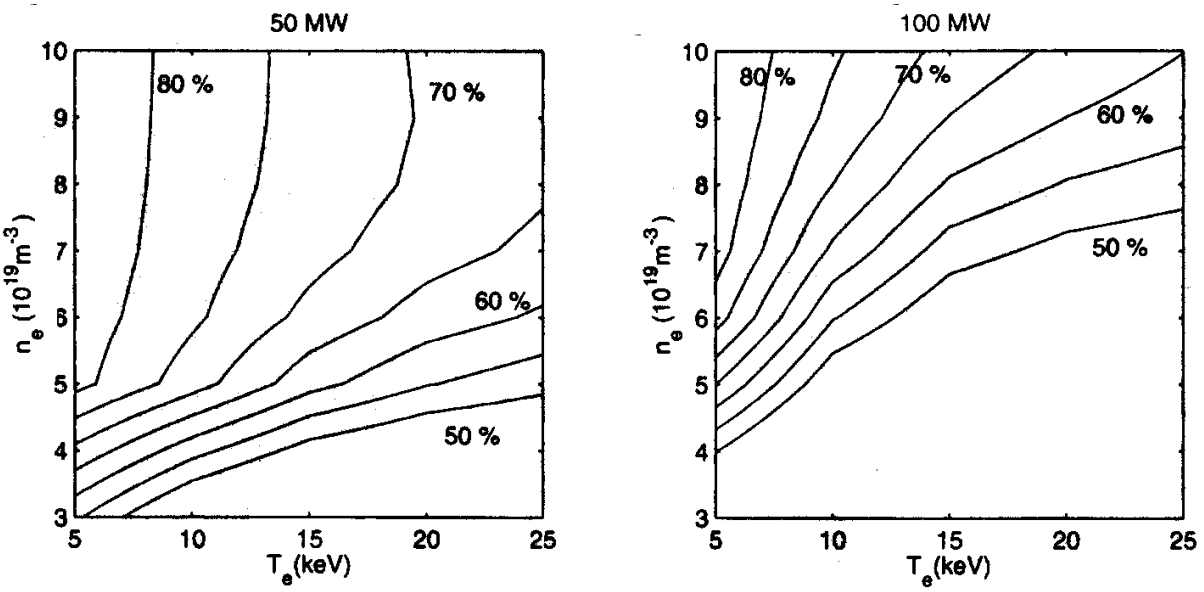

Figure III-40: Ion heating fractions in ITER-EDA for different temperatures and densities. The injected powers are 50 MW for the figure on the left and 100 MW for the figure on the right. At each point, T_i=T_e, and T_e represents the central temperature on each figure.

Considerable ion heating fractions are obtained, mainly at low power. When the plasma density is low, ion heating is poor, since suprathermal ions reach excessive energies, and the energy is redistributed by collisions to the plasma electrons. When considering high temperature and density scenarios, ion heating is limited by competition with direct electron absorption mechanisms, ELD and TTMP, whose efficiency increases with n_eT_e. At high power, the performance in terms of ion heating is degraded, because the ions receive higher power densities and the suprathermal tail develops further than in the 50 MW case.

^{3}He minority

As in the case of $2\omega_{cT}$, an optimised scenario was used, with polychromatic heating. Mode conversion was tested using the 1D ISMENE code. Dipole phasing was used for these simulations. The obtained ion heating fractions are given in figure III-41.

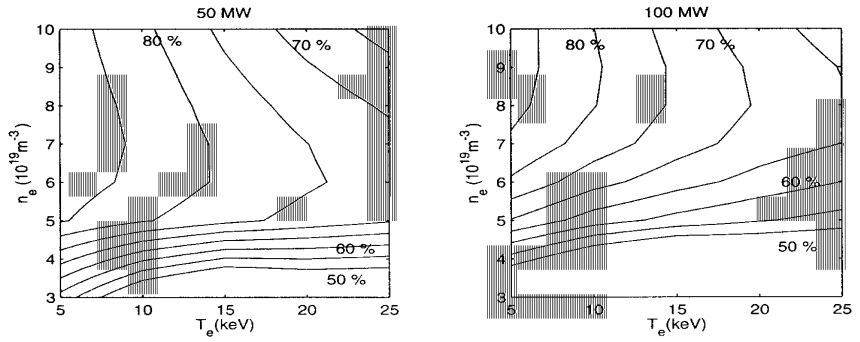

Figure III-41: Ion heating fraction obtained with the minority ^{3}He scenario for 50 MW and 100 MW of injected power.

Increase in plasma reactivity

Thanks to ion heating, it is possible to increase the plasma reactivity. Indeed, in a tokamak type reactor, the energy equipartition time between thermal ions and thermal electrons is not negligible compared to the energy confinement time (τ_{ei}~2s, τ_E~5s). There is thus enough inertia that heating the ions or the electrons is not equivalent. The effects of ion heating have been demonstrated by using a simplified transport model, implemented in the TETINE code, using transport coefficients of the Rebut-Lallia-Watkins type, normalised so that the confinement time of the simulations is equivalent to the confinement time given by the multi-machine scale law H_{98}. The ion heating fractions and the ion and electron power deposition profiles are given by the PION code. It was thus possible to test the performances of two machine configurations (ITER-LAM and IAM). The results are given in figure III-42. In a small tokamak, the ion heating fraction is very similar to that obtained in the ITER-EDA configuration (60% in a stationary regime). Two contradictory effects compensate each other:

- the size of the machine being smaller, the power density increases, which tends to take particles beyond the critical energy E_c, and to increase electron heating;
- the electron pressure being lower, the ELD/TTMP absorption mechanisms are less efficient, thus favouring ion absorption.

The plasma volume being smaller in IAM, the quality factor is lower than in LAM. The use of FCI heating for 60% of ion heating increases the quality factor by 20% versus the case of pure electron heating in the LAM case, and the increase is of 30% in the IAM case.

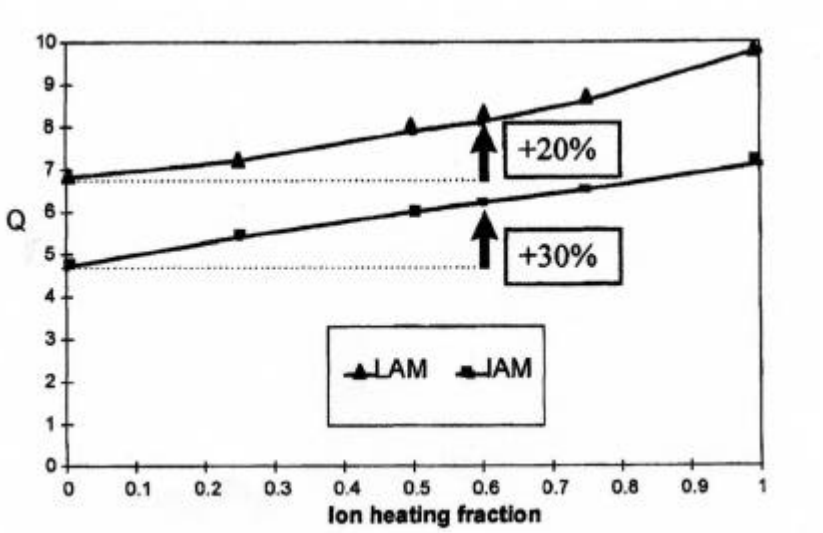

Figure III-42: Quality factor ($Q=P_{fus}/P_{add}$) as a function of the ion heating fraction in the LAM and IAM ITER configurations.

The minority ^{3}He heating scenario is very promising to maximise the ion heating fraction. Indeed, it combines the advantages of a high absorption scenario to those of a rather collisional species, which quickly redistributes its energy to the plasma, thus favouring ion heating.

Attempts to provide elements allowing the optimisation of the concentration to be used in ITER were made. This means a compromise between three problems :

1. obtaining a good ion heating by using enough ^{3}He,
2. avoiding the absorption on alpha particles, again using ^{3}He,
3. preventing the introduction of ^{3}He from diluting the plasma too much. The influence of dilution on plasma is very sensitive. For example, introducing 5% of ^{3}He in the plasma is equivalent to a reduction in efficiency of 19% if the dilution effect is the only factor considered.

We recommend a ^{3}He concentration of 2%, which allows absorption by the alphas to be controlled and a good ion heating fraction to be obtained (60%), while limiting plasma dilution (P_{fus} reduced by 7.2% by the dilution effect, which is more than largely compensated for by the gain due to ion heating). The efficient ^{3}He absorption, along with the existence of an adiabatic barrier for passing alpha particles (III.3.2.2), helps to limit the direct losses of fusion products. Lastly, the effect of super-adiabacity on the parasite absorption of alpha particles was evaluated based on the results of the MOKA code, combined with a simple model of alpha particle distribution function. The decrease in the parasite absorption is of about 40% in a scenario with minority ^{3}He heating.

The final modifications to the ITER design (ITER FEAT) require a quantitative re-examination of these results, but do not change the qualitative conclusions.

III.3.1.3. Dynamic of fast ions in a tokamak

Influence of non-standard orbits on the power deposition of the FCI wave

The influence of non-standard orbits and the spatial transport induced by the interaction with the waves on the FCI power deposition have been studied with the code SELFO, in a collaboration with the Stockholm Royal Institute (Swede). This code combines, in a self-coherent way, a 3-D calculation of the resonant ion distribution function with a full wave code calculating the power deposition. For example, such simulations show that absorption can be dominated by non-standard orbit passing ions on the low field side.

Super-adiabatic of fast particles with FCI wave (MOKA code)

The effect of phase correlation between the fast magnetosonic wave and the particles cyclotron movement is at the origin of the super-adiabaticy of fast particles. Former studies give an elegant description of super-adiabaticy, but are not realistic enough to accurately determine the appearance of correlation phenomena. The present study allows the adiabatic barriers to be accurately located in the phase space (energies where the behaviour of particles submitted to the interaction with the FCI wave is no longer diffusive). With this in view, the MOKA code was written in order to calculate the path of particles during several hundred poloidal revolutions, while keeping the information on the cyclotron phase. Associated to an indicator of stochasticity, X, based on the self-correlation function of the particle energy variations, this gives an accurate image of stochastic and regular behaviour over the entire velocity space. The X factor is shown in figure III-43, simulating 400 particles in Tore Supra (#23418) in a minority D(H) heating scenario.

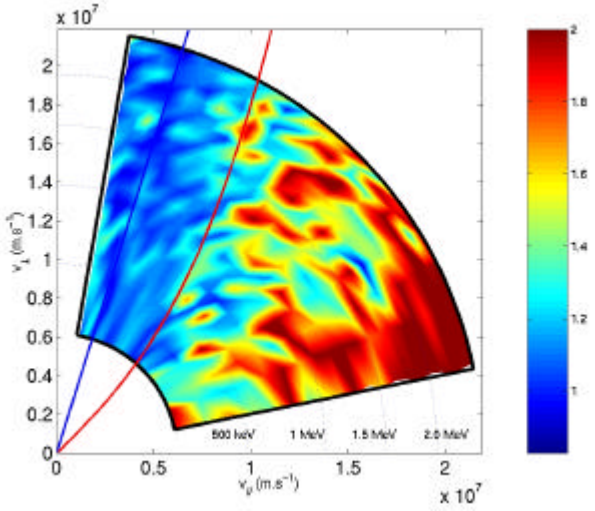

Figure III-43: X factor in the ($v_{//0}$,$v_{\wedge 0}$) plane. The blue zones correspond to diffusive behaviour (X factor close to 1), whereas the red zones correspond to super-adiabatic behavior. The border between the two gives the shape of the adiabatic barrier.

This figure shows that super-adiabaticy greatly depends on the shape of the particle path. In the area of the plane ($v_{//0}, v_{\perp 0}$) where the particles are trapped, diffusive behaviour is systematically found in the energy range studied. However, for passing particles, an adiabatic barrier appears between 1 MeV and 2 MeV. The super-adiabatic behaviour is observed for high-energy passing particles, as predicted by the Hamilton theory. Figure III-44 illustrates the crucial importance of the FCI wave toroidal spectrum for the study of this phenomenon : all the power (7 MW) is injected in a single toroidal wave-number ($N_{//}$=20) for this figure, whereas figure III-43 represents the same calculation with the same power distributed over a complete toroidal spectrum.

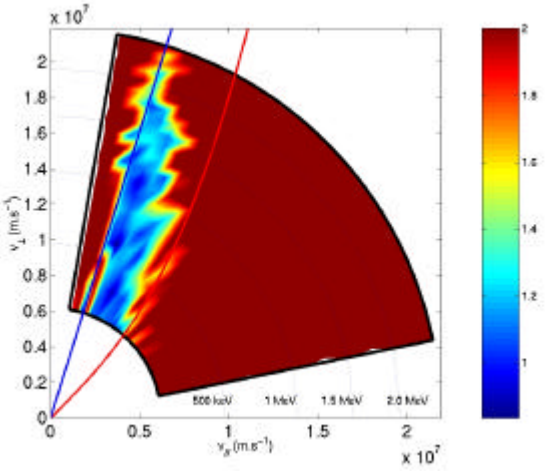

Figure III-44 : X factor in plane ($v_{//0}, v_{\wedge 0}$) in the case of a spectrum reduced to the wave number $N_{//}$=20

The super-adiabaticy map calculated by including the effect of collisions is essentially the same as that obtained without collisions (that in figure III-43). At high energies (E>200 keV), collisions have a very small de-correlation effect (electron slowing-down). The pitch angle dispersion is not very efficient at such energies, and this mechanism is the one mainly responsible for collisional de-correlation. At lower energies, collisions do not modify the diffusive behaviour ensured by inherent de-correlation.

Correlation effects at high energy generate a decrease in the diffusion induced by FCI heating. The power absorption is shown to be greatly reduced for high-energy particles. This effect occurs for particles with energies of about 1 MeV, and mainly concerns passing particles. In the case of minority heating, this thus occurs prior to the effects described by Mantsinen (1999). Indeed, the ions cannot diffuse beyond energies of approximately several MeV, because of the conjugated action of the wave components polarised on the left and on the right. The super-adiabatic effect does not concern many ions in present tokamaks, since energetic ions have essentially trapped trajectories. The case of a tokamak reactor, for which these correlation effects play a role, has been studied : it is mainly the high-energy passing particles which are submitted to these effects. The FCI power fraction absorbed by the alpha particles is thus reduced by the correlation effects. Figure III-45 shows the alpha particle behaviour as a function of their position on a plane ($v_{//}, v_{\perp}$), in a of minority ^{3}He heating scenario (with a concentration of ^{3}He of 2%). The effect of these correlations on the parasitic absorption of the FCI heating by alpha particles can then be estimated : the reduction in diffusion decreases the parasitic absorption to 9%, instead of the expected 16% when not taking into account this phenomenon.

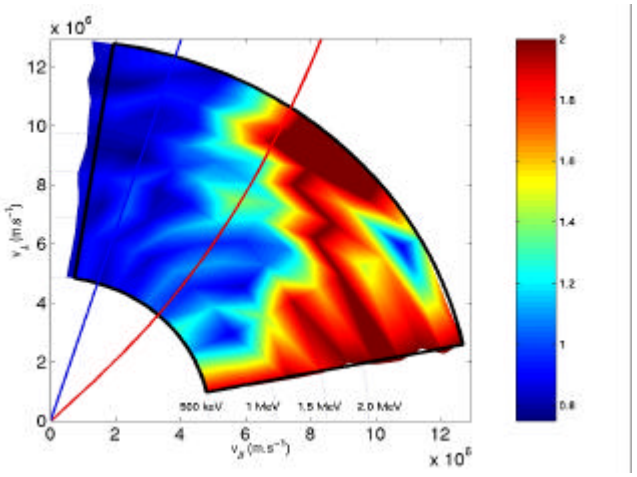

Figure III-45 : X factor expressing the correlation degree in the case of alpha particles for an ITER-EDA scenario of minority ^{3}He. X~1 : diffusive behaviour. X~2 : correlated behaviour.

III.3.1.4. Plasma rotation in the presence of FCI heating

Tore Supra plasmas with a high concentration of minority hydrogen (§III.3.1.1.c) show improved confinement (nearly by a factor of 2) compared to the L mode prediction. This improvement in confinement goes along with a toroidal acceleration of the plasma in the same direction as the current, even though FCI heating does not inject any toroidal couple into the plasma, contrary to neutral injection. It is not yet established whether this rotation is the cause of this confinement improvement. Experimental observations and theoretical studies however show that it is possible to stabilise the turbulence in a plasma by shear rotation. Consequently, it is very important to understand the origin of such a rotation in a plasma.

Experimental observations

There are two possibilities : the fast ions created by the FCI heating are responsible for this rotation, or else, this is a phenomenon linked to transport in a thermal plasma. The experimental results on Tore Supra however show that there is a definite link between rotation and ion pressure (figure III-46).

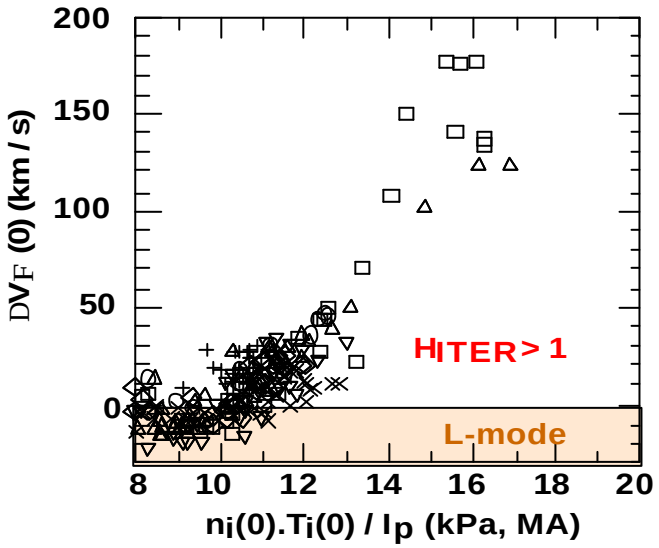

Figure III-46 : Plasma rotation velocity versus ion pressure (normalised at plasma current)

Rotation induced by fast ions

It is clear that part of the rotation is induced by fast ions, even if it is still not possible to explain all the experimental observations. The direction of this rotation depends on several factors.

a/ If the FCI antennae radiate waves with a low toroidal wave-number, the study of the differential couples produced by fast ions shows that the pitch angle dispersion plays an important part in the rotation direction. More particularly, for an ion cyclotron resonance layer on the low field side, the fast ions can induce a rotation in the same direction as the plasma current if their average energy is not much greater than the critical energy of the pitch angle dispersion. However, if the fast ions have a high average energy, which is often the case if the concentration of resonant ions is low, the induced rotation is in the opposite direction. For a dipole antenna spectrum (symmetrical spectrum, most often used) with rather high toroidal wave-numbers, the physics is more complicated.

b/ Initial simulations have been made with the SELFO code. This code combines, in a self-coherent way, a 3D calculation of the resonant ion distribution function with a full-wave code, which calculates the power deposition. The simulations show that fast ions can locally absorb some of the kinetic wave momentum. In particular, fast ions can absorb some of the kinetic momentum in the same direction as the plasma current in the plasma centre, and in the inverse direction towards the plasma edge. It is possible to have a rotation induced by fast ions in the same direction as the current for a resonance on the high field side as well as the low field side.

III.3.2. Interaction of the FCI wave with the edge plasma

III.3.2.1. In limiter configuration

Modelling of RF sheath phenomena in realistic geometry has been ongoing since 1999, in collaboration with the LPMIA laboratory of the Nancy I University. The simulation tool is organised into several successive modules :

- The RF electric field in the absence of plasma perturbation is evaluated around the FCI antenna, using the 3D self-coherent code ICANT (LPMIA Nancy). Several modifications improved the realism of the antennae and plasma description : integration of the slow wave and of a poloidal field in the target plasma, thick bars for the Faraday screens, antenna boxes in the shape of parallelograms.
- A module of field line plotting determines the topology of the open magnetic lines near the FCI antennae, with the actual Tore Supra antenna map and a realistic magnetic configuration in limiter mode. This module was used to validate analytical expressions for the magnetic connections around the FCI antennae. As an example of application, the shadowing of the Faraday screen corners by the lateral antenna protections was studied as a function of plasma geometry.
- The RF parallel electric field is integrated along these open field lines. Each of the flux tubes is considered as a 1D RF sheath. Thus a 2D mapping of the DC plasma potential in a poloidal section near the antenna can be drawn up.
- The re-organisation of the density in this poloidal section is then calculated with a fluid particle transport code, in the presence of an « E×B » convection introduced by the differential polarisation of the nearby flux tubes (CELLS code).

All these codes were linked in 2000. They were used to explain asymmetries in heating noticed on the FCI antennae, as due to density asymmetries produced by RF convection. Experiments made in the limiter configuration in 1998/1999 were also simulated :

- Parametric studies with HF power and central plasma density.
- Radial movement of the antenna versus the last closed magnetic surface.
- Effect of antenna structure changes performed during the 1998/99 shutdown.

The parametric variations of the simulated heat flux are in at least qualitative agreement with the surface temperature variations observed with infrared cameras.

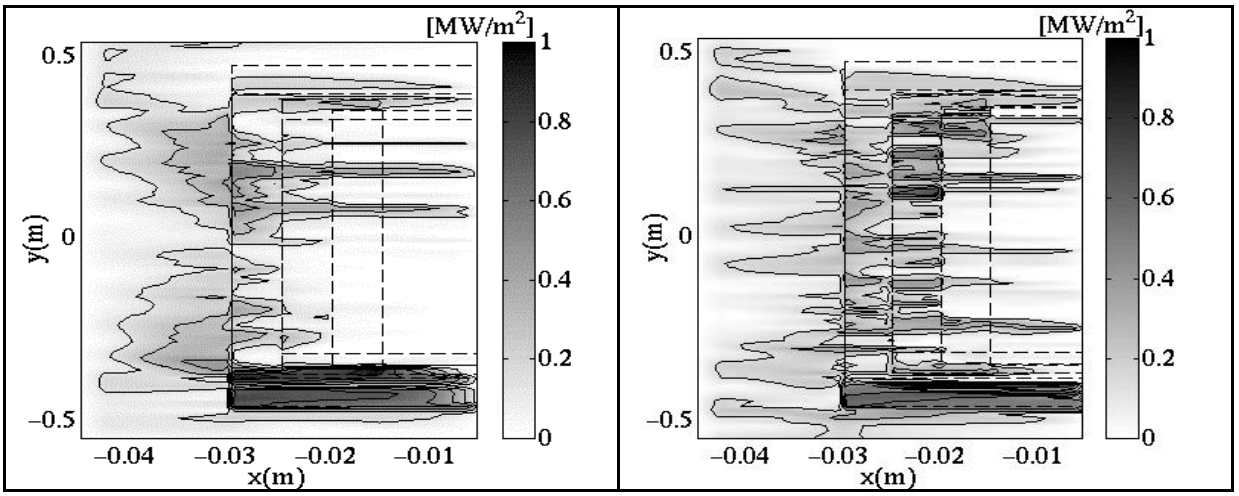

Figure III-47 : 2D mapping in a poloidal plane of heat fluxes on a FCI Tore Supra antenna. The confined plasma is on the left of the figures, the torus vessel on the right. Dotted, the projection on the reference poloidal plane of the antenna material elements is super-imposed : from left to right, successively, lateral protections, Faraday screen frame, septum tip, shielding bars. Left hand figure : dipole phased antenna; right hand figure : monopole phased antenna. A significant top-bottom asymmetry and differences between monopole and dipole can be seen.

III.3.2.2. In ergodic divertor configuration

The heating of the FCI antenna corners was characterised in the ergodic divertor regime using infrared and visible cameras. The results of the two diagnostics are coherent. The edge plasma density was modified in three very different ways (change of central density, change of base gas, or introduction of the pumped limiter in the ergodic region). A correlation exists between a high density on the divertor Langmuir probes, an easy coupling of the FCI wave and very bright spots on the Faraday screens. A local density effect on the hot spots is thus confirmed.

The FCI power coupling (minority scenario) in the ergodic divertor configuration increases with edge density (figure III-49b). The edge density is very sensitive to any perturbation in the high recycling regime (which is always obtained in the ergodic divertor configuration) whereas the average density variation is moderate (figure 49a). One of the control parameters on Tore Supra is the gas injection, mainly influencing the average density : this sensitivity of the coupling resistance to the edge parameters, perturbed by detachment instabilities, makes the injection of FCI power difficult in these high density regimes, even in the presence of the automatic adaptation system. Partly detached regimes, with or without inhomogeneities in edge density and temperature, induced by the presence of flux tubes in the laminar zone, are therefore obtained for the high coupling resistance values.

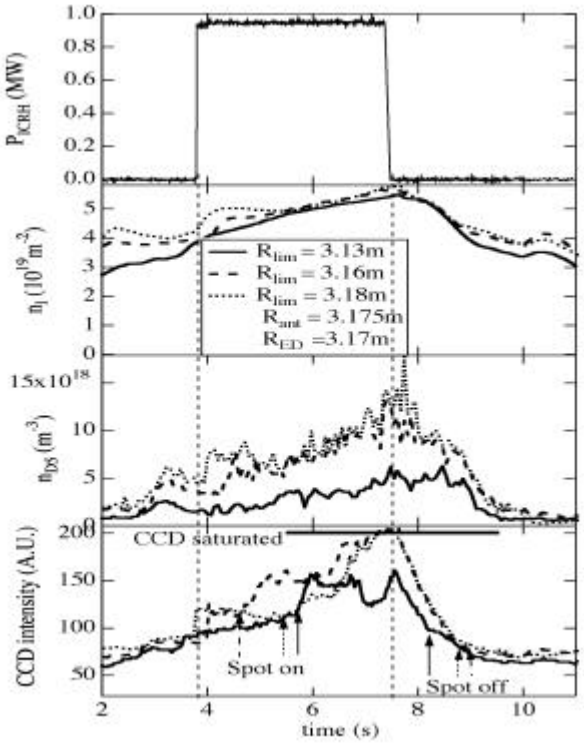

Figure III-48 : Comparison of three discharges in the ergodic divertor regime. The density of the confined plasma is kept constant, the pumped limiter is progressively inserted in the ergodic layer. This affects the local density on a divertor module Langmuir probe, and the heating of the antenna corner observed with a visible CCD camera.

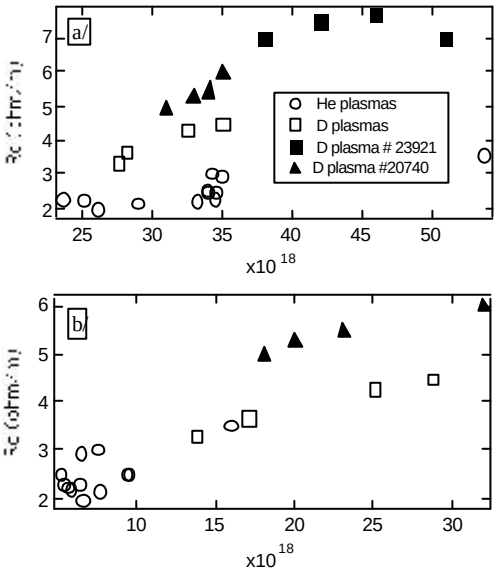

Figure III-49 : Coupling resistance in minority FCI heating in the ergodic divertor configuration as a function of average density (a/) and edge density (b/).

III.3.3. Magnetic ripple physics

III.3.3.1. Ripple modelling with the FIDO code

The ripple modulation of the Tore Supra toroidal magnetic field is relatively high, reaching 7% at the plasma edge on the low filed side. Consequently, the losses of ions accelerated by FCI heating can be

very high. Losses up to 20% of the injected power were measured during FCI heating. It is therefore important to accurately simulate these losses. With this in mind, a module to estimate these losses was added to the Monte Carlo FIDO code. This code solves a 3D Fokker-Planck equation averaged on an orbit concerning the accelerated ions distribution function. It takes into account finite orbit width effects and spatial transport induced by FCI heating. The ripple modelling treats both the losses caused by ion trapping in the magnetic field mirrors and the space diffusion induced by the ripple (collisional and stochastic). This diffusion in space is treated by adding a diffusive term to the Fokker-Planck equation averaged on an orbit, whereas a Monte Carlo sub-loop is used for the ions submitted to trapping in the magnetic field mirrors.

The FIDO code simulations were compared to the experimental results. The code reproduces very well the tendencies observed experimentally. An example is given in figure III-50, showing the ripple losses, measured and simulated, as functions of the injected power for typical Tore Supra discharges.

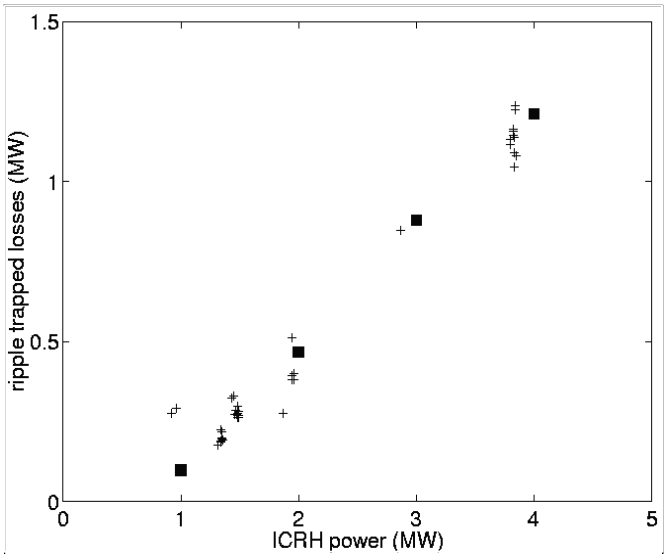

Figure III-50 : Power lost in the magnetic ripple as a function of injected power.

III.3.3.2. Experiments and CIEL configuration for electrons and ions

The design of protections from suprathermal electrons trapped in the toroidal modulation of the magnetic field (ripple) was validated with the experiments conducted in 1999. Each Tore Supra upper port, submitted to the electron flux (F_R) generated by the hybrid or FCE wave, is now protected by a set of actively cooled tubes, similar to that of the prototype (figure III-51).

The incident flux was experimentally determined using the prototype installed in 1999 (temperature measurement by infrared camera), the scaling laws being deduced by current measurements from a diagnostic devoted to these losses (which is also installed for the 2001 and 2002 campaigns) :

$$\Phi_R = [18\ MW/m^2] \times [P_{LH} / 8\ MW]^{1.06} \times [I_P / 1.6\ MA]^{0.8} / [nl / 2\ 10^{19}\ m^{-2}]^{1.75}$$

This calculated flux must not exceed 10 MW/m^2 (i.e. 50 % of the maximum acceptable value for the tube, which is 20 MW/m^2). The red curves plotted in figure III-52 represent the power corresponding to the 10 MW/m^2 limit. The calculation of this maximum is integrated in the VME AHYB, and the power is automatically limited to this value by the feedback control (to be validated at low power at the beginning of the campaign).

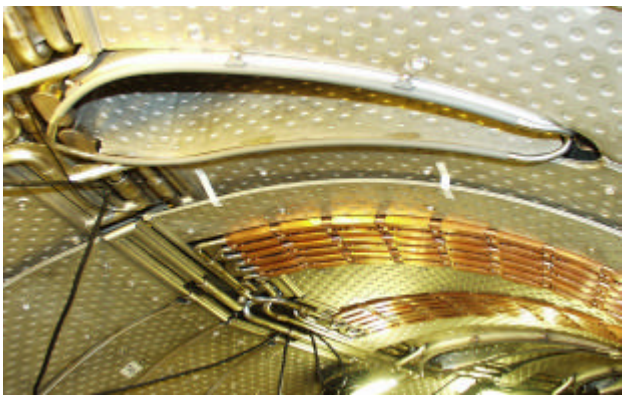

Figure III-51 : View of ripple protections

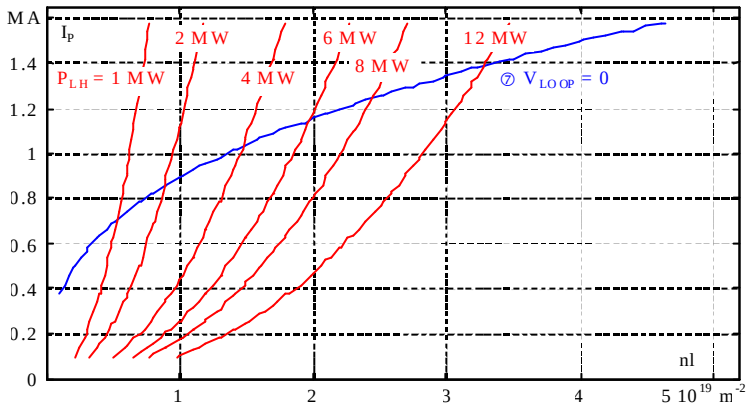

Figure III-52 : Maximum allowed power as a function of line density and plasma current. The line corresponding to the operation at zero loop voltage with the maximum allowed power is plotted for an efficiency of 0.65 10^{19} A/W.m^2. It shows the maximum current which can be generated in a stationary regime for a given density value. Any value greater than I_P is only possible in partly inductive regimes.

Concerning the ions, most of the suprathermal ions reach the toroidal limiter. Figure III-53 shows the estimation of this flux for an injected power of 1 MW, the flux varying linearly with power. In some configurations (hydrogen minority, ion cyclotron resonance layer on the high filed side), some of the suprathermal ions flux will not be intercepted by the limiter (major radius < 2.20m). A protection has been installed to retrieve these ions. Infrared surveillance in these scenarios is initially required to evaluate this flux.

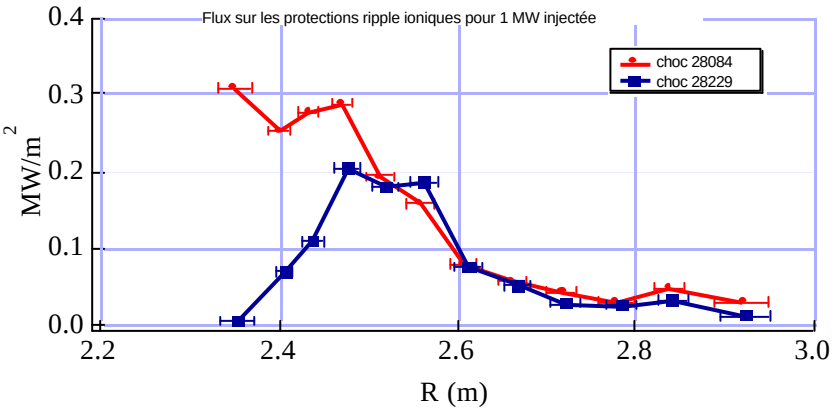

Figure III-53 : Flux on the toroidal limiter for two heating configurations (red: heating outside the magnetic axis on the high field side; blue: heating on the magnetic axis). There are no measurements for R<2.35m, R being the major radius.

III.3.3.3. CIEL scenario with low ion ripple losses D (^{3}He)

When using the FIDO code, it is possible to make predictions for different heating scenarios within an advanced scenario producing 100% of non-inductive current. It is a priori forecast to use 20 MW of power (9 MW of FCI power, 9MW of hybrid power and 2 MW of FCE power) for the scenario called CIEL 2. The two scenarios tested with the FIDO code are scenarios with hydrogen minority and helium-3 minority, both in deuterium plasmas. Heating by the fundamental helium-3 cyclotron resonance is a very promising scenario, allowing the minority ion energy to be controlled by the high collisionality of the ^{3}He ions. The results are given in Table III-2.

Scenario	Losses in ripple mirrors	Total losses
Hydrogen minority	2.8 MW (31%)	3.8 MW (40%)
Helium-3 minority	0.3 MW (3%)	0.4 MW (4%)

Table III-2 : Power lost in the ripple for helium-3 minority and hydrogen minority heating in the CIEL configuration.

Even though this scenarios has a high density, the losses predicted by the FIDO simulations are very high. This is due to the fact that the scenario is at low plasma current, in which the q safety factor values are high. Since stochastic diffusion processes greatly depend on the q value, they become dominant in this scenario and are responsible for the very high losses (40% of the power lost in the ripple for the case of minority hydrogen). The same simulation made without stochastic losses predicts total losses of 11%, clearly showing the increase in minority ion transport linked to stochastic diffusion. The ^{3}He minority heating scenario provides a good alternative to limit the losses due to the magnetic ripple. The minority species in this case being more collisional than hydrogen, the resonant ions reach much less high energies (figure III-54a and b). The ions are thus much less likely to be affected by ripple effects, i.e. collisional trapping or stochastic diffusion. The ripple losses predicted by the FIDO code are about ten times lower than in the case of minority hydrogen. Experiments made during the 1998 experimental campaign also confirm that the losses are reduced by the use of minority ^{3}He scenarios. Figure III-55 shows a comparison between discharge #26355, which had a ^{3}He injection, and discharge #25020, which is a classic case of hydrogen minority heating. The injected power, plasma current and electron density were similar for both plasmas. However, the ripple losses measured by the DRIPPLE diagnostic are five times lower for discharge #26355. The stochastic losses in both cases can not be evaluated, but they are efficient for ions with an energy greater than that of the ions concerned by trapping mechanisms. Thus, it is thought that the stochastic losses are likely to be negligible in the case of minority ^{3}He.

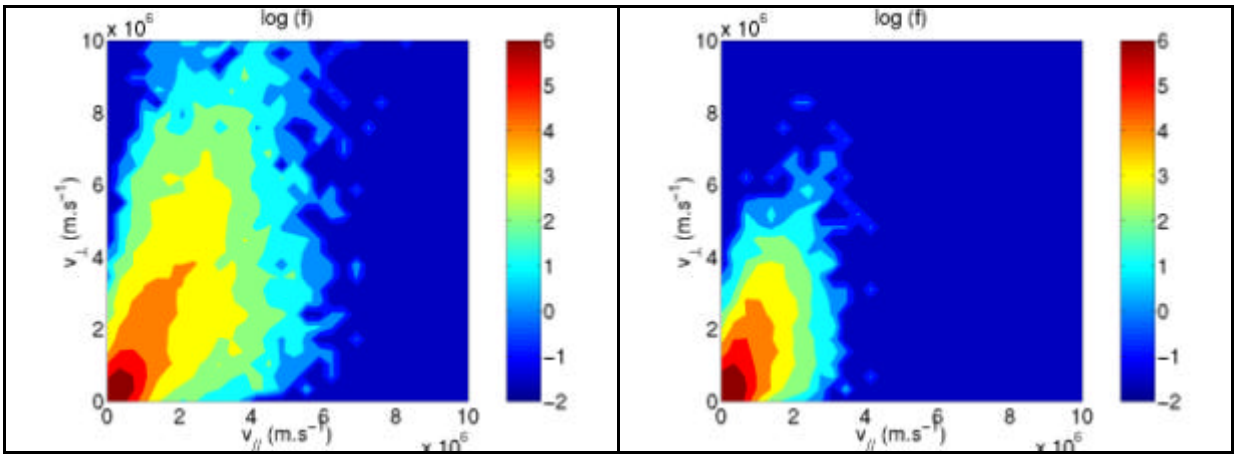

Figure III-54 : a/ distribution function for a CIEL 2 scenario with hydrogen as minority species; b/ distribution function for a CIEL 2 scenario with helium-3 as minority species.

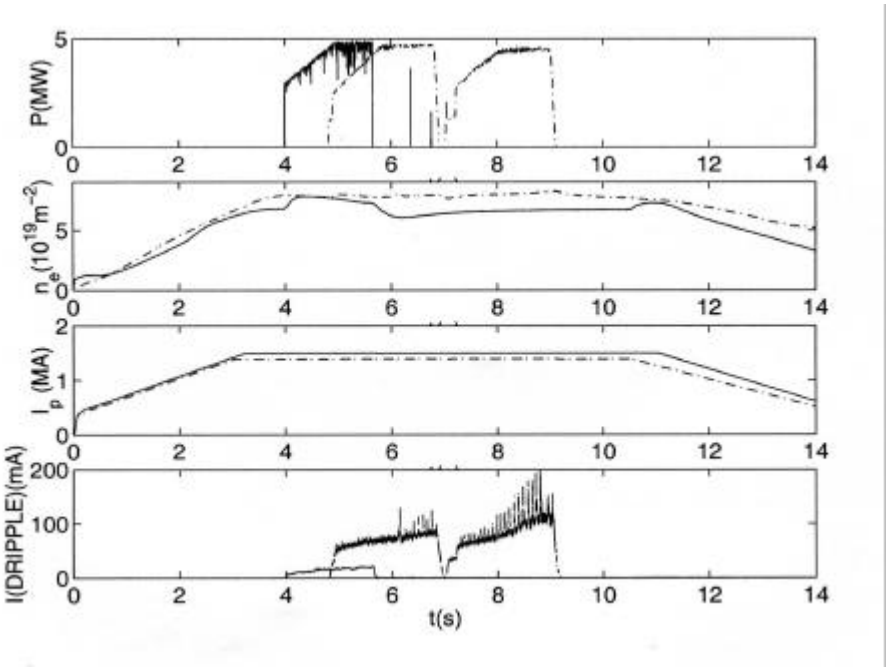

Figure III-55: Comparison of two Tore Supra plasmas with equivalent plasma conditions, but having different heating scenarios: a/ ^{3}He minority, b/ hydrogen minority. The first graph shows the FCI injected power, the second gives the average density, and the third the plasma current. Lastly, the fourth is a comparison between the signals detected by the DRIPPLE diagnostic for both plasmas.

III.3.3.4. Asymmetry of ion losses due to the magnetic ripple

In some FCI low power heating scenarios (< 1 MW) on Tore Supra, ion losses due to the ripple modulation of the magnetic field show a toroidal asymmetry: fast ions are mostly lost around the FCI antennae. Power fluxes larger than those which can be estimated with the usual toroidal symmetry assumption (with period 2π/N) might then be deposited on the plasma facing components and thus create particularly dangerous hot spots.

The importance of the toroidal precession $\Delta\phi/\tau_b$ of the fast ion "banana" paths compared to the transport mechanisms towards the local magnetic mirrors induced by the magnetic ripple has been studied. The time Δt required for a fast ion, initially in the good confinement area, to be lost in these mirrors under the effect of angular dispersion and stochastic diffusion, was analytically estimated using a Fokker-Planck calculation. A comparison with numerical simulations from a Monte Carlo code was made. This code has a module allowing the resonant ion interaction with the FCI wave to be modelled. A satisfactory agreement was found in so far as our analytical model does not take into account either the magnetic ripple effect on transport or the effect of the radio frequency wave. The first results show that Δt is sensitive to the fast ion energy and to the vertical position of the "banana" orbit tips with regard to the zone of good confinement. Δt only greatly decreases at high energy (starting at 200 keV) when particles are initialised near a region of strong magnetic ripple. The toroidal position $\Delta\phi$ of the losses, given by $\Delta\phi/\tau_b * \Delta t$ in all the other cases, is not linked to the initialisation position of the "banana" tips. The toroidal precession period is too short compared to the oscillation period τ_b on a "banana" trajectory. A uniform distribution of the lost power between each pair of toroidal coils is then possible, as shown by the symmetry of the ripple losses in the case of high power FCI heating.

The initialisation of the banana tips at the edge of the confinement zone corresponds to a low power heating, for which the FCI wave is weakly focalised at the plasma centre. More experiments are necessary, but already the possible role of cavity modes might explain the Δt decrease for unusually large energies absorbed by the fast ions at low powers.

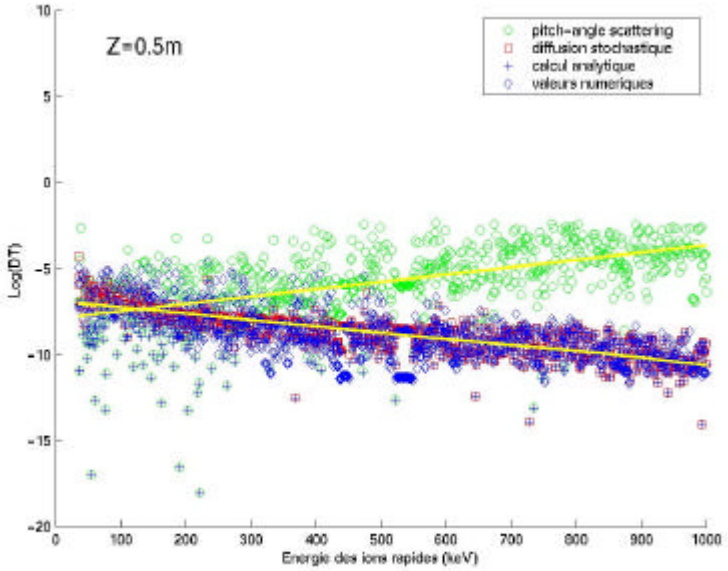

Figure III-56 : Evolution of Dt as a function of energy for ions initialised on the ion cyclotron resonance layer at the centre of the good confinement zone at Z=0.5 m. At high energy, stochastic diffusion is more important and $Dt_{stochastic}$ decreases, whereas pitch angle scattering is weaker, so that the total time Dt does not decrease, which means a symmetry effect of the ion ripple losses

III.3.4. LH experiments analysis

III.3.4.1. Analysis of the PPI 1999 water leak

The experimental Tore Supra campaign prematurely ended in 1999 because of a water leak on the first internal wall (PPI). The leak localisation has permitted to attribute its origin to a very localised fast electron impact produced during lower hybrid heating. The acceleration and the loss of these electrons are very different from what had previously been observed in the case of high energy de-coupled electrons created during disruptions or of low energy electrons accelerated in front of the hybrid grill. This subject is very important for future machines and a study has been started using the Tore Supra diagnostics (hard X-ray and CCD cameras).

These electrons, whose average energy is 100 to 200 keV, are accelerated in the central plasma by the hybrid waves and lost by a slow diffusive process. The scenario during which the leak occurred (hybrid waves coupling and low plasma density) is the most unfavourable one for the material surfaces interacting with the edge plasma, since thermal fluxes of more than 10MW/m^2 can be obtained.

The purpose of the future Tore Supra experimental campaigns is to generate long duration plasmas using, among other things, high power hybrid waves coupled to low density plasmas. This fast electrons phenomenon will therefore be further investigated in order to protect the Tore Supra limiters.

III.3.4.2. Dynamic of fast electrons accelerated by lower hybrid waves

The dynamic of fast electrons produced by the hybrid wave was studied in detail with the tomography of hard-X ray bremsstrahlung radiation, which allows to follow the dynamics in space of the velocities and configurations as functions of time.

In the absence of sawteeth, the non-thermal bremsstrahlung X emission is linearly dependent on the plasma current I_p, and independent of the ratio P_{LH}/n_l , in which P_{LH} is the injected power and n_l the central line density. Such a dependence is in agreement with the fact that collisional relaxation of the fast electrons produced by the wave, is the dominant energy transfer process with thermal electrons. This suggests that the radial transport of fast electrons, if it exists, plays a small role, as confirmed by the theoretical models (cf. hard-X ray modelling).

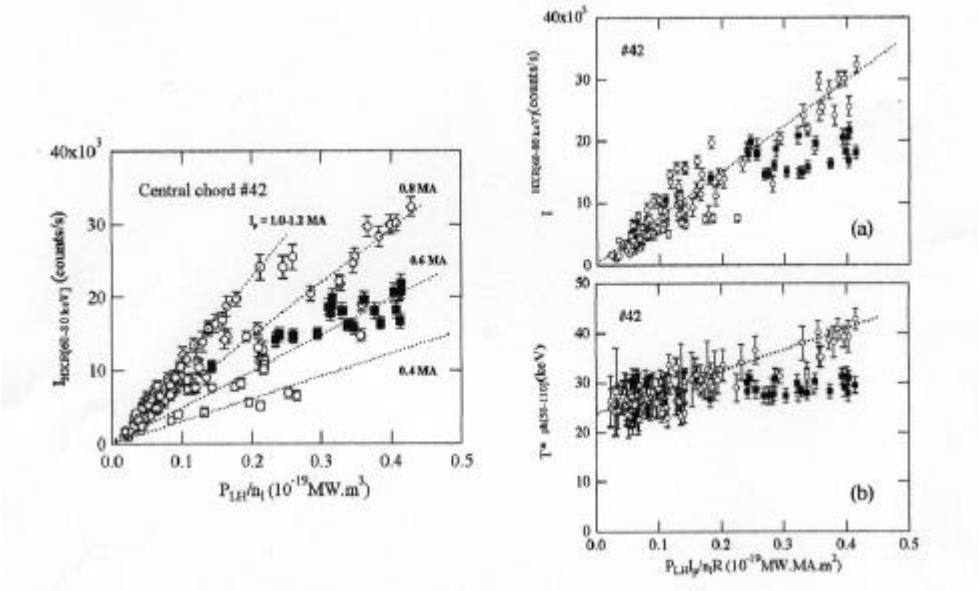

Figure III-57 : Bremsstrahlung radiation intensity between 60 and 80 keV, and photon temperature T_{ph}^{*} defined between 50 and 110 keV. The empty circles correspond to regimes without MHD, and the black squares with MHD.

The simultaneous increase, at constant P_{LH}/n_l, of the intensity of the X-ray emission and of the photon temperature, T_{ph}^{*}, with I_p, is a new result, which provides essential information on the dynamics of the fast electrons produced by the hybrid wave. Indeed, the fact that these two phenomena are concomitant indicates that the non-thermal tail tends to spread towards higher energies when increasing I_p. These electrons being less collisional, there is an improvement in the efficiency of current generation by the hybrid wave, which is actually observed in totally non-inductive regimes.

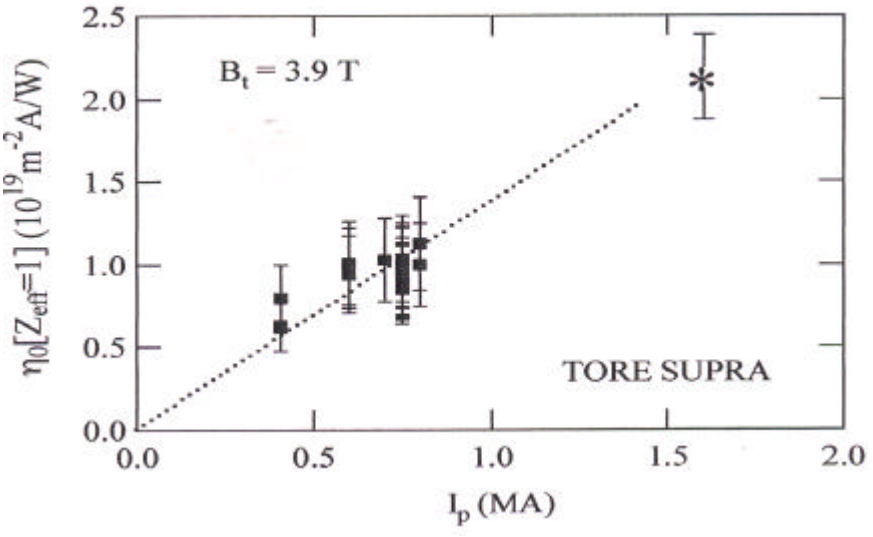

Figure III-58 : Improvement of the efficiency of hybrid wave current generation in totally non-inductive regimes, as a function of plasma current I_p

It must be noted that the electron losses in the local mirrors between two toroidal coils entirely confirm this analysis, since the average energy of the lost electrons greatly increases with plasma current, at constant collisionality.

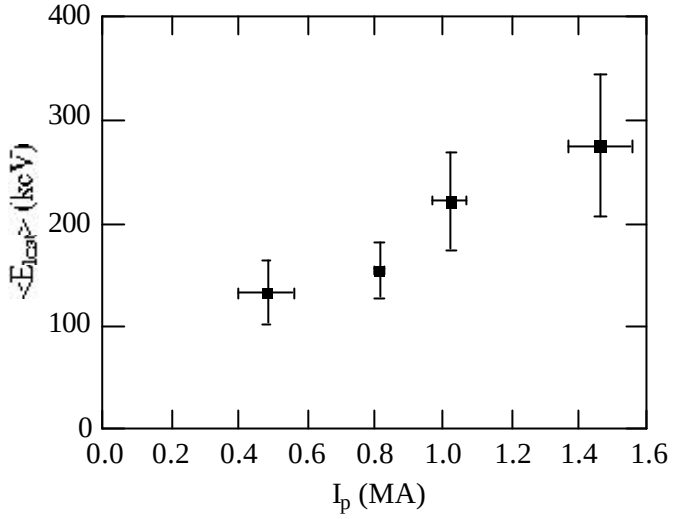

Figure III-59 : Average energy of fast electrons determined by the diagnostic of losses in the local mirrors.

Such a result has very significant consequences on non-inductive current generation scenarios and on extrapolations to a reactor, since the parametric dependence of the hybrid wave efficiency, η_{LH}, versus the volume averaged electron temperature, $<T_e>$, is only one of the indirect consequences, the energy confinement also improving with the plasma current. Such a dependence probably results from the broadening of the hybrid wave propagation domain with I_p, the electrostatic wave being able to propagate with lower $n_{//}$ values, resonant electrons then having a much higher energy. A ray tracing study confirms this analysis. It is important to note that this result suggests that the wave absorption is complete after a reduced number of plasma crossings, which is coherent with the parametric dependence of the power deposition profiles as functions of the antenna phasing. Indeed, in the inverse case, i.e. in very low absorption regimes, the initial phase memory would have been lost.

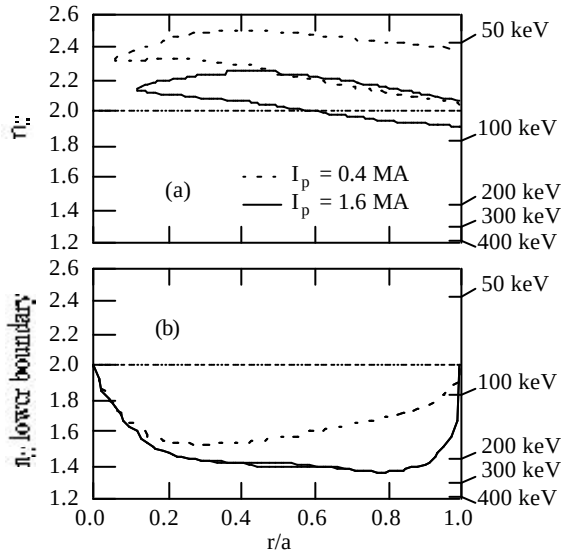

Figure III-60 : Evolution of hybrid wave propagation domain as a function of plasma current, all the other parameters being constant. The effect of plasma current on the ray trajectory under similar plasma conditions is also shown. The resonant electron energy is indicated on the right.

The comparison of regimes with and without MHD (mode tearing, m/n= 2/1) allowed the role played by the fastest electrons to be confirmed. Indeed, in the presence of MHD, at constant plasma current, a significant decrease in the hybrid wave current generation efficiency is noted, and is correlated with a significant decrease of X-ray intensity and photon temperature. The simultaneous decrease of these

three parameters can only be interpreted by the loss of the most energetic electrons produced by the hybrid wave, which is coherent with the fact that these are the same electrons which are most sensitive to a magnetic perturbation in the plasma.

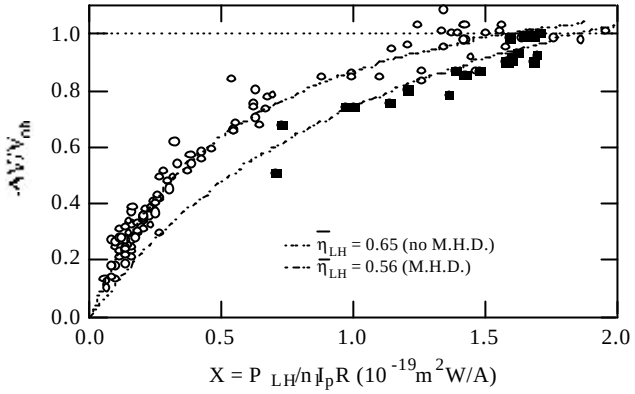

Figure III-61 : Relative variation of the loop voltage in the presence of a hybrid wave, without (white circles) and with (black circles) MHD; I_p = 0.8 MA. The parametric adjustment helps to estimate the average value of the hybrid wave current generation efficiency.

The hypothesis advanced on the role played by the fastest electrons of the distribution tail in non-inductive regimes were studied using the solution of the 2D relativistic Fokker-Planck equation in the velocity space. Based on a simplified but realistic modelling of the electrons quasi-linear diffusion process, induced in a resonant way by the wave electric field along the field lines, the role played by the most energetic electrons was confirmed. A measured 40 keV photon temperature in the absence of MHD is compatible with the minimum value of $\eta_{//}$ of about 1.6, very close to the values deduced from the propagation conditions of the hybrid wave, the electrons thus being accelerated up to energies of approximately 160 keV. A significant wave downshift thus occurs, the spectrum of the injected hybrid wave being centred on $\eta_{//}$ = 2. The fact that, experimentally, T_{ph}^* decreases by 10 keV in the presence of MHD indicates that electrons with an energy over 110 keV are de-confined before being able to participate to the current generation process. The result is a decrease of 50% in the intensity of the X ray emission intensity between 60 and 80 keV, whereas the current generation efficiency only decreases by 10-15%, relative values very close to experimental observations. It is interesting to note that in this regime, the minimum value of the wave-number in the plasma is comparable to that for which the power spectrum is maximum. The residual ohmic electric field effect on the bremsstrahlung radiation remains weak, the observation domain corresponding to the energy interval where the wave plays a dominant role.

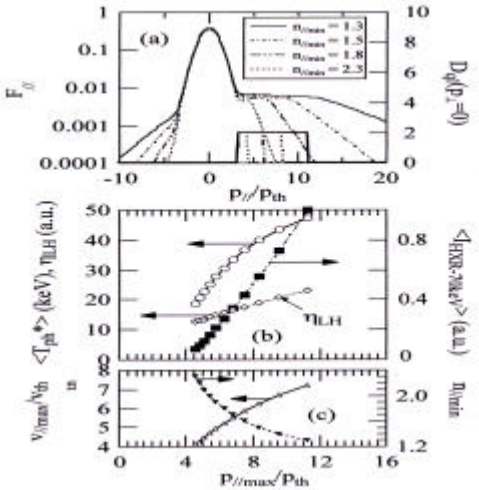

Figure III-62 : Parametric dependence of the photon temperature, of the bremsstrahlung radiation intensity between 60 and 80 keV, and of photon temperature calculated in the 50-110 keV interval as functions of the upper limit of the quasi-linear diffusion domain.

The behaviour of the fast electrons generated by the hybrid wave was studied at high plasma current (I_p = 1.4-1.6 MA), in the presence of giant sawteeth (m/n = 1/1) and of a several MW cyclotron heating. The bremsstrahlung X-ray emission between 20 and 40 keV shows, in the centre of the plasma, strong amplitude modulations, correlated to those observed on the central electron temperature. This modulation tends to disappear at higher energies.

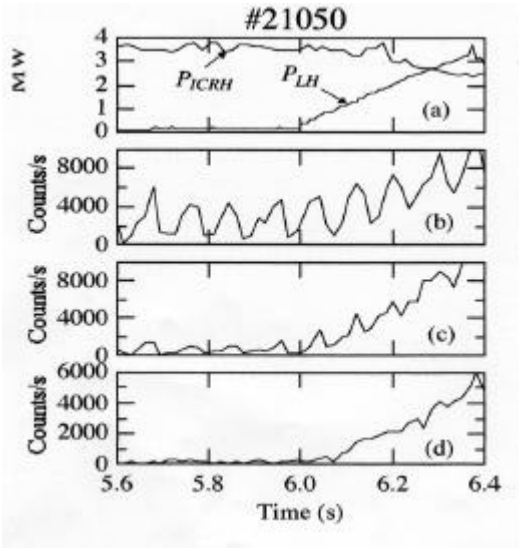

Figure III-63 : Evolution of modulations associated to saw teeth at different X-ray radiation energies, (b) 20-40 keV, (c) 40-60 keV, (c) 60-80 keV.

A detailed study has shown that this effect is due to the spatial localisation of the electrons outside the surface q = 1, because of the strong plasma current and the high density in this regime to allow an optimal coupling of the FCI power. The results of this analysis, based on a ray tracing calculation coupled to a Fokker-Planck 2D code, are that the fast electrons transport is very weak, and that the dominant mechanism is collisional relaxation. A natural follow up to this study would be to treat regimes for which the hybrid wave power deposition is more central, inside q=1, so as to follow their space-time dynamics.

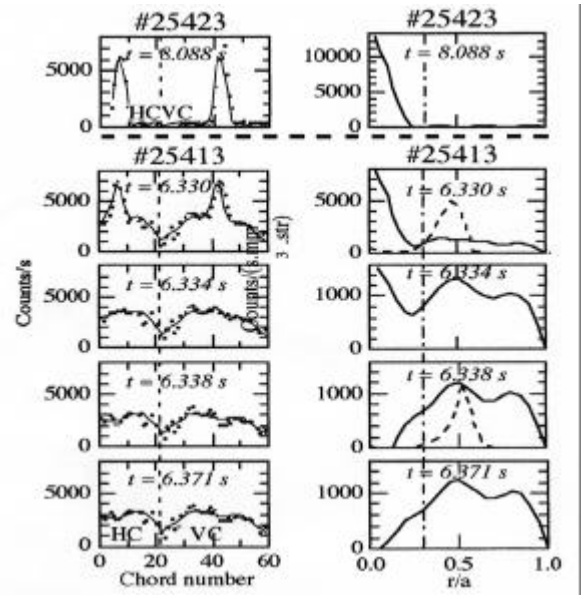

Figure III-64 : Evolution of the X ray emission radial profile between 60 and 80 keV during a sawtooth cycle (left: profiles integrated on the lines of sight; right: local profiles after Abel inversion). Dotted lines show the profile predicted by the tracing code coupled to the Fokker-Planck equation, and the vertical dash-dot line at r/a ˜ 0.3 represents the position of the surface q = 1.

III.3.4.3. Role of MHD in LHEP experiments

The role of the wave-guides phasing on the current profile control has been clearly demonstrated. By increasing the phase, the hard X ray emission profile, which is the faithful representation of the power deposition, tends to significantly broaden, in correlation with the decrease in internal inductance.

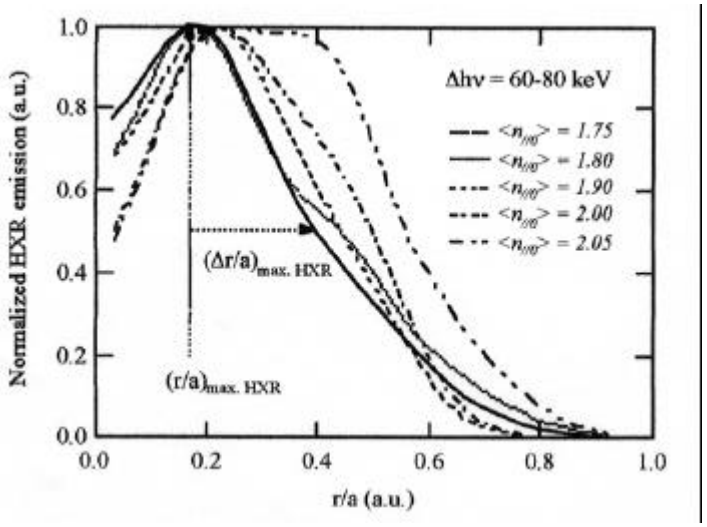

Figure III-65 : Evolution of power deposition profile of the hybrid wave with antenna phasing.

When the flattening of the safety factor profile becomes significant, at zero loop voltage, an improvement of the confinement in the region with flat magnetic shear is observed. During the last campaign, it was not possible to maintain this regime for longer than a few seconds, of the order of the resistive diffusion time; the appearance, with a precursor, of a global tearing mode led to an irreversible performance deterioration, in terms of confinement and current generation.

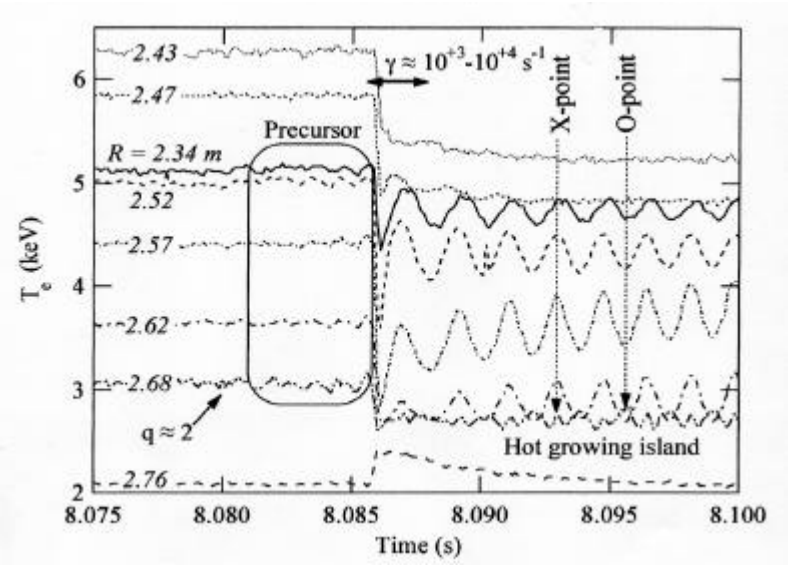

Figure III-66 : Time evolution of the electron temperature observed by the radiometer. The appearance of a precursor is clearly observed before the tearing mode starts (m/n = 2/1)

For current generation, the observed decrease remains limited, since the loss of the fastest electrons is localised in the island region, which can be clearly seen for the first time by hard X ray tomography. This result is promising for the reactor since the region concerned by such a mode, if destabilised, will have a marginal radial extension compared to the plasma size.

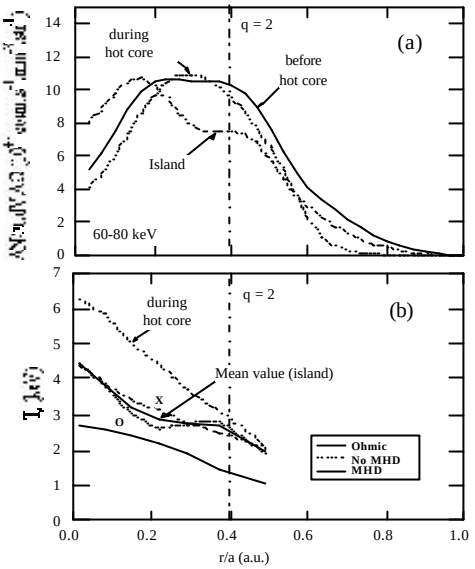

Figure III-67 : Evolution of the hard X-ray emission profile between 60 and 80 keV, as well as of electron temperature profile, before and after the starting of the tearing mode. A flattening in both types of profiles near q = 2 is observed, showing the existence of a global island, approximately 10 cm in width.

It is interesting to note that the island associated to the tearing mode is large, its width being approximately 10-12 cm. It is clearly seen with the superheterodyne radiometre (T_e), but also with the hard-X ray tomography. The island time evolution shows that it is a heated island, which is coherent with the fact that there are still fast electrons in this island in spite the high MHD activity, as evidenced by the hard X-ray. The appearance of the MHD activity, which is systematically associated to a tearing mode (m/n= 2/1) is very closely correlated to the localisation of the hybrid power deposition, at zero loop voltage. When this deposition is central (case $<n_{//0}>$ = 1.8), no MHD activity is observed for more than 10 s, but no transition to an improved confinement regime is obtained. The correlation between the two effects is clearly identified.

The calculation of the current profile resistive evolution in the plasma, using the hybrid current source directly from the hard X ray emission profile between 60 and 80 keV, shows with great accuracy that the MHD activity systematically starts if the flattening of the safety factor profile around q = 2 is too marked. With the CASTOR code, it is shown that when the hybrid power deposition is broad, i.e. the q profile is progressively flattened over a large area (r/a < 0.4) around q = 2, the discharge trajectory at low β_p (about 0.35) invariably enters the region where the tearing mode (double or global) is unstable. By increasing the value of β_p, it is possible that an operational stability window exists. At too high a value of β_p, the infernal resistive modes take over. It is not possible to consider stabilising the tearing mode by injecting FCE power in the island, as the required power levels are too high. It is preferable to avoid entering the unstable area by increasing the value of β_p, therefore by strongly heating the plasma in this regime. It is however not sure that this stability window exists, since it is very dependent on the plasma electric conductivity. An experimental validation of this point is essential.

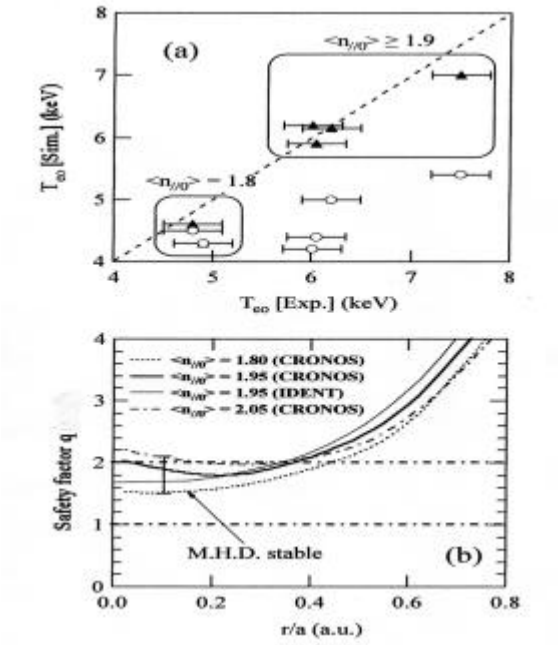

Figure III-68 : Correlation among the safety factor profile q(r), the appearance of an improved confinement regime (black triangles), and the triggering of MHD.

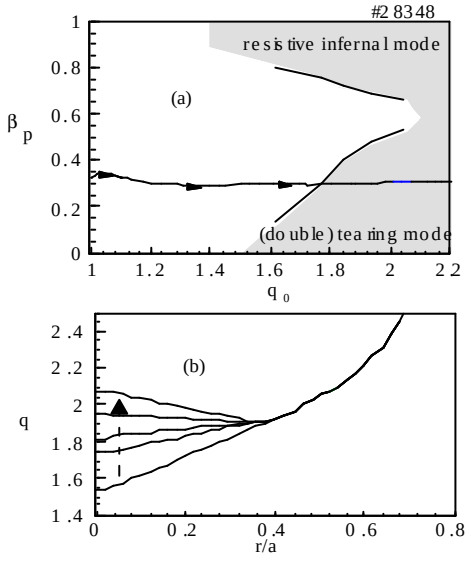

Figure III-69 : Stability of a LHEP discharge as a function of the safety factor profile, q(r), time evolution.

The role played by the low order rational surfaces has been identified not only for q = 2, but also for q = 3/2. Indeed, before entering the improved confinement regime, there is systematically a roll over, characterised by a fast decrease of plasma performances. This behaviour is associated to the triggering of a tearing mode (m/n= 3/2), whose consequences on the confinement are less disastrous than for the case (m/n = 2/1), the magnetic shear not being close to zero near q = 3/2 when the current profile evolves.

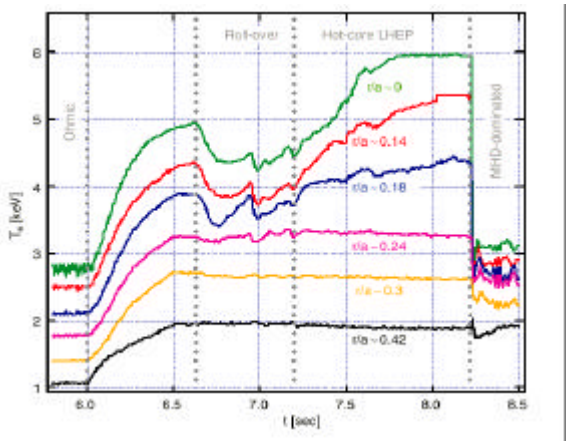

Figure III-70 : Time evolution of plasma temperature measured by the superheterodyne radiometer. The presence of the roll over can be seen, as well as the improved confinement regime, and then the MHD phase.

It is particularly interesting to note that the simultaneity of improved confinement and MHD, clearly identified for the physics associated to q = 2, is also found for q = 3/2, and, moreover, in a dynamic way. Indeed, the transition to the improved confinement regime of LHEP type is associated to the progressive disappearance of the surface q = 3/2 in the plasma. It is possible to monitor this confinement improvement from the time evolution of relaxations with a saw tooth shape, associated to the annular cyclic re-connection of the double tearing mode around q = 3/2. The inversion of the sawtooth shape for a given line of sight is the signature that the sawtooth inversion radius moves radially as does q = 3/2, and it is noted that this inversion is associated to a local transition towards improved confinement, as shown by the resulting irreversible temperature increase.

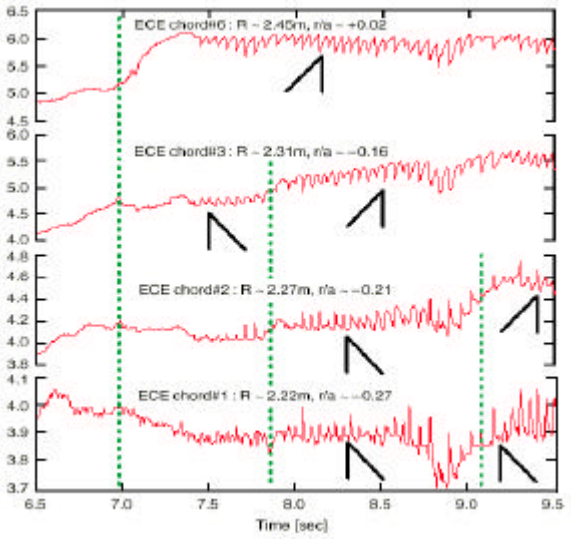

Figure III-71: Time evolution of the temperature at four different radii, and of the relaxations associated to the cyclic re-connection of the tearing mode m/n=3/2. Each sawtooth inversion is associated to a jump in temperature, reflecting a local confinement improvement. This process does not appear at the same time at different radii, thus reflecting the radial evolution of the q(r) profile as a function of time.

The link between low order rational surface and confinement improvement, which was identified in an analogous way on T-10 with the FCE wave, is not taken into account in the simulations carried out with CRONOS. Only a criterion of magnetic shear flattening is taken into account in the bifurcation to an improved confinement regime. That is why the roll over observed on the electron temperature is not described by the code.

III.3.4.4. Bremsstrahlung radiation code

Based on the work done at the beginning of the '90s, a multi-machine code on bremsstrahlung radiation was developed. It was initially devoted to circular or elliptical plasmas, knowing hat its structure could be extended to calculate plasmas with an X point. With a graphic interface and on line help, this tool allows the thorough investigation of the evolution of non-thermal bremsstrahlung radiation in the presence of LH or FCE waves, and especially a detailed comparison with experimental results. It is now operational on Tore Supra, HT-7 (China), and C-MOD (United States). The calculation of distributions is either based on simplified modelling of wave physics - for a fast investigation, filled with the physics content of parametric dependencies (3D Fokker-Planck, kinetic drift equation, 3 temperature distribution, simple beam) -, or based on wave propagation and absorption codes integrating the plasma equilibrium, such as KOLTRA (wave diffusion + 3D Fokker-Planck) and DELPHINE (ray tracing with all equilibria plus relativistic 2D Fokker-Planck). A detailed analysis at different photon energies shows that the power deposition predicted by the present models is still too narrow compared to experiments (KOLTRA or DELPHINE). A better quantitative agreement is obtained for high energies ($h\nu > 100$ keV) by introducing a radial transport proportional in intensity to the component $v_{//}$ parallel to the magnetic field of the electron velocity, $D = D_0 v_{//}/v_{th}$ with $D_0 = 0.2$ m^2/s. However, between 40 and 100 keV, the radial dependence remains very poorly described. On the other hand, with KOLTRA, it was possible to quantify the LH+FCE synergy experimentally observed on Tore Supra during the 1999 campaign. The effect remains weak, in good agreement with the experiment. It is to be noted that the energy dependence of non-thermal bremsstrahlung radiation is generally very well described by simulations, especially the photon temperature T_{ph}^*, which measures the exponential decrease of the radiation intensity with photon energy.

Future improvements are planned for the bremsstrahlung radiation code : integration of the helicity of field lines, trapped particles, X ray retro-diffusion of the walls and contribution of recombination radiation.

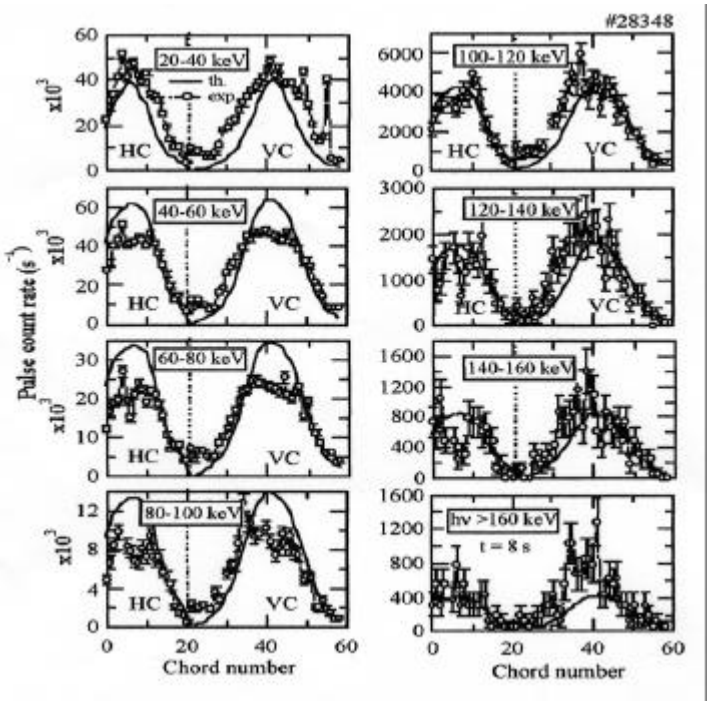

Figure III-72 : Radial profiles integrated along the DSPX diagnostic cords at different energies (circles : experiment; full line : simulation based on KOLTRA code); Tore Supra discharge #28348 at t = 8 s.

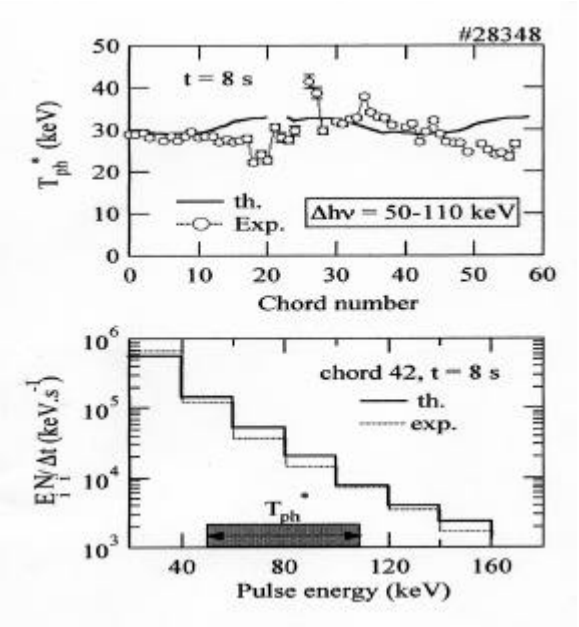

Figure III-73 : Energy and photon temperature (T_{ph}^*) spectra (simulation based on KOLTRA code) for Tore Supra discharge #28348 at t = 8 s (central cord number=42).

III.3.4.5. Power deposition on walls by parasitic absorption of LH power

The power deposition on the lateral protections of the new hybrid coupler has been compared to that measured by IR thermography on the first generation of coupler protections. For the same injected HF power, the deposited power flux is lower for the new coupler. This result is in agreement with the theoretical model predicting that the scaling parameter is the electric field (lower for this new antenna), and not the coupled power. By plotting the deposited power flux versus the HF power density (proportional to the average HF field at the antenna mouth), a univocal relation is seen for both couplers (figure III-74).

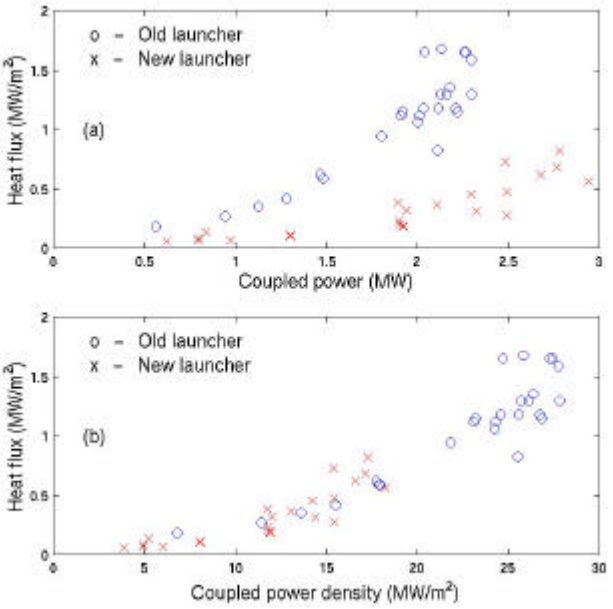

Figure III-74 : Power flux deposited on LH antenna lateral protections as a function of coupled HF power (a), and coupled HF power density (b).

From a theoretical point of view, within the collaboration with the EURATOM/IPP.CR Association (Prague), a new modelling of the particle dynamics near the antenna has been started. It takes into account the random fields which can be spontaneously excited. These fields reinforce the particles acceleration and lead to a power absorption over a radial width more similar to the experimental one. A 3D fluid model was developed, showing that the high electrostatic potential which develops, contributes to accelerating both the ions and electrons. Two HF probes were installed on the new hybrid coupler so as to particularly show the effect of these random fields.

III.3.5. First experiments with electron cyclotron frequency wave

III.3.5.1. Tearing modes stabilisation by non-inductive current generation

Applications and theoretical developments of the theoretical model developed in 1998-1999 to describe tearing modes stabilisation by non-inductive current generation have been made. This model couples the Rutherford equation, which describes the evolution of the magnetic islands width, to a kinetic equation for the evolution of the electron distribution function under the effect of wave absorption. An important characteristic of the model is the inclusion of island rotation effects and of the finite response time of the electromotive force due to current generation. The same model has been, on the one hand, extended to the stabilisation of neo-classic tearing modes (NTMs), by coupling it with a self-coherent calculation of the bootstrap current, made by solving a pressure evolution equation, by including parallel and perpendicular transport effects. On the other hand, the effects of island geometry were studied by developing a specific code. Applications were made to the stabilisation experiments of the NTM modes made on ASDEX Upgrade, with very satisfactory results. This experimental validation allowed this model to become the reference model for the stabilisation of NTM modes on ITER. Figure III-75 shows a calculation of the evolution of a (3,2) island, in the presence of localised current generation by electron cyclotron waves on ITER.

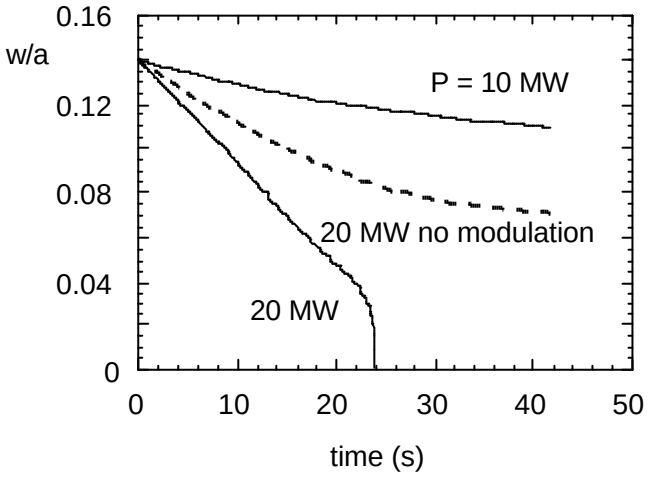

Figure III-75 : Calculation of the evolution of a (3,2) island with localised FCE current generation on ITER.

III.3.5.2. Elaboration of models for heating and current generation

Heating and non-inductive current generation are influenced by both kinetic effects and macroscopic heat and current transport. In regimes where the confinement greatly depends on the current profile shear, this leads to non-linearities, which make predictive modelling of these regimes difficult. In view of the importance of these types of regimes in the achievement of long duration discharges on Tore Supra, a numerical model combining the kinetic equation, lower hybrid and cyclotron electron wave propagation equations, and macroscopic transport equations, has been developed. The main aim of this work is the systematic study of the fundamental properties of a complex system of this type, where the current and temperature profiles are coupled through the absorption of waves and the dynamics of the 3D electron distribution function. The existence of stationary regimes obtained by LHCD and characterised by the presence of an electron transport barrier was demonstrated by a self-coherent

calculation. These stationary regimes greatly depend on the initial conditions (especially the minimum value of q, as is shown in figure III-76). It is possible to control the position of the barrier by injection of waves at the electron cyclotron frequency of power comparable to the LH waves (figure III-77). The synergy phenomena between the two waves have been demonstrated by a self-coherent calculation. The same phenomena were also studied with an analytical approach. Other complex kinetic phenomena occur when the power density coupled to the electrons is very high. A complex numerical calculation, using a high-resolution kinetic code with parallel programming, has shown the possibility of distortion of the electron distribution function at low velocity, under the effect of intense electron heating. For example, for parameters typical of electron cyclotron heating experiments on FTU (P_{ECRH} ~ 0.8 MW, n_e ~ 3 10^{19} m^{-3}), the calculated distribution function shows a flattening for velocities lower than the thermal velocity, as shown in figure III-78a, to be compared with the Maxwellian distribution (figure III-78b). This distortion has a deep impact on the electron cyclotron emission spectra measured by a Michelson interferometer. These spectra cannot be reproduced by a calculation which uses a Maxwellian function. However, the high-resolution kinetic calculations are in excellent agreement with the experimental spectra, for several discharges (figure III-78c). An important consequence of this study is the existence of out of equilibrium regimes, in which the heat transport cannot be described in terms of electron temperature, but only in terms of the average kinetic energy associated to the non-Maxwellian distribution function.

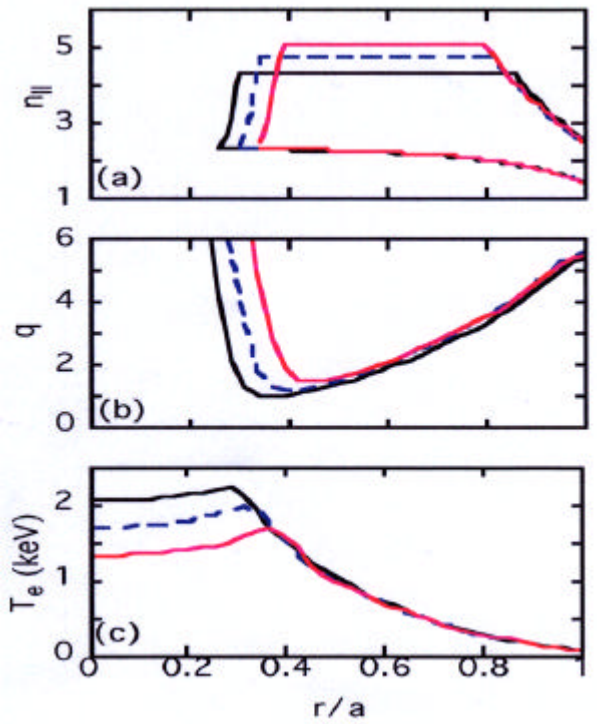

Figure III-76 : Three stationary states obtained by self-coherent calculation of the distribution function of electrons and of heat and current transport, for three different initial conditions (thin full line : q_{min} = 1 ; dashed line : q_{min} = 1.5 ; thick full line : q_{min} = 1.6). a) propagation region of LH waves ; b) q profile ; c) T_e profile. Tore Supra parameters: B = 2 T, n_{e0} = 3.5 10^{19} m^{-3}, P_{LH} = 3 MW.

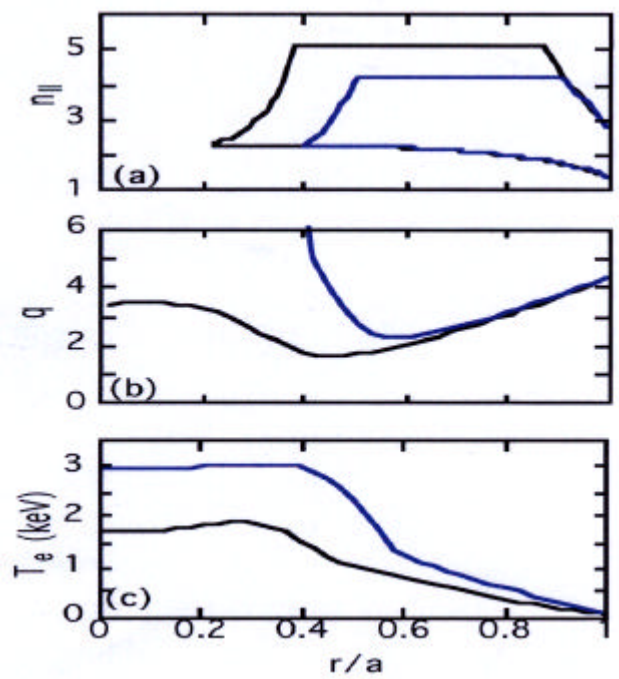

Figure III-77 : Stationary states in the presence of only 3 MW of LH waves (thin line) and with 3 additional MW of ECRH power absorbed at mid-radius (thick line).

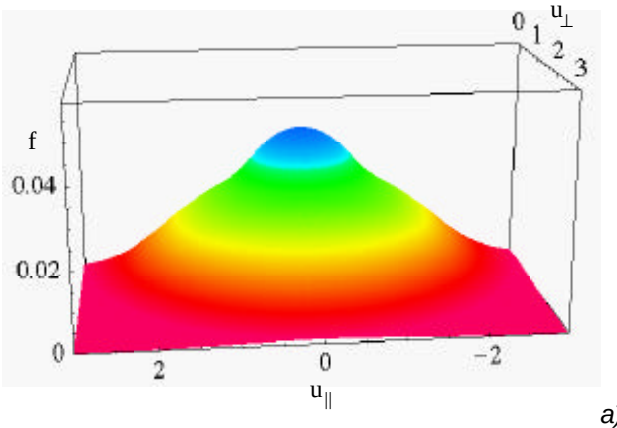

a)

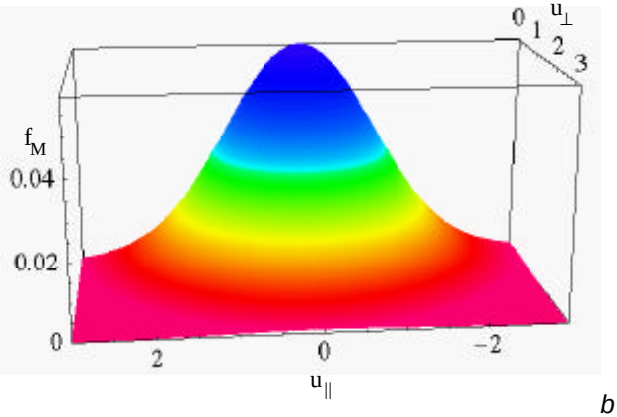

b)

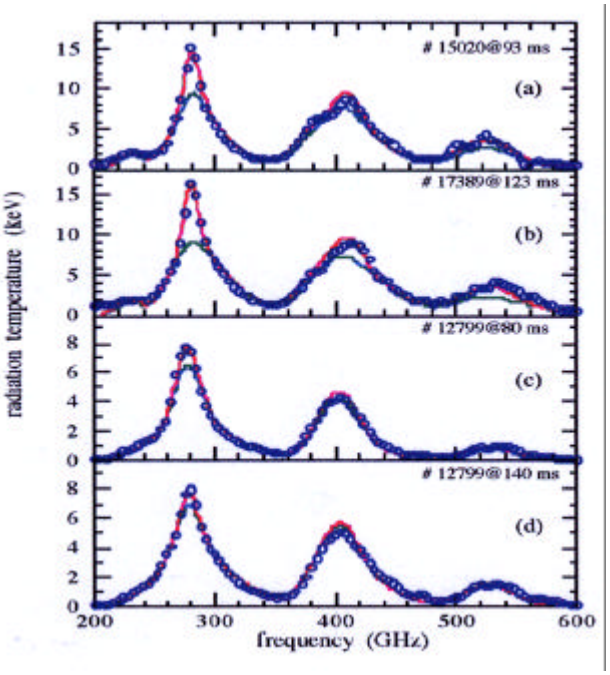

c)

Figure III-78 : a) Electron distribution function calculated in the presence of FCE heating. The velocities are normalised to the thermal velocity. b) Maxwellian distribution function for the same parameters as in a). c) Electron cyclotron radiation spectra measured for several FTU discharges (circles), and calculated by the kinetic code (red curves) and the Maxwellian code (green curves).

III.3.5.3. Theoretical studies on synchrotron radiation in tokamaks

The problem of synchrotron radiation in a tokamak and the associated losses in a reactor have been considered. The theory of these losses is still based on the work of Trubnikov, particularly concerning the effect of reflections by the walls. This theory uses the hypothesis that synchrotron radiation is proportional to $n_e^{1/2}$, where n_e is the electron density. A recent study determined a somewhat different scaling law (n_e^{α}, with $\alpha \sim 0.4$). The consequences on the reflections by walls are significant : for values of the wall reflection coefficient R of about 0.9, the losses by synchrotron radiation can be reduced by a factor of 1.5. This loss reduction is shown in figure III-79 as a function of R, for three values of α.

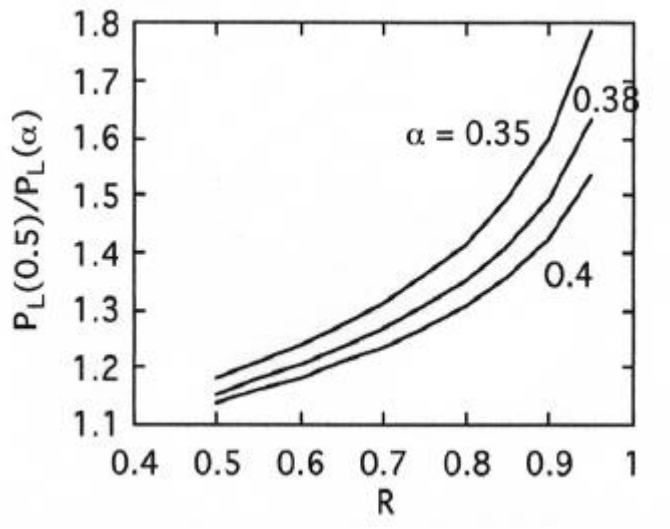

Figure III-79 : Loss reduction factor for synchrotron radiation, relative to the Trubnikov formula, as a function of the wall reflection coefficient, for three values of the exponent α.

A complete formulation of the synchrotron radiation transport has been elaborated for realistic conditions of toroidal geometry, with a poloidal section presenting an elongation, and for arbitrary density and temperature profiles, by using an exact method to calculate the absorption coefficients. In particular, this formulation allows the calculation of losses by synchrotron radiation for plasmas with an arbitrary aspect ratio and temperature profiles characteristic of Advanced Tokamak modes, which the previous formulations did not take into account accurately. It has been found that the temperature profile effect is quantitatively significant. As an example, it has been shown that in the high temperature plasmas considered for a stationary commercial reactor, synchrotron radiation losses represent about 20% of the total losses. In view of the quantitative importance of the above effects, a new scaling law (with 7 parameters) for a fast calculation of synchrotron radiation losses was proposed. This law gives an accuracy of about 6% within a range of parameters covering the entire domain useful for controlled thermonuclear fusion.

III.3.5.4. FCE heating experiments on TS

At the end of 1999, the first experiments on electron cyclotron heating were carried out on Tore Supra, using a 118 GHz gyrotron. The analysis made during the years 2000 and 2001 revealed problems with the mirrors orientation and the polarisation of the injected waves. Once these problems were solved, the experiments resumed after Tore Supra started up again. The gyrotron power was this time modulated at different frequencies from 4 to 20 Hz. The electron cyclotron emission signals showed an excellent response to the heating of electrons (figure III-80), thus allowing to clearly localise the power deposition, in agreement with the propagation and absorption calculations. This is a good basis for the use of modulated electron cyclotron heating for the study of heat transport in several Tore Supra operating regimes.

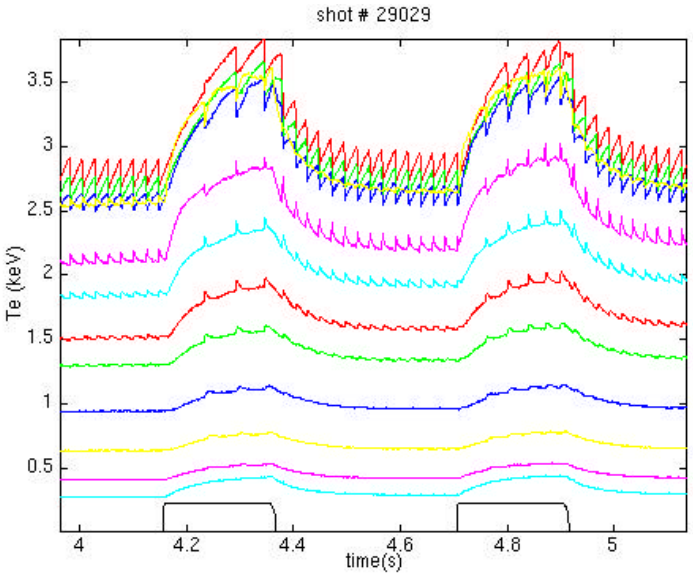

Figure III-80 : Response of electron temperature (measured by the different ECE cords) to two FCE pulses (approximately 500 kW each). This shows that the wave power was absorbed near the sawtooth inversion radius.

III.3.6. Experiments with combined LH and FCE waves

III.3.6.1. Tore Supra

Finding a synergy between the hybrid wave and the electron cyclotron frequency (FCE) wave is an important research subject, one of the aims being to improve the efficiency of current generation obtained with the hybrid wave by accelerating the electrons in resonance with this wave at even greater energies. Experiments have been carried out, in a totally non-inductive regime, with 4 MW of hybrid power. The available FCE power not exceeding 300 kW, it can only induce a simple

perturbation to the general dynamics of the electrons produced by the hybrid wave. When the FCE wave is injected perpendicularly to the toroidal direction (ECRH regime), no effect on the energetic electrons is observed. With a 30° toroidal injection angle (ECCD regime), a clear increase of the X-ray radiation intensity is observed at all energies, up to 200 keV, indicating without any doubt a direct interaction of the FCE wave with the high energy electrons. The change in the slope of the emission spectrum is however too weak, compared to the error bars, to be able to prove a synergy mechanism. Indeed, an increase in the photon temperature T_{ph}^{*} is the most obvious signature of a synergy effect. This synergy effect is only experimentally observed when the FCE wave power deposition predicted by a ray tracing code, coupled to a Fokker-Planck module, coincides radially with that of the hybrid wave. When this radial alignment is absent, no effect of the EC wave on the fast electrons is observed.

III.3.6.2. FTU

The simultaneous use of electron cyclotron frequency (FCE) and lower hybrid frequency (LH) waves opens interesting perspectives for the control of the current profile and, therefore, of the confinement. The absorption of electron cyclotron waves by the fast electron tail created by the hybrid waves, in the absence of a «cold » resonance in the plasma, extends the application domain of electron cyclotron heating to very high magnetic fields. These two types of application were tried out on FTU (Euratom-ENEA Association, Frascati), in close collaboration with the DRFC, with the loan of the hard X-ray camera and a significant participation in the preparation, achievement, analysis and interpretation of the experiments.

The main results were the following :

- Heating of the plasma by FCE wave absorption by the fast electron tail created by the LH waves was demonstrated in conditions of absence of a « cold » resonance in the plasma (figure III-81 a and b),
- A regime with a very marked transport barrier was obtained, by using as target a plasma with inverted shear produced by the LH waves, and by heating with the FCE waves in the region with s = 0 (figure III-82a). The transport model which reproduces well the target plasma (Bohm/gyro-Bohm with shear function f(s)) under-estimates the temperature in the LH+FCE, phase, which implies the establishment of a regime of better confinement. Excellent agreement is obtained using a shifted shear function, i.e. f(s) $\rightarrow$ f(s-0.5) (figure III-82b). This seems to indicate a stabilising role of the pressure gradient (alpha-stabilisation), already observed on DIII-D, and predicted by the theory of ITG type turbulence.

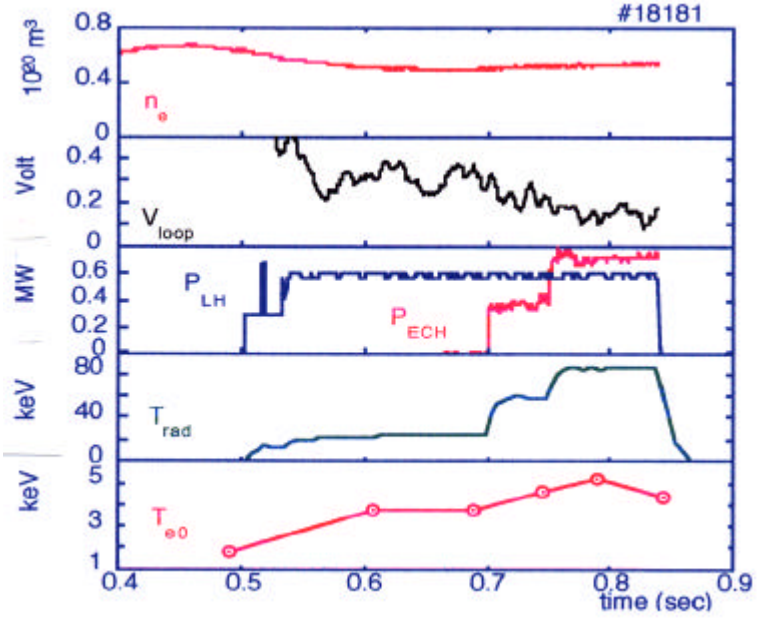

a)

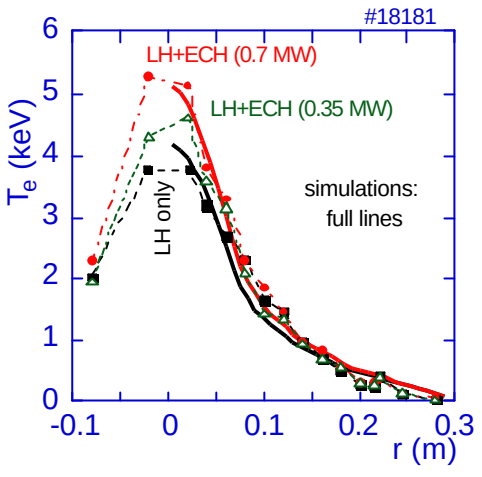

b)

Figure III-81 : a) FTU, discharge #18181 at B = 7.2 T. Time evolution : 1) average line density, 2) loop voltage, 3) power of the two waves, 4) suprathermal cyclotron emission (Michelson); 5) central electron temperature (Thomson scattering). b) FTU, discharge #18181 at B = 7.2 T. Electron temperature profiles measured by Thomson scattering in the LH phase and in the LH+FCE phase. Simulations made using the ASTRA transport code.

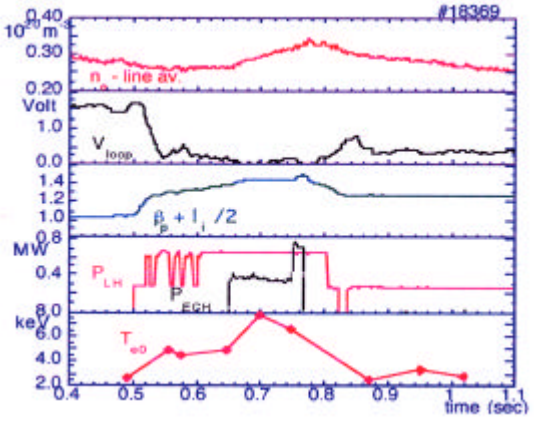

a)

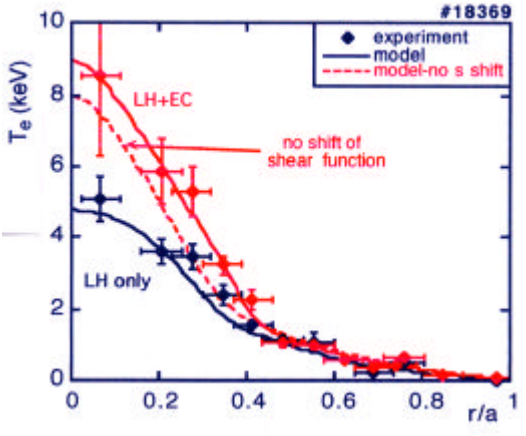

b)

Figure III-82 : a) FTU, discharge #18369 at B = 5.3 T. Time evolution : 1) average line density, 2) loop voltage, 3) $b_{pol}+l_i/2$; 4) power of the two waves, 5) central electron temperature (Thomson scattering). b) FTU, discharge #18369 at B = 5.3 T. Electron temperature profiles. Experimental points and results of transport simulations (lines) by using the Bohm/gyro-Bohm model with shear function f(s).P_{LH}=0.65 MW, P_{ECH}=0.36 MW. To reproduce the LH+EC phase, the shear function was shifted, i.e. f(s) ® f(s-0.5). The dashed curve corresponds to the simulation without this shift.

III.3.7. Modelling of runaway electrons

Runaway electrons are mainly created during plasma disruptions and can damage the first wall. They can therefore raise a serious problem in tokamak plasmas. These runaway electrons can also appear, in fewer quantities, in normal discharges, especially at low density. They then give useful information on magnetic turbulence. It is thus important to understand the physics governing their behaviour.

The ARENA code (Avalanche of Runaway Electrons Numerical Analysis) was developed to obtain realistic numerical simulations of runaway electrons. The ARENA code solves a relativistic Fokker-Planck equation, averaged over a complete orbit, by a Monte Carlo method. This code treats the generation of runaway electrons, both by the usual Dreicer acceleration mechanism and by close collisions, namely the avalanche effect. Synchrotron radiation also generally plays an important role and is included in the modelling.

A study on the influence of runaway electron radial transport on the avalanche effect was carried out with the ARENA code, in collaboration with the UKAEA Culham (U.K.). An analytical theory was developed. This study shows that the radial transport induced by magnetic fluctuations could indeed eliminate the avalanches of runaway electrons during a disruption if the amplitude of the fluctuations is greater than $\delta B/B \sim 10^{-3}$. An important element of the last version of the ARENA code is the integration, in a self-consistent manner, of the electric field induced by runaway electrons. A specific algorithm was developed, since the obvious solution leads to unstable solutions. It is to our knowledge the only code taking into account the electric field in a self-consistent way. After a disruption, the current carried by the runaway electrons can be important, and in some cases decreases over a time of a few seconds. To simulate this runaway electron current decrease, it is very important to properly model the induced electric field. This can be seen in figure III-83, showing three different simulations for typical parameters of the JET tokamak. The first simulation only takes into account collisions. The second one adds the effect of synchrotron radiation and the third is a complete simulation, including the self-consistent electric field. It must be noted that synchrotron radiation plays an essential role. It is however obvious that it is absolutely necessary to include the self-consistent electric field in these simulations.

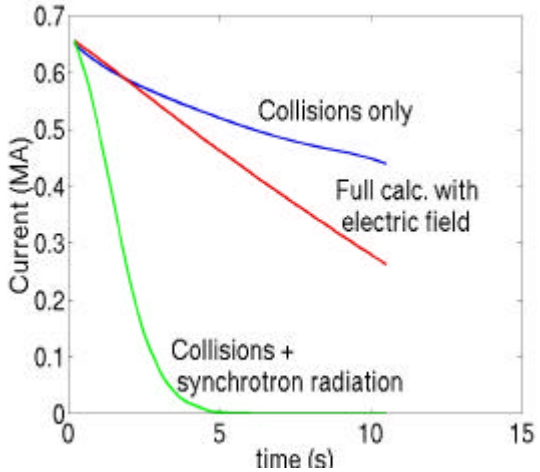

Figure III-83 : Calculated decrease of runaway current for a JET type plasma

III.3.8. Current and heat diffusion

An important effort over several years has been made from a numerical point of view to develop the CRONOS code. This code allows to analyse or to predict the space-time dynamics of profiles (current, pressure), and also to study the control possibilities, in a self-coherent way with the toroidal plasma equilibrium, the heat and current sources. This work corresponds to a coherent effort of integration, around a common architecture, of numerous analysis tools (equilibrium, heating and current generation codes…), more specifically developed at DRFC. This integration is necessary to numerically study stationary tokamak operation in the advanced regime. Indeed, under conditions

where a large part of the plasma current is generated non-inductively, there are significant non-linear couplings between confinement, current and heat sources. For example, the non-inductive bootstrap current which is self-generated, proportionally to the plasma pressure, can change the current profile and consequently improve the plasma confinement and pressure, resulting in an increase of the bootstrap current. These couplings are surely at the origin of the bifurcation process of the heat transport towards improved confinement states, which can be simulated by CRONOS by integrating all this physics. Independent codes could not account for this dynamics.

In its recently improved version, the CRONOS code solves current, heat and particle transport equations in a coherent way with the 2D equilibrium solution (Grad-Shafranov equation). The coherence between the equilibrium and evolution equations is ensured at each time step by an iterative method. The CRONOS code can now treat different equilibria in a predictive or interpretative way : circular (Tore Supra), with X-point separatrix (JET and ITER), with high poloidal beta, with high triangularity (ITER), …. In addition, a user-friendly interface of the code was written so that CRONOS be easily accessed by the different users. This code is now interfaced with the Tore Supra and JET databases; in the following, the use of the code is illustrated with Tore Supra and JET data.

The CRONOS code was recently used in an interpretative way in a current resistive diffusion mode to simulate performing discharges in Tore Supra and JET. It allows in particular to reconstruct the evolution of the safety profile factor and to determine the current fractions generated non-inductively (self-generated bootstrap current, current generated by hybrid waves…). The determination of the time dynamics of the current profile is important since the safety factor plays an essential role in both the macroscopic stability and the thermal energy confinement of the discharge. Figure III-84 shows the complete analysis of the resistive diffusion of a Tore Supra discharge in which the plasma current is entirely generated by the hybrid wave. The calculation of the current profile (figure III-84b) is validated by simulating the time evolution of the loop voltage (V_s), of the internal inductance (ℓ_i), and of the integrated Faraday rotation angle measurements. In this discharge, the safety factor profile goes from a standard monotonous profile in the ohmic phase to a non-monotonous profile. A similar analysis was also made with discharges approaching a zero loop voltage regime recently obtained on JET. The difficulty in the simulation is in the coherent calculation of the evolution of the profiles in the situation of a strongly perturbed plasma equilibrium : high elongation equilibrium with separatrix, the current on the magnetic axis being close to zero and the plasma pressure, normalised to the poloidal magnetic field pressure (factor β_p) being large (regime with internal transport barrier and reduced plasma current). One of the greatest advantages of the code is that it allows the direct reconstruction of the raw signals measured by the current profile diagnostics : this is a unique characteristic among all the available codes. This reconstruction of measured signals can be obtained by using the coherent resolution of the 2D plasma equilibrium. Figure III-85 (a-b) shows the time evolution and the profiles of the Faraday rotation angle and the polarisation angles of the impurity lines by the Stark effect (MSE diagnostic). These two independent diagnostics both measure the plasma safety factor. The agreement between the experimental and simulated values gives confidence in the non-inductive currents estimation (figure III-85c). Thus, in the example shown in figure III-85, 80% of the plasma current is maintained non-inductively and the bootstrap current reaches a value of 1MA.

Lastly, the code can also be used predictively to simulate the coupled evolution of the current and temperature profiles. Figure III-86 shows this use of CRONOS for a Tore Supra discharge. The simulation was performed for an experiment in which a transition of the central electron temperature (T_{eo}) is observed at approximately t=7s. To reproduce in a self-coherent way this confinement bifurcation, a dependence on the local shape of the current profile was included in the electron transport model. When this dependence is taken into account, it is possible to describe the existence of several electron heat transport states and to reproduce the transport bifurcation process towards a better confinement state. Indeed, the electron heat transport coefficient attains in the plasma centre a level near that observed in the ohmic heating phase, in spite of the application of 4.6 MW of additional lower hybrid power.

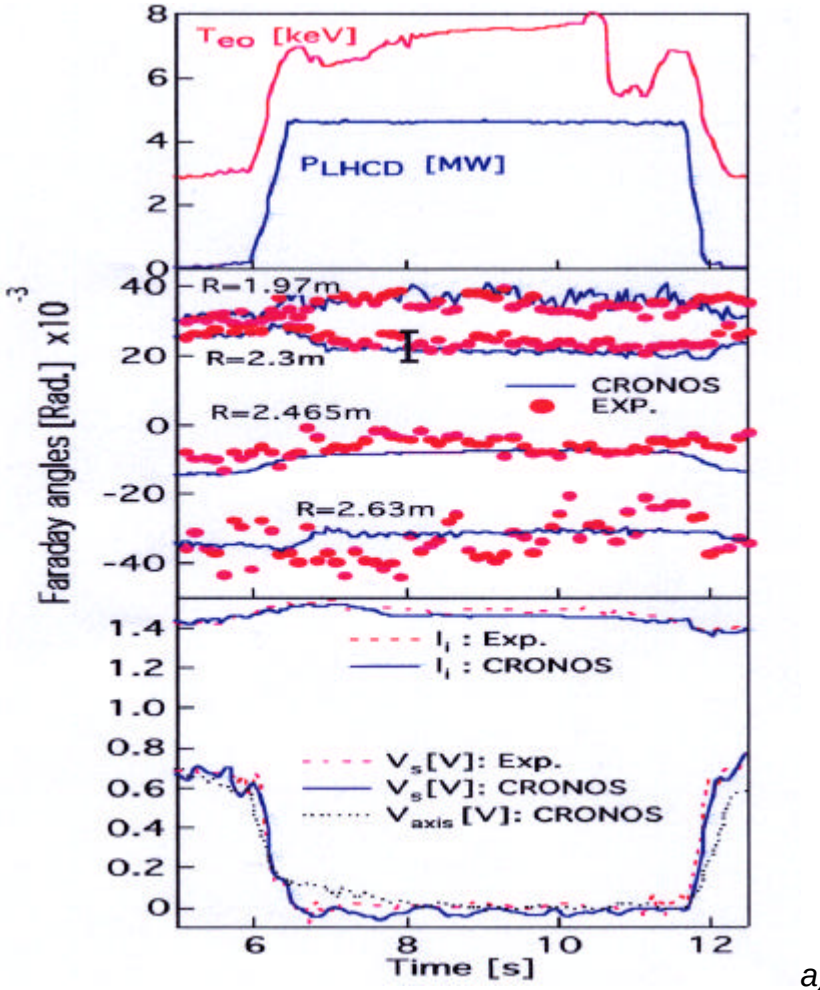

a)

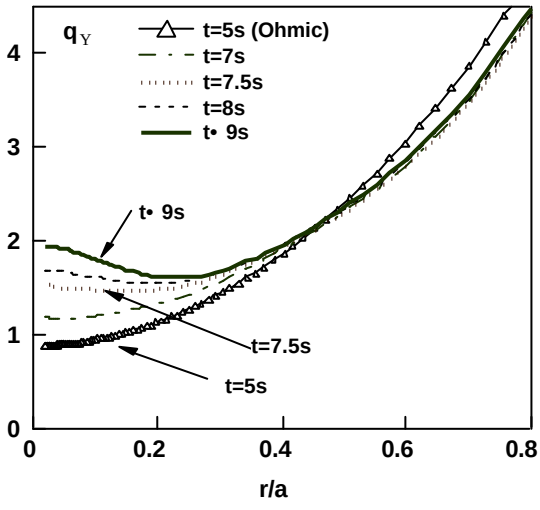

b)

Figure III-84 : Analysis of resistive diffusion (CRONOS) of a Tore Supra discharge with zero loop voltage (#28342) with a large current fraction generated by the hybrid wave. a) time evolution of experimental and simulated signals by CRONOS. b) resistive evolution of the current profile.

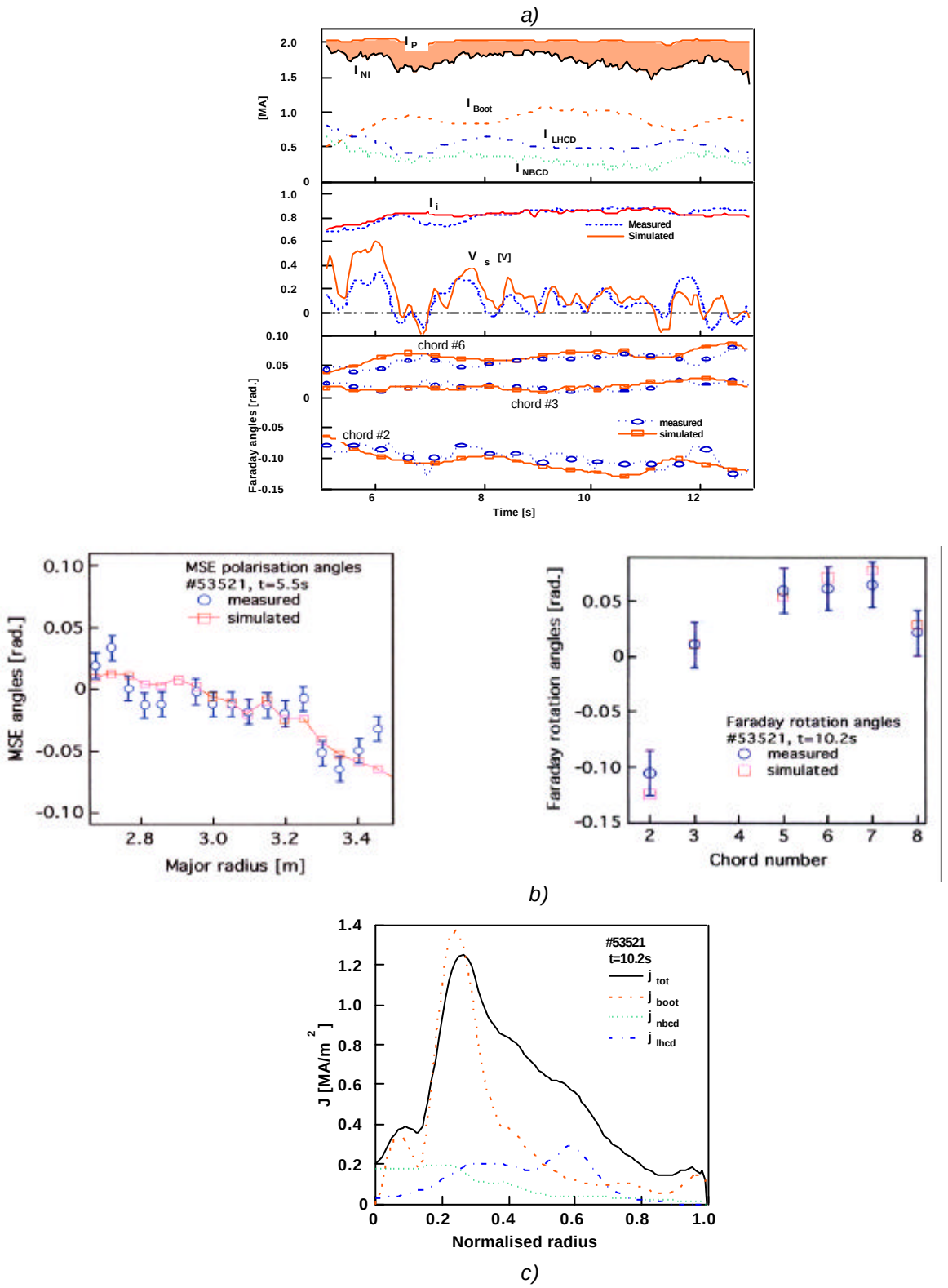

Figure III-85 : Analysis of resistive diffusion (CRONOS) of a quasi-stationary discharge in JET (#53521) with a large non-inductive current fraction. a) time evolution of bootstrap current (I_{Boot}), of neutral injection (I_{NBCD}), of lower hybrid (I_{LHCD}) of the sum of non-inductive currents (I_{NI}); time evolution of loop voltage and internal inductance, and of Faraday rotation angles (measurements : dots, simulation : full line). b) Measurement and reconstruction of MSE polarisation angles as functions of the major radius (t=5.5s) and of Faraday rotation as a function of the measurement cord number (t=10.2s). c) total and non-inductive current profiles (t=10.2s)

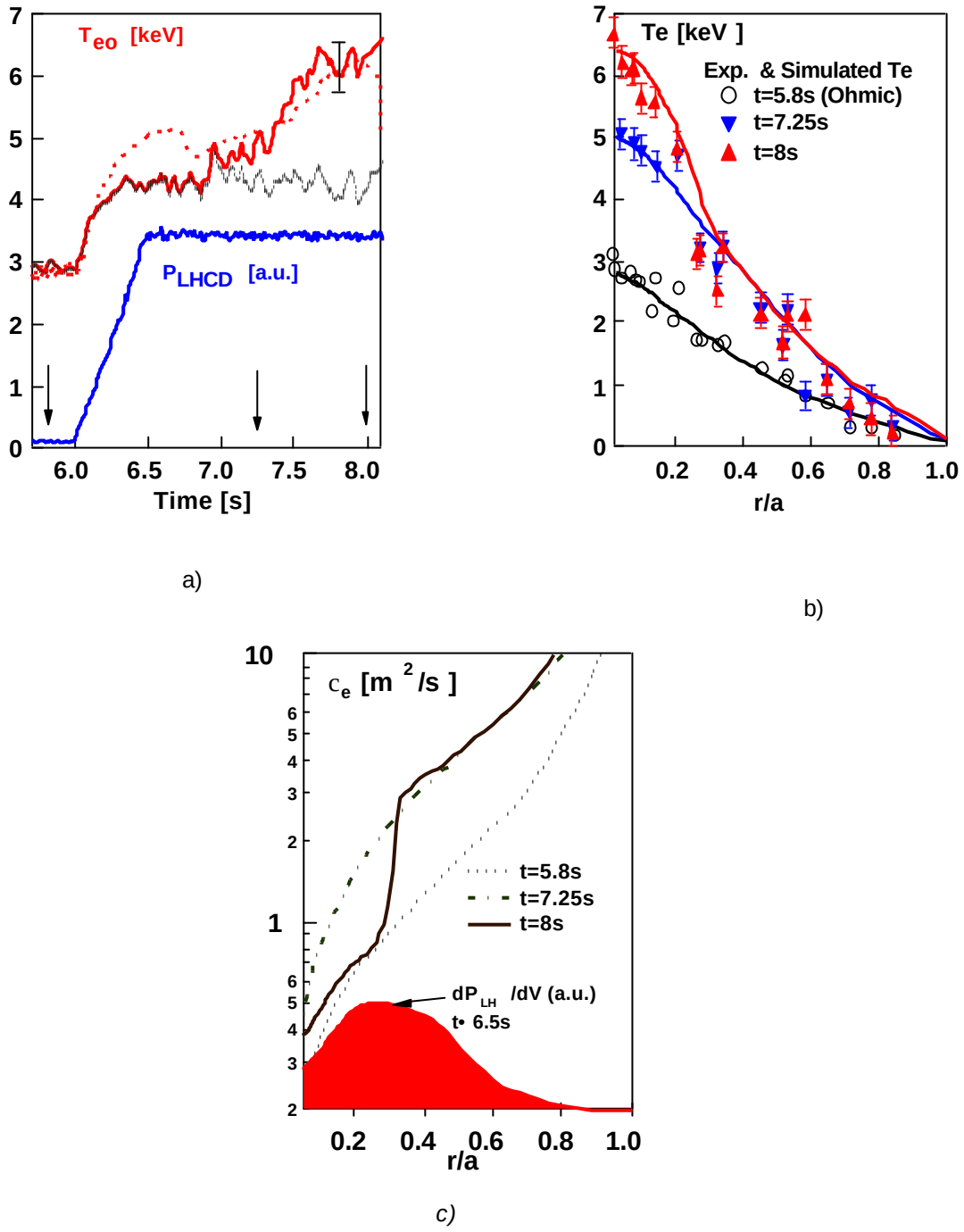

Figure III-86 : Predictive simulation of electron transport in a stationary Tore Supra experiment characterised by a bifurcation of electron transport at the plasma centre (#28348). a) time evolution of the central electron temperature, T_{eo},; full line : simulation taking into account the current profile role in heat transport to reproduce the T_{eo} bifurcation; vertical line : measured T_{eo}; dashed line : simulation without taking into account the current profile role in heat transport. b) electron temperature profiles (full line) and experiment. c) electron diffusivity profiles and LH power deposition deduced from hard X-ray radiation profile measurements.

III.4. Transport, turbulence and MHD

III.4.1. He transport in advanced scenarios with internal transport barrier

This work is one of the results of a collaboration between the Euratom-CEA Association and the Euratom-OAW Association (Austria). Within this framework, advanced scenarios with ITER-type plasmas were numerically studied in the presence of an internal transport barrier. Helium transport was modelled by introducing a « two groups » model, by separating fast alpha particles and helium ashes. This is a step forward compared to previous simulations. It has been assumed that the ion thermal transport coefficients given by the Bohm/gyro-Bohm model were also valid for the transport of helium ashes. Another progress concerns helium recycling, which was described as a source term of particles coming from the wall. As an entry parameter to these simulations, the effective helium recycling coefficient was used (recycling coefficient including the pumping efficiency at the edge), R_{eff}, rather than the ratio of effective helium confinement time to the energy confinement time, τ^*_{He}/τ_E. Indeed, even for a given scenario, the τ^*_{He}/τ_E ratio is a quantity which is strongly time-dependent, and it is not constant, as was assumed in previous studied. Parametric studies of the recycling influence and of the pumping efficiency are therefore possible. It is concluded that a very good knowledge of the actual recycling coefficient is necessary to make more realistic simulations.

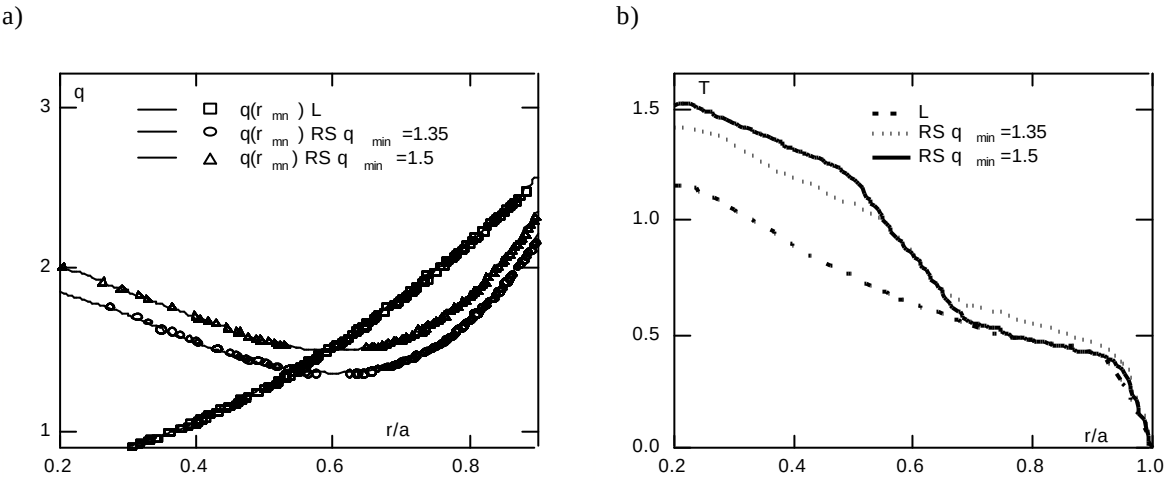

Figure III-87 : a) Monotonous and inverse safety factor profile (two values of q_{min}, one being close to the « simple » rational 3/2). b) Corresponding temperature profiles.

III.4.2. MHD

Traditionally, there are two ways to explain transport barriers with inverse magnetic shear. The first explanation is based on a weakening of the exchange instability when the magnetic shear is negative. The second one is based on the decrease of the number of resonant surfaces near the nil magnetic shear region. 3D fluid simulations of an ion turbulence with monotonous or inverse safety factor q profile (figure III-87a) show that an ion temperature barrier appears when the shear is inverse (figure III-87b). The barrier appears near the nil magnetic shear region. The confinement is better if the minimum safety factor is close to a «simple » rational (here 3/2). This result is in favour of an explanation based on the resonant surface density near the minimum safety factor. These simulations also show that the barrier broadens due to the poloidal velocity shear, which appears when the pressure gradient increases. A variation in heating power indicates that there is no power threshold when the q profile is sufficiently inverted.

The density profiles in a tokamak are generally modelled by invoking a particle flux directed towards the magnetic axis. This flux is called pinch. To this day, there is no satisfactory model to explain this particle pinch. The neo-classic theory predicts a pinch proportional to the loop voltage, called Ware pinch. However, this pinch is in agreement with the experimental values only in the most central parts

of the plasma. It seems that the pinch in the more peripheral areas is linked to turbulent transport. Two explanations have been proposed. One is linked to the magnetic field gradient; it predicts that the pinch is proportional to the safety factor gradient. In the absence of particle sources, the «natural » profile is inversely proportional to the safety factor. The second type of model is based on the thermo-diffusion phenomenon, appearing when the diffusion coefficient in the phase space is energy dependent. A component of the particle flux is then proportional to the temperature gradient. A pinch appears when cold particles diffuse faster than the fast particles. In this case, the natural density profile is a power of the temperature profile. This situation occurs naturally in the presence of an electrostatic turbulence. When the turbulence is of a magnetic nature, the inverse phenomenon occurs : fast particles diffuse more rapidly than the slow ones and the particle flux component proportional to the temperature gradient is directed outwards. The validity of this argument has been tested by calculating the test particle diffusion coefficient with electric potential perturbations. In order to do this, the trajectories of the guide-centre of 1000 particles were calculated for different perturbed potential parameters and several initial velocities. The diffusion coefficient was calculated from the particle exit time. The shape of the diffusion coefficient as a function of the initial velocity, normalised to the thermal velocity, is shown in figure III-88 for different values of the potential amplitude normalised to the temperature. It appears that the diffusion coefficient of slow particles is larger than that of fast particles. By assuming that the distribution function remains close to a Maxwellian, the particle flux can be calculated. The flux component associated to the temperature gradient is directed towards the magnetic axis. Thermodiffusion is therefore a possible explanation for the particle pinch.

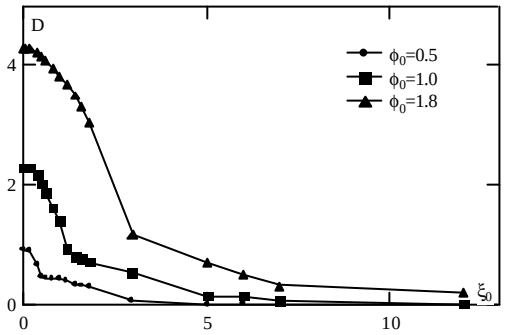

Figure III-88 : Diffusion coefficient as a function of the particle initial velocity for different values of the potential normalised to the temperature.

III.4.3. MHD in type II supraconductors

The scalar equation of the « critical state », which shows the effect of the vortexes anchoring force in type II supraconductors, limits the current perpendicular to the magnetic field, but does not limit the parallel current. This equation is classically used to study the evolution of macroscopic magnetic configurations inside a supraconductor in the case where the force lines are plane. It is not sufficient in the general case where the force lines are helicoidal, and where the current parallel to the magnetic field plays an important role. In this case, the evolution is based on an MHD constraint introduced by Josephson in 1966, which gives the magnetic variations caused by the «vortex » movement, and which is very similar to the MHD constraint applicable in hot plasmas. This MHD constraint must be completed by the law giving the vortexes velocity, as it is caused by magnetic and anchoring forces. Thus a complete model is obtained which theoretically solves all the evolution problems, starting from the initial situation and the evolution of the external conditions.

Particular interest was given to the case of configurations called « quasi without force », for which the current is nearly parallel to the magnetic field, which theoretically allows for large magnetic fields, not limited by the critical state equation limiting the transverse current. The study on the stability of these configurations, using traditional MHD plasma tools, is however essential. It provides an order of magnitude of the maximum current density, which can circulate in a supraconducting wire. This current, nearly parallel to the magnetic field, triggers instabilities of the « kink » type if it exceeds the « Kruskal-Shafranov limit », well known in tokamaks. However, when the energy reservoir due to the parallel current is too low, the unstable mode remains under the control of the vortexes anchoring force, appearing only as a small quasi-static deformation of the configuration. The current density can

then be increased until the perturbing force exerted on the vortexes is of the same order as the anchoring force. From this point, the configuration can no longer be maintained. Thus, a new stability criterion can be defined, which in fact allows for a current much greater than the Kruskal-Shafranov limit. The values given by this new criterion are in good agreement with experimental results.

In the case of a coil “quasi without force”, the current in each wire can be increased up to a limit calculated by the stability criterion above. However, non-acceptable kink instabilities, on the scale of the entire coil, should appear if the total current exceeds the Kruskal-Shafranov limit determined by the coil global geometry. Nevertheless, it still seems possible to stabilise the magnetic configuration beyond this criterion, by using a stabilising counter-reaction, since the unstable mode develops slowly. This type of configuration, which has not actually been experimented up to now, could be promising for producing high magnetic fields, particularly when high critical temperature supraconductors are used, for which the anchoring force is low, but the critical field is very high (≈ 100 T).

III.4.4. Electron transport

III.4.4.1. Analysis of electron transport in TS and ASDEX Upgrade

Tore Supra plasmas obtained during the stable (20 to 120 times the energy confinement time) phase of FCI direct electron heating (Fast Wave Electron Heating, FWEH) are characterised by a power deposition strongly peaked on the magnetic axis, a purely electron heating, a low coupling between ions and electrons, and the absence of energetic particles. They are an excellent tool for analysing electron transport and validating proposed models. Moreover, their conditions are similar to those which will be found in the future reactor. A base of 41 TS discharges has been made, gathering the results of helium plasma with hot electrons ($T_e > 2\ T_i$), covering a relatively wide range of parameters (injected power, density, plasma current,…). An analysis of electron heat transport, using FCE heating, was also made on the ASDEX Upgrade tokamak, within the framework of a collaboration with IPP Garching.

Different transport models were tested on the Tore Supra data-base of plasma using the FWEH scenario : Bohm/gyro-Bohm mixed models, Rebut-Lallia-Watkins (RLW, linear model with offset), Weiland-Nordman, and a model based on electrostatic turbulence (ES) or electromagnetic turbulence (EM) generated by ETG (Electron Temperature Gradient) modes. The ETG electromagnetic turbulence model gives the best results to reproduce the Tore Supra data (figure III-89). The other models simulate experimental data in an acceptable way, but with an accuracy lower than that of the electromagnetic ETG model (figure III-90).

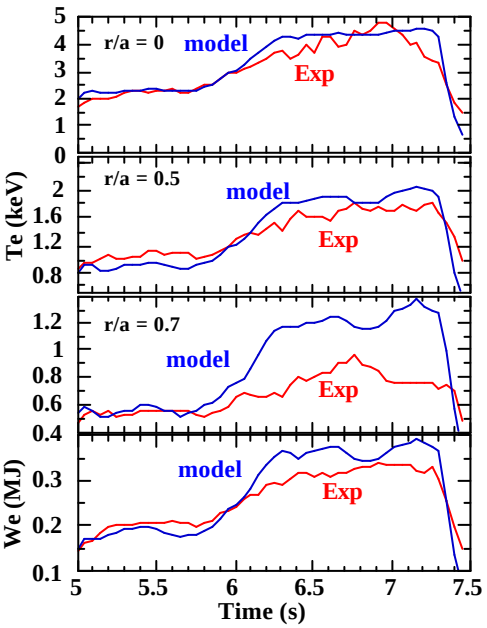

Figure III-89 : Simulation of a FWEH discharge with the electromagnetic ETG model (I_p = 0.65 MA, $n_e(0)=6.5x10^{19}\ m^{-3}$, P_{FW} = 3-6 MW)

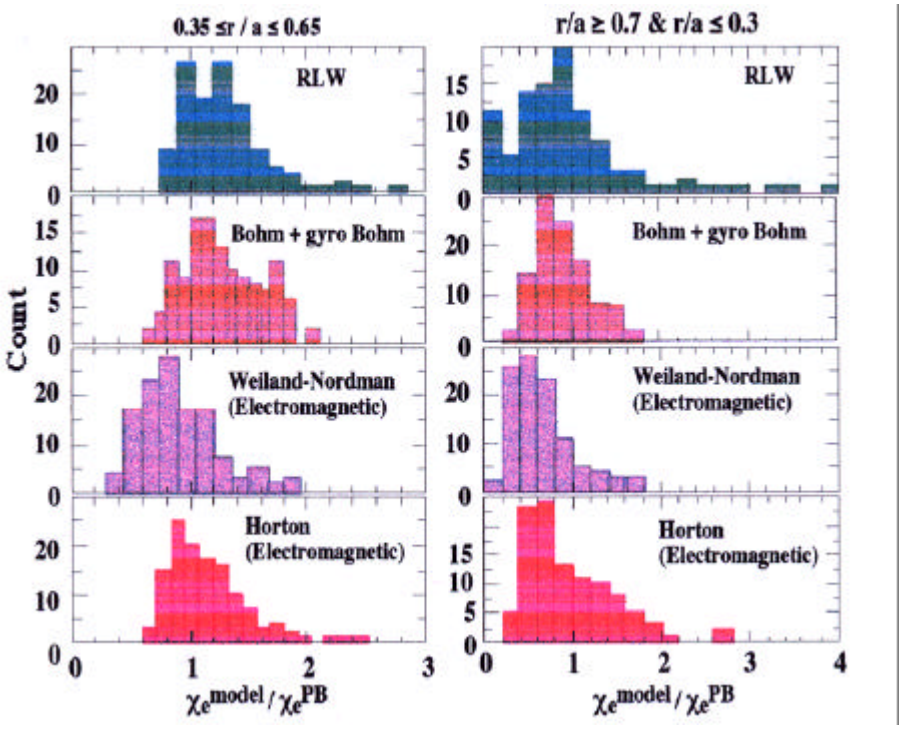

Figure III-90 : Histogram of results of different transport models, tested versus the experimental diffusion coefficient (Power Balance, PB), on the database. The RLW model was tested without the critical gradient term, the mixed Bohm/gyro-Bohm by dividing by 2 the constant used for JET, Weiland-Nordman by imposing a low value of the parameter $(k_q r_i)^2$ » 0.03.

It has been possible to show the existence of a critical gradient (figure III-91). The radial profile of this critical threshold, characterised by the inverse of the normalised electron temperature gradient length, and its dependence on the magnetic shear s and on the safety factor q were also determined. The experimental dependence is as follows : $R\nabla T_e/T_e \approx 5 + 10(s/q)$, where R is the plasma major radius. This dependence is in good agreement with linear gyro-kinetic calculations (figure III-92).

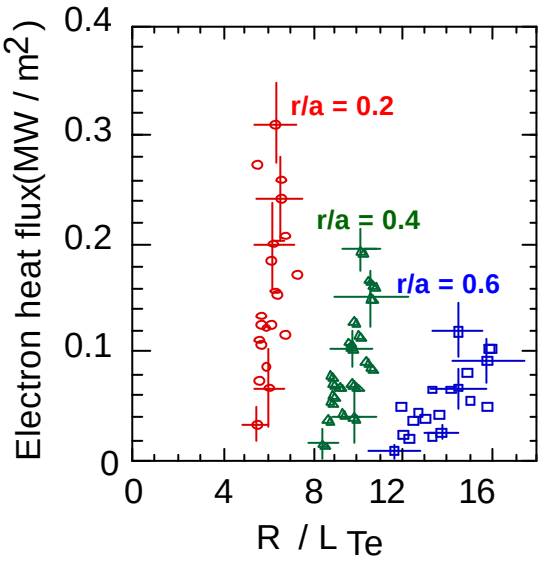

Figure III-91 : Electron heat flux as a function of the inverse of the normalised electron temperature gradient length (R / L_{Te} where $L_{Te} = T_e / \nabla T_e$) at several radial positions in the plasma and for heating powers varying from 1.5 to 7.4 MW.

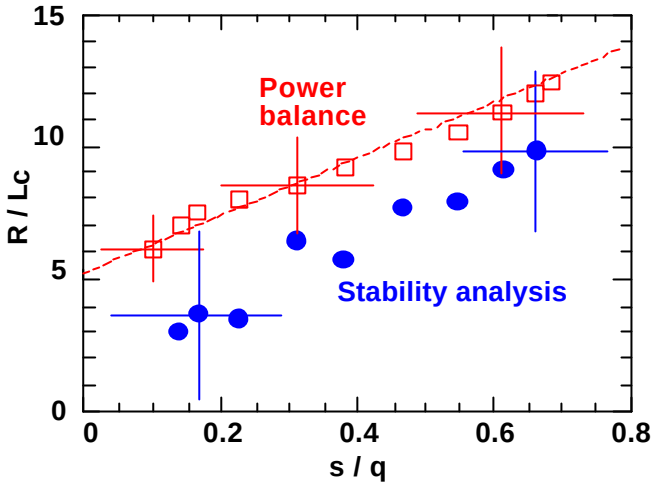

Figure III-92 : Inverse normalised critical gradient length as a function of s/q. Circles : experimental values ; squares : theoretical values.

An analysis of electron heat transport was realised on the ASDEX Upgrade tokamak, within the framework of collaboration with IPP Garching. The analysis of purely electron heating experiments by FCE waves has shown the existence of a critical threshold in the dependence of the diffusion coefficient as a function of the inverse of the electron temperature gradient length, above which heat transport considerably increases (figure III-93).

This result is all the more interesting as it opens the way to accurate comparisons with the Tore Supra results on electron transport, where the existence of critical gradient lengths was also shown. An interesting research subject for the future is particularly that of the linear dependence of the critical threshold as a function of the s/q parameter (ratio of magnetic shear to safety factor), deduced from the measurements made on Tore Supra, and which has not for the moment been found on ASDEX Upgrade.

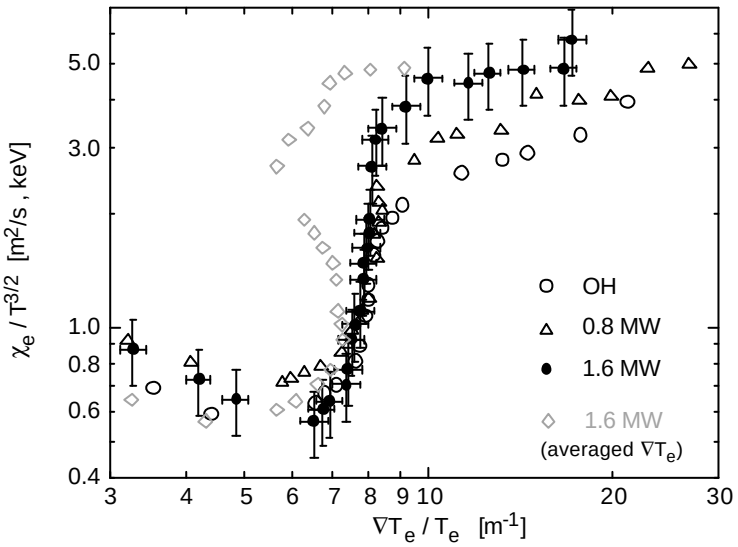

Figure III-93 : Diffusion coefficient normalised by an electrostatic gyro-Bohm dependence as a function of the inverse of the electron temperature gradient length, for different FCE heating powers (open circles : ohmic; triangles : 0.8 MW; full circles : 1.6 MW; diamonds : 1.6 MW; curve estimated from a temperature gradient averaged on the entire flux surface). Except for the diamond curve, the temperature gradient is estimated by the measurement on the low field side, in agreement with the turbulence hypothesis based on ballooning.

III.4.4.2. Modelling of FCE power modulation experiments on AUG

Experiments using modulated heating power are an exceptional tool for heat transport studies, since the analysis of the propagation of transient phenomena provides additional information compared to the stationary energy balance. Within the framework of a collaboration with the IPP Garching on electron heat transport, the modulation experiments, performed on ASDEX Upgrade with FCE waves, were modelled with a simple empirical model, based on the existence of an inverse electron temperature critical gradient length.

This model has shown to be very well adapted, qualitatively and quantitatively, to simulate ASDEX Upgrade modulation experiments. Indeed, the main result of these experiments was the existence of two different regimes of heat propagation generated by modulation, when a stationary, localised, heat source is added at mid-radius. Outside the stationary source position, the heat puffs propagate much faster than the prediction using the diffusion coefficient deduced from the stationary energy balance; on the other hand, inside this position, the propagation speed is of the same order of magnitude as the prediction using the stationary diffusion coefficient. This difference in propagation regime was interpreted as a consequence of the existence of an inverse electron temperature critical gradient length. A parametric study also allowed the dependencies of the diffuison coefficient as a function of temperature and inverse gradient length to be determined. The best agreement with experimental data is obtained with an electron temperature dependence at the power 3/2 (electrostatic gyro-Bohm dependence) and an almost linear dependence on the difference to the critical threshold .

This study, and the interest of its results, open the way to similar experiments foreseen on Tore Supra with the new FCE heating system.

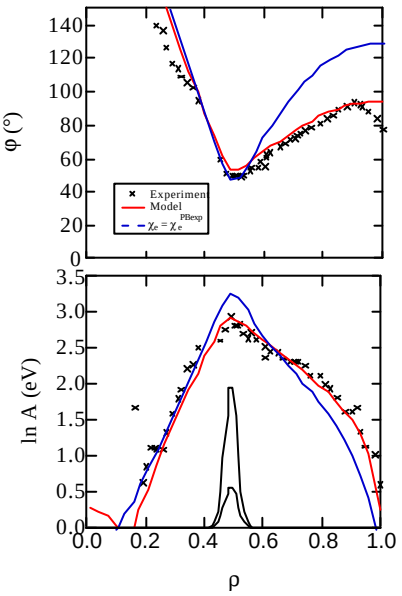

Figure III-94 : Phase and amplitude of the electron temperature modulation with the FCE deposition localised at mid-radius, a small part being modulated at 30 Hz. Outside the FCE deposition position, the heat pulses move much faster than predicted using the diffusion coefficient measured at equilibrium.

III.4.4.3. Non-local transport in TS

Non-local transport (TNL), characterised by an instantaneous increase of the central temperature following a sharp drop in the edge temperature (see figure III-97), was confirmed by perturbation experiments on Tore Supra. Two thresholds were found for the observation of this phenomenon : a density and temperature threshold, $n_e(0)/T_e(0) = 0.6\times10^{19}$ m^{-3}/keV; and a second threshold on the pellet size, $\Delta n/n = 0.5$. In the LH regime, the TNL effect on the amplitude is larger than in the ohmic regime. There is also an extension of the operating domain for the observation of TNL on density and current, and the threshold on the pellet size is less restrictive in the LH regime than in the ohmic regime: $[\Delta n/n]_{crit} > 0.5$. Lastly, a broadening of the « heated » region was observed in the LH regime. Analyses

seem to indicate that the mechanism governing the TNL is decoupled from the plasma current, thus excluding in the mechanism MHD modes toroidal coupling, current redistribution in space, and magnetic shear. However, some indications show that the plasma rotation shear (or radial electric field E_r) could play a key role.

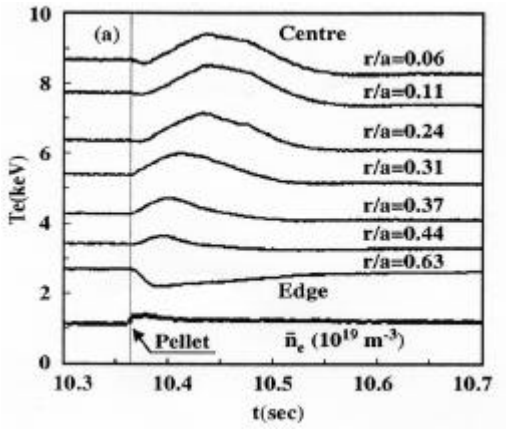

Figure III-95 : Time evolution of the electron temperature (ECE) and average line density $\overline{n}_e$ before and after the injection of a pellet in an LHCD regime with 100% non-inductive current.

III.4.5. Turbulent transport by avalanche

According to the standard approach, the non-linear dynamics of pressure, temperature or density fluctuations (i.e. of Fourier modes $(m,n)\neq(0,0)$, m and n being the poloidal and toroidal wave-numbers, respectively) is governed by an *equilibrium gradient maintained constant*. A heuristic transport coefficient is then deduced from the amplitude of these fluctuations, as well as from their length and time correlation. Two essential reasons motivated this « frozen gradient » approach. The first one, physical, is based on the up to now usually admitted idea that there is a scale separation between equilibrium and fluctuations : the latter occur on much shorter space and time scales than equilibrium. The other one, numerical, is due to the limited computer resources.

Recent results, both experimental and theoretical, have questioned the assumption of scale separation, the calculation power developing at the same time. New models were then found. In this new approach, the system total dynamics is taken into account at each instant, from equilibrium to fluctuations. The latter are then allowed to generate local relaxations of the equilibrium on times much shorter than the confinement time. *Forcing* is no longer ensured by a fixed gradient, but by *a flux*, of matter or heat.

In this case, it appears that a diffusive process can no longer properly describe the turbulent transport. On the contrary, it is intermittent and dominated by large space scale event, called avalanches.

III.4.5.1. Avalanche transport physics

In this approach, several electrostatic instabilities are studied in the fluid limit and the developed turbulence regime. First, one must mention a 2D code treating the interchange instability (analogous to Rayleigh-Bénard) in the edge plasma « in the shade of the limiters » (SOL), where the field lines intercept wall elements. The system is forced by a constant particle flux going through the separatrix. The resulting turbulent transport presents significant analogies with the experimental measurements made by Langmuir probe or reflectometry. More particularly, the flux histograms have an exponential wing towards large amplitude events, which are characteristic of avalanches. Also, an average density profile with exponential decrease is found, experimentally interpreted as resulting form a diffusive transport : $\lambda_{SOL}^2 = D_\perp L_{//}/c_s$. A 3D model is also used to study the RBM (Resistive Ballooning Mode) instability in the edge zone in the presence of the static magnetic field of the ergodic divertor. In agreement with the experiment, the DE has the effect of reducing the amplitude of the pressure fluctuations, whose large structures are preferentially stabilised; the turbulent flux remains practically

unchanged. The numerical results help to understand this apparent paradox : they indeed show that velocity fluctuations strongly increase. The strongest amplitude avalanches are the only ones to go through the stochastic zone.

A 3D model treats the ITG (Ion Temperature Gradient driven mode) instability in the core plasma. When the safety factor profile is inverted (negative magnetic shear s), a transport barrier develops in the nil shear region *s*=0, because the resonant magnetic surfaces in this region become rare. The polodial velocity shear, self-generated by turbulence via the Reynolds tensor, has the effect of extending the barrier beyond the strict region *s*=0. Lastly, as shown in figure III-96, avalanches do not cross easily the transport barrier. This result can be explained by the fact that, in this region, the turbulent cells are greatly sheared by the poloidal velocity.

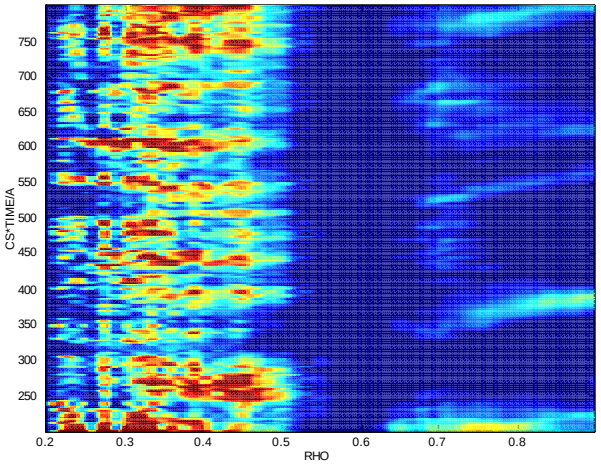

Figure III-96 : Turbulent flux (averaged on the magnetic surfaces) as a function of time and normalised radius. The safety factor profile is inverted, the magnetic shear being zero around rho=0.6

III.4.5.2. Towards a 1D transport model

Along with the development of these complex codes with high dimensionality, an effort was also made to establish a reduced dimension model containing the essential of the avalanche transport dynamics. The long-term objective is to propose an alternative solution to the turbulent transport description by a heuristic transport coefficient.

With this in mind, a generic model was developed using the interchange instability in the SOL. This system, forced by a source term, studies the dynamics of the equilibrium profile coupled to the fluctuation dynamics. Two mechanisms are in competition to dampen the fluctuations : the non-linear coupling of modes, which tends to transfer the energy to the small scales where it is then dissipated, and the relaxation of the equilibrium profile, generating avalanches. It then appears that the turbulent transport transits from a diffusive regime to an avalanche regime when the non-linear coupling coefficient is increased or, in an equivalent way, the system is excited far from the instability threshold.

III.4.5.3. Determination of heat transport scaling laws from microturbulence numerical simulations

Two microturbulence simulation codes were developed and used to study the parametric dependence of the thermal conductivity of ions and electrons as a function of the different non-dimensional parameters ρ^*, β, the safety factor, the power injected; etc. The aim was to determine the transport scaling laws using sufficiently fundamental plasma dynamics models. The ETAI3D code solves the three equations of evolution of a fluid model of ITG turbulence generated by the ion temperature gradient, which determines the fluctuations of three fields, electric potential, ion temperature and plasma velocity parallel to the field lines. The domain of simulation is the region included between two arbitrary magnetic surfaces. To study the corresponding ETG electron turbulence, the new ETAE3D code was used. In this case, the three interesting fields are the electric potential, the electron

temperature and the electron fluctuating parallel velocity, which is directly proportional to the magnetic field fluctuations. This model is thus electromagnetic and allows to study the dependence on β. The study of the dependence on ρ^* gives a scaling law of gyro-Bohm type, $\chi \propto (cT/eB)\rho^*$, for the thermal conductivities of ions and electrons. The dependence on β of the electron conductivity, from the ETG model, is weak for the β values considered in the study (between 1% and 16%.) This result is in agreement with the gyro-kinetic simulations of other authors. Lastly, a detailed study of the dependence on the safety factor q, from the ITG model, obtained by varying the current profile at fixed magnetic shear, shows that this dependence cannot be put into a simple scaling law. This dependence requires the use of a threshold function in the expression of effictive conductivity, $\chi \propto q^{\alpha}(\nabla T - \nabla T_{crit}(q))$, where the critical gradient depends on q. This results seems to be in agreement with the Tore Supra experiments.

III.4.6. Gyro-kinetic modelling

To describe the plasma response to electromagnetic field fluctuations, two approaches are possible : the fluid approach, which solves fluid mechanics equations, and the kinetic approach, where the fluid equations are replaced by particle trajectory equations, or by a kinetic equation. The coherence of the problem is ensured by the Maxwell equations, which link the fields to the charge and current densities. The second approach is the most used, since it is technically advantageous (3D instead of 6D); however, it does not account for the resonant interactions between waves (fields **E** and **B**) and particles (distribution function), known as Landau effects. In fact, these two descriptions lead to very different results : the linear instability thresholds differ (figure III-97), and the fluid turbulent transport coefficients are typically overestimated by a factor of two.

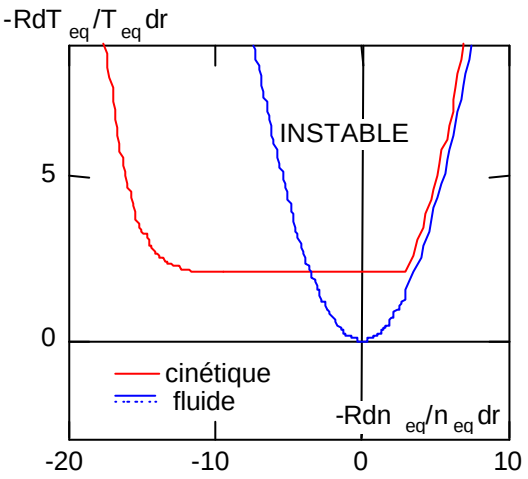

Figure III-97 : Linear instability thresholds with fluid (blue) and kinetic (red) approach

III.4.6.1. From kinetic to gyro-kinetic : theoretical developments

In a tokamak plasma, the turbulence characteristic frequency ($\leq$ 500 kHz) is very much lower than that of the cyclotron motion (the cyclotron frequency of a proton is about 45 MHz at 3 Tesla). It is therefore reasonable to average the motion over the fast cyclotron phase. Within this limit, called adiabatic, particles are assimilated to their guide-centre. Starting from the Vlasov equation, the first difficulty resides in deriving an equation governing the evolution of the guide-centre distribution function : the gyro-kinetic equation. It uses gyro-averaged electromagnetic fields, and the guide-centre trajectories. The system is 5D plus time. The operation of gyro-averaging is essential in a non-collisional problem, since it ensures, among other things, the dampening of small scale fluctuations.

A second difficult point is the fact that the charge and current densities, which satisfy the Maxwell equations, are those of real particles and not those of their guide-center. Thus, these densities must

be linked to the guide-centre distribution function, whose evolution is given by the gyro-kinetic equation.

Two codes are now under development within the framework of this project. These are global codes, with scales ranging from the Larmor radius to the plasma radius. They study the electrostatic instabilities associated to ions, describing the dynamics of the total distribution function (equilibrium and fluctuations) of the guide-centres. In this framework, the electrons are assumed to be adiabatic.

- The first code aims at studying the instability associated to trapped ions. This instability is known as being potentially dangerous in tokamaks. Within the limit of a low frequency turbulence (lower than the bouncing frequency of trapped ions), the problem can be reduced to two spatial dimensions (r and $a = j - qq$) by averaging on the cyclotron and bouncing motions. The particle kinetic energy is then a parameter.
- The second code concerns the Ion Temperature Gradient (ITG) instability in cylindrical geometry. This instability is assumed to control the heat turbulent transport in the tokamak core. To simplify, the non-linear problem is brought back to 4D by neglecting finite Larmor radius effects and because of the absence of trapped particles. This last property comes from the uniformity of the magnetic field chosen for this study. The geometry of the system is cylindrical, the curvature drift for the moment not being considered. The coordinates are the 3 cylindrical spatial directions (r,q, z) and the parallel velocity $v_{//}$.

III.4.6.2. First numerical results

Because of their high dimensionality, and of the importance of non-linear couplings, these codes require efficient numerical techniques and the use of super calculators. The two codes now used at DRFC are parallel and calculate on the Compaq machine at Grenoble.

Trapped ion instability (2D code)

This code is the first example of a «Vlasovian » kinetic code working in a developed turbulence regime. The first results obtained in this regime show that the non-linear saturation phase in turbulent regime is characterised by the development of large radial structures of the electric potential, which govern the spatial evolution of the distribution function. The Fourier spectrum is coherent with an energy inverse cascade process. Moreover, even though the imposed average temperature gradient is much larger than the linear instability threshold, the temperature profile in the non-linear regime is not very different from the marginal profile. In fact, in a large central region, the gradient remains close to the critical gradient. This result underlines the rigidity of the profiles. Lastly, the Landau resonances result in a deformation of the distribution function (figure III-98), which seems to indicate particle acceleration to supra-thermal velocities.

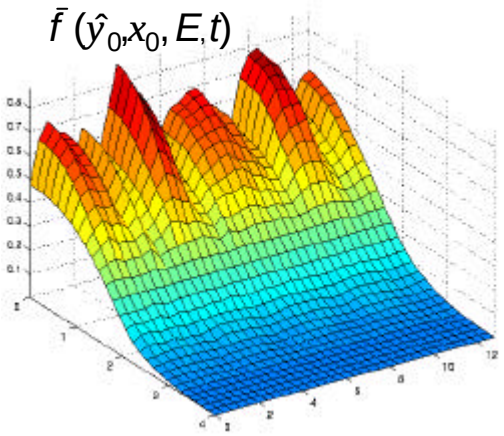

Figure III-98 : Evolution of the distribution function

4D code

A comparison of the growth rates obtained numerically with the linear analytical growth rates shows good agreement. Convergence problems in the Newton algorithm, used to calculate the trajectories, do not yet allow the non-linear saturation phase to be reached. The correct simulation of this non-linear phase will certainly require the integration of finite Larmor radius effects, which tend to dampen the small spatial scales excited by non-linear couplings. This work requires the integration of the adiabatic invariant μ as a parameter. This code should then gain another dimension.

III.4.7. Coherent structure spectrum in a turbulent environment

The intermittent transport in the tokamak is associated to highly turbulent regimes where non-linearities generate quasi-coherent structures (observed both experimentally and by numerical simulations). The theoretical approach based on the re-normalization of the distribution function response is inadequate; a statistical set composed of the exact solution (the Hasegawa-Mima vortex) and of a drift wave field with random phases has been considered. The correlations of the entire field are obtained by using the partition function, which is the functional integral over this set. The calculation (which was made analytically) implies the extremum of the action functional (Martin-Siggia-Rose) plus the domain near the function space. The result is the spectrum of the coherent structure modified by the interaction with the turbulent environment. Numerous applications are possible.

III.4.8. Magnetic study of transport barriers : localisation on « noble » surfaces

An original approach was developed for a purely magnetic study of the localisation of internal transport barriers (ITB), observed in tokamaks « around » the rational values of the safety factor (q), whereas non-linear dynamic system theories predict, on the contrary, barriers at irrational q values. By using the chaos theory, the number theory and by localising the rational convergent island sequences according to Fibonaci series, the ITB was identified as being composed of two permeable Cantori (destroyed Kolmogorov-Arnold-Moser surfaces) with «noble » q values (the most irrational). This result remains compatible with the experimental observations and the analytical models ("q-comb model" developed at Rijnhuizen), which identify the ITBs « near » the rational q values. This is also the case here since the barrier is composed of two noble Cantori surrounding a simple rational q value. The study of the diffusion of a set of magnetic lines shows that the usually assumed radial diffusion regime is not valid in this case. The demonstration of the validity of these results, linked to the chaos and number theories, required the development of graphic tools (GIF, JAVA, etc.), as well as mathematical studies and the construction of numerical codes to localise high periodicity magnetic islands.

III.4.9. Test particle transport

III.4.9.1. New statistical physics method for the analytical treatment of non-linearities in turbulence

The description of the test particle motion in stochastic velocity fields by means of Langevin type equations helps to determine the transport coefficients in turbulent plasmas from known eulerian statistical characteristics. For the particle guide-centre motion in two dimensional electrostatic turbulence, existing methods give results which are not always correct in low frequency turbulence, because of phenomena of *trajectory dynamic trapping* which are usually neglected. A statistical description in terms of conditional probabilities and of « decorrelation trajectories» has been developed, allowing this complex trapping process to be studied, especially for plasmas. It has been shown that the trajectory dynamic trapping has a significant influence on particle diffusion and on scaling laws for turbulent transport, by modifying the lagrangian statistical characteristics of trajectories : appearance of a long time tail in the velocity self-correlation and of a non-gaussian distribution of mouvements.

The effects of several factors always present in plasmas were studied : particle collisions, particle motion along the magnetic lines and plasma poloidal rotation. These are de-correlation mechanisms, which are known to decrease the diffusion coefficients. It has been shown that, in low frequency turbulence, they determine, on the contrary, a significant increase in the diffusion coefficient. Long series of numerical calculations of the de-correlation trajectories occurring in the analytical results helped to determine the effective diffusion coefficient as a function of the turbulence parameters (Kubo number, *K*) and of the parameters of the three additional processes. « Abnormal » transport regimes were found in conditions for which trajectory trapping is important. The main results are summarised in the following paragraphs.

The general conclusion of these studies is that the dependence of the transport coefficients on the turbulence parameters (Kubo number) is not only determined by turbulence, but also by other factors such as collisions, parallel velocity or plasma rotation. Consequently, the estimation of the transport coefficients based on the experimental measurements of the turbulence parameters must take into account other parameters such as the rotation velocity, but also the temperature and density, which determine the plasma collisionality. The method of decorrelation trajectories was extended to the self-consistent case of drift instabilities this year.

III.4.9.2. Influence of collisions on diffusion in electrostatic turbulence

In magnetic turbulence, it is well known that particle collisions completely change the effective diffusion coefficients and generate several transport regimes. However, there was no analysis of the influence of collisions in electrostatic turbulence. By means of the method of decorrelation trajectories, it has been demonstrated that the effective diffusion is determined by a significant non-linear interaction between collisions and stochastic field. The diffusion coefficient is presented in figure III-99 as a function of the Kubo number, *K,* for different values of the Péclet number, $P = b/c$, taking into account collisions (c is the collisional diffusion coefficient and b the Bohm diffusion coefficient). The non-collisional case is represented by the dotted line.

A significant increase is observed for diffusion in the domain of large *P* and *K* values (i.e. for the slightly collisional particles in low frequency turbulence). In these conditions, not only is the value of the diffusion coefficient modified, but also its scaling law in *K* : a super-Bohm regime is obtained for *K>>P>>1*.

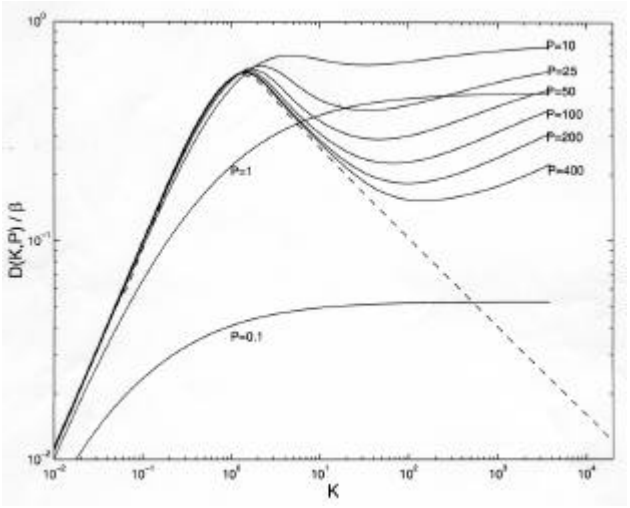

Figure III-99 : Diffusion coefficient as a function of Kubo number, K, for different values of the Péclet number, P

III.4.9.3. Influence of rotation on diffusion coefficient

The plasma poloidal rotation results in a significant decrease of the diffusion coefficient if the parameter V_d (ratio between the rotation velocity and the amplitude of the fluctuating velocity induced

by the turbulence) is greater than 1. It has been demonstrated, by means of the method of decorrelation trajectories, that in a low frequency turbulence, even a small plasma rotation ($V_d<1$) modifies the diffusion coefficients by a non-linear interaction mechanism between rotation and trajectory trapping. Under these conditions, a significant increase of the poloidal diffusion was obtained, as well as a significant reduction of the radial diffusion. The poloidal (D_{11}) and radial (D_{22}) diffusion coefficients are shown in figure III-100 as functions of V_d for different values of the Kubo number. The non-linear effect appears for $KV_d>1$ and $V_d<1$. In the limit of fixed turbulence, a poloidal super-diffusion and a radial sub-diffusion are noted.

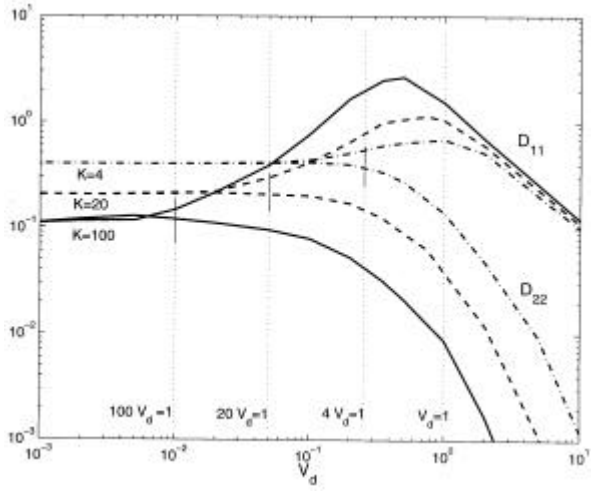

Figure III-100 : Poloidal (D_{11}) and radial (D_{22}) diffusion coefficients as functions of V_d for different values of the Kubo number

III.4.9.4. Effect of parallel motion on diffusion coefficient

The particle motion along the magnetic lines can influence the radial diffusion in an electrostatic turbulence with a finite parallel correlation length. It is known that this motion results in particle decorrelation and in a decrease of the diffusion coefficient. It has been shown that in a low frequency turbulence ($K>1$), the effect is inverse and a significant amplification of electron diffusion appears because of the non-linear interaction of the parallel motion with trajectory trapping.

It has been demonstrated that the radial diffusion coefficient increase is the most important for « passing » electrons with large velocities along the magnetic field. For low parallel velocity electrons, trapped in the potential mirrors along the magnetic lines, the radial diffusion is also influenced by the parallel motion : the process is much more complicated in this case, since there are two types of trajectory trapping. A non-linear regime similar to that of the passing electrons was obtained, but with a lower growth of the diffusion coefficient.

III.4.10. Fluctuations

The experimental activity on turbulence is essentially a joint research effort. The University/CNRS laboratories participating in the experimental and modelling effort through LRC (Laboratoire de Recherche Conventionné) contracts are the LPMI laboratory of the Henri Poincaré Nancy University, the PIIM laboratory of the of St Jérôme Marseille University, and the LPTP laboratory of the Ecole Polytechnique in Palaiseau. Lastly, foreign collaboration is essentially centered around the program on dynamic control of turbulence made in the CASTOR tokamak, within the framework of the Czech association.

III.4.10.1. Exchange between edge and core fluctuations in TS

The experimental results on most tokamaks show that it is not likely that the turbulence measured in the confined zone originates in the shadowed region of the plasma (even though this is where

turbulence is strongest). One could imagine that the strong turbulence existing in the limiter shadow diffuses towards the plasma interior. This idea was rejected thanks to experiments using polarisation of electrodes placed in the limiter shadow. This polarisation creates a sheared radial electric field, which generates a significant modification of the turbulence in this same region, modifying the power deposition on limiters, without modification of the plasma particle and energy global confinement. On the contrary, when the sheared radial electric field is created in the confined zone and affects the turbulence in this same zone, this is immediately seen as a change in the plasma confinement properties and a change in the heat deposition on the limiters. It is therefore the inverse which is probably true, namely, that the modification of turbulent transport in the confined zone can affect the turbulence in the shadow zone. This does not mean that the core turbulence and that in the shadow of the limiters are identical, but that there is a reciprocal interaction through the radial flux at the separatrix. However, there are situations in which a specific turbulence can be created and exist simultaneously in both regions (shadow of the limiters and confined plasma). An example of this was studied on Tore Supra near a limiter on which the plasma leans. The results obtained with a turbulence measurement diagnostic by coherent diffusion show that the turbulence created near the limiter is detected in both regions. This turbulence is somewhat the analogous in a magnetised plasma of that created in nature by a bridge pier in a river. It does not create radial transport, which explains the invariance of the plasma confinement properties.

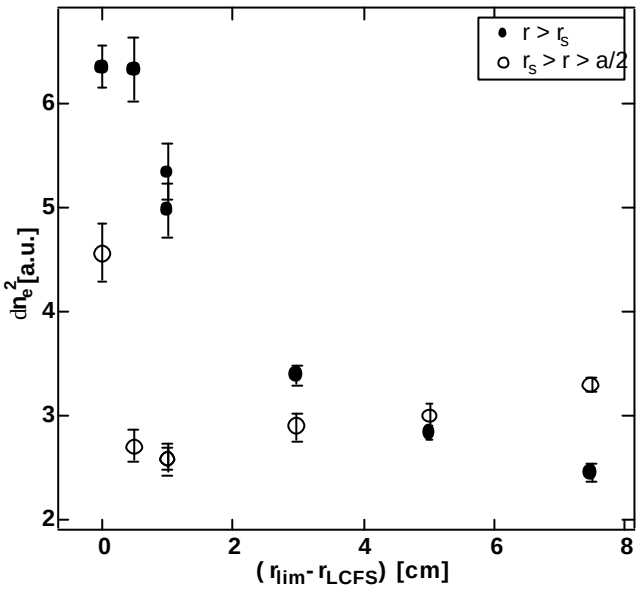

Figure III-101 : Turbulence level in the shadowed section (black circles) and in the confined edge zone (white circles) as functions of the position of one of the lower limiters relative to the last closed magnetic surface. It is seen that when the limiter gets close to the last closed magnetic surface, the turbulence level (k_q=10 cm^{-1}) increases in both regions.

III.4.10.2. Intermittence and flushes due to turbulence in CASTOR

Statistical methods were used to approach the problem of the nature of turbulent transport. Within the framework of a theory describing turbulent transport as being the result of a global relaxation of profiles when a critical gradient is reached, the turbulent signal is shown to have very long term correlations. It is possible to highlight these correlation properties by calculating the signal self-similarity on the corresponding times. The calculation of the exponent characterising the self-similarity is in fact a fractal dimension. The method based on the calculation of the Hurst exponent was used (this calculation is largely used in the literature as proof of the existence of long term correlations); this has shown that for long times this parameter is not adequate, since it essentially characterises short time correlations. Within the framework of the collaboration with the Czech Association, studies of the turbulent radial flux of particles in the CASTOR tokamak shadowed region were conducted. A 64 probes radial and poloidal matrix was used to observe the dynamics of the radial flux in this region. A film of this dynamics was made; the observations made can be summarized as follows. Flushes are observed, starting near the separatrix. They have dimensions of nearly 5 mm in the radial direction

and 12 mm in the poloidal direction. These flushes then propagate towards the wall. A radial propagation is easily detected up to 1.6 cm from their initial position, beyond which the signals dynamics is no longer sufficient for a reliable observation. The visual observation shows that the radial flux in the shadowed region is essentially convective. A spectral study of the flux reveals that all the time scales equally contribute to the average flux up to 100 kHz. The contribution of times beyond 100 kHz (namely for times t<10 µs) quickly drops. A study on the dependence of the average radial flux as a function of signal amplitude reveals that the flux decreases exponentially, with an exponent giving a characteristic amplitude for the transport. This amplitude is in the intermittent domain, in other words it corresponds to an amplitude which is encountered in the signal only inside turbulent flushes. This confirms the importance of turbulent convective transport in the shadow of the limiters.

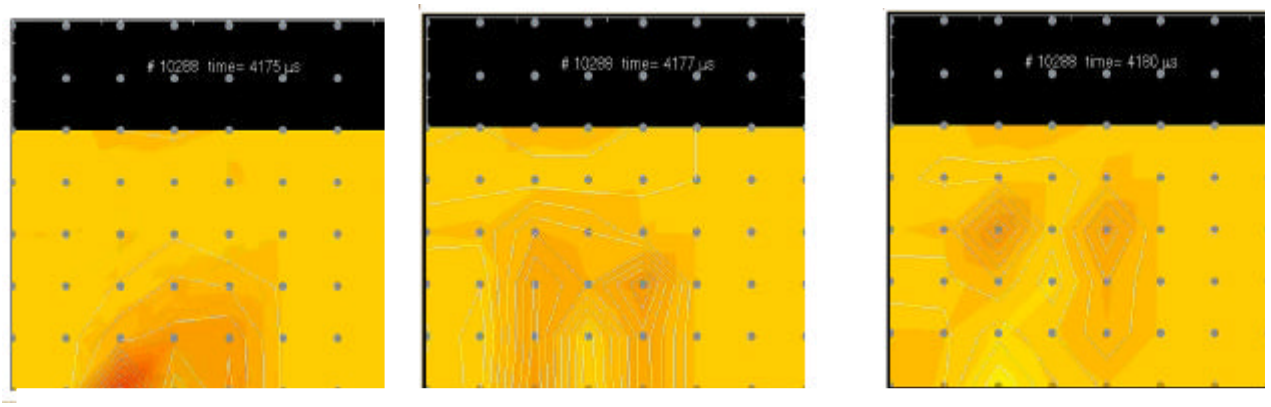

.

Figure III-102 : Three sequences of the film showing the flux propagation in the radial direction. The separatrix is located at the bottom of the figure, the wall at the top. The horizontal axis corresponds to the poloidal direction. The position of the probes is indicated on each picture. This series show a flush originating near the separatrix and propagating to the wall. The time between the first and last picture is 5 µs.

III.4.10.3. Experiments in CASTOR

The main collaboration program on turbulence between the Czech Association and DRFC is centered on the dynamic control of turbulence and of the associated transport in the shadowed region and the confined edge zone of the plasma. It is to be noted that in parallel, more classic turbulence studies were also carried out (see preceding paragraph). To obtain the control, turbulence retroaction methods are used along with techniques of open loop forcing. The open loop forcing consists in making a coherent electric field turn around the poloidal section of the tokamak, the spatial symmetry (poloidal wavelength), time periodicity (frequency), and amplitude being imposed. The electric field rotation direction is the same as that of the turbulence. The parameters are chosen so as to have a maximum of interaction with turbulence. Figure III-103 shows the fluctuations of the floating potential during the application of the electric field rotating over half of the poloidal perimeter. The controller, which is a poloidal crown of 32 plates, is located in the region shadowed by the limiter. The potential fluctuations are dominated by the rotating wave. This situation caused a change in the poloidal limiter current, proof that the density profile in the shadowed region was modified. A local measurement of the turbulent flux with a set of probes on the poloidal crown shows that it was modified through a phase change between density and poloidal elelectric field fluctuations, the flux coming from the product of these two quantities.

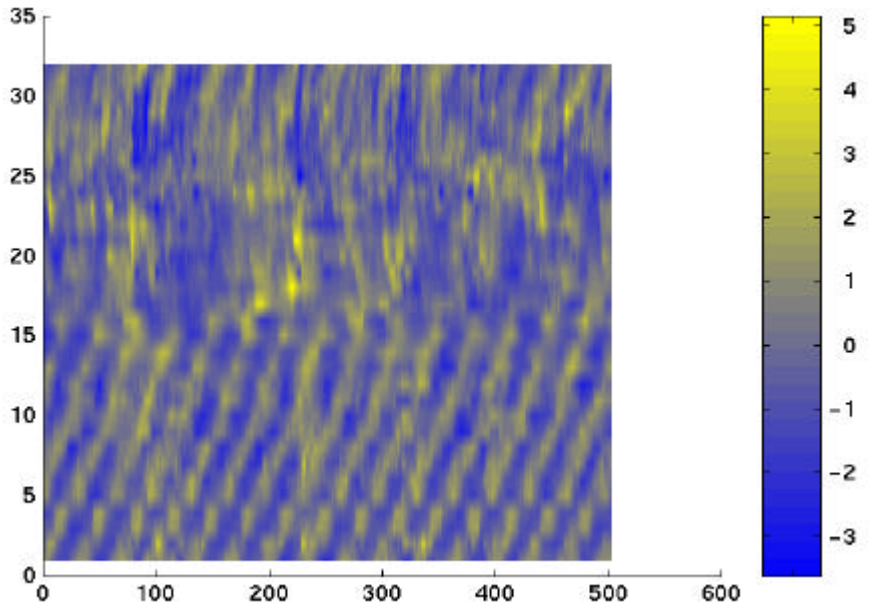

Figure III-103 : CASTOR. Potential fluctuations measured by the probes inserted in the poloidal ring plates during the open loop control phase. On the vertical axis is the probe number, the 32 probes corresponding to a complete poloidal rotation. Control is only applied on the first 16 plates. The rotating mode imposed has the following characteristics : a 30 kHz frequency, and a poloidal wave-number corresponding to m=5 . The amplitude of the signal on the plates is of 30 V peak to peak.

IV. TORE SUPRA : SUB-SYSTEM OPERATION, MAINTENANCE AND ENHANCEMENT

IV.1. Operation of Tore Supra in 2001

IV.1.1. Tore Supra start-up

IV.1.1.1. Tore Supra conditioning

The conditioning phase, which lasted about 3 weeks, is represented in figure IV-1. It is to be noted that this conditioning was interrupted at the beginning of September, because of a problem of the B30 pressurised water loop. The total length of the luminescent discharges was of 5.5 days in deuterium and 4.5 days in helium. The average levels of hydrogen and water, measured using a differential mass spectrometer, dropped by more than a factor of 10 during this time, allowing the first plasma to be made on 19 September. During this entire conditioning period, 40 g of water were retrieved and the particularly high level of hydrogen, due to the presence of a large surface (~14m^2) of «new » CFC composite on the CIEL elements is to be underlined. After 50 days of operation, 20 grams of hydrogen were pumped.

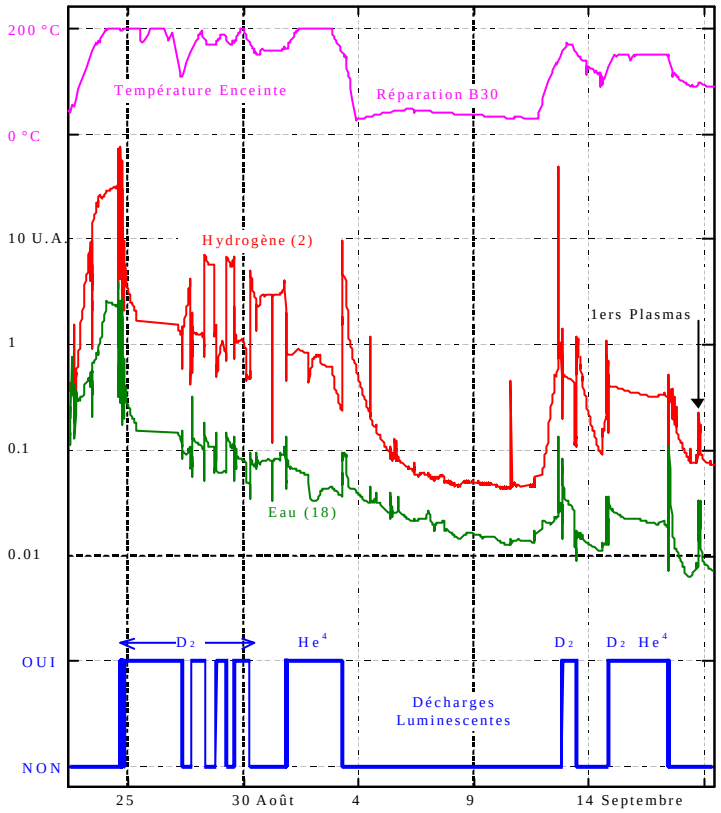

Figure IV-1 : Conditioning during Tore Supra start-up in 2001. Evolution of chamber temperature, partial pressures of hydrogen and water. Main gas making up the luminescent discharge.

IV.1.1.2 First Plasma on LPT/LDC

The first plasma breakdown occurred on 31 August 2001 and the first controlled plasma of 600kA for 6s (see figure IV-2) which marks the beginning of the Tore Supra experimental campaign was

obtained on 19 September 2001. This two-week interruption was due to an incident on loop B30 (rupture of a seal on a pipe under pressure). This plasma was limited by the LPT. The new control in position on the plasma was very satisfactory (see section IV.3).

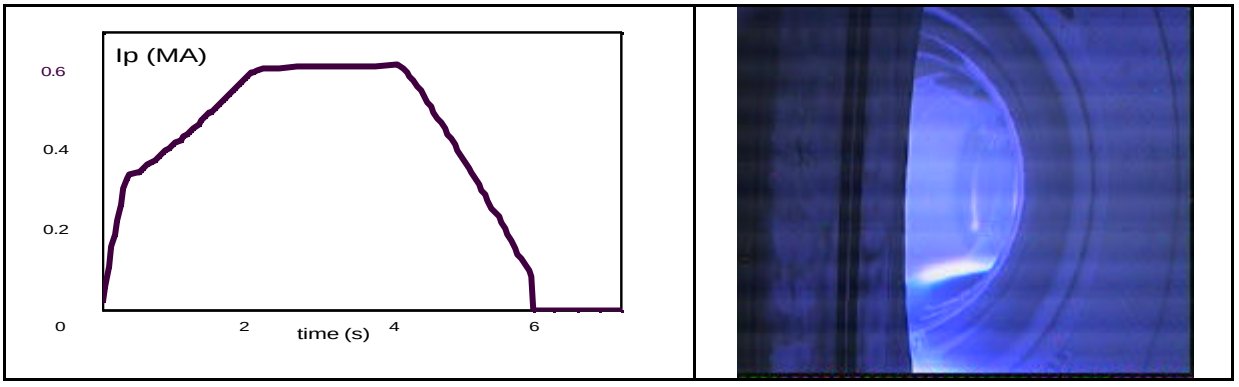

Figure IV-2 : First plasma of Tore Supra campaign in LDC/LPT configuration.

4.1.1.3. Incident on the LPT/LDC

An important problem quickly appeared during the experimental campaign started at the end of September 2001, which led to interrupting the plasma experiments. A strong current, induced in the LDC/LPT structure during a disruption, circulated in the LDC and LPT carbon plates and fingers. This current circulation, a priori impossible since the LPT sectors were first isolated from the LDC, was made possible due to arcs or contacts, visible upon inspection of the chamber after the incident (see figure IV-3).

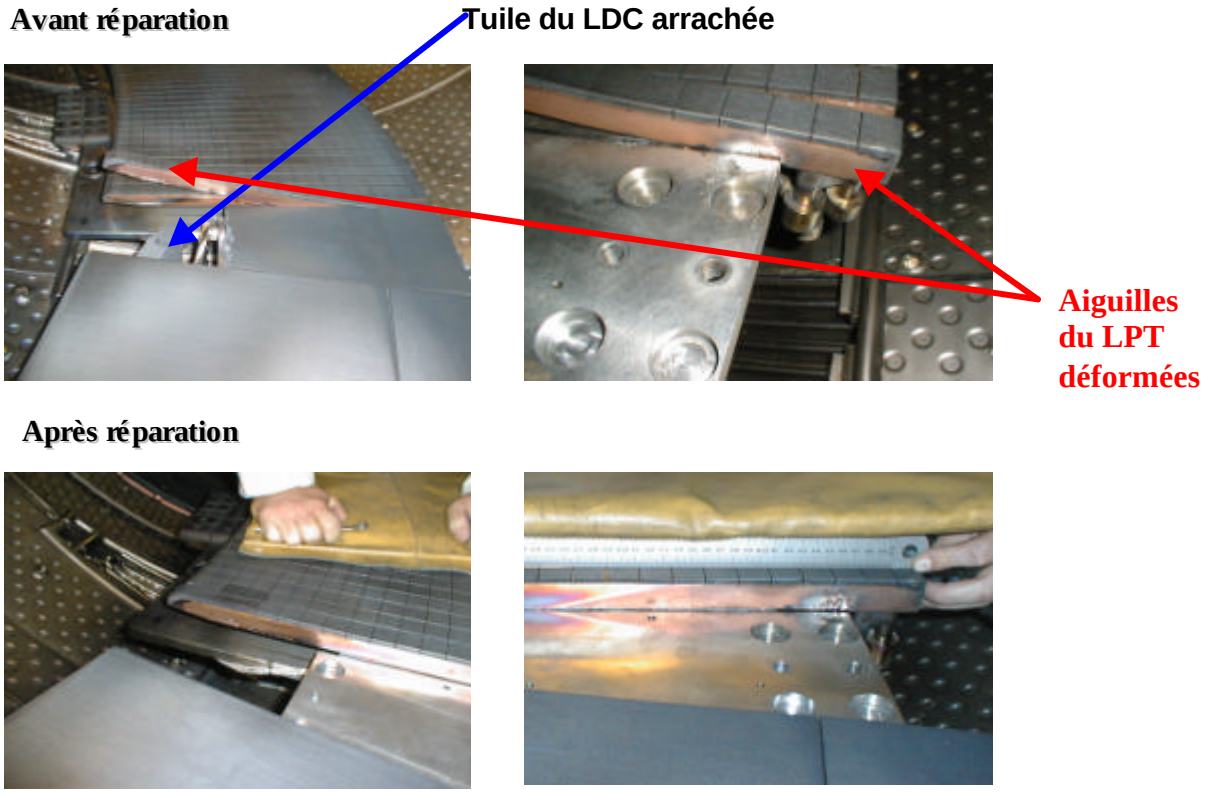

Figure IV-3 : Consequence of the disruption and repair of LPT fingers.

In the presence of a radial magnetic field, the force obtained, estimated to be several tons per meter, resulted in some of the LDC tiles being ripped off or in significant deformations of the LPT fingers (see diagram in figure IV-4).

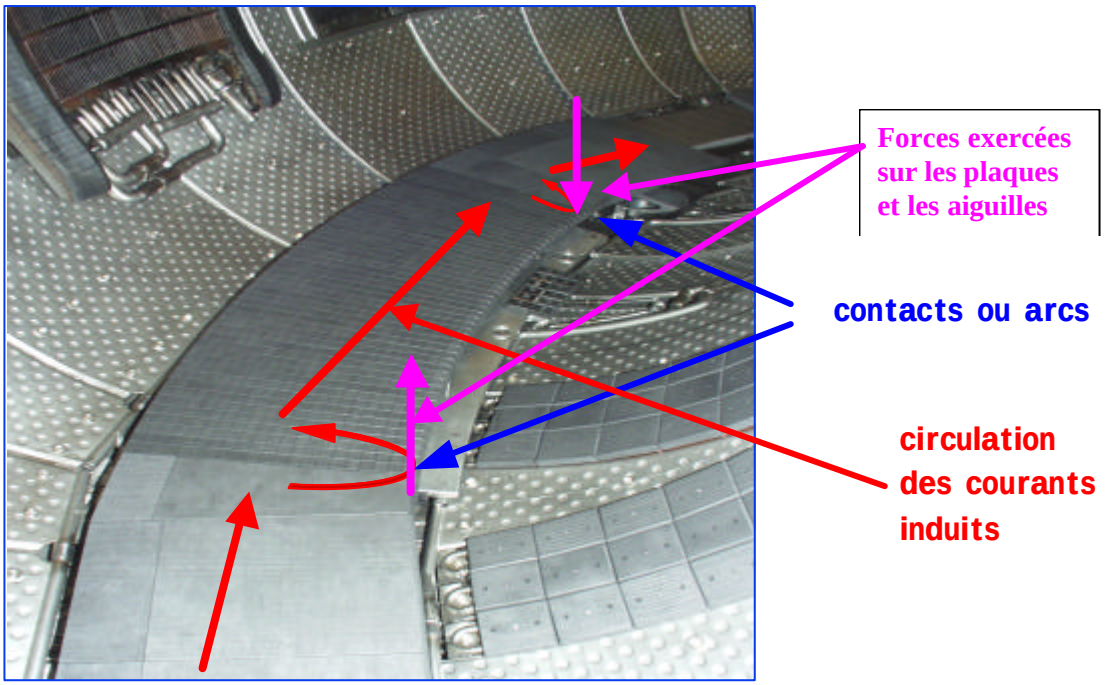

Figure IV-4 : Diagram describing the current circulation in the LPT/LDC during disruption.

The deformed fingers were repaired in situ and the ripped off plates replaced. So as to prevent this incident reoccurring, the LPT and LDC sectors are now electrically connected so that the current generated during the disruptions be toroidally drained, thus minimising the risks of ripping or of deformation. Calculation showed that the maximum current thus drained in the LDC/LPT beam during a disruption will be less than 160 kA (I_p=1 MA and t_{dis} =cste=5 ms) resulting in vertical forces tolerable by the LDC support structure. A study of the consequences of disruptions for plasma currents up to 1.5 MA was carried out during the 2001 campaign to validate this modification and verify whether the LPT would not be damaged if such a disruption were to occur.

IV.1.1.4. Start-up with LDC in short circuit

The plasma experimentation in this configuration was started on 16 November 2001. There were some difficulties because, during start-up, the current induced in the LDC beam (≈30 kA) attracted the plasma towards the LDC, as can be seen in figure IV-5, and plasma breakdown failed.

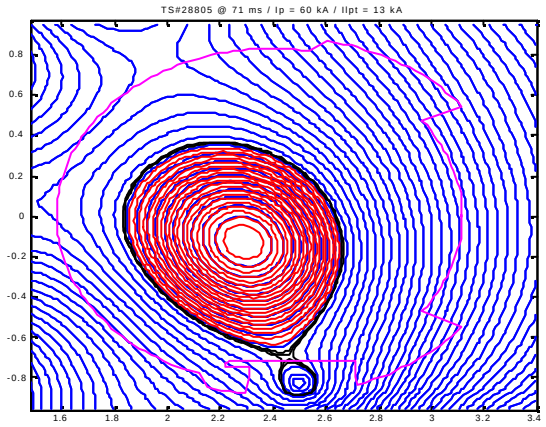

Figure IV-5 : reconstitution of flux map during plasma breakdown. The areas in colour are those where the plasma current is located.

In order to try to prevent this effect, preliminary adjustments of the poloidal coils, which allow the plasma to be placed away from the beam, were made. This led to obtaining a value of the breakdown plasma current greater than 90 kA, allowing the current to increase

IV.1.1.5. Current circulating in the LDC beam during a disruption

The first disruptions obtained after start-up confirmed the estimated current values in the beam obtained during disruptions. In figure IV-6, the plasma current during a disruption is shown. The decrease time constant is of 4 ms. The induced current generated in the beam (LDC current) during the disruption reached a maximum value of 125 kA, equal to 12% of the I_p value at the plateau. This value is in agreement with that foreseen by calculation.

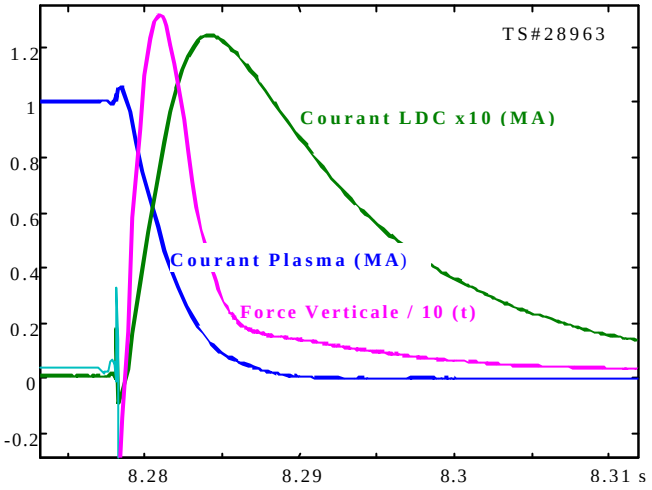

Figure IV-6 : Evolution of plasma current, of current induced in LDC and of the vertical force applied on the LDC during a disruption.

The vertical force induced on the LPT reaches 13 tons at its maximum value (in other terms over 2 tons per jack). This value is considerably lower than the limit, evaluated at 60 tons.

IV.1.2. Organisation of Tore Supra operation and experimental campaign

The Tore Supra operation was modified in depth in spring 2001 by the implementation of 24 hour a day shifts for safety reasons (PMS), coupled to safety duty. This new organisation, involving 20 people in the department, ensures the safety of the Tore Supra facility outside working hours. In parallel, reflex index cards, which help the employees during their safety duty/PMS, have been drawn up and are still under development. Feedback from the experience will be included during the winter shutdown, which will enable these index cards to evolve.

Moreover, with the aim to optimising the scientific operation of Tore Supra in 2001, the experimental day now lasts 13 hours, from 8 am to 9 pm. Two teams of employees, consisting of pilots, physicists, diagnosticians, are in charge, daily, of the Tore Supra operation, the change-over being between 1 pm and 4 :30 pm.

IV.1.3. Safety

Safety at the DRFC is understood as the operating safety of the systems in the industrial sense and also as nuclear safety. In both these areas, the following have been achieved over the period under consideration :

- When the machine was started up in 2001, the systems intervening in facility safety were controlled and verified. This mainly concerned the control of personnel access and safety, the safety procedures for dangerous equipment, the protection system of the toroidal magnet and that associated to the protection of the vessel from the vapour risk, which was completed by an additional rupture disk.
- All the new systems installed on the machine were initially electrically verified with significant non-respects of regulations being corrected. An inspection of all the tanks under pressure was also made by an accredited organisation, so as to check their conformity in view of changing regulations.
- The zoning of the facility for the management of Very Low Activated (TFA) components is operational. It was set up during the shutdown and is integrated to the waste references in application on the centre.
- The radiological zoning is being re-defined because of the implementation of the active dosimetry system, DOSICARD.

IV.2. Machine sub-systems

IV.2.1. The Tore Supra toroidal magnet

During the prolonged shutdown of Tore Supra since 1999, several changes have been made on the toroidal magnet within the framework of the CIEL project : inversion of current direction, change over to VME of mechanical instrumentation system using constraint gauges, change of the incident analyser. The tests conducted during start-up did not show any abnormality on the magnet on the electrical and mechanical levels, but a degradation of the instrumentation system, requiring the replacement of accessible detectors. The operation of the machine in September 2001 resulted in 3 fast discharges of the toroidal magnet induced by cryogenic faults. These discharges allowed the safeguards installed to be checked for proper operation.

IV.2.2. The cryogenic refrigeration system

IV.2.2.1. Cryogenic refrigeration of the toroidal magnet

The Tore Supra cryogenic system was completely overhauled from 1999, at the beginning of the CIEL shutdown, and ended in 2001 with the start-up of the facility. The entire control command system was changed, and the initial ARC7 system has since been replaced by last generation programmable industrial automates (API). The automatic programs have all been re-written integrating the experience acquired during the 11 years of magnet operation. The operation tests started in March 2001. There were several significant problems linked to the difference in writing of the automatic programs on API. These problems, causing many operation errors and which were solved along the way, did not prevent the magnet from being cooled. The cryogenic system operation is now very satisfactory, since the toroidal magnet has been at 1.8K since August 2001.

Moreover, significant modifications on the facility were caused by the new regulations on the protection of circuits under gas pressure (decree of 04/12/98), essentially concerning over-pressure relief valves. The general analysis of the facility components revealed the need to change the HP exchanger (He/H_2O), whose operating pressure was too close to the calculated pressure. A technical file with a calculation note was established for all the safety valves.

IV.2.2.2. Cryogenic developments

The cryogenic fluid supply system for the interfero-polarimetry diagnostic was achieved and installed during the first semester of 2001. This system is now operational. In addition to the insulation of the liquid nitrogen supply circuits, the liquid helium supply system is entirely automated. Thus, the buffer tank of the system is filled by the SC4 cryogenic satellite with a flow rate of 60l/h, without disturbing the cryogenic system of Tore Supra. The pre-cooling system of the lines was optimised and allows the cryostats to be quickly filled with very small losses.

IV.2.3. The water refrigeration system : loop B30

The cooling loop which controls the plasma facing components (PFCs) temperature (B30) had been designed at the beginning of Tore Supra for a total flow rate of 540 t/h, a maximum temperature of 230°C, a maximum operating pressure of 40 bar and a components ΔP of 4 bar. The total flow rate during the 10 years of operation never exceeded 270 t/h.

Within the framework of the CIEL project, this loop must go, in phases, from these previous values to a flow rate of 1100 t/h with a components ΔP of 7,5 bar to supply the entire LPT. In order to achieve this, two pumps will have to be used simultaneously. During the winter shutdown of 2001-2002, a second pump will be installed and the networks in building 510 will be changed.

During the 2001 start-up, the flow rate was of 600 t/h with a components ΔP of 6 bar. As the maximum operating pressure of the loop cannot be modified (for safety reasons) and the components ΔP is larger, the low pressure at the machine outlet will be of 24 bar instead of 28 bar.

The modifications due to CIEL concerned all the B30 components :

B30 networks in the upper part of the machine

Studies and mechanical calculations of the module supply networks were made. The High Pressure system was made in a factory and the Low Pressure system was modified. Both were installed on Tore Supra in October 2000.

B30 networks in middle and lower parts

During the period corresponding to the 2000 shutdown, mechanical studies and calculations of the networks were realised. The pipes were pre-fabricated and their on site assembly was carried out.

B30 networks at -6m

It was also necessary to increase the B30 pipe diameters between building 510 and the torus hall and to re-build the network in the torus hall at -6m.

Once the main loop networks installed, the final hydraulic approval test at 60 bar was carried out in the spring of 2001. Water filling was done in June and the last heat insulation work just prior to the pressure and temperature increase for the conditioning of the machine (August 2001).

In parallel, the P30 pump dedicated to the plasma operating mode was equipped with a new motor and a new variator. The present operating point of the B30 in the start-up configuration (LPT sectors and the LDC) in plasma mode is :

- Total flow rate = 640 m^3/h, including upper part flow rate = 340 m^3/h,
- ΔP(pump)=6 bar.

Figure IV-7 shows that the operating points measured are very close to the values predicted by calculations taking into account the hydraulic characteristics of all the components.

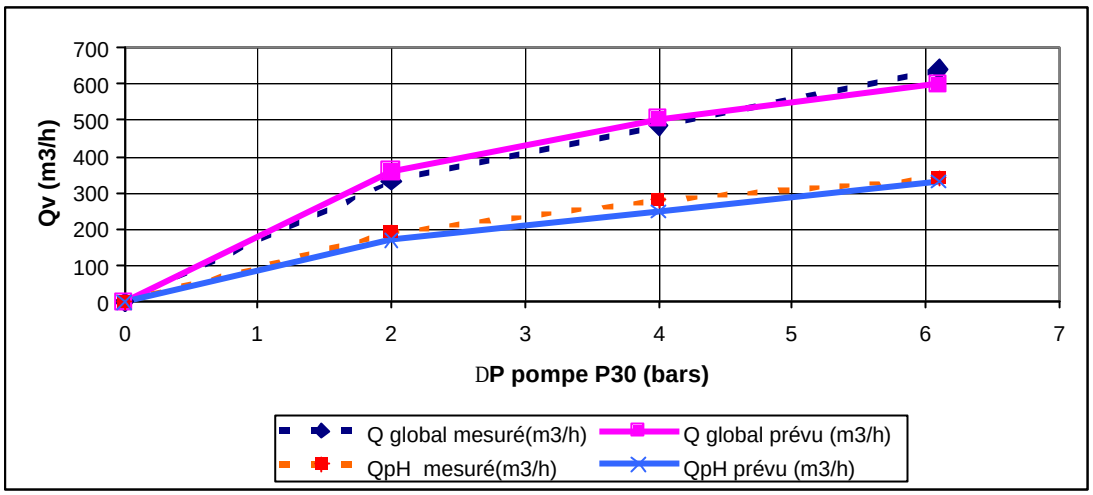

Figure IV-7 : Comparison of measured and calculated flow rates on loop B30 (global flow rate and upper part flow rate QpH).

Aid to B30 filling and drainage

A control panel for the pneumatic valves installed on the drainage/filling circuits of the different B30 sub-systems was designed and built. This panel allows a gain in time during filling and drainage operations for B30 or for its sub-systems (for example, the cooling circuit of the HF heating antennae). The system is operational and was successfully tested during the filling/drainage of B30 for the hydraulic testing of the loop. Moreover, the nitrogen network, which is used to flush out the water from the networks during drainage of the machine, was re-built for safety reasons.

Calorimetric diagnosis

Significant changes were made on the calorimetric diagnosis (§II.4.3). The calorimetric measurements were used to evaluate and correct the horizontal setting of the LPT sectors (see §II.1.3.3).

Modification of STEFI machine

To ensure the cooling of the optical systems internal to the infrared endoscopes, the STEFI-machine loop had to be re-built. The STEFI-machine is used to cool the diagnostics placed in the upper Tore Supra ports, the FCI antenna capacitances and the hybrid coupling windows. A safeguard system on the water supply in the upper part of this loop in case of loss of electrical supply or compressed air was designed and built.

IV.2.4. The supply systems and electrical networks

IV.2.4.1. Work associated to changing the magnetic configuration

In order to make the system compatible with the magnetic configuration foreseen for CIEL, the polarity of the poloidal field coils at the level of the connections of co-axial cables on the coils was inverted in April 2000. Insulation tests were made to validate this operation. In the same way, the new current supply bar of the lower B coil in Sector Q6 was installed and tested. All these changes are operational and the first plasmas were made without any problems from a magnetic configuration point of view.

IV.2.4.2. Studies and work associated to replacing the fast contactors

The answers to the call for tenders on the replacement of the Driescher fast switches equipping the poloidal installation arrived in October 2000. These devices, essential to starting up the plasma, will be replaced by switches designed for ITER by the Russian Institute Efremov (Saint Petersburg) and

adapted to Tore Supra. A preliminary study report was handed in at the end of March 2001. They should be installed during the next Tore Supra shutdown, at the beginning of 2002.

The maintenance cost of the Driescher fast switches, still in operation on Tore Supra in 2001, is very high. To allow the 2001 plasma campaign and the operation in good conditions without carrying out this maintenance, two fast switches which were very rarely used were removed so as to increase the stock of spare parts. The fast plasma management graphs were also modified before start-up to integrate this modification.

IV.2.4.3. Studies associated to ground distribution

In collaboration with the RFX team in Padova, a new detection system for mass loops adapted to the surveillance of the LPT sector insulation and to the machine, was studied and developed. This system has been in operation since the facility start-up and has detected faults on the Q1B, Q2B, Q5B and Q6B sectors during their deterioration end of September 2001 during the operation of Tore Supra in the presence of plasma.

IV.2.5. Data processing and electronics

Changes in data processing systems due to the objectives of improving reliability, performance and maintenance were made during 2000-2001. Other actions resulted in changes in the machine systems in CIEL configuration. The following can be mentioned :

IV.2.5.1. Control command system

During start-up in spring 2001, all the control command system of Tore Supra had been changed into APIs. The APIs of cryogenics, refrigeration, vacuum, LH/FCI/FCE heating systems, diagnostics, and the unit in charge of safety, of controls in position and of supervision were validated
All the supervision PCs were changed to Windows NT. The NT server PC was validated and started up. It ensures that information is centralised on safeguards and archives, the administration system of all the supervision PCs and the safety and protection of the entire facility.

IV.2.5.2. Data acquisition

The TAXI system of transmission of measurements by optical fibres has changed in its performances and principle, now allowing a recopy in both directions of any signal type : it is now the MIONET system.

A dozen acquisition units were changed into the VME standard at Tore Supra start-up and are operational today : the poloidal control, the gas control, interferometry, bolometry, Langmuir probes, FCI heating, DDUO spectrometry, Thomson scattering, reflectometry, magnetic measurements and calorimetry. The acquisition unit of the DSIR spectrometer is in its final installation phase. The new chronology VME card is now in operation on half of the Tore Supra diagnostics.

The 3rd generation integrators for the magnetic measurements were validated and installed. Developed with a view to measure long discharges, these new integrators provide a better measurement quality, and a semi-automatic calibration capacity.

The continuous data from the control command system and the acquisition system of the diagnostics are operational, including the continuous acquisition of the calorimetric diagnosis.

IV.2.5.3. Networks and computer systems

The main network equipment was replaced by more efficient gigabits materials, which improved communication between the different buildings and computers. The new data storage system connected and managed by the Compaq ES40 bi-processor server (667 MHz) has been operating since the beginning of May 2001. All the TS data, whether raw or treated, have been gathered on this system of safe disks, which offers significant extension possibilities. The storage and data access programs now take into account the continuous data, whether these be acquired on the diagnostics (calorimetry) or coming up from the control command system.

On the calculation servers, a variable priority system for the execution of calculation codes has been set up in close connection with the users. This should replace, in the long term, the batch manager, which is not adapted to our needs.

For the DRFC personnel working abroad, namely at the JET, a new server using the Citrix protocol was installed. This allows them to access under proper safety conditions to the computer environment of Tore Supra.

With the aim to gain experience and thus improve the service to our personnel, a statistical study was set up on our ability to meet the demands on UNIX. In figure IV-8, the solving time of the declared incidents is mentioned on a monthly basis. Each month over 50 calls are recorded and 70% of the requests are solved in less than 3 days.

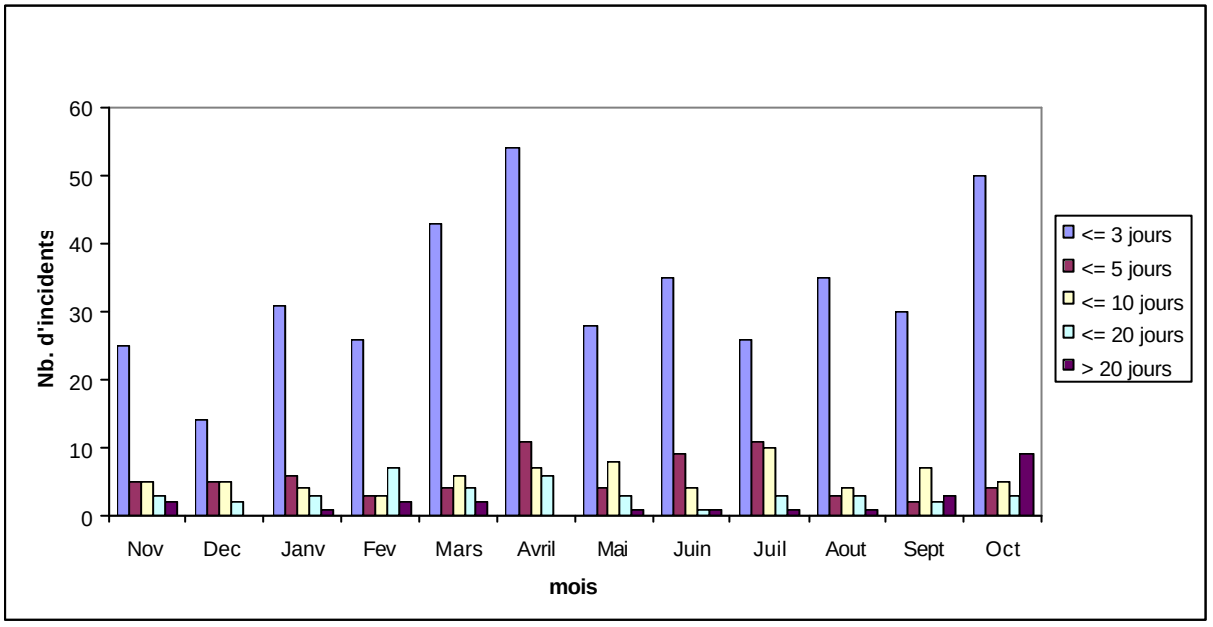

Figure IV-8 : Solving time of incidents for end of 2000 and 2001

IV.2.5.4. Parameter and data exploitation tools

The Pavane program has been improved so as to integrate the management of experimental days in 2 teams and the demands of the users for the preparation of experiments. The program now allows the recording in its base of an experiment sheet under .pdf file format and then associating it to a day of operation.

IV.3. Control

IV.3.1. Plasma safeguards

A set of Tore Supra exploitation regulation index cards has been implemented. These cards define the operational limits which can only be exceeded after obtaining the approval of the Experimental Committee of Tore Supra. These concern the definition of plasma vacuum quality as well as possible magnetic configurations or even acceptable plasma conditions for the injection of HF power. The experience gained will be used during the winter shutdown of 2001-2001 to upgrade these operation cards.

IV.3.2. Feedbacks : plasma controls

The control of the shape and position of the plasma was greatly modified in the CIEL configuration : the number of measurement points was multiplied by 3, the saddle coils were eliminated, the limiters are all new…This was very successful as soon as the first plasmas were made at the machine start-up. The plasma was positioned a few millimetres from its desired position and its circularity guaranteed. Figure IV-9 shows the residual deformations of the plasma as functions of the poloidal angle, compared to an ideal circle.

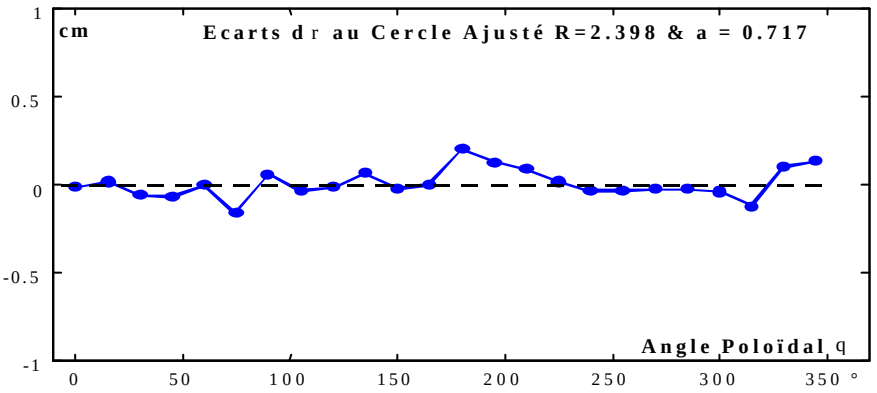

Fig. IV-9 : Plasma deformation versus ideal circle

The dynamic response of the control was also studied. In figure IV-10 a displacement of 4 cm in 100 ms is programmed between 7 and 7.5 seconds. The average radius and the contact radius with the LPT are in agreement with the reference within a few millimetres (the contact radius is no longer defined for the most external position of the plasma).

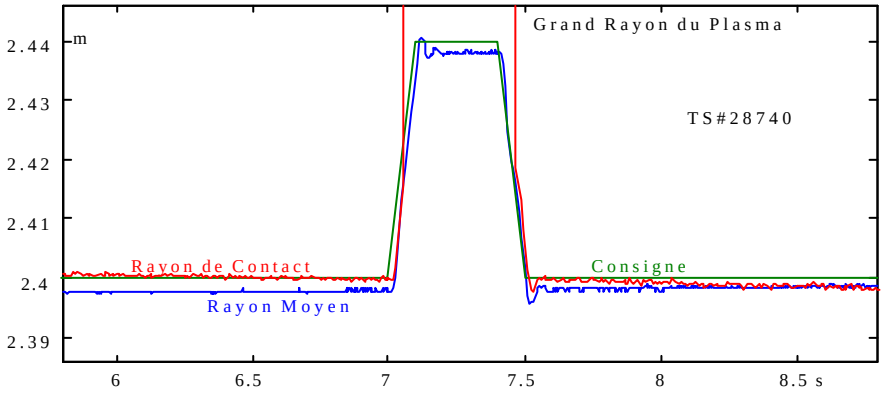

Fig. IV-10 : Fast movement of plasma. Difference with reference

IV.3.3. Pulsed supersonic injection of matter (ISPI)

In addition to the traditional gas injection, a pulsed supersonic injection system was developed for Tore Supra. This allows the injection of gas with characteristics close to those of pellets (0.5 $Pa.m^3$ / 0.5 ms at 10 Hz). The aim is to increase the gas injection efficiency without too much investment.

To achieve this rapid injection, a fast opening valve is used, actuated by the shock of a piston, itself accelerated by the injected gas. Such a system, with a relatively simple design, has been installed on Tore Supra since September 2001 in a safety ring for a qualification test campaign. This prototype injector allows the injection of between 0.1 and 1 $Pa.m^3$ in 2 to 4 ms at a maximum frequency of 12 Hz. The quantity of gas injected can be adjusted between each plasma experiment and the maximum flow rate is very high, over 100 $Pa.m^3/s$.

The first results obtained on the plasma are discussed in III.2.3.

IV.3.4. Tore Supra conditioning

Tore Supra has just been equipped with a set of 12 electrodes for luminescent conditioning discharges in the vacuum chamber. Each newly designed electrode is made of a CFC briquette mounted on a stainless steel support plate and covered by an insulating alumina coating (see figure IV-11). The support plates are placed on the inner vacuum vessel above each port and integrated in the loop B30 cooling circuit. The electrodes cannot be moved and are exposed to plasmas.

The new glow electrode system was successfully implemented during luminescent conditioning discharges made when Tore Supra was started up again in 2001 .

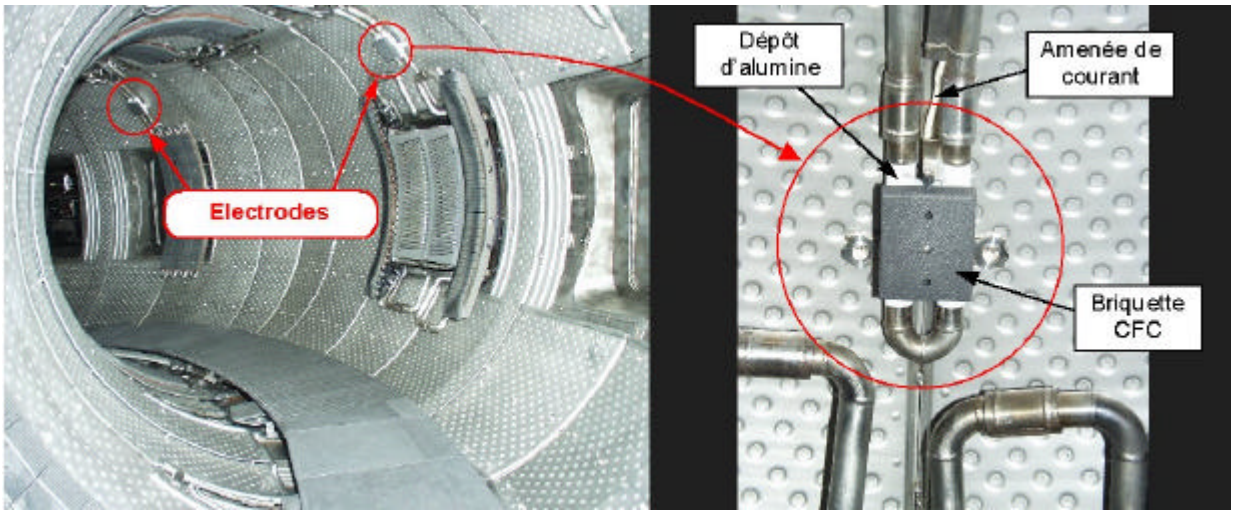

Figure IV-11 : New luminescent discharge electrodes in the machine.

V - PARTICIPATION IN JET OPERATION

V.1. Introduction

The overall changes of the JET tokamak operating conditions starting on 1st January 2000 have very significant effects on DRFC operation, and in general on the EURATOM-CEA Association. The JET machine is now managed by the JET Implementing Agreement (JIA) within EFDA (European Fusion Development Agreement) : all the Associations back its operation. In addition to its very active participation in the definition itself of these agreements and in the different Executive or Management Committees, DRFC has immediately responded to all the operational demands of JET under EFDA.

V.1.1. CEA participation to JET Close Support Unit

Since September 1999, J. Paméla has been the EFDA JET Associate Leader (JAL) at the head of the Close Support Unit (CSU). The Association is also in charge of, within the CSU, the administrative and operational departments. Moreover, support to logistics and to the JET-EP project is also part of the functions of CEA personnel. The global commitment in the CSU first concerned 4 then 5 employees over the period considered.

V.1.2. CEA participation to JET Operation Contract

The technical operation of the JET facility is insured by the UKAEA, through the JET Operation Contract (JOC). The CEA participates to the JOC via several employees, transferred for long periods of time to the UKAEA, either for 100% or for a fraction of their time which also allows them to participate in the scientific and technical activities (see §V.2) and/or developments (§V.5). The Association has thus been involved over the last two years in three main activities linked to the JOC :

- *JET operation* : control, operation and development of the real time system, operation of HF heating systems (ICRH, LHCD), operation of diagnostics (MSE, CXRS, ECE, polarimetry). 8 CEA employees or post-doctoral students have been involved in these activities, at the rate of 9 man-year for 2000-2001,
- *the direction of the plasma facing components group*. 1 man-year per year,
- *safety of tritium plant*. 1 man-year per year.

V.1.3. CEA participation to JET developments.

The CEA has committed itself to four large JET development projects, within the so-called framework of JET-EP. Thus, the CEA is responsible for three projects : 'Divertor Design', 'Infrared Viewing', and 'Real Time', and is greatly involved in the 'ICRH antenna' project. A summary of the work done is given in §V.5 below. These projects entail the department providing 5-6 men-years.

V.1.4. CEA participation to Scientific and Technical tasks

Scientific and Technical tasks (S/T) cover all the work done in preparation for the S/T JET experimental campaigns. There were three of them in 2001 (C1, C2 and C3), and one in 2001 (C4), for a total of 35 weeks of operation (350 sessions). These S/T tasks consist in participating on site to the experimental days (7.45 men-years in 2000 and 3.42 men-years in 2001 for the Association), and work at distance (preparation and analysis, publications) (about 11 men-years in 2000-2001 for the Association). The Association managed Task Force S2 in 2000-2001 and, since the fall of 2001, manages Task Force T, and the coordination of Task Forces S1, S2 and FT.

These Scientific and Technical tasks gave rise to a very large number of participations to conferences and publications, mainly during 2001. The EURATOM-CEA thus participated to 47 contributions at the 28th EPS Conference (Madeira, Portugal), 11 of which as first author, 10 contributions to the Topical RF Conference (Oxnard, USA), 2 of which as first author. It also participated to 24 other contributions in different workshops. For publications, accepted or being reviewed, the Association is now involved

in about thirty papers, ten of which with a first CEA author. The work done in these Scientific and Technical tasks is detailed in §V.2 below. This work, in 2000-2001, was the focus of a concentration of means on a reduced number of objectives in agreement with our skills and/or planned developments (cf V.1.3) : study and control of advanced regimes, particularly sustained by a significant fraction of non-inductive current; plasma edge and characterization of ELMs; LHCD coupling; ICRH scenarios; support to the operation of some diagnostics, vital to advanced scenarios.

V.1.5. Remote participation

DRFC has also been very active in the definition and necessary tests to improve their remote participation within EFDA. The coordination of the project on defining the technical infrastructure and an active participation in the users club were among these actions (§V.4).

V.2. 2000-2001 campaign results

V.2.1. S1 and E Task Forces

V.2.1.1. Characterization of ELMs : effect of triangularity on ELMs and confinement in H modes

A systematic study was conducted on the energy losses and heat fluxes in the divertor during type I ELMs. Former experiments on JET, DIII-D, AUG, and JT-60U showed an improvement in the confinement of high triangularity plasmas. The work on the C1 and C2 campaigns on this subject was focused on the study of the new 'ITER-like' configuration with an elongation ε=1.7, and a maximum triangularity δ_{upper}~0.5, δ_{lower}~0.44 (average triangularity : $<\delta>$=0.47) (figure V-1). In this experiment, a good confinement (H_{97}~1) and a very high normalised density (n_e/n_{GR}~1) were obtained simultaneously in the $<\delta>$~0.47, q=3 configuration (wall temperature : T_v=200° and T_v=320°) (figure V-2), without transition to type III ELMs, which normally cause significant confinement degradation (cf. type III points in figure V-3).

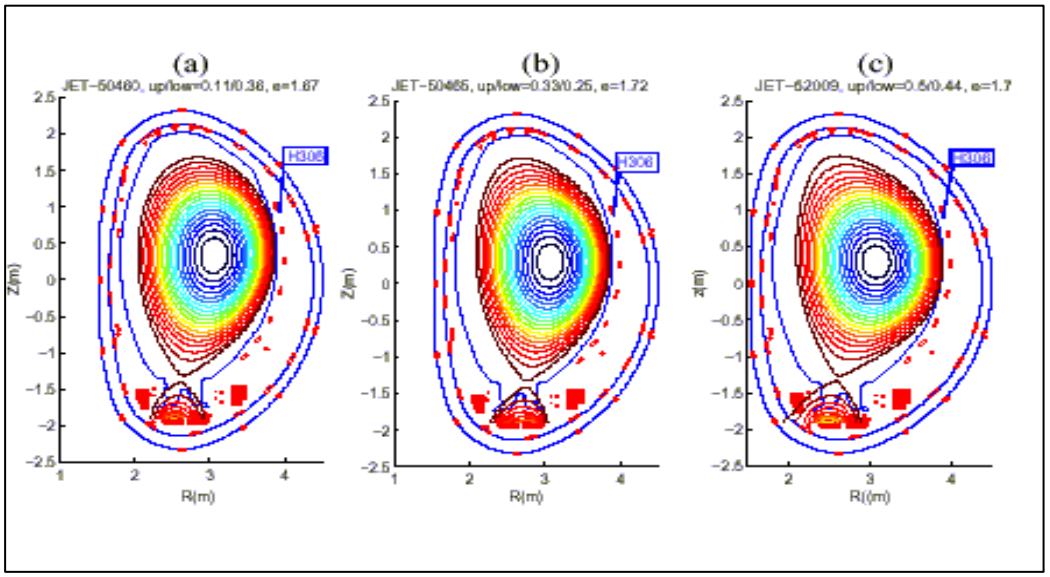

Figure V-1 : Configuration of plasma with different triangularity : (a) d_{upper}/d_{lower}=0.11/0.36, elongation e=1.67 ; (b) d_{upper}/d_{lower}=0.33/0.25, e=1.72 ; (c) ITER-like configuration in JET : d_{upper}/d_{lower}=0.5/0.44, e=1.7.

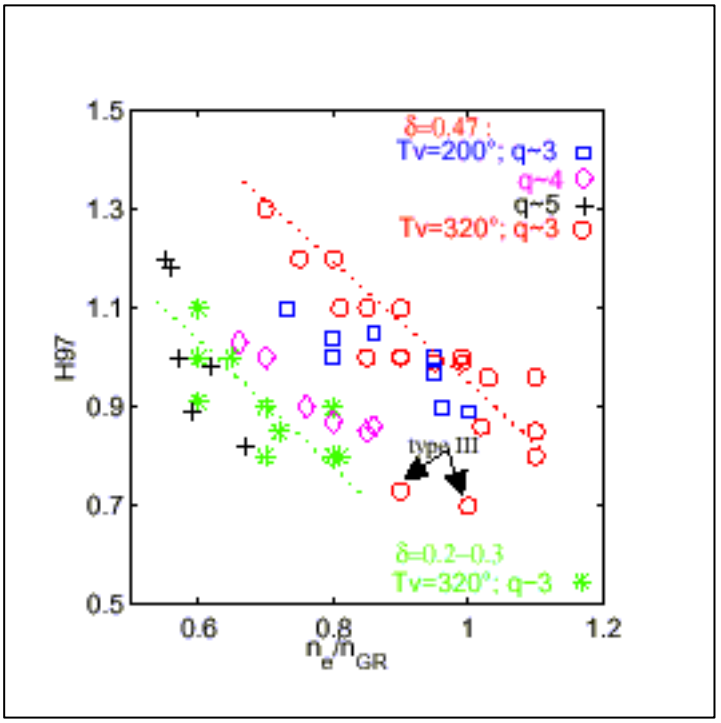

Figure V-2 : Confinement factor H_{97} versus the density normalised to the Greenwald density (n_e/n_{GR}) for different triangularities (<d>~0.47(ITER-like) and <d>~0.2-0.3) and safety factors ($q=q_{95}$=3 ;4 ;5). Two wall temperatures (T_V=200° and 320°) were tested.

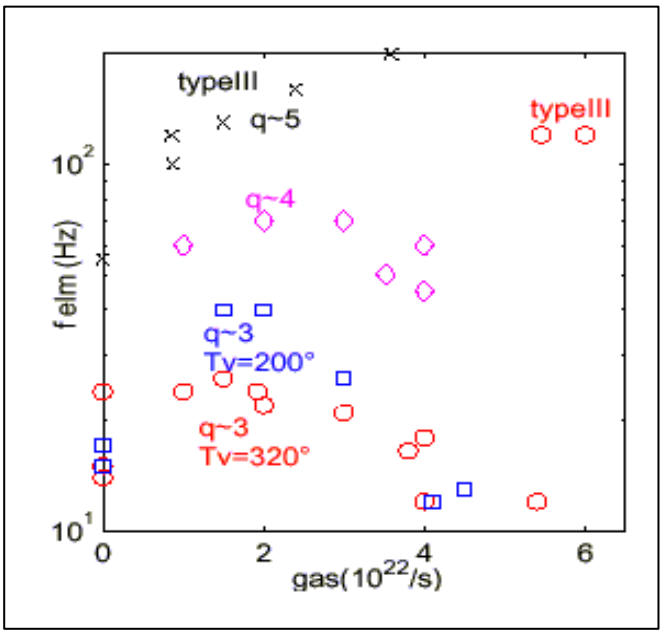

Figure V-3 : Dependence of ELMs frequency with the gas injection rate for the plasmas of fig.V-2.

The energy losses per ELM also decrease with density: ~3% of W_{dia} per ELM (n_e=1.1n_{GR}), instead of 6% (n_e=0.8n_{GR}). A very high increase in the magnetic turbulence was observed on the Mirnov probes at the plasma edge, suggesting an increase in electron transport between ELMs (figure V-4). This is a very favorable regime for ITER. This type of fluctuations was called type II ELMs by analogy with the observations on ASDEX. The theoretical analysis and the experimental facts suggest the possibility of access to the stabilization region of MHD ballooning modes thanks to the magnetic shear effect, which changes along with the shape of the plasma, particularly with triangularity.

Analysis shows that the limit pressure in the pedestal before the ELM is always higher in high triangularity configurations. With a very strong gas injection, the ELM frequency shows an abnormality : it decreases compared to the situation normally observed during gas injection (figure V-3).

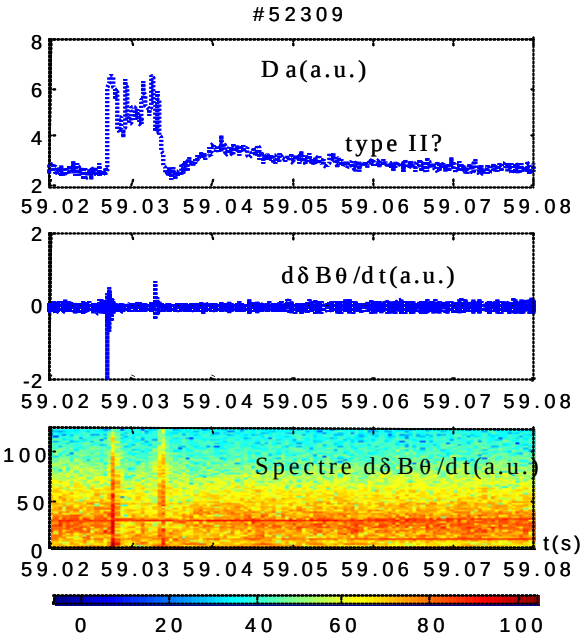

Fig V-4 : Da signal and Mirnov probe signals, and frequency spectrum (kHz) obtained by Fourier analysis of the Mirnov probe signal

V.2.1.2. Particle balance, retention, change to helium

Particle balance and retention

The particle balance of a plasma experiment provides access to information on the exchange of particles between the plasma and the wall and also a better understanding of the density control mechanisms. It also allows the evolution of the particle content of the walls in interaction with the plasma to be monitored and information on tritium capture to be obtained. This study is paramount for both JET in the case of tritium experiments and for future machines such as ITER.

The total number of particles pumped (N_p) by a pumping system is equal to the product of pressure (P) by pumping rate (S) at the location of the pressure measurement : $N_p \propto PxS$. Because of the presence of high pumping rate cryo-mechanical pumps (divertor cryopump and neutral injection boxes), the pumping rates in the divertor and vessel set the dominant terms for the particle balance. Since the absolute pressures are known, the particle balance was then determined during the plasma discharges (figure V-5), between the discharges and during the conditioning periods.

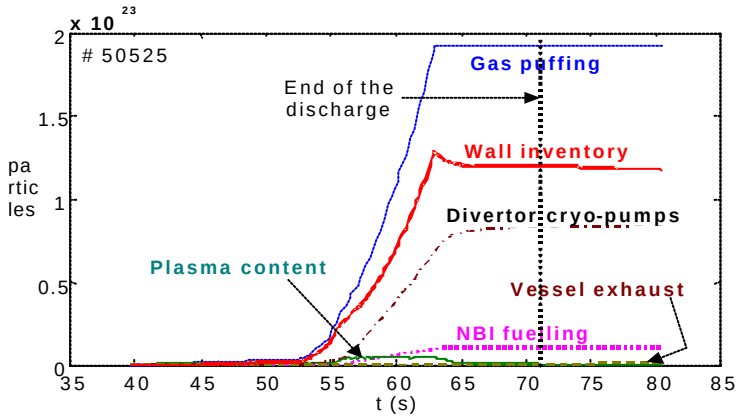

Figure V-5 : Example of particle balance for a JET discharge (ELMy H-mode : 2.8 MA/3.0 T)

Thus, it was demonstrated that 50% of the particles injected were captured in the walls after the end of the plasma. These particles were then slowly desorbed, resulting in a long-term retention of about 8 to 10% of the injected atoms.

Change from deuterium to helium

D_2 is the gas mostly used in JET plasmas. A series of experiments in helium were conducted with the aim to determining the evolution in the D_2 content in the walls, and to find out what the dominant gas was in the edge plasma when helium was injected. The helium percentage (R) in the D_2 and helium mixture was characterized by partial pressure measurements of the gas neutralized in the subdivertor, as well as by spectroscopy measurements in the SOL (photomultiplier and filters centered on helium and deuterium spectral lines).

The first point which is interesting to note is the decrease by a factor of 10 of the number of particles concerned in helium plasmas, compared to equivalent D_2 plasmas. This difference is explained by the pumping of D_2 by the walls, this effect being negligible for helium. Figure V-6 represents the evolution of the helium percentage in the discharge versus time. Discharge #53936 was performed in D_2, and the following one in helium. Starting with this first plasma with helium injection, the R ratio increased up to 85%, independently from the power injected (ohmic or with FCI additional heating in this case) both in the subdivertor (pumped gas) and in the SOL. When additional power is applied, some D_2 is extracted from the walls, which contributed to decreasing R. This method thus helps to reduce the hydrogenoid particle content of the wall, and will also be important in tritium experiments.
This series of experiments confirmed that in D_2 the particle balance was totally dominated by the gas injection, and by the D_2 trapped in the walls ; the particle content in the plasma being negligible (10%). Even with walls saturated in D_2, the proportion of helium in the SOL and the subdivertor is dominated by the gas injection, which suggests a possible control of the gas composition in the plasma.

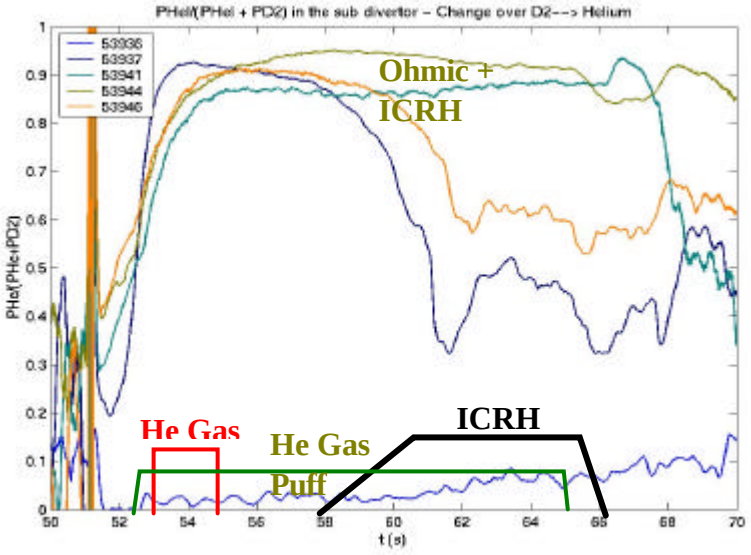

Figure V-6 : Percentage of helium versus time for plasmas with helium injection

V.2.1.3. IR fast camera

Obtaining efficient discharges with an acceptable power deposition for the plasma facing elements is of prime importance for research on controlled fusion. The power deposited inducing a temperature increase in the divertor tiles, the analysis is conducted by infrared thermography. Because of the geometry of the MkIIGB divertor, direct observation does not allow the zones interacting with the plasma to be seen (impact points on the high and low field sides). An endoscope, installed on a middle port, simultaneously aims at two different places of the divertor, thus allowing an observation of the power deposited on the internal and external parts of the divertor. A fast camera was developed for the specific needs of JET. The detector has a focal plane of 128x128 pixels (3 MHz frequency), the

acquisition is done in parallel on 4 converters, at a rate of 725 pictures per second, in other terms a time resolution of 1.3 ms. By reducing the number of pixels per line and column, it is possible to increase the number of pictures per second. However, fast events such as ELMs require a time resolution of about 100 µs. Because of the operating mode of this camera, by reading line per line the pictures and by assuming a toroidal symmetry of the power deposition, a temperature profile on the divertor with a time resolution of 20 µs is obtained. Figure V-7 shows a picture obtained with this camera and the endoscope. An image treatment program written in Matlab reconstructs the temperature profiles on the divertor (figure V-8). After having changed and tested the command electronics and calibrated the camera, at the beginning of January 2001, many data were acquired during the C4 campaign, allowing the power deposition in L-mode and H-mode in deuterium and helium to be compared. It was demonstrated that during the deuterium plasmas, the radiation from the inner part of the divertor does not follow the black body law; the additional contribution to the photon flux seems to be due to the co-deposited layers with a small thermal contact with the substratum.

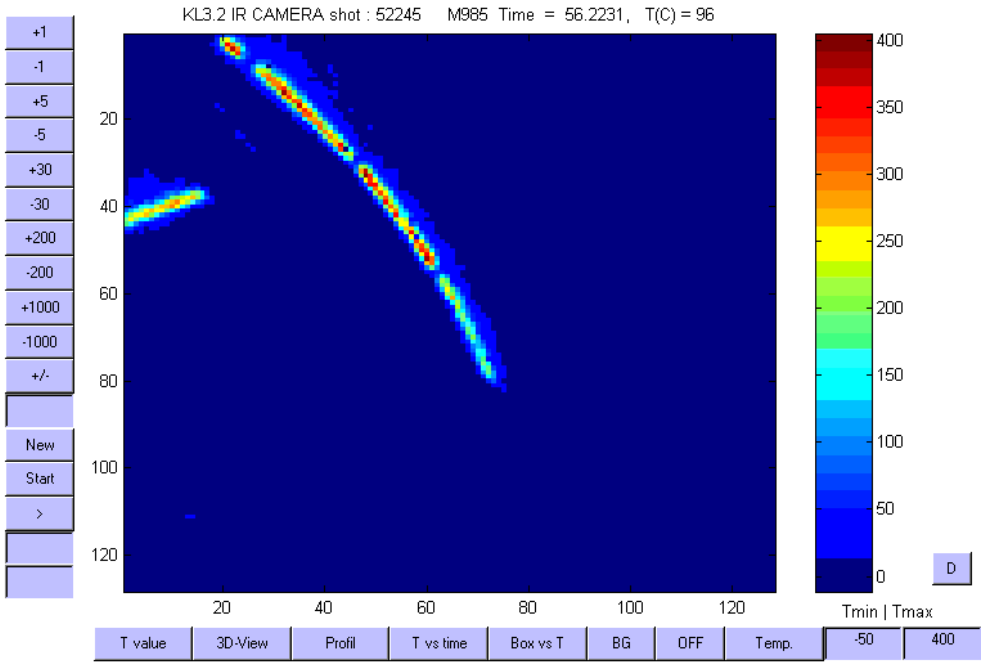

Figure V-7 : Infrared picture of MkIIGB divertor; outer strike point : from the top to the bottom of the picture; inner strike point : on left of picture

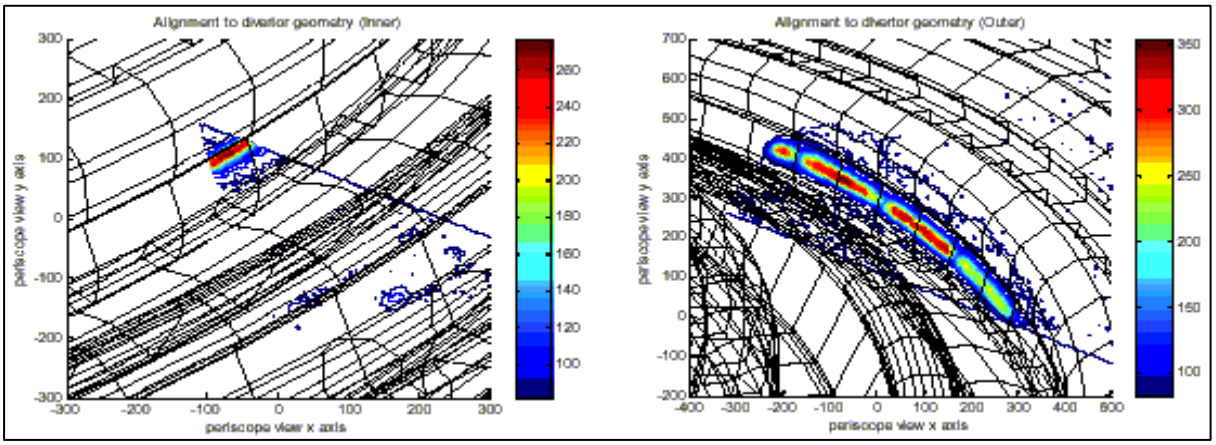

Figure V-8 : Reconstruction of infrared picture of MkIIGB divertor; on the left : inner divertor; on the right : outer divertor

V.2.1.4. Alpha heating

The experiment described below was conducted during the DTE1 JET campaign at the end of 1997. The deuterium and tritium mixture was changed from 0% to 92%. Several plasmas were made with a given composition, so as to ensure the same isotopic ratio at the wall, by loading it step by step, and in the neutral beam. The results on electron heating have already been published. The following analysis, conducted in 2000-2001, concerns the behavior of the ion temperature.

Figure V-9 shows the central ion and electron temperatures as function of power for each mixture. The alpha power produced during these experiments is around 1 MW, of the same order of magnitude as the typical variations in neutral beam power; the data are therefore shown as functions of total power. According to the calculations, the alpha power distribution between ions and electrons should be favorable to electrons. However, experimentally, the ion temperature is found to increase much more than the electron temperature (2.6 keV per MW of alpha power for the ions versus 0.9 keV per MW for the electrons).

Several approaches were used to understand this phenomenon. First, the experiment was repeated using FCI heating instead of alphas : the 1.2 keV increase per FCI MW of the ion temperature is similar to that forecast by equipartition. This difference in behavior thus indicates that this effect is inherent to heating by alphas, thus possibly indicating a drop of the ion conductivity in the presence of alphas.

There could be three explanations for this : (i) that the usual calculation on the power transferred from the alphas to the ions is questionable, because of, for example, the appearance of cyclotron or Alfven waves ; (ii) that a transport barrier is triggered by the alphas, since they produce a radial electric field ; (iii) that the ion turbulence is highly sensitive to the electron temperature. The first two points are very unlikely. Indeed, point (i) leads to assuming a negative electron conductivity, and no plasma rotation was observed, whereas the latter should be induced by an electric field in the case of point (ii). Thus, the explanation in point (iii), with a drop in ion conductivity due to turbulence effects seems more likely.

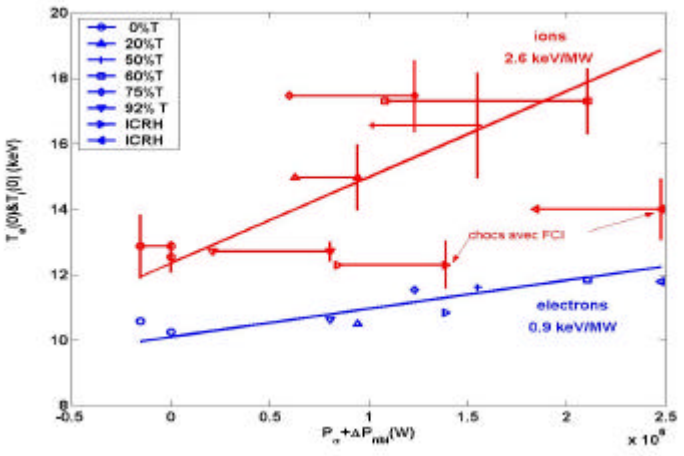

Figure V-9 : Central ion (in red) and electron (in blue) temperatures as functions of total power for each D-T mixture and for two plasmas with FCI heating to replace alphas heating. The horizontal bars show the change in neutral beam power. The red dots on the left of the bars thus correspond to the ion temperatures versus alpha power.

V.2.2. Task Force S2

The EURATOM-CEA Association has generally committed itself to research on Advanced Tokamaks, by providing its expertise on stationary regimes. The main results obtained in the C1 to C4 campaigns by the Association (or with a high involvement of the Association) are both experimental and interpretative. These can be divided into several categories :

V.2.2.1. Study on the influence of the target current profile on the formation and quality of the barrier.

This study, using additional power (particularly LHCD) during the plasma current increase, has clearly shown that target plasmas with inverted current profiles have a threshold for the establishment of internal transport barriers (ITBs) lower than those with a monotonous profile (ITB in the ion channel); figure V-10. Moreover, this study confirmed the appearance of barriers in the electron channel as soon as a sufficient level of LHCD preforming power is applied, very similar to the LHEP regime in Tore Supra. Moreover, this additional preforming of the current profile during the plasma current increase resulted in a very significant reproducibility of ITBs triggering, as well as the adjustment of the current profile to a desired profile already in the low performance phase (small current diffusion time), thus allowing "freezing" this profile in the high performance phase at values very close to the stationary values (figure V-11).

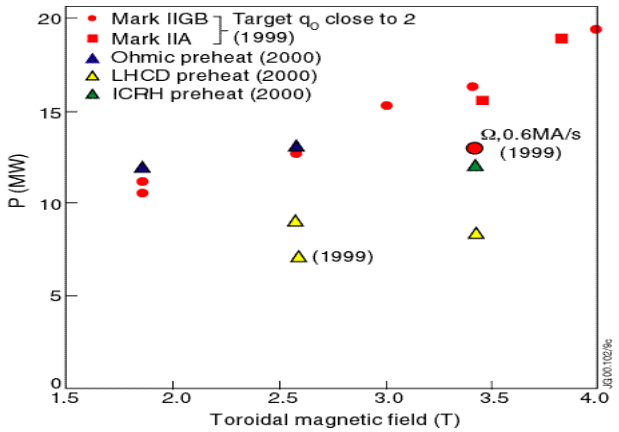

Figure V-10 : Power required to trigger an ITB on JET as a function of the magnetic field, for different pre-heating situations during the current increase phase

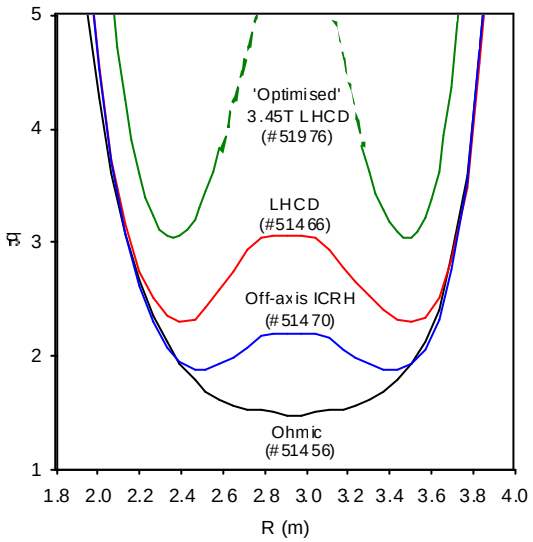

Figure V-11 : Target current profiles obtained at the end of the current increase phase, using different pre-heating means and levels (EFIT reconstructions with MSE data).

V.2.2.2. Study of ITBs triggering physics

Fine studies of the ITBs triggering mechanisms, already started on plasmas with monotonous current profiles, have been completed on plasmas with inverted current profiles. These confirm the predominant role not only of the magnetic shear profile, but also that of the safety profile itself on the trigger threshold and mechanism (figure V-12).

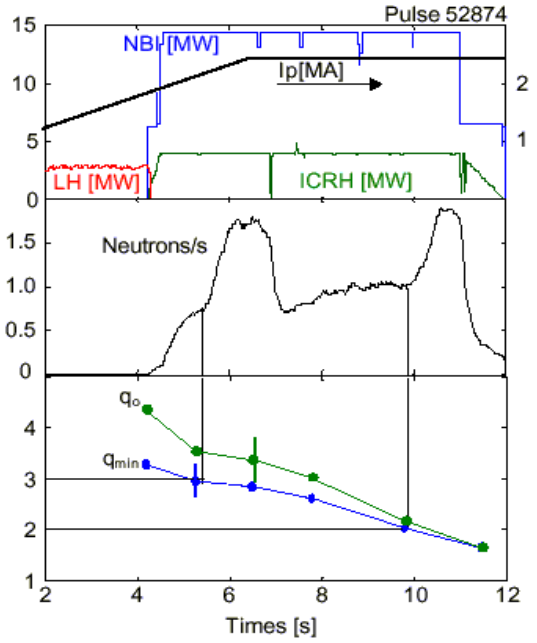

Figure V-12 : Example of correlation of the triggering of efficient internal barriers and the safety factor profile, during the evolution of the current profile in an advanced discharge with inverted current profile.

In the same way, in order to both understand and conduct research on identical advanced regimes in different machines, advanced discharges with monotonous current profiles, usually having q_{min}=2 or 3 on JET, were successfully extended to q_{min}=1 (figure V-13). This type of discharge now enables a systematic research on similarity to be conducted with machines such as AUG, and therefore to start a study of scaling laws for the advanced regime itself.

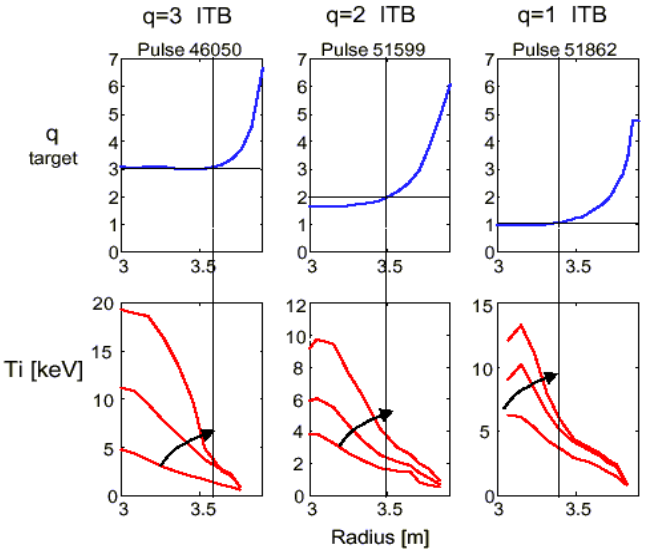

Figure V-13 : examples of three JET discharges with ITB and monotonous current profile, with minimum safety factors around 3, 2 and 1.

V.2.2.3. Research on stationary regimes

Advanced regimes research on tokamaks involves stationarity. A campaign of ITB discharges was undertaken on JET under conditions where the plasma current is entirely sustained in a non-inductive

way. In order to achieve this, an effort on coupling of the LHCD power was jointly conducted with Task Force H (cf V.2.4.2) which allowed up to 3MW to be coupled in the high power ITB discharge phase. ITB discharges with a nearly zero loop voltage were thus obtained for a few seconds, the current being typically sustained in equal parts by LHCD, NBCD and the bootstrap effect (figure V-14). Their study shows the quasi-stationarity of such discharges, in so far as the current profile thus obtained is near its final state, and the barrier thus obtained is resistant to MHD type perturbations, and even to internal radiative collapses. These collapses, a consequence of the neo-classical accumulation of heavy impurities due to the large ion temperature gradients, justify the need to optimize and control the pressure profile under such regimes (see below).

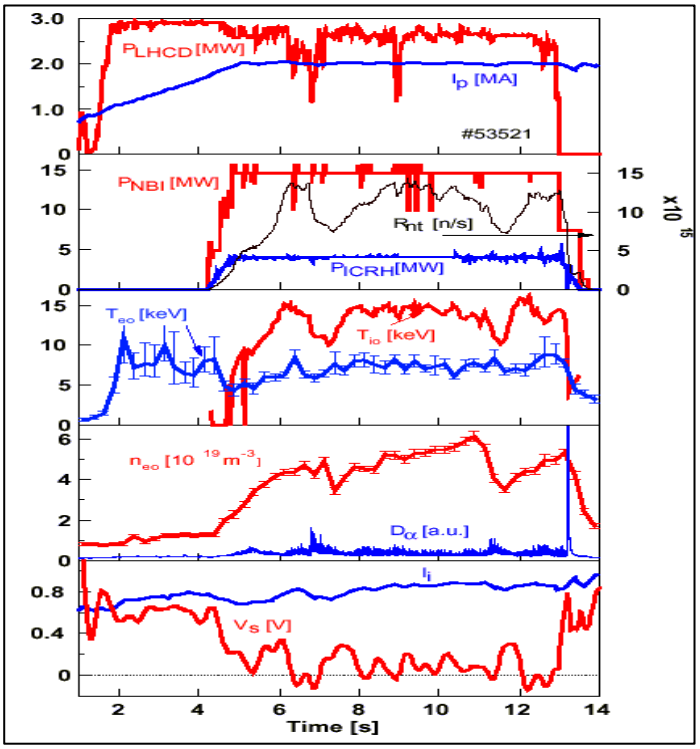

Figure V-14 : JET #53521 discharge, achieving a ion ITB for about 8 s (27 t_E) and an electron ITB for 11 s.

An additional effect evidenced in these discharges is the very satisfactory behavior of the edge plasma (cf. the Dα behavior in figure V-14): the study concerned the characterization of type III ELMs, which are compatible with the internal transport barriers (ITBs), and with type I ELMs, which correspond to a higher pedestal pressure and which cause erosion and sometimes the destruction of ITBs (figure V-15).

The experimental comparison of standard H-modes and advanced scenarii with the same configuration showed that the power scaling law for this transition is very different for the two scenarii (figure V-16). Even at very high power (~5*$P_{thresholdL/H}$) the discharges with ITBs have a plasma edge with type III ELMs. The analysis indicates that the plasma edge current, which is higher in the case of advanced plasmas, is the determining factor in the transition between type III and type I ELMs.

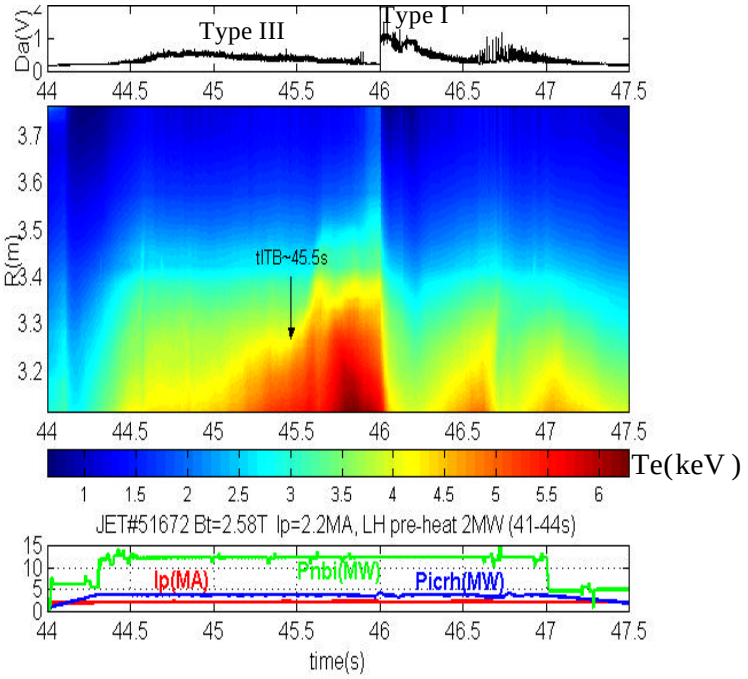

Figure V-15 : Dα signal and electron temperature during the ITB (starting at ~45.5 s) The end of the ITB coincides with the transition to type I ELMs.

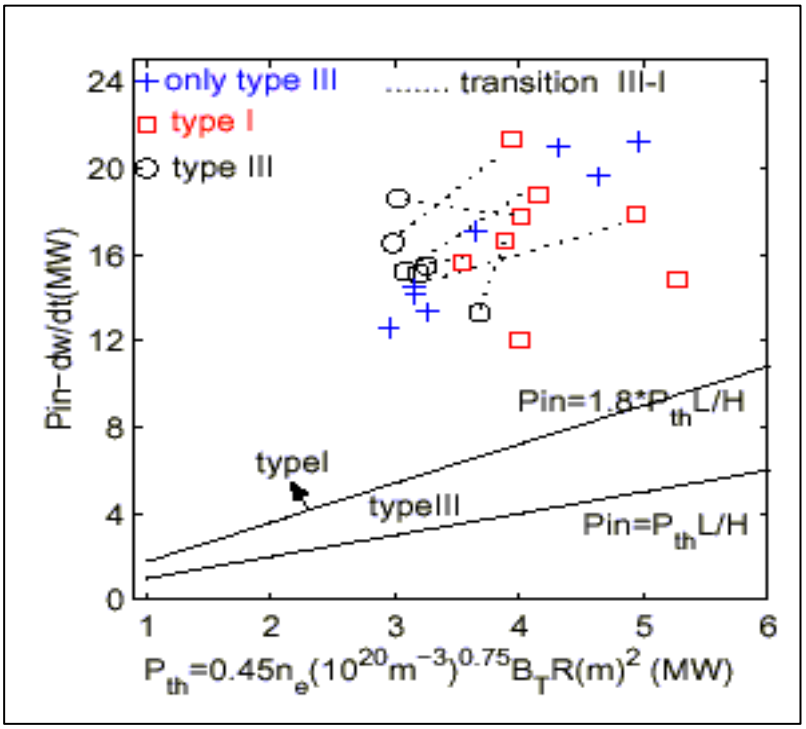

Figure V-16 : Comparison of power scaling of the transition between type I and type III ELMs in H-mode plasmas (P_{in}=1.8$P_{L/H}$) with ITB.

V.2.2.4. ITB characterization

It soon became obvious that a quantitative characterization criterion for ITBs (appearance, localization, intensity …) was needed for the analyses (individual, figure V-17, or statistical) of the discharges obtained, but especially for the detection and monitoring of these ITBs in real time, so as to study their control. The Association has conducted a joint study leading to a quantitative criterion in

complete agreement with the observations (based on a simple parameter, the ratio of the ion Larmor radius to the temperature gradient characteristic length), to the implementation of the necessary real time signal acquisition (including all the superheterodyne radiometer measurements) as well as of retroaction loops between the diagnostics, the plasma supervision systems and the additional heating systems, and, finally, to the algorithms and discharge planning to be made in order to validate such operating methods for advanced regimes. A stationary regime with ITB has been sustained in a completely non-inductif plasma for 7 s (see below).

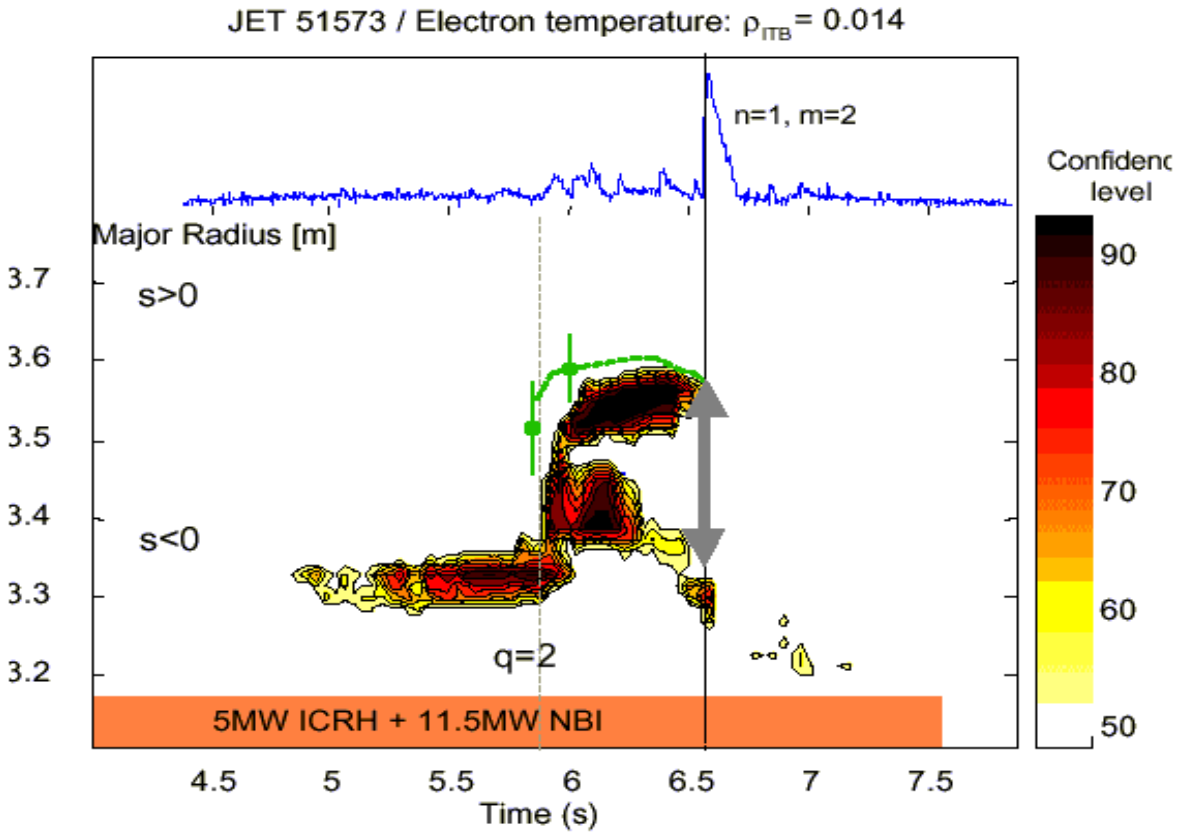

Figure V-17 : Example of analysis of an ITB discharge using the criterion implemented by the Association. This figure shows the space-time localization of the barrier (a criterion calculated using ECE data) as well as information on current profile, the evolution of zero magnetic shear surface (in green) and the envelope of MHD signals (in blue).

V.2.2.5. Self-coherent modelling of discharges

The Association also focused its pluri-annual efforts on the 1-D self-coherent modelling of this type of regime. Thus, the CRONOS code is now able to simulate in an interpretative or completely predictive way advanced discharges. CRONOS thus provides the time evolution of all the profiles (density, temperatures, currents,...) by combining in a self-coherent way the transport and evolution of the current profile in a plasma equilibrium with whatever geometry (figure V-18). CRONOS benefits, among other things, of the main codes on power and current deposition by additional heating systems developed at DRFC over several years. It is now directly coupled to Tore Supra and JET data, and also allows the development and testing of all the real time algorithms prior to their integration.

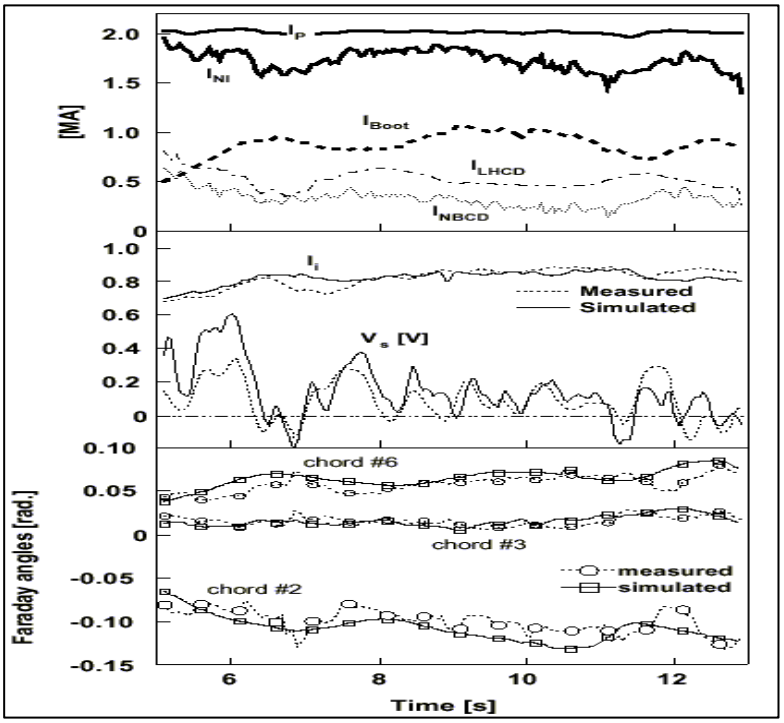

Figure V-18 : Example of complete analysis of advanced discharge (JET #53521, cf figure V-14) by the CRONOS code, with determination of different contributions to total current and reconstitution of the measured physical quantities characteristic of the current profile (self-inductance, loop voltage, MSE angles).

V.2.2.6. Performance of advanced discharges controlled in real time

For the first time in the world, the Association made on JET advanced-mode discharges in which : i) the current profile is prepared and sustained close to a stationary situation (particularly thanks to LHCD during the entire discharge), ii) the quality of the barrier is controlled in real time through a loop linking the FCI power to a normalised predetermined T_e gradient (criterion of barrier existence), iii) the discharge is also controlled in real time by means of a second loop linking the NBI power and the neutron rate produced by the discharge. The best discharge thus obtained showed an ITB (T_e, T_i, n_e, rotation) which was under control for 7.5 s (figure V-19).

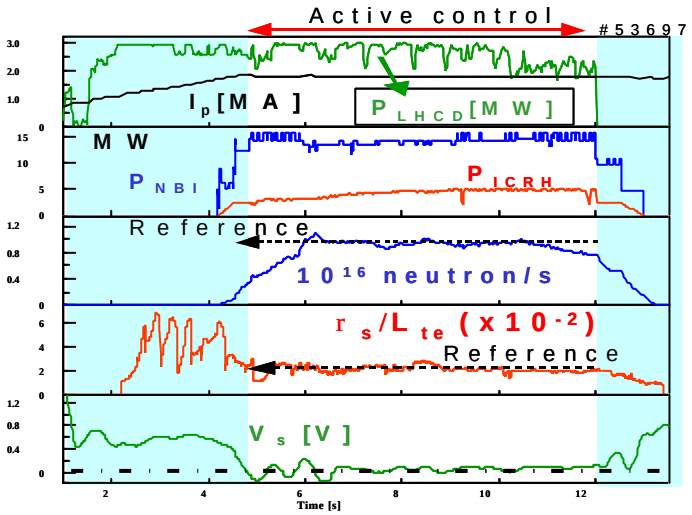

Figure V-19 : Example of advanced discharge (JET #53697) doubly controlled in real time (maximum normalised gradient controlled by ICRH and neutron rate by NBI) and close to zero loop voltage (by means of LHCD additional power)

The next step is under study (cf V.5.4). This means obtaining enough information on the current profile in real time so as to create a third counter-reaction essentially linking the current generator actuators and the current profile. This type of discharge is programmed for the C5 and C7 campaigns of 2002, based in particular on real time polarimetry data.

V.2.3. Task Force M

V.2.3.1. MHD in advanced scenarii : the 'current hole'

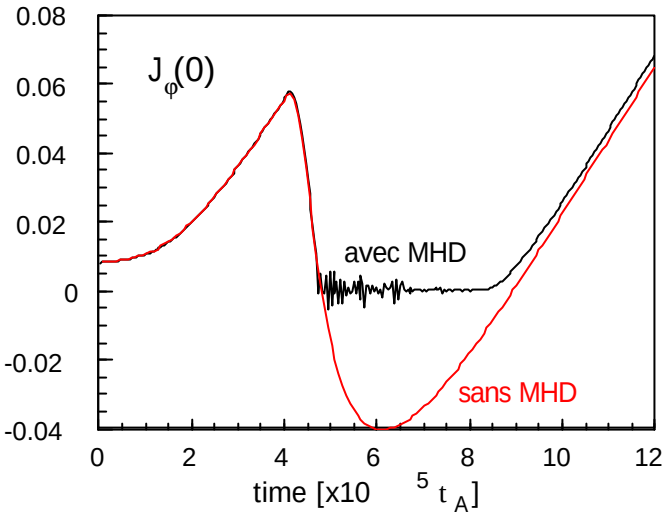

Figure V-20 : Comparison of central current evolution with and without the MHD mode.

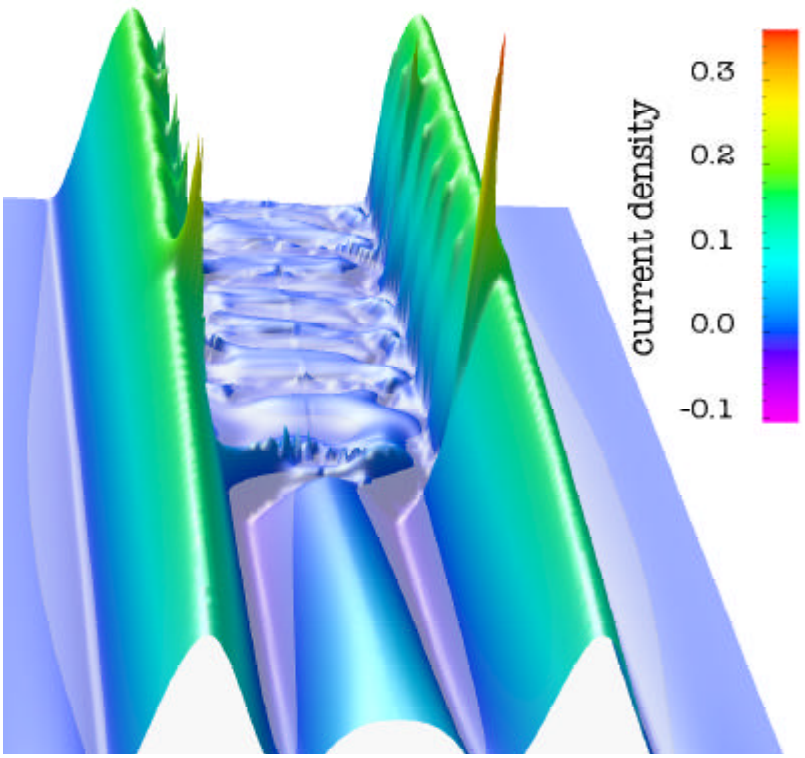

Figure V-21 : Current density profile evolution from 3-D calculations

At JET, in advanced mode scenarii with hybrid heating during the current increase phase, a region with current density close to zero is observed in the center of the plasma. In JT-60U, the same type of current profile, named « current hole », was measured in the presence of a high bootstrap current. The conventional current diffusion with hybrid current outside the magnetic axis predicts a negative current in the center. However, such a negative current in the plasma center has never been observed. MHD stability analysis shows that a plasma with negative current (therefore with a $q=\infty$ surface in the discharge) is unstable to an axisymmetrical kink resistive mode (n=0). The effect of such a MHD mode on the evolution of the current profile has been studied by numerical simulation of the current diffusion with reduced MHD equations. This required a time resolution of about the Alfven time (10^{-6} à 10^{-7} s), whereas the current increase time is of a few seconds (figures V-20 and V-21).

V.2.3.2. Modelling of ion diamagnetic effects on ideal MHD modes

The pressure gradient in the edge pedestal of the H-mode is limited by MHD modes. The ballooning modes are excited by this pressure gradient, kink modes by the bootstrap current due to the pressure gradient. The ELMs are probably a combination of these two instabilities. Generally, the effect of the ion diamagnetic velocity linked to the pressure gradient is not taken into account in MHD stability calculations. However, it is well known that the diamagnetic velocity can have a strong stabilizing effect on ideal MHD modes. In order to study this, the ideal MHD stability code, MISHKA-1, has been modified.

The amplitude of the contributions linked to the diamagnetic velocity to MHD equations increases with the τ parameter, which is the inverse of the ion cyclotron frequency normalised to the Alfven time. Consequently, the effect of the diamagnetic velocity is greater in smaller machines or at low density.

The first case studied is the stability of ballooning modes in the edge pedestal as a function of pedestal width and of toroidal wave-number n ($0 < n < 40$). The effect of the diamagnetic velocity is shown in figure V-22 for one value of pedestal width.

The effect of finite Larmor radius on the ballooning mode, through diamagnetic stabilization, gives an image similar to that of the access to the second stability regime. The modes with high n are stabilized first, and the modes with intermediate n are the most unstable. Diamagnetic corrections to ideal MHD introduce a dependence in density of the stability limit. The modes are more stable at low densities. At high densities, the ideal MHD limit is again reached.

To quantify the importance of the stabilizing effect on MHD limits, the kink and ballooning mode limits were calculated for a JET plasma (hot-ion H-mode) as functions of the parameter τ (figure V-23). The difference between the ideal MHD limit (τ=0) and the limit with the diamagnetic velocity effect is of about 30% for the kink and ballooning modes. The most unstable ballooning mode changes from n=8 to n=10-15 for the experimental value of τ.

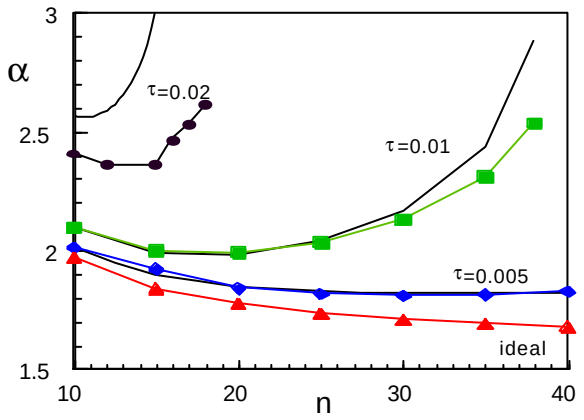

Fig. V-22 : Ballooning limit as a function of toroidal wave-number, n, for four values of τ, the cyclotron frequency normalised to the Alfven time.

In conclusion, the ion diamagnetic velocity has a very significant stabilizing effect, especially at low density, and must be taken into account to evaluate the MHD stability limits of the edge pedestal.

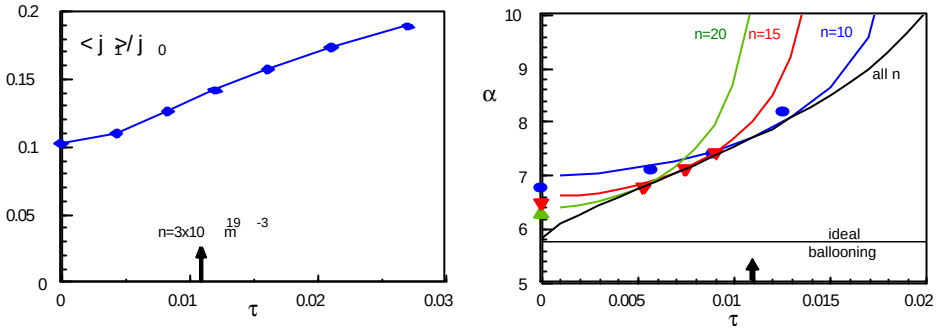

Fig. V-23 : MHD stability limit of kink mode n=2 (on the left) and ballooning mode, n=10, 15 and 20 (on the right) as functions of the parameter t for JET hot-ion H-mode plasma #42677. The arrow indicates the experimental value of t.

V.2.4. Task Force H

V.2.4.1. Non-inductive current generation by fast magneto-sonic wave on JET

Different experiments were conducted on the JET tokamak within the framework of Task Force H to determine the current generation possibilities using the fast magnetosonic wave with the A2 antennae.

Non-inductive current produced by minority FCI heating and sawteeth stabilization

Firstly, different scenarios of minority current drive, out of axis on the high field side, were tested in deuterium plasmas to locally change the magnetic shear and influence the sawteeth behavior. Sawteeth stabilization is observed at + 90° (corresponding to a wave propagating in the direction of the plasma current, i.e. in the trigonometric direction inverse and colinear with the toroidal magnetic field) in current generation with a minority scenario D(H) (ramp of B_T=2,3 ->2,8 T, 42 MHz) (figure V-24). With an inverted phasing of the antennae (-90°), a monster sawtooth is also obtained but at a higher magnetic field. These results can be explained by both a flattening effect of the magnetic shear profile induced by the « minority CD » around the surface q=1 and a fast particle pressure effect in the center. The latter is increased in the case of phasing at +90° by an effect of trajectory pinching induced by the FCI wave. It is to be noted that these results differ from the former JET results obtained with the A1 antennae : sawteeth stabilization was only obtained for waves in the direction opposite to the plasma direction (the plasma current was then in the inverse trigonometric direction).

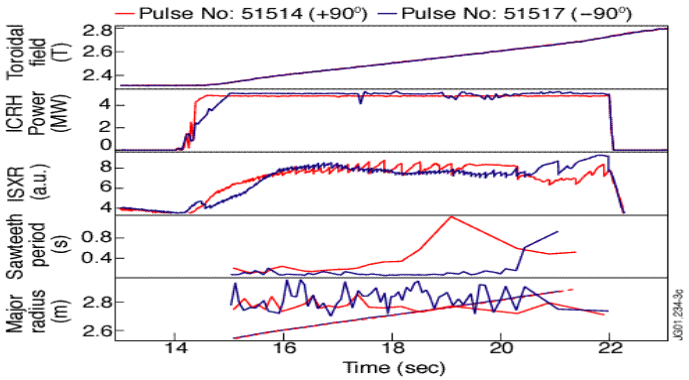

Figure V-24 : discharges #51514 (+90°) in red and #51517 (-90°) in blue. a/ ramp of magnetic field, b/ FCI power, c/ soft X-rays, d/ sawtooth period, e/ ion cyclotron resonance layer (dotted lines) and sawtooth inversion radius

A direct measurement of minority current drive was first made thanks to the MSE diagnostic, by difference between current density profiles with phases at +90° (#51522) and –90° (#51523) (figure V-25) : a difference of 18 kA for 5 MW of FCI power was estimated. This difference in current density profiles is comparable to that obtained with a numerical simulation using the SELFO code. A flattening of the safety factor profile is observed for both plasmas, but the nature of the inverse profile cannot be confirmed, being in the measurement error bars.

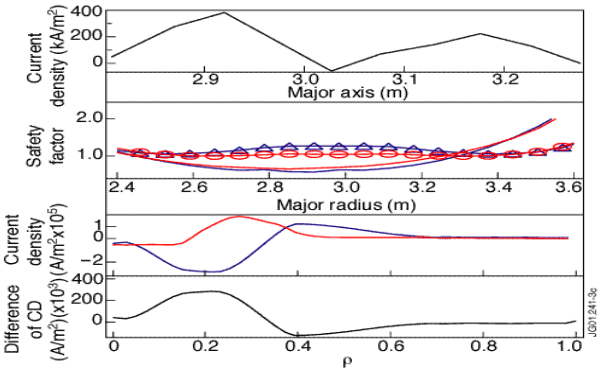

Figure V-25 : a/ difference in current density profiles (MSE measurements) between plasmas #51522 (+90°, in red) and #51523 (-90°, in blue) as a function of major radius; b/ safety factor profiles for #51522 and #51523 (line before FCI, and line with circles during FCI) as a function of the major radius; c/ non-inductive current profile calculated by SELFO as a function of normalised radius, d/ difference in current density profiles calculated by SELFO as a function of normalised radius.

It is to be noted that the monster sawteeth crash obtained under these conditions produces a magnetic island grain of sufficient size to generate « Neoclassical Tearing Modes » (NTM), known to limit tokamak performances (figure V-26).

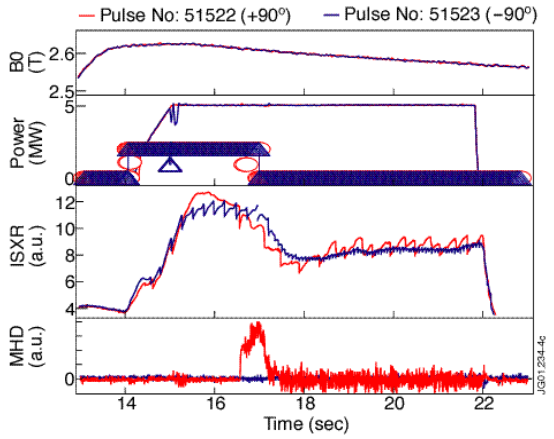

Figure V-26 : plasmas #51522 (+90°) in red and #51523 (-90°) in blue, a/ magnetic field, b/ FCI and neutral beam powers, c/soft X-rays, d/ MHD modes (n=2)

This has the effect of reducing the beta threshold value necessary to obtain NTMs. A contrario, sawteeth can be destabilized with an inverse phasing or by using minority CD on the second harmonic on the low field side. This then helps to increase the beta appearance threshold of the NTMs. These studies, more specifically focused on NTMs, were conducted jointly with TF M. The analysis of heating at the second cyclotron harmonic of hydrogen out of axis on the high field side was made with the ALCYON code, whereas the minority current drive on the second cyclotron harmonic of hydrogen out of axis on the low field side was obtained with the FIDO code.

Non-inductive current generation with FCI wave (FWCD)

For the first time on JET, FCI power was coupled in a FWCD scenario with a high magnetic field (B_0=3.45 T) without an efficient absorption layer of the FCI wave on the ions (figure V-27). The MSE current density measurements in the center indicate a current difference of about 300 kA between +90°(#51643) and –90° (#51644) phasings of the A2 antennae (figure V-28).

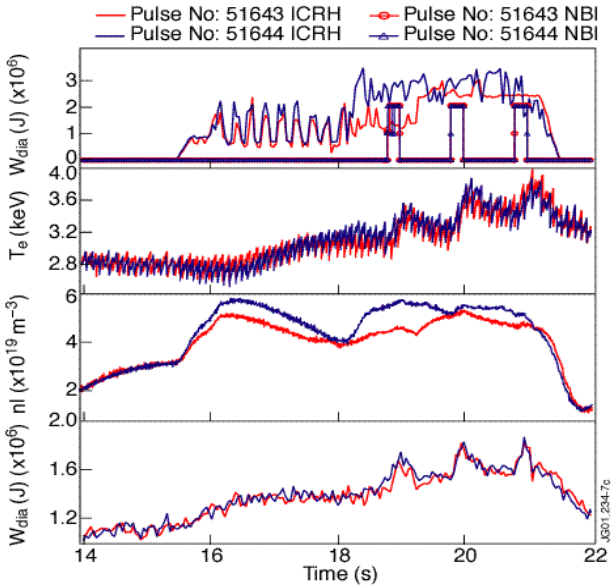

Figure V-27 : a/ ICRF and NBI powers for plasmas #51643 (+90°, in red) and #51644 (-90°, in blue), b/ Electron temperature (KK3, R=2,93 m), c/ average density, d/ diamagnetic energy

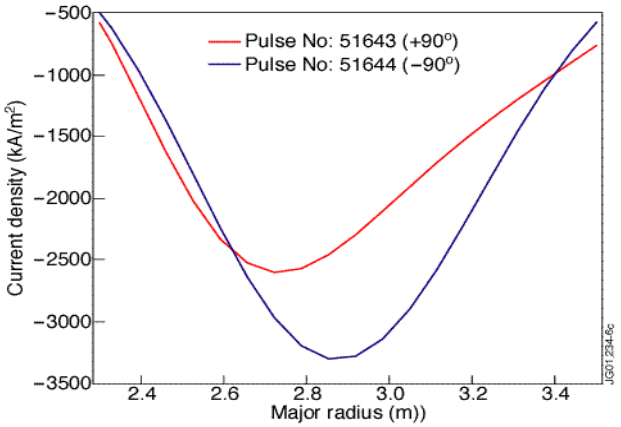

Figure V-28 : current density profiles deduced from MSE measurements, # 51643 in red and #51644 in blue, at t=20,9 s

Direct electron heating (FWEH) with Internal Transport Barrier

Additional experiments with the same scenario as that of FWCD at 3.45 T with pre-heating by lower hybrid wave (2 MW) were carried out during the C4 campaign. A central electron temperature of 6 keV (figure V-29, # 53779 in red) was obtained with 3 MW ICRF power with dipole phasing. By adding 7.5 MW of neutral beam injection on this type of scenario, an electron ITB was formed and produced a central electronic temperature of 8 keV with 6 MW of ICRF power (figure V-29, #53782 in blue). This result is particularly encouraging for future FWCD tests in advanced scenarii in JET, since the absorption of the FCI wave by electrons increases with electron temperature. Within the framework of

our collaboration with the Euratom-Max-Planck Institut für Plasmaphysik Association, a comparison of FWCD scenarios was made for the JET, ASDEX-Upgrade and DIII-D tokamaks.

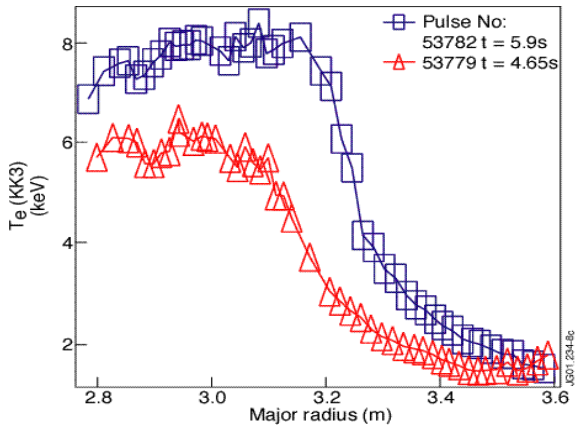

FigureV-29 : Electron temperature profiles (KK3) for # 53779 (red triangles) and # 53782 (blue squares)

V.2.4.2. Fast particle dynamics

DRFC has actively participated in the study of a ^{4}He suprathermal tail by acceleration of a ^{4}He beam by absorption of FCI power at the third ion cyclotron harmonic of ^{4}He. This is particularly interesting since it allows the simulation of 3.5 MeV fusion alpha particles. It is to be noted that the high collisionality of alpha ions in a ^{4}He plasma requires the presence of a sufficiently energetic ^{4}He beam to accelerate this tail (as opposed to a deuterium plasma for which this scenario results in a suprathermal deuterium tail from the thermal plasma, i.e. without neutral beam injection).

V.2.4.3. Mode conversion of the FCI wave into a Bernstein wave

DRFC has participated to mode conversion studies on JET in D-^{3}He and ^{4}He-^{3}He plasmas. An efficient direct coupling to the electrons of the converted wave was observed and the parametric dependence of the localization of the maximum power deposition on the electrons is consistent with the theoretical predictions on mode conversion.

V.2.4.4. Plasma rotation in the presence of FCI heating

DRFC has also participated in studies on plasma rotation in the presence of additional FCI heating. The toroidal rotation profiles show structures which depend on the position of the ion cyclotron resonance layer, the presence or absence of MHD modes, or the plasma confinement mode (L or H).

V.2.4.5. Coupling of hybrid wave on optimised shear plasmas

Coupling experiments and modelling

Coupling of the hybrid wave is very difficult in the presence of ELMs in the H-mode, which is the typical scenario studied on JET and considered for ITER. Significant improvement was made through the injection of CD_4 gas by means of a tube located near the antenna.

It has been demonstrated that if the injection flow rate (expressed as an electron flow rate) was less than 8 10^{21}, the transport barriers are not affected and coupling is greatly improved. Reflection coefficients lower than 6 % and an injected power of 2.5 MW were routinely obtained.

Modelling of the hybrid wave coupling in L-mode was carried out with the SWAN code. The new geometry of the JET hybrid antenna was taken into account. Indeed, after modification of the plasma shape, the antenna front face was machine-finished. The consequence is that the self-adaptation properties of the antenna multi-junctions are highly degraded. In ideal geometry, the reflection coefficient at the antenna input is the square of that existing at the plasma antenna interface. The scattering diffraction matrix of the present antenna has been re-calculated. The agreement between the experimental and theoretical coupling values is better, except for the modules located at the top of the antenna. An explanation could be that the latter are very degraded (presence of large traces of fusion, cracks).

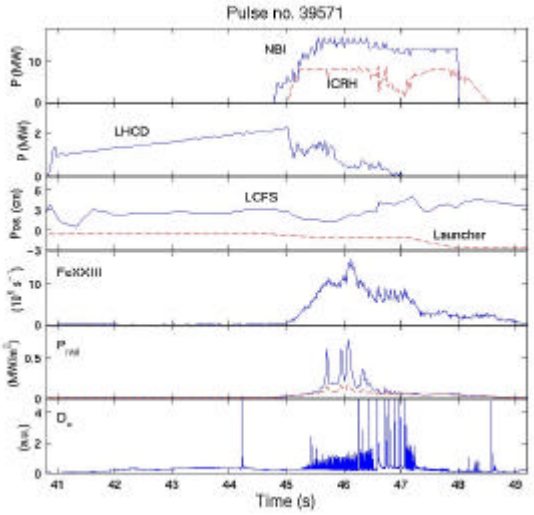

Figure V-30 : One of the first attempts of LHCD use in experiments with optimised shear. During the discharge, impurities are produced, because of the proximity of the plasma. In spite of the small distance, wave coupling is poor (with injection of D_2)

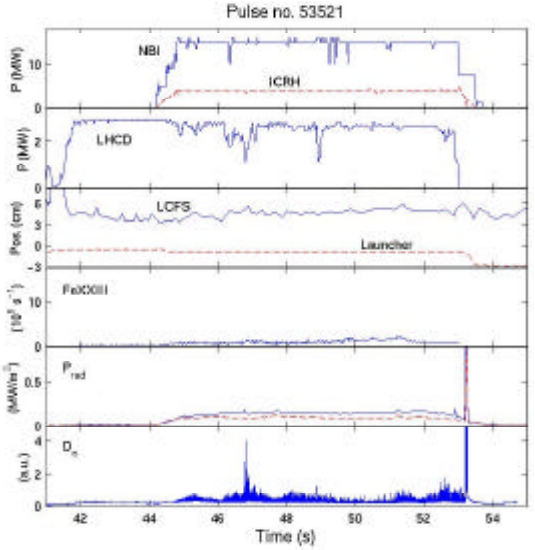

Figure V-31 : Recent discharge with LHCD during the high power phase in an optimised shear type discharge. The LHCD power is maintained during the period with ELMs. No impurity was produced (with injection of CD_4)

During the gas injection experiments, the effect on the coupling was greater on the upper modules than on the lower modules. The gas to be injected enters the injection tube on the upper side. The latter having several holes, the interpretation was that the flow rate was no longer sufficient for the lower modules. The excess upper holes were therefore plugged so as to even out the flow rate over the entire antenna.

Reflected power safety system (SPR)

During a plasma discharge, each klystron is stopped on average four times, which means 96 interruptions per shock. Stopping a tube has two consequences :

- the coupling of modules close to those of the stopped tube is degraded because of inter-coupling,
- the electric field may no longer be sufficient to ionise the gas so as to maintain sufficient electron density for the coupling in the presence of ELMs.

The SPR system is based on the following principle : each klystron supplies two antenna modules by means of a hybrid junction. Conditions are placed on the maximum acceptable values of the ratio and difference of reflected powers measured at the level of the two modules. During the C4 campaign, due to the antenna machine-finishing, the limits in the ratio of the reflected powers are already reached even on an adapted charge. It is therefore clear that this system must be adapted.

V.2.5. Task Force D

V.2.5.1. Equilibrium, current profile, RT control

Recently, the CEA effort in this domain has focused on the validation of the equilibria produced by the EFIT equilibrium code and on the integration of infrared polarimetry and motional Stark effect (MSE) measurements in this code. The expertise in the department on the EFIT code enabled the active participation to the validation of the JET iron core model, needed for magnetic reconstruction. The former iron core model was shown not to correctly reproduce the magnetic measurements; it was therefore improved and is now under testing and installation. The basic reconstruction functions were also improved so as to take into account the increase in the number of inner flux local measurements by MSE. The «B-splines » functions now allow details on current profile to be integrated, which reconstructions with polynomes did not.

CEA has significantly contributed to the determination of current profiles with the MSE and polarimetry diagnostics, particularly during the experiments of Task Force S2. Magnetic reconstruction with these measurements showed the wide variety of inverted current profiles that the JET tokamak can produce. A detailed analysis of the variation of MSE angles during electron ITBs evidenced a strong correlation between the major radius position of this barrier and the current profile. The MSE measurements also revealed the presence in some cases (hybrid wave heating during the plasma current increase, for example) of a zero current region in the center. This phenomenon resulted in MHD analyses to determine the stability of this type of magnetic configuration (cf. §5.2.3). A statistical comparison with infrared polarimetry measurements showed differences, which allowed significant improvements on the magnetic reconstructions with the measurements of the two diagnostics.

V.2.5.2. Impurities, charge exchange

CEA has actively contributed to the work on alignment and absolute calibration improvement of the charge exchange diagnostic. The alignment improvement has helped to determine the uncertainty on the active volume of the neutral beams used by the measurement. The radial position of the lines of sight (LOS) was obtained by using «shrinking » plasmas. Moreover, the development of a new technique for the LOS relative calibration very significantly improved the quality of the charge exchange measurements. This calibration is based on the use of a narrow helium (rather than deuterium) spectral line, and on the radial sweeping of the plasma in order to reproduce the same measurements on several different LOS. A detailed study of the error sources completed this work and the calculation of new error bars was introduced in the calibration of charge exchange spectra. This important work on the charge exchange diagnostic resulted in a much finer study on neon transport as a function of magnetic shear in discharges with a transport barrier.

V.2.5.3. Electron temperature measurement by electron cyclotron emission (ECE)

CEA has contributed on the technical level to the electron cyclotron emission diagnostic (ECE). The calibration procedures and the data treatments improved the routine use of this essential diagnostic.

V.2.6. Task Force T

The JET Transport Task Force (TF-T) was created in 2001 with two main missions :

1. ensure the transport modelling effort in support of the JET experimental program,
2. promote experiments on JET allowing a better understanding of particle and heat transport in a tokamak.

The TF-T action has for the moment resulted in several initiatives in preparation of the 2002 campaign :

- a call for proposals to transport experts in Europe and the United States. 30 proposals on modelling (4 of which from the States) have been received, corresponding to 51 proposals on experiments directly linked to transport studies on JET in 2002.
- the organization of training sessions for the use of the main analysis or transport prediction codes in JET.
- the coordination of the modelling activity in work groups around six main themes :

  1) particle transport (especially understanding the density peaking mechanism),
  2) transport of impurities and their possible impact on turbulent transport,
  3) fast particle transport and link with toroidal speed generation,
  4) integration between edge conditions and transport in plasma core,
  5) heat transport, especially the question of the « rigidity » of temperature profiles,
  6) transport barrier physics (appearence, maintaining and controlling).

- the organization of long stays (>1 month) of theoreticians at JET during experimental campaigns. 39 european experts are expected at JET in 2002, as well as 6 american experts.

V.2.7. Task Force FT

In 2001, within the framework of JET operation, DRFC was involved in the Fusion Technology Task Force. Indeed, an employee of the department was nominated to be Task Force Leader Deputy and thus participated to the selection of european tasks, which will be undertaken at JET in 2002 in this framework. The different subjects which are under consideration are essentially the study of tritium trapping in the tokamak and its characterization as well as any process necessary to detritiate the machine. Disruptions and characterization of material activation for ITER will also be studied.

V.3. 2002 Program

The Association signed at the end of 2001 the 2002 Task Agreement for JET operation. This Task Agreement continues the Association commitment at all levels of the JET tokamak operation (CSU, JOC, S/T Tasks and Enhancements). More specifically, for experimental campaigns C5 to C7, the Association will participate with 7.2 men-years in Orders and 7.8 men-years in Notifications. The five main themes are :

1. Edge plasma and ELMs (TFS1, TFE, TFS2, TFT) :
This concerns a better understanding of ELM behavior versus a certain number of key parameters (plasma shape, edge current density, wall saturation degree, type of heating source), of modelling it and proposing mitigation techniques. This activity is in direct relationship with the design and optimization of the JET-EP divertor.

2. Quasi-stationary controlled operation of advanced scenarii (TFS2, TFH, TFT) :
This concerns pursuing the development work on a quasi-stationary advanced scenario, based on regimes with very high, controlled, non-inductive current fractions. A support to the development of current generation ability by ICRH is also proposed. These points are perfectly adapted to the operational strategy of Tore Supra and our involvement with the « real time » project on JET-EP. In 2002, an increase in NBI power (campaign C7) and real time acquisition of diagnostic will be implemented.

3. ICRH induced rotation (TFH, TFT) :
This subject, already started in 2000, is of great interest to DRFC, and concerns the plasma rotation induced by ICRH and its capacity to trigger possible ion ITBs. Experiments are scheduled on TS, a Ph.D. is being started. The JET contribution in this area is considerable.

4. Transport studies (TFT, TFS1, TFS2) :
The first type of proposals in this area is a consequence of the experiments we propose (effect of ICRH on ELMy H-mode confinement and triggering of ITBs, effects of T_e/T_i, inter-machine comparisons for TFS2 in order to draw up more reliable scaling laws). The second type of proposals « offers » our analysis and modelling expertise in the areas of advanced scenarii with current profile control and of transient transport. Also to be noted are the pellet ablation studies.

5. System optimization (TFH, TFD, TFS2) :
This last theme is in support of the others (and of the JET activity in general). The proposals concern the septum effect on advanced discharges, optimization of ICRH and LHDC coupling (which is crucial to the program we want to perform in TFS2), as well as vital improvements of the MSE and CXRS diagnostics. A series of generic piggyback experiments on real time control is also proposed.

V.4. Remote participation

The Department has been greatly involved, within the framework of a European Task, in setting up and monitoring remote participation techniques. This is particularly due to our very high involvement in the JET program, which must now be able to operate with the help of scientists who are not present on the site.

The different aspects of remote participation can be described in the following five ways :

1) Remote Data Access (RDA) :
80 DRFC employees can presently access JET data remotely. This is possible due to web sub-programs incorporated in Matlab as well as other data analysis programs. However, the european networks are not fast enough to allow a large number of data to be transferred. In this case, remote access to JET computers should be considered (RCA).

2) Remote Computer Access (RCA) :
This allows safe connections to local computers. Thus, the screen is transferred, not the data. The “Citrix” servers as gateway computers were chosen, coupled to a safety system by personal SecurID electronic cards. 50 DRFC employees are authorized to connect through this to the JET computers. The DRFC personnel at JET can also connect to Tore Supra with a similar system.

3) Communications :
DRFC physicists are in daily contact with those present on the JET site. Theis is increasingly done electronically and a participation space has been installed which allows us to directly participate in the JET operation as if we were in the control command room. A video conference room is also operational at DRFC and several meetings have been successfully attended in a similar room at JET. Network speed is here an essential element.

4) Network surveillance :
Several control tools for network surveillance are used: statistics are made, response time and traffic between all the laboratories are monitored, including the automatic emission of alarm signals.

5) Support :
This support activity is essential to the success of remote participation. Two DRFC employees ensured the development of techniques and training of personnel.

V.5. JET EP Projects

V.5.1. JET EP Divertor Design

The JET EP divertor project consists in studying, fabricating and installing on JET a new divertor able to manage up to 50 MW of injected power for about 10 s. The aim is to propose a divertor design authorizing equilibria with high triangularities representative of ITER as well as being compatible with high beta scenarii allowing advanced tokamak studies, all the while preserving a pumping capacity.

This project has been led by DRFC since July 2000 with the participation of different units in Europe (EFDA CSU Garching, CEA/DEN Saclay, IPP Garching, FZJ Jülich, ENEA Padova, UKAEA at Culham and IST at Aveyro), the controlling structure (EFDA CSU JET) being in Culham.

The physics studies resulted in proposing a design optimised to manage heat and particles in different configurations. The support structures were designed to maintain the carbon tiles in the defined geometry, whatever the electromagnetic strains. These structures were adapted to integrate all of the diagnostics and allow the divertor to be installed by remote handling.

The technical specifications needed to launch a call for tenders for fabrication will be ready in January 2002.

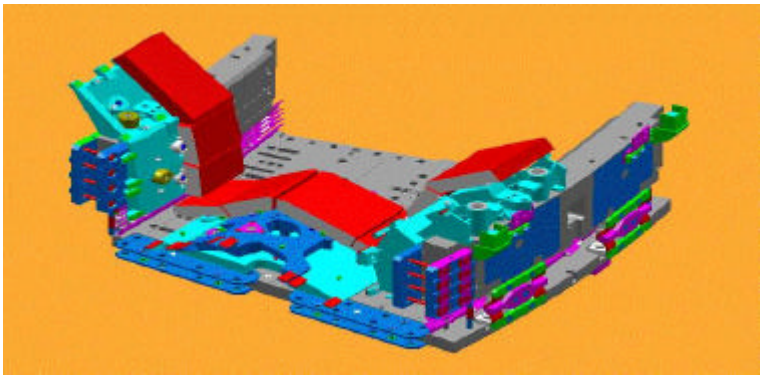

Figure V-32 : View of JET EP divertor module

V.5.2. EP IR Viewing

Within the JET-EP, DRFC was selected to be in charge of an infrared thermography diagnostic. The project proposed by DRFC for the JET-EP is ambitious, innovative, compatible with an operation in tritium and pertinent for ITER. The aim is to be able to observe the power deposition on all of the internal components (divertor, first wall, antennae…), while maintaining a high spatial resolution to study very peaked deposition patterns, such as on the divertor strike points or possible hot spots. To meet these demands, the choice was made of a reflective optical system using metallic mirrors (thus resisting to neutron radiation in the upstream part of the endoscope), associated to a conventional optical system equipped with a zoom for the downstream part. Moreover, to study ELM physics and in particular measure the power and energy distributions during ELMs, the time resolution must be less than the characteristic ELM time, in other terms 100µs.

The project was approved during an EFDA sub-committee meeting on 5 October 2001. It is financed by Task 5.1b, for the time being allowing the design phase of the endoscope optical system to be launched.

V.5.3. FCI antenna

A contribution was made to the JET-EP ITER-like antenna project team, especially on the following points :

- analysis of electrical circuit and establishment of electrical specifications for connection components,
- design, fabrication and measurement of Radio Frequency electrical characteristics of a low level, scale 1, mock up of a module representing half the antenna,
- thermo-mechanical analysis of tunable components (capacitances by COMET) and establishment of specifications for fabrication of three prototypes,
- achievement of fatigue tests on a RF power test bench of the three prototype tuning capacitances within the framework of an EFDA/ITER contract.

Moreover, proposals for the evolution of the design were made with the aim to solve the technical difficulties, which especially appeared on tunable components.

V.5.4. Real Time Project

The real time project was prepared during 2001 so as to meet the increasing demand for control of advanced tokamak plasmas. It aims at :

- increasing the real time calculation capabilities of a certain number of diagnostics,
- preparing the real time algorithms on current profiles, temperature, and density,
- designing control algorithms for the experiments.

This project was approved by the EFDA steering committee in July 2001. It has a budget of 80 k€ for material, 6 to 7 men-years for human means. Four associations and a university are actively involved (CEA, University of Nice, ENEA-RFX, IST Lisbon, UKAEA). Over twenty people are directly involved.

Many diagnostics and codes are concerned by this project :

Diagnostics	*Concerned real time measurements*	*Data production time*
Magnetic	MHD modes n=1 and n=2	2 ms
Charge exchange	Ion temperature and rotation profiles	<50 ms
ECE	Electron temperature profiles	<10 ms
Interferometry and polarimetry	Density and current profiles	<10 ms
MSE	Current profiles	<50 ms
Plasma limit code	Confinement parameters, plasma geometry	2 ms
Real time equilibrium code	Current profile, surface flux mapping	25 ms

This will provide JET in 2002 with a unique tool for all the current profile control experiments.

VI. DEVELOPMENT FOR THE NEXT STEP AND THE LONG TERM

VI.1. Prospective studies

In the hypothesis of lack of agreement on the ITER construction, the European Community, in compliance with the recommendations of the "Airaghi" report, is studying a fall back project which could be acceptable at the European level. A machine of 5.20 m major radius with aspect ratio and elongation identical to those of ITER, but a higher magnetic field ($B_t \cong 6$ T), was the object of a preliminary study. The scaling law ITER98(y,2) for the energy lifetime and the same hypothesis as ITER on profiles and impurity contents were taken. In the inductive mode, with a plasma current of 14 MA, giving an edge safety factor of 3, an operating point for this machine is obtained at Q= 10 and 400 MW of fusion power, with a density of 80% of the Greenwald limit, a reasonable margin for the L-H transition and an acceptable maximum flux at the divertor. The poloidal system of the machine can withstand discharges of this type for about 300s. In a non-inductive current generation mode, and with assumptions identical to those considered for ITER in the same conditions, a reasonable operating point is found at Q = 5. The toroidal and poloidal magnetic fields are generated by hardened copper coils. A steel band surrounds the toroidal coils ; it is aimed at reducing the explosion strains on the copper. A preliminary modelling of the mechanical structure of the machine was made for the calculation of strains with the CAST3M code ; it takes into account the plate structure of the toroidal coils. Thermal effects, as well as the effects of the different poloidal current configurations, have been studied. For a choice of Inconel as a structure material for the box containing the toroidal coils, the strains were found compatible everywhere with the limitations of the different materials.

An effort to validate the results of the CAST3M code was made in a pedagogical case without steel band and with only the toroidal field. The results of the code are found in this case to be identical to those given by an accurate analytical calculation of the vertical force and similar to those provided by an accurate analytical calculation of the centring force.

The design of the M2 machine (Q = 5, supraconducting) was actualised by using the ITER rules on geometry (aspect ratio and elongation), confinement, density limit, margin versus L-H transition and discharge time in inductive mode. This results in a larger machine that that obtained in 1999 (R = 5,60 m instead of 5,24 m). A re-estimation of the cost of this machine by interpolation of the ITER cost rules results in 3 G€.

VI.2. Developments

DRFC is responsible within the Euratom-CEA Association of the studies started within the framework of the European Fusion Technology Program. These activities concern the developments necessary to the achievement of the next step and studies whose objectives are longer term, but whose importance is paramount in establishing credibility for fusion energy (development of structural materials for example).

DRFC ensures the technical and financial aspects but also the program orientations of these studies, which represent over one fourth of the activity of the Association. These studies are mostly conducted with the collaboration of other CEA units or with the industry (figure VI-1). The main participants are the Nuclear Energy Directorate (CEA/DEN), for the activities on tritigenous blankets, safety studies, nuclear materials, and the Technological Research Directorate (CEA/DRT) for work on robotics, advanced welding, development of new materials. Execution of this work is controlled by the DRFC with whom the different partners (CEA or not) are under contract.

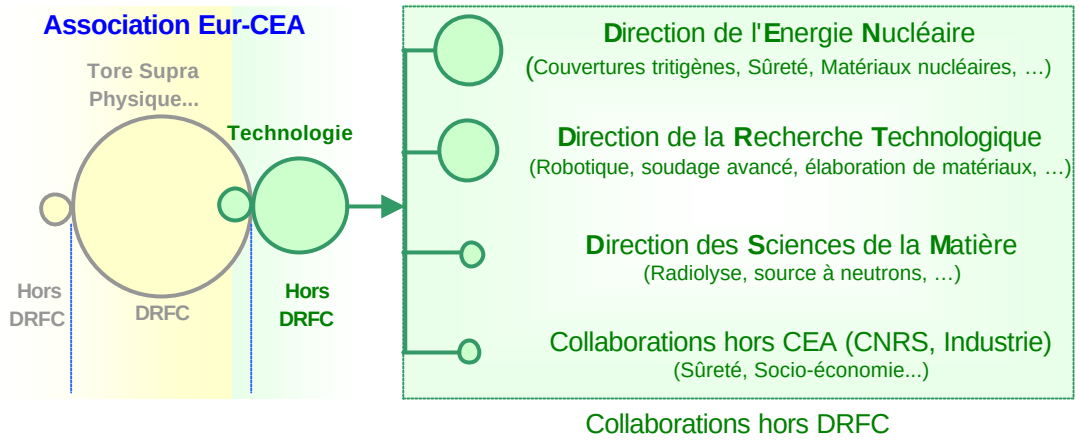

Figure VI-1 : Technological activities of the Euratom-CEA Association. In green : technological developments for the next step and the long term.

In the following paragraphs, the presentation will be limited to the work done at DRFC itself : plasma engineering, high flux components, supraconducting magnets. The reader can refer to the "FUSION TECHNOLOGY Annual Report of the Association EURATOM/CEA 2000 " documents and to the 2001 report (to be published) for a complete description of all the activities conducted by the Euratom-CEA Association. These references are available on the Association website.

VI.2.1. Plasma engineering

VI.2.1.1. Negative ions

JAERI/CEA collaboration on the development of negative ion sources, D^-

This collaboration concerns the study and improvement of the performance of the Kamaboko III source (designed and built by JAERI, Japan, as a « model » of the source for ITER injectors). Experiments were conducted on the MANTIS test bench at DRFC. The main goal was to demonstrate beams of 1000 s in D^- with 200 A/m^2 and a pressure in the source of < 0.3 Pa. Obtaining these long duration beams required several modifications to MANTIS :

- change of the resistances in series with the discharge with water cooled resistances ;
- increase of the water flow rate to cool the source ;
- replacing the source diagnostic flanges by properly cooled flanges ;
- making the accelerator protection system more reliable ;
- modifications of the grid supports in the accelerator ;
- implementation of remote control to reduce the neutron fluxes to the operators to an acceptable level.

The most important part of the ITER task, producing beams of H^- and D^- for 1000 s with a pressure and a power in the KAMABOKO III source of 0.3 Pa and 55 kW respectively, was achieved (figure VI-2). Unfortunately, the accelerated current density during long duration beams, 80 A/m^2, was 40 % lower than the foreseen value, which explains nearly all the difference between expectations and obtained performance. The reason for this phenomenon could be due to the material of the plasma grid (molybdenum), and/or to the temperature at the source walls, which is higher than with short duration beams. These assumptions can be verified during the next campaign of 2002, when a copper-zirconium grid will be used.

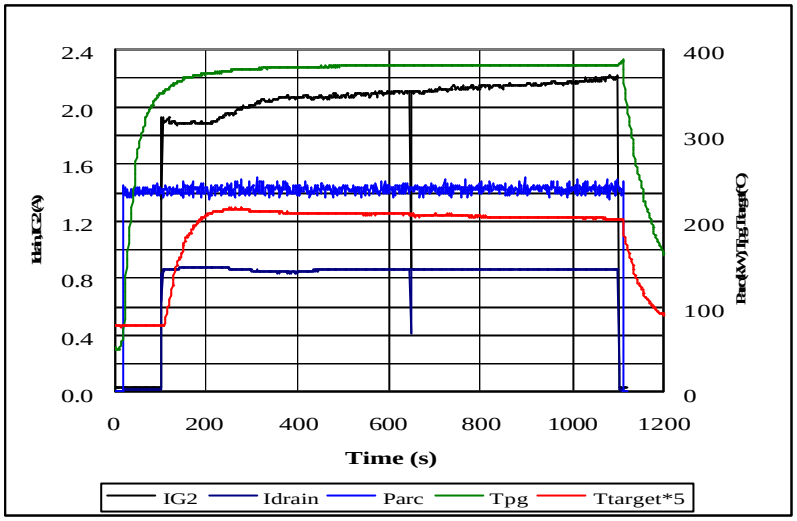

Figure VI-2 : 1000 s D- beam, with KAMABOKO III source, in ITER-like conditions. Pressure in the source of 0.3 Pa, Pdischarge 47 kW, Vextraction 6 kV, Vacceleration 25 kV.

During the long duration beam campaign, the rate of use of caesium was 500 times greater than the expected rate; this can be a very serious problem for ITER. The reason is probably linked to the way of using the system : to obtain constant current during the shocks, the plasma grid temperature must be at equilibrium ; the discharge is thus started more than 100 s prior to the application of the high voltage. Since the Cs in the source is estimated to be ionised at 98%, during this time it can escape from the source. This can be prevented if the plasma grid is polarised positively versus the plasma before the application of high voltage, or if the high voltage is applied earlier on. These two scenarii will be studied during the next experimental campaign. The negative ion density measurements in the source by means of the "laser cavity ringdown" diagnostic failed, as the limits imposed by the holes in the MANTIS flanges prevented the cavity from being aligned. Enlargement of these holes should allow a new alignment test to be performed during the next experimental campaign.

IPP/CEA collaboration on the development of a HF negative ion source

Study of the negative ion HF source, called "type 6", is underway in Garching. This source uses a small cylindrical HF source attached on a rectangular source body, thus improving confinement. As in all the other HF sources, the addition of argon increases the density of H^- extracted from the source. Also, when the source is «clean », the addition of Cs increases the density of the extracted H^-. Unfortunately, the beneficial effect of caesium cannot be reproduced. The best performance up to now is 150 A/m^2 of H^-, with a HF power of 145 kW in the source, but with a high pressure, 0.7 Pa. Recently, it was shown that the addition of Ne, Kr and Xe also increases the efficiency of H^-, but less than Ar. The mechanism responsible for this effect is still unknown : there is no significant change in the plasma characteristics (measurements made with a Langmuir probe), nor improvement with a filament source of negative ions. A new version of the HF source, "type 6.2", has been built and will soon be tested. The specificity of this source is its two cylindrical sources attached to the rectangular source body ; it could demonstrate the possibility of extrapolating to larger HF sources.

SINGAP

The development of a 1MeV «SINGAP» accelerator (an ITER task) started up again in 2000. The 1 MV isolator was re-assembled with the first 8 isolators in epoxy glass and the ninth in ceramic. The isolator is leak-proof with the transmission line at a large SF_6 pressure, 0.35 MPa. After high voltage tests on each isolator, the complete isolator was conditioned up to ~ 600 kV under vacuum, and then up to 1.04 MV with addition of gas (H_2) to obtain a pressure of 10^{-3} Pa in the system (see below). This conditioning was very fast (two hours with voltage, corresponding to a week of real time).

When voltage is applied to the plots of one or several crowns, a significant « black » current is measured, causing a degassing of the isolator and/or of the electrostatic shields. This current decreases when the pressure in the system increases (between 10^{-6} and 10^{-2} Pa). The black current and degassing decrease with the application time of the voltage. The composition of the gas released during the conditioning always being the same (independently from the composition of the isolator), it can be concluded that the degassing comes from the electrostatic shields. Conditioning of the entire isolator is done with the « anode » of the accelerator at the high voltage (≤ 1.04 MV). In this situation, the « cathode » is the wall of the system, with a surface of about 50 m^2. This surface emits electrons (the black current) which bombard the anode, which degasses. However, the current being limited to < 100 mA by the supply system, the anode heating does not seem to be sufficient, either to reduce the degassing to zero nor to condition the cathode. Therefore, the pressure had to be increased to reduce the black current ; this enabled 1 MV to be obtained on the isolator.

After the end of the 1 MV test bench (reconfigured) use for the development of the positive ion source, it was put back in the negative ion configuration, using the negative ion source "sourcette" and the SINGAP accelerator. The 1 MV isolator and the accelerator were first conditioned up to > 600 kV under vacuum. The variation of the beam profiles (therefore the beam optics) with the extraction and pre-acceleration energies was studied with an infrared camera, which looks at the back of a carbon target (the target is located about 3 m from the accelerator). The first results are in agreement with the predictions of the 3D OPERA code; detailed comparisons are underway.

An example of D- beam profile at 900 keV (seen by the infrared camera) is shown in figure VI-3.

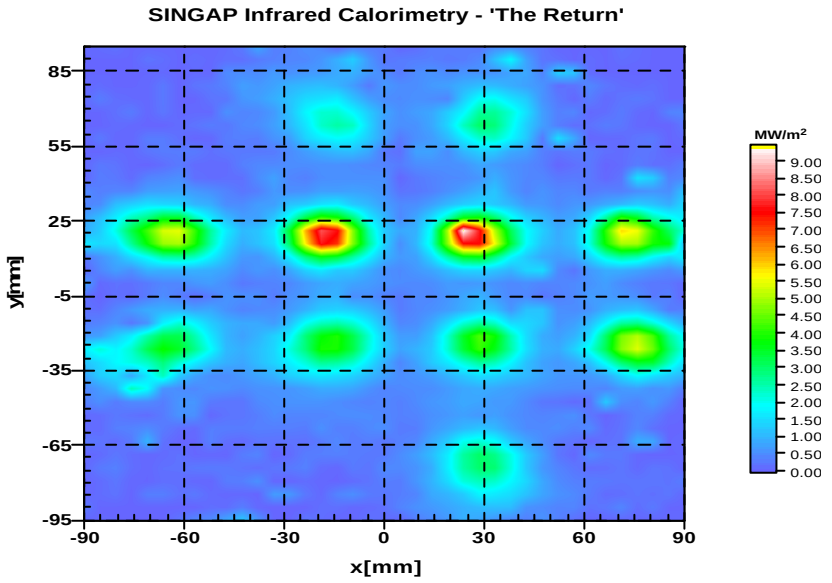

Figure VI-3 : Profiles of a D- beam at 3 m from the accelerator. The small beams from the 11 holes of the pre-accelerator can be seen.

SINGAP accelerator design

A thorough study of the SIINGAP accelerator optics was submitted to ITER-FEAT. The use of a SINGAP accelerator for low energies was also considered; such an accelerator had been envisaged for several applications in Europe, for example on JET-EP. The result of this study is that generally SINGAP is not the best choice for energies under 350 keV, but is certainly good for those above 400 keV.

VI.2.1.2. RF heating

FCI

- Within the framework of an EFDA task, a contribution was brought to the definition of an electrical configuration for an antenna allowing the power density coupled per surface unit to be increased (in view of the greater demands in this area in the reduced ITER-FEAT configuration), especially by the analysis and comparison of several alternate configurations.
- Within the framework of an R&D EFDA task, a cw power test bench was designed and is being fabricated for use during 2002.
- Following a conceptual design activity on tuneable components, two technical options were studied by making a low level, scale 1, mock up, which electrically validated the concept. Moreover, a first series of tests under vacuum of electrical contacts of the « multifoil » type in fixed position was done on a test bench, allowing a current of 1 kARMS (in other terms 60 A/cm) during 60 s to be reached, without any trace of degradation found during the dismantling inspection.

LH

Current generation by hybrid frequency waves is presently considered in ITER-FEAT only to obtain stationary scenarii at zero loop voltage in which the production of fusion power corresponding to Q=6 is aimed at. The plasma current then being of 9 MA to benefit from a greater ratio of self-generated current (50%), the injection of hybrid waves is considered to generate the current at the edge of the discharge in a region where the electron density and temperature are lower and where it is therefore more efficient.

The power injected in a quasi-continuous regime must be of 20 MW. Within the framework of EFDA contracts, in partnership with ENEA, ITER JCT, IAP nizny Novgorod and VTT (Finland), all of the hybrid system has been designed. Two more detailed reports on the study of the antenna and transmission line were written.

The most important aspects of the hybrid system are as follows :

- The generator consists of 24 cw klystrons of 1 MW each. The frequency considered is 5 GHz. This value comes from a compromise between the klystrons technological limits and the need to increase the frequency to avoid that a portion of the power be coupled on alpha particles. The required klystrons characteristics are an efficiency of at least 60% and a gain greater than 50 dB.
- The klystrons are supplied in groups of 4. Since the considered tubes do not have any modulation anode, power switches would be a possibility to isolate the elements raising problems. The HF control system has two sources shifted by 10 MHz, so as to bring all the measurements back to this frequency.

The klystrons rectangular wave-guide outputs are grouped 4 by 4 by recombiners to feed 6 lines made of a circular wave-guide in which the excitation of the TE^{O}_{01} mode is aimed at in order to minimise losses. The length of the transmission line is 70 m. The circular line part includes :

- mode filters (to attenuate higher modes),
- quasi-optical bends (to minimise diffraction losses).

At the output of the circular line, a divider is used to separate the power into 4 and to feed 4 rectangular guides which are then connected to the antenna. The evaluation of the transmission losses is of 9.5% for the diffraction losses and of 1.8 % for the joule losses.

The study of each component was carried out with the HFSS (High Field Structure Simulator) electromagnetic code. The recombiner, which is also used as a divider, requires additional study.

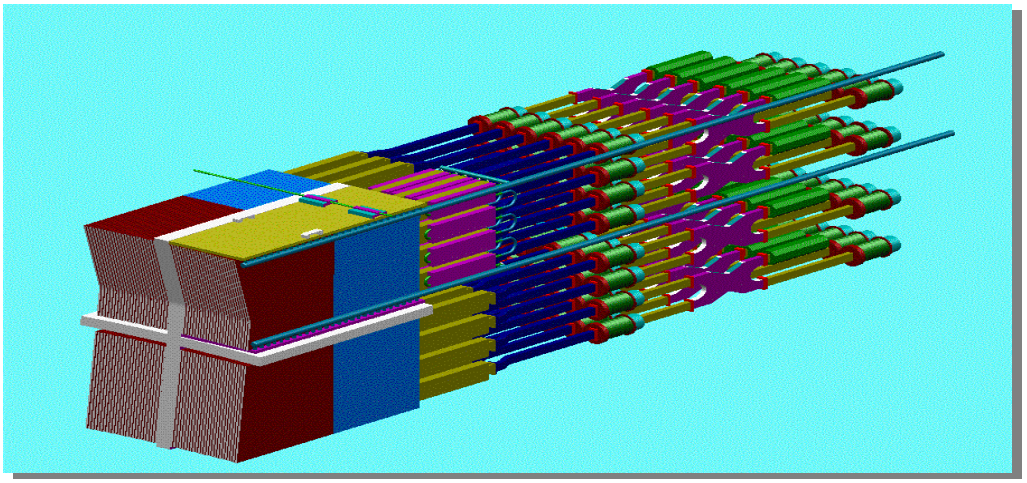

Figure VI-4 : Drawing of the antenna whose principle is based on the use of Passive Active Multijunction (PAM)

The antenna has two parts. The first one (located in the cryostat vacuum) has 24 beryllium oxide windows on the cryostat flange, 48 windows (same type) on the vacuum vessel flange, and 24 hybrid junctions to divide the power by 2. The second part (located in the machine vacuum) has 4 blocks, each made of a PAM. Each of them is supplied by a 3x4 TE_{10} - TE_{30} mode converter. A PAM has 12 rows of 24 active and 25 passive ducts. The geometry of the antenna is chosen so as to be able to work at a power density of 33 MW/m^2, a value extrapolated from that of Tore Supra, and to radiate a spectrum whose main peak value is $N_{//}$=2.

A complete study of the antenna was carried out :

- all the HF components were modelled and studied with the same electromagnetic code as that used for the elements of the transmission line ;
- the coupling calculations were made using the SWAN code. The power directivity is greater than 60% and the reflection coefficients are less than 5% on a large range of electron density variation (a factor of 10) ;
- calculations of heating due to the neutron flux, to the HF losses and to the plasma radiation have been made. The PAM concept, very efficiently cooled, allows to remove the power. The antenna tip is made of beryllium and the antenna is made of special copper. CFC, which was initially considered for the tip, was eliminated because of the excessive shearing strain between CFC and copper ;
- the degassing and pressure calculations in the antenna were done. They show that, in all cases, a pressure of less than 10^{-5} mbar can be ensured. This pressure level is sufficient to ensure proper operation of the antenna ;
- the thermo-mechanical constraints and those due to disruptions have been evaluated. In all cases, it has been shown that it remains in the elastic domain ;
- studies on electron acceleration in the field close to the antenna were made. The sheet thickness was chosen so as to minimise the part of the power radiated at high $N_{//}$ values. It was demonstrated that under these conditions, very little power would be lost through this mechanism ;
- neutronic calculations to evaluate the doses at the antenna flange on the machine vacuum side were made. The result is that the antenna design meets the specifications. In fact, the dose rate is lower than 100 µS/h, which is the necessary condition to be able to work on the antenna without any radiological protection.

The study of the hybrid frequency system has shown that it is perfectly conceivable, from a technical point of view, for a machine like ITER FEAT.

VI.2.2. Plasma facing components (CFP)

VI.2.2.1. CFP ITER activities

Concerning the plasma facing components, the technologies under consideration as « reference » for the divertor or the first wall as well as the associated non-destructive controls, have been improved. The department worked through contracts or european Tasks using the FE200 high heat flux station and the SATIR infrared characterisation bench.

High flux elements

a) Contract 98/480 : FE200 and SATIR tests

Six mock-ups of different divertor parts were tested under thermal fatigue :

- three right hand samples of the ITER divertor baffle ; CFC monoblock technology in NB31, but assembled under cold isostatic pressure (cold HIPping). The mock-ups withstood up to 1000 cycles at 17 MW/m^2 without failure, but presented significant heterogeneities of surface temperatures. These tests proved the robustness of the monoblock concept, despite the presence of interface defects due to the fabrication process ;
- a curved sample of the ITER divertor baffle also presented remarkable results, since it withstood 1000 cycles at a surface temperature of 2000°C, corresponding to 13 MW/m^2 absorbed in water. The fabrication of a curved monoblock is a first and offers many design possibilities which were up to now impossible for this technology ;
- two prototypes of the ITER divertor dome made of compacted copper on stainless steel, then covered with a thick tungsten-copper mixture plasma deposit, were submitted to up to 1000 cycles at 3 MW/m^2 without damage ; however, one of these elements cracked after 900 cycles at 4 MW/m^2 : this is the maximum acceptable heat flux for this technology.

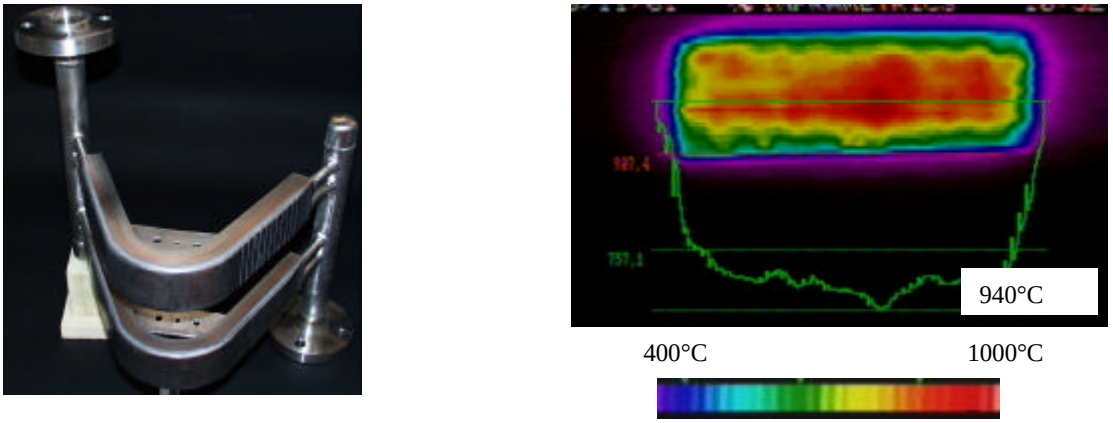

Figure VI-5 : Infrared view of dome prototype under a 3 MW/m^2 flux

b) DV4.3 Task : Risk of domino type fall of tiles and FE200 tests

This study consists in evaluating the risk of tiles coming off in a domino style as soon as one defective tile falls. A preliminary study was done with finite element calculations. This is a concept with flat CFC tiles on a hyper-vapotron tube, which allows for fluxes much greater than 10 MW/m^2. These calculations showed that slightly after the drop of a tile, a temperature of 3000°C is reached on the edge of the adjacent tile submitted to the parallel flux. This temperature goes back down to ~2100°C when the CFC erosion starts up. The flux through this adaptation layer was also calculated with different hypotheses on eroded thicknesses. The calculations predict, with a rather significant probability, a detachment of the adjacent tile.

The preliminary study determined the charges to be applied to the mock-ups in order to perform these tests of domino detachments, foreseen in 2002 on the FE200 high flux station.

First wall elements - Contract 98-485 : FE200 tests

Four small scale mock-ups in hardened copper (CuCrZr or Glidcop) welded by Hot Isostatic Compression (CIC) on massive stainless steel 316L back plates of the first ITER wall were tested on FE200. The incident heat fluxes varied during the tests from 2,5 to 5 MW/m^2 (5 to 10 times the nominal value expected in ITER) with the aim to accelerating the propagation modes of cracks or defects at welded interfaces (N.B. : the mock-ups have already been submitted to 30000 cycles at 0,7 MW/m^2 without damage). In addition, one of the aims of the study is to correlate the damage at the interfaces with non-destructive controls. Each test phase is also controlled with ultrasounds at VTT (Helsinki).

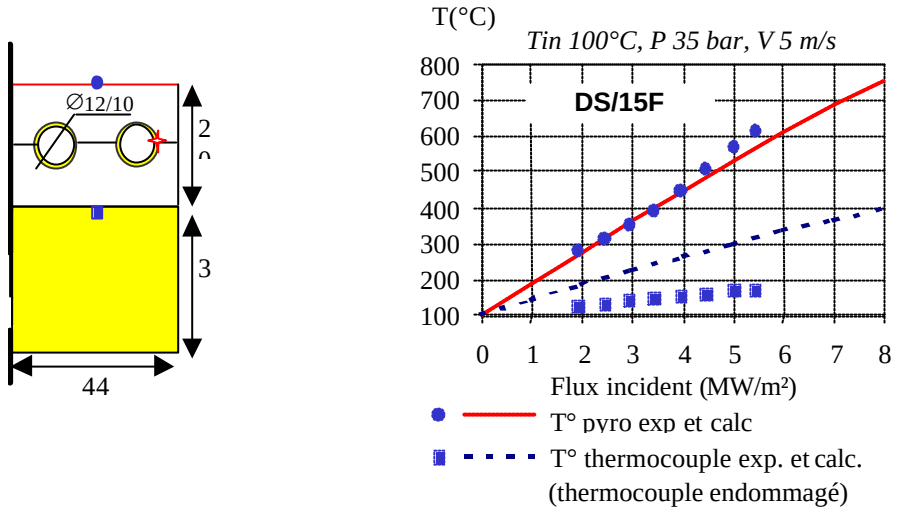

Figure VI-6 : Cross sectional view and comparison calculation/experiment for the DS/15T mock-up (Glidcop).

The results are coherent with the present knowledge on the concept and control tools : imperfections in CIC weldings had been detected by US control on the triple generator level (cf. red star in figure VI-6) of a CuCrZr mock-up. The imperfections quickly propagated (less than 100 cycles at 5 MW/m^2 have been sufficient) in the interface plane, which did not resist (cf. open interface in figure VI-7). The three other mock-ups resisted to 1000 cycles without damage.

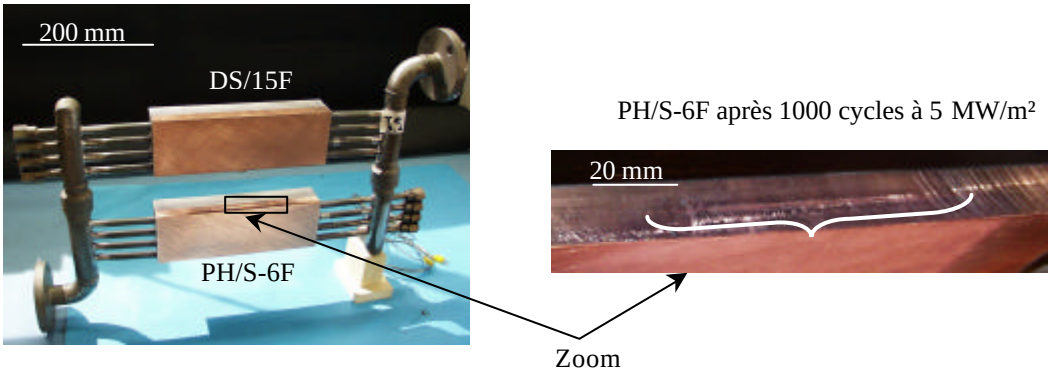

Figure VI-7 : Two of the four mock-ups tested and a view of the de-cohesion on PH/S-6F (CuCrZr).

Future contracts and work organization

Four additional contracts between CEA and the European Community were signed during this time; the corresponding tests will not be conducted until 2002. Two contracts concern thermohydraulic tests on NB31 monoblocks and on hardened copper hypervapotrons, the other two concern fatigue tests at

high thermal flux on six, scale 1, prototypes of the ITER divertor. The amplitude of the corresponding workload (estimated to be three years of testing) required negotiating a new financial structure for the FE200 station with the other two partners, EFDA and FRAMATOME-ANP. A new contract between CEA and FRAMATOME-ANP for 2002-2004 is being drawn up.

VI.2.2.2. SATIR thermographic test bench

The SATIR facility allows the testing of plasma facing components by determining the quality of the thermal transfer between the part of the component submitted to the thermal flux on the plasma side and the cooling structure. The control consists in evaluating the difference in temperature response ΔT_{ref} of the tested element versus a reference element when they are submitted to a front of hot then cold water in their cooling circuit.

Presently, SATIR is part of the reception and qualification control of incoming components for high heat fluxes of Tore Supra. The facility ensures the control of all the LPT fingers of the CIEL project, i.e. over 600 fingers, some of which have been tested several times, prior to and after repair (see section II.1.1.1). To meet this high demand, the organisation of the tests was reviewed, with a team operating in shifts. The acceptation criterion ($|\Delta T_{ref}| < 3°C$) as been slightly relaxed, in order to have, before the end of 2001, the number of fingers necessary for the LPT installation.

Moreover, between the control campaigns of different LPT finger batches, several mock-ups for the validation of new fabrication concepts for ITER were controlled (figure VI-8).

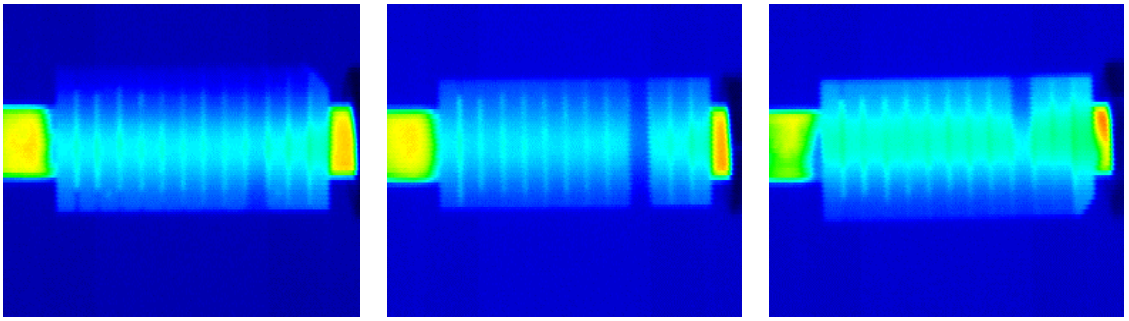

Figure VI-8 : Example of SATIR control on tungsten ITER mock-up (three views of the same defect)

This facility has been described in several publications and many industrialists in the fusion domain are willing to test on it their components under development. Consequently, the control bench was assessed this year in view to improving it (european contract EFDA 00/565). The most significant improvement should be obtained through the acquisition of a numerical camera, associated to the development of a new infrared image treatment program. The pressurisation of the water loop, which would allow hotter water to be used (180°C for 10 bars), is also a means of improvement, but the gain in measurement sensitivity would be less.

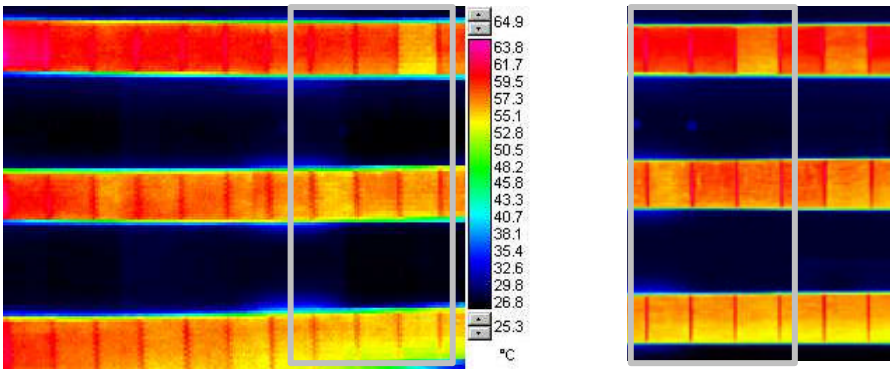

Figure VI-9 : Comparison of LPT finger infrared images between the presently used sweeping camera, on the left, and a focal plane camera, on the right.

The change of camera improves by a factor of two the detection sensitivity of defects on Active Metal Casting (AMC) assemblies of the Tore Supra type (plasma facing material: CFC ; structural material : copper OFHC) (Figure VI-9). This factor reaches three for the Hot Isostatic Compression assemblies of ITER type (plasma facing material : tungsten ; structural material : copper OFHC). A financing proposal of this detector by the PACA region is being evaluated.

VI.3. Supraconducting magnets

The activity in this domain is carried out through contracts with EFDA for the ITER magnets.

VI.3.1. CSMC model coil and CS Insert

The model coil of the ITER central solenoid is the largest solenoid in Niobium-Tin ever made, with a stored energy of about 600 MJ and about 5 km of conductors supplying 46 kA at 13 T. This coil, made in the United States and Japan, was installed in Naka (Japan) for tests which were conducted from March to August 2000. The Euratom-CEA Association participated in the CSMC model coil tests, as well as in the CS insert tests, made by Japan and used for exploring the performances of the central solenoid conductor. The results obtained are remarkable :

- the nominal performances were obtained without quench with a very good behaviour of the fifty connections included in the coil. The temperature margin is of 2K in compliance with the predictions.
- the coil showed a very good behaviour in pulsed regime, by going in 30 s to nominal current without quench. This is the first supraconducting coil of this size to operate in such a regime.

These large-scale tests help to validate the design criteria of the ITER magnetic system.

A european workshop was held on 5/6 February 2001 in Cadarache on the analyses of the performances of the model coil and of the CS insert. The conclusions of this meeting indicate that there exists a very inhomogeneous current distribution between the six petals making up the conductor cable. This phenomenon causes an earlier appearance of the resistive voltage at transition.

VI.3.2. TFMC model coil

The Euratom-CEA Association participated in monitoring the fabrication in the industry and to the tests in Karlsruhe of the model coil for the ITER toroidal field (TFMC). This coil, made by Europe, was in its final fabrication phase at the end of the first quarter 2000 with the welding of the box. This operation was followed by :

- impregnation of the coil ;
- installation of helium inlet and outlet tubes ;
- a global leak test of the coil ;
- assembly with the coil of the NbTi bushbars ;
- installation of the instrumentation (temperature measurements, voltage, …);
- control tests including measurements on global charge losses on all the hydraulic circuit, as well as high voltage tests.

The TFMC coil was delivered in FZK on 11 January 2001, assembled on the inter-coil structure and positioned in the TOSKA test station in March 2001. Figure VI-10 shows the TFMC inserted in the inter-coil structure.

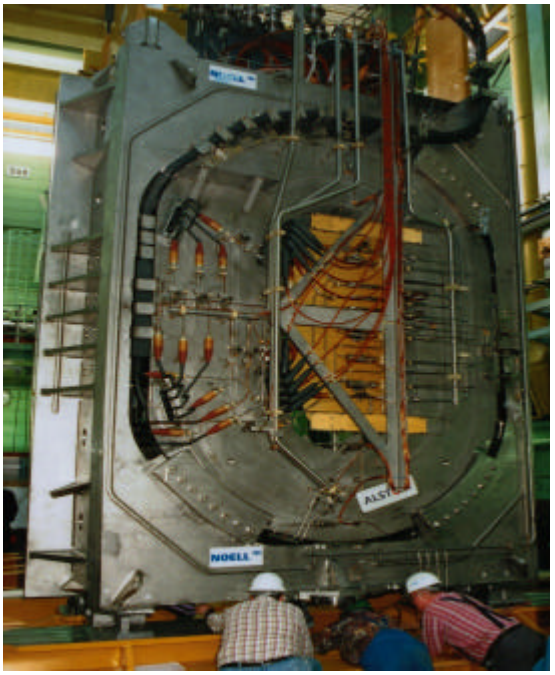

Figure VI-10 : TFMC model coil inserted in inter-coil structure (ICS) at Karlsruhe

The supraconducting transition was observed around 18K on 6 July 2001 and the temperature of 4.5K reached on 9 July. The main result was the achievement of the nominal current of 80 kA on 25 July without any difficulty.

The first analyses on the measurements taken during the tests helped to show that the electrical resistance of each connection was between 1,5 and 2 nΩ, in agreement with predictions. The particularly low value of this resistance, as well as the small dispersion observed, lead to the validation of the twin box concept developed by CEA. A conductor transition was obtained around 8,7K for 80 kA, which is in agreement with the expected theoretical value. Moreover, the mechanical measurements showed a very good agreement with the predictions obtained using the FZK finite element model.

VI.3.3. R&D on ITER FP coil conductors

The ITER FP coil conductors are made with Niobium-Titanium because of the low value of the magnetic field. Few experiments exist on Niobium-Titanium supraconducting cables using forced cooling. An important question is the coating of the strands making up the cable. An R&D program established a choice between five possible coatings. The choice was made of an electro-deposited 1 µm nickel coating. This coating is a good compromise between the variable field losses and the current distribution in the strands. The cost of this coating is low compared to the cost of the strand.

Two strands, representative of the ITER solutions, were then tested with variable temperature and field at the High Field Test Facility of CNRS Grenoble in a variable temperature cryostat : an ALSTOM strand and an EM-LMI strand. The results obtained allow the FP coils of the ITER poloidal field system to be designed, based on experimental values which are representative of the critical current density at 6.5K, which is the temperature used to design the conductors. These two samples of sub-cables were made at DRFC as soon as the ENEA conductor lengths were available in April. These samples (figure VI-11) were tested in the JOSEFA facility at DRFC. CEA also designed a scale 1 sample of a prototype conductor and connection (PF-FSJS), whose fabrication in industry and tests will be made in 2002.

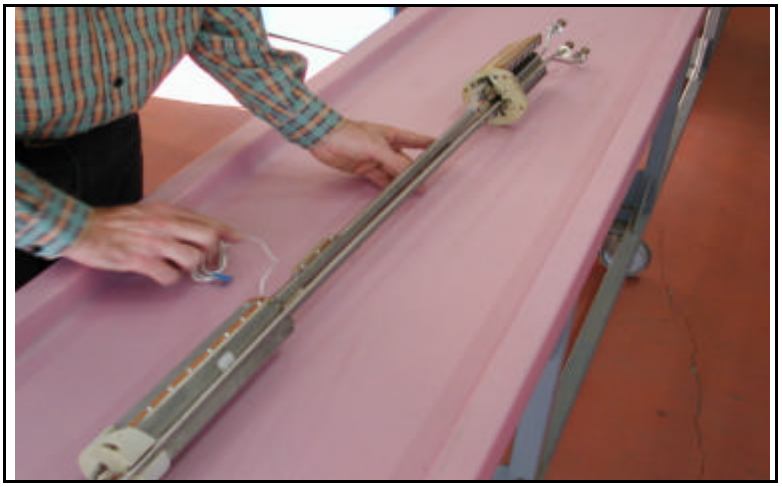

Figure VI-11 : PF1-SSJS sample of FP conductor sub-cable in NbTi

VI.3.4. TF insert

The TF insert is a single layer coil whose aim is to test the properties of a TF type conductor (similar to that of the TFMC, but with a titanium cladding) at a nominal current of 46 kA and under an induction of 13 T. The low temperature tests in the CSMC model coil of the TF insert (supplied by the Russian Federation) started in Naka on 17 September. The main result is obtaining without difficulty a current of 46 kA under an induction of 13 T. CEA participates in the analysis of the results of these experiments.

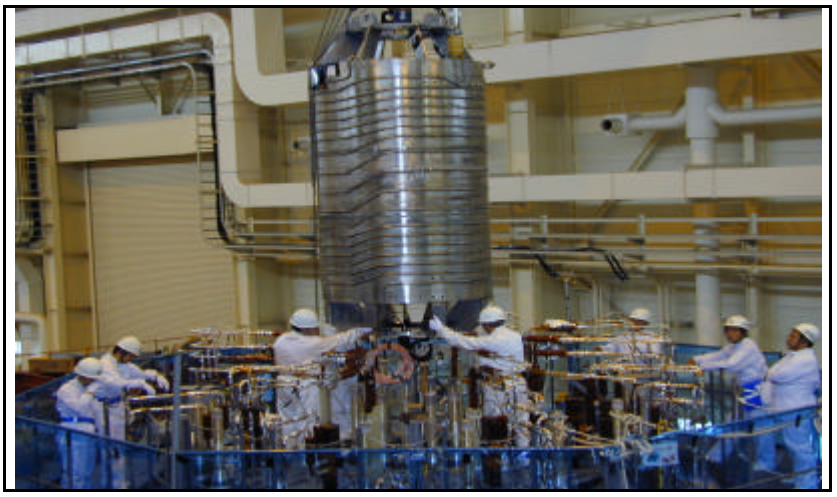

Figure VI-12 : Installation of TF insert in model coil CSMC in Naka

VI.3.5. Design and analysis of ITER PF coils

We have obtained the contract of design and analysis of ITER PF coil operation. This contract includes both the electromagnetic and thermohydraulic operation of the FP coils during a typical scenario and the design and analysis of the coil connections. The design and analysis of the helium inlets in the CS coils is also included in the contract.

The electrical and thermohydraulic analyses resulted in proposing an overlapping connection concept of the «handshake » twin boxes type, with a horizontal interface plane. The mechanical design is based on the combination of a flexible electrical connection and a rigid mechanical link between pancakes.

Analysis of the coil operation taking into account electromagnetic, neutron, and radiative heat losses showed that the minimum temperature margin of 1.5K was always respected.

A concept for the helium inlet based on an elliptical hole was proposed and analysed mechanically using a finite element model : it was possible to optimise the geometry to allow for both the wetting of all the six conductor sub-cable by helium, the preservation of the conductor clad on its external face and the limitation of the strain concentration factor to 1.15, so as to allow operation during 30 000 cycles. A hydraulic qualification experiment in the OTHELLO test station of DRFC was started using a conductor sample from the TFMC.

VII. COLLABORATIONS

VII.1. CEA internal collaborations

For some technological developments, the competencies of the different CEA units are used. Particularly, within the Direction of Material Sciences, the Service of Low Temperatures (SBT) develops pellet injectors at high speed as well as a cryomechanical pump for Tore Supra, whereas the Service of Cryogenic and Magnetic Techniques (STCM) is responsible for the test on the supraconducting coils of the stellarator W7X.

Within the DRT, the main work concerns the welding and implementation of materials for the internal components of ITER.

The DEN closely participates to the site studies for ITER and also contributes to other technology program studies : development of low activation materials, design of a future fusion reactor, safety and waste management studies.

The DRFC, by way of the EURATOM/CEA Association, co-ordinates these technological activities which are mostly conducted in other CEA laboratories.

VII.2. Collaborations : CNRS and Universities

The collaboration effort of the Association with French universities and the associated CNRS laboratories was kept up during the reference period. These joint projects are carried out within the framework of the Tore Supra and JET operation, but also that of theoretical research. They are financially sustained by EURATOM, within the Association contract, thus increasing their efficiency by, for example, allowing the concerned laboratories to finance material, travel, or an additional post-doctoral contract for a young scientist.

We have now signed 4 LRCs (Université de Provence, Université de Nancy, Ecole Polytechnique, Université de Nice), two of which this last year.

For 2001, these joint projects concerned 21 teams in 8 laboratories, for a total of 23.5 person-year; the total amount involved is 0.4 M€ (the figures for 2000 were not very different). Many projects are obviously with the Université de Provence. The two main themes concerned are plasma-wall interaction and its effects on the edge plasma (Universités de Provence and St. Etienne), and turbulence (Universités de Provence and Nancy, Ecole Polytechnique, …).

Even though it is not strictly a CEA-CNRS-University collaboration, the joint organisation by DRFC and the Université de Provence of the "1st Theory Festival " must be mentioned. This working meeting was held at the Faculté de Lettres of the Université in Aix-en-Provence, lasted 3 weeks in July 2001 and gathered 27 participants, including 5 astrophysicists (added to that 9 students and young scientists from both organisations) on the theme "Self Organisation and Transport in Electromagnetic Turbulence".

The program was built on two talks of one hour per day, 5 guided discussion a week on pre-determined subjects, and spontaneous discussions on different subjects. The discussions were interesting and very productive. The big advantage of this type of program is to be able to maintain the interaction on a given theme over a long period of time, which is impossible to do in a conference. Another success of this meeting was the interaction between analytical theory specialists and numerical specialists. Several work programs and papers were initiated, one of which on intermittence and prediction power. A few new physics points to be noted are :

- « Electromagnetic » effects on transport. The results of numerical simulations show that the transport coefficients increase rapidly near the MHD limit (Alfvenic turbulence). The part of the transport linked to the fluctuating magnetic field however remains low.
- Analogy between the turbulent generation of magnetic field at large scale (dynamo) and the generation of sheared velocity in fusion plasmas. This is a very significant stabilising effect. During the meeting, the fact that at high β the effect disappears was verified.
- Questioning of the description of transport based on diffusion coefficients. An approach taking into account the formation of intermittent structures should be found. A possibility is given by a statistical description in terms of non-gaussian probability distribution of the turbulent flux.

A summary of the main results will be written up by those responsible of the main themes and submitted to Plasma Phys. Control. Fusion. This type of meeting will again be organised in 2003.
An overview of the joint activities is given in Table VII-1.

VII.3. International collaborations

Apart from the participation to JET and ITER-related activities, the Euratom-CEA Association has maintained substantial exchanges with other laboratories in the European Union and other international partners on a number of subjects. The opening to European scientists of the different experimental possibilities offered by the Union was encouraged so as to best benefit from the human scientific potential and the existing machines. The DRFC is attempting to interest European scientists in the next experimental campaigns by organising meetings during which these scientists can propose experimental themes.

Outside the European Union, activities with the new states linked by contract to Euratom have started : Rumania and the Czech Republic.

Outside of Europe, the agreement between Europe and the United States has just been renewed. This means re-discussing the collaboration program. The collaboration agreement of the CEA with MINATOM (Russia) has also been renewed. This agreement contains a part on fusion, which will be discussed with our Russian partner at the beginning of 2002.

The DRFC has participated to the evaluation actions of the Korean supraconducting tokamak KSTAR within the framework of a Europe-Japan collaboration project. There are no new actions scheduled for 2002. The main actions are as follows (most were described in detail in the previous chapters):

VII.3.1. Within the framework of the Euratom program

- *ENEA (Italy)* : Two types of combined LH + EC experiments were conducted on FTU : at high magnetic field (7.3 T) and at lower magnetic field (5.3 T). In the first case, the EC waves interact with the suprathermal electrons, in the second case, with thermal electrons. In both cases, combined simulations (heat and current transport + Fokker-Planck) were made. Measurements with the TS hard X-ray camera were made during the ECCD and LH experiments on FTU ; energy re-calibration of the diagnostic. The results are being analysed.

- *EPFL (Switzerland)* : A gyro-kinetic code has been developed, describing trapped ion instabilities in 2 space dimensions and 1 energy dimension, to predict ion heat transport in a simplified geometry. At the same time, Lausanne developed a code in cylindrical geometry on the same principle (Vlasovian code), to describe passing ions instabilities. The short-term objective is to make a single code describing both types of instability.
  The heating and ECR current generation experiments on TCV, simultaneously using two gyrotrons at different frequencies, can only be interpreted by using the kinetic theory. Our 3D Fokker-Planck code, adapted to the TCV configuration, was successfully used to model these experiments.
  The hard X-ray camera was used for the third time on TCV. Experimental results are numerous, and are being analysed. Cadarache provided the TS data analysis code and participated to its adaptation for TCV. We are also working on the multi-machine hard X-ray calculation code. Following the problem of power limited to 300 kW observed on the fist series gyrotron, the latter was transferred to Lausanne and tested on the CRPP test bench to check its operation. A slightly higher power (360 kW) with the same operating point was reached ; however, by increasing the

beam current beyond the nominal value, a power of 420 kW was obtained. The diamond window, developed by FZK, was tested on this gyrotron at Cadarache, and was submitted to a power of 300 kW for 111 s. The losses measured in the window are 1.4 kW, i.e., a value 40 to 50 times that expected after the low level characterisation. The gyrotron mock-up for W7-X was satisfactorily tested in Karlsruhe. The power/duration couples obtained for the pulses are 900 kW/7.8 s, 750 kW/45 s, and 450 kW/180 s. The time limitations for powers of 900 kW and 750 kW are not due to the gyrotron, but to arcs appearing in the charge.

- *IPP Garching (Germany)* **:** The ECRH modulated power experiments made on Asdex-U were simulated by the ASTRA code, using different models of electron transport. It was thus possible to confirm, in addition to the energy balance analysis without modulations, the existence of a critical temperature gradient length for heat transport via the electron channel.
  The spectra measured by reflectrometry in ASDEX-U show a shift towards higher frequencies during the L-H transition. A simple model, based on the Doppler effect due to the plasma toroidal rotation, qualitatively reproduces these observations, the observed shift corresponding to the appearance of a significant rotation shear in the cut-off layer. A more quantitative analysis requires the use of theoretical and 2D code results. Thus, reliable 2D codes are investigated to allow the characterisation of fluctuations and modelling of the Doppler effect. The Nancy and Lisbon time codes are being compared with a more accurate, although stationary, Helmholtz code. The effects of MHD type perturbations in these codes satisfactorily model some experimental results from TS.
  The Association participated to the development of a HF (1 MHz) source of negative ions; it provided IPP an accelerator for negative ions, a calorimeter and the programs needed for the data acquisition and analysis. The experiments are ongoing in Garching with our participation.
  Discussions (and participation to the 'Workshop divertor W7X') on a possible collaboration program on actively cooled components for W7X ; with no result to this day. Participation to tests of the W7Z coils on the cryogenic test bench at Saclay.

- *IPP Prague (Czech Republic)* : Experiments on the control of edge turbulence (by interaction of a coherent wave with adequate wavelength in resonance with the turbulence by synchronisation of the poloidal rotation), as well as studies on poloidal and toroidal flows induced in edge plasmas by polarisation of an electrode, were made on CASTOR with the participation of Association physicists.

- *IST-Lisbon (Portugal)* : Collaboration on the modelling of reflectometry, with the Universities of Marseille and Nancy.

- *ÖAW (Austria)* : Simulation of the control of current and pressure profiles in advanced regimes. In particular, work was directed to the simulation of helium transport in the advanced scenarios considered for ITER. Helium transport is treated by a model with two groups, by solving transport equations for the fast alpha particles and helium ashes. The recycling of helium ashes is also modelled. These developments are a progress in making simulations more coherent for fusion plasmas close to ignition.

- *TEC (Trilateral Euregio Cluster* : Germany, Belgium and the Netherlands) : Conditioning discharges created by ion and electron cyclotron frequency waves were made and compared in TEXTOR. The conditioning efficiency is 5 to 10 times greater for ICR discharges.
  A new series of experiments on the effects of an electric field applied between the toroidal pump limiter ALT-II and the internal TEXTOR walls was made : negative polarisation and inverted I_p and B_t compared to the usual configuration. A large increase of the parallel flux collected in the limiter throats is obtained with a polarisation of -75 V. Moreover, measurements made at the same time with the Gundestrup TS probe also show a clear dependence of the parallel and perpendicular Mach numbers versus the polarisation voltage.

- *UKAEA (United Kingdom)* : The ARENA (Avalanche of Runaway Electrons, Analysis) code, which solves a kinetic equation for runaway electrons with a Monte Carlo method, was improved. The code can now integrate, in a self-consistent way, the electric field produced by these electrons. In order to do this, a new numerical method was developed ; also included were operators for synchrotron radiation.

- *Université Libre de Bruxelles (Belgium) - IRST-Bucharest (Rumania)* : Study on the dynamics of chaotic magnetic lines in a toroidal geometry : the tokamap model (Hamiltonian mapping) allows the reproduction of the island structure in tokamaks and the study of the position of internal transport barriers and of the diffusion of magnetic lines.

- *Université de Dublin (Ireland)* : Development of negative ion sources. Diagnostic on the MANTIS test bench with a sliding Langmuir probe ; preparation of a "Laser Cavity Ringdown" system to measure the density of negative ions in the Japanese source KAMABOKO III.

- *NILPRP in Bucharest, Institutes of Physics and Mathematics of the University of Krakow, Université de Timisoara* : The recent entry of Rumania in Euratom has allowed the creation of a team of 9 Rumanian physicists and mathematicians actively collaborating with our laboratory in the theoretical field on turbulent transport and stochasticity (3 in Bucharest, 3 in Mathematics and 2 in Physics at the University of Krakow, 1 in that of Timisoara)

VII.3.2. Outside the Euratom program

- *ASIPP (China)* : Two Chinese physicists spent a year in Cadarache (they have just gone back home) ; they worked on the treatment of images from endoscopes and infrared cameras. A scientist from the University of Hefei participates to a multilateral project (MIT, Madison, Cadarache) on the hard-X radiation calculation code which must be adapted for HT-7.

- *INRS (Canada)* : Edge flow problems : modelling and experiments (on TEXTOR and TS).

- *JAERI (Japan)* : A four wave-guides lower hybrid module (graphite with copper on the surface, actively cooled), fabricated by JAERI, was tested in Cadarache at high power density (125 MW m^{-2}), on long impulses (900 s), for which thermal equilibrium is obtained and wall degassing is nearly stationary.
  A bolometre (gold on mica) was tested in the JMTR reactor in Japan for three cycles of 25 days each (0,03 dpa/cycle). During the first irradiation cycle, the bolometre resistance practically doubled, but the initial value was not retrieved at the end of the cycle ; this increase could be due to the nuclear transmutation of gold into mercury. During the cooling phase at the end of the first cycle, all the electric connections were short-circuited; a few recovered at the beginning of the second cycle, but were definitely lost at its end. The preliminary conclusion is that platinum should be used instead of gold.

- *PELIN-Inc (Russia)/ DRFMC-SBT* : Continuous pellet injector. A first test campaign on the optimisation of PELIN and SBT fast valves, used to accelerate the pellets, was conducted in St Petersburg. The quantity of gas released at each shot is compatible with an assembly on TS, if using a reasonable pumping capacity. Modifications of the valves were suggested by the results obtained to reduce this quantity of gas and increase the pellet velocity; they will be tested next semester. A test bench was installed in SBT to test a new pellet fabrication process. Very promising results were obtained, with the capacity to launch a hydrogen pellet at 1.9 km/s every 12 seconds.

- *Moscow Engineering and Physics Institute (Russia)* : Development and operation of a mobile sample carrier, and of a degassing analysis device. Modelling of the carbon-deuterium interaction and particle balance (microscopic level).

- *US-DOE (United States)* : A presentation of the Tore Supra activities took place end of November 2000, at the US-DOE in Washington D.C., to try and give a new impetus to this collaboration, which has changed over time, on technological subjects for long pulses, to much more physically oriented subjects (analysis and interpretation of TS experimental data). The Association insisted on the need of having a more balanced co-operation, through “in kind” contributions (MSE, reflectometry, RF antenna), in addition to the participation of physicists (the participation of American physicists to JET through the Associations was also mentioned). A list of possible joint projects was discussed ; this should give rise to a formalisation in the near future of DOE-EUR-CEA Association collaboration projects.
  Despite the absence of a formal framework, several joint projects, which had been started a long time ago, were continued. Among these :

With the IFS, University of Texas, the study of electron transport, more specifically the critical gradient and its parametric dependence. The ETG and ITG/TEM theories were tested with the TS experimental database, using the TRANSP (PPPL) and BALDUR (IFS) codes. With PPPL, Princeton, the analysis and interpretation of TS experiments using the TRANSP code. The simulation of LHCD experimental data allowed the validation of the corresponding module of the code. With UCSD, California, the study of large scale transport events (called streamers) in edge turbulence simulations. The streamers play a large part in the abnormal heat transport. When the poloidal velocity shear increases (in the H-mode case, for example), these streamers have a smaller size and the associated transport is reduced. A predictive expression, giving the heat flux as a function of the shear velocity, was deduced. Lastly, the collaboration with ORNL, Oak Ridge, which has existed for a long time, concerns the use of the 3D Monte Carlo BBQ code to interpret edge plasma spectroscopic data. During the reference period, work was carried out on the coupling between BBQ and the 1D radial transport codes of impurities in the confined plasma (use of BBQ to calculate the flux of entering impurities, which are the edge conditions of 1D codes) and on the interpretation of radial emission profiles.

Table VII-2 provides an overview of the joint projects underway.

Tableau VII-1 : CONVENTIONS LRC ET CONTRATS AVEC UNIVERSITES/CNRS: 2000-2001

Université	LRC Contrat #	Responsable Association	Responsable Université	Personnes x An Univ.	Thésards (T) Postdocs (P)		Thèmes de recherche
					Univ.	CEA	
				(données pour l'année 2001)			
Univ. Provence Aix-Marseille I/LPIIM CNRS UMR 6633	DSM 99-14 (1/01/99) #V3130.001 avenant 2	X. Garbet Ph. Ghendrih	S. Benkadda	3.35	2T 1P		Modélisation/simulation transport turbulent dans plasma tokamak de bord
		E. Gauthier	J.M. Layet	1.8	2T		Interaction plasma/surface et erosion chimique dans TS
		C. De Michelis	R. Stamm	1.13		1P	Diagnostic spectroscopique du plasma de bord
		H. Capes	R. Stamm	1.12	1T 1P		Physique atomique et transport au bord du plasma
		F. Clairet P. Devynck	F. Doveil	2.1	1P		Etude expérimentale de la turbulence
		M. Ottaviani	D. Escande	0.25			Auto-organisation magnétique des plasmas de fusion
		P. M.-Garbet C. Brosset	P. Roubin	0.3	1T		Mesure de porosité des surfaces en contact avec le plasma
		P. M.-Garbet C. Brosset	A. Allouche	0.35			Rétention H du graphite: aspects quantiques des interactions plasma-surface
		R. Reichle	C. Arnas	0.35		1T	Signature IR du graphite et ses poussieres sous bombardement i/e
Univ. Henri Poincaré Nancyl/LPMIA CNRS UMR 7040	DSM 99-18 (1/01/99) #V3134.001 avenant 2	X. Zou L. Colas	S. Heuraux	1.1			Interaction onde-plasma
		X. Garbet	P. Bertrand	1.65		1T 2P	Modélisation gyro-cinétique des plasmas de tokamak
		P. Devynck	G. Bonhomme	2.75			Caractérisation du transport et contrôle du bord du plasma
Ecole Polytechnique/ LPMI CNRS UMR 7648	DSM 01-23 (1/01/01) #V3232.001	R. Sabot	J.M. Rax	3.55	1P		Etude de la turbulence

Univ. Nice/Sophia-Antipolis CNRS UMR 6621	DSM 01-24 (1/01/01) #V3254.001	E. Joffrin	J. Blum	0.75	1P		Identification temps réel du profil de courant dans un tokamak (en 2000 à l'Univ. Grenoble/LMC)
		X. Garbet	Y. Bernier	0.3			Approche gyro-cinétique de l'equation de Vlasov
Ecole Polytechnique/ LPMI CNRS UMR 7648	#V2939.003 avenant 6	R. Sabot	D. Gresillon	0.9			Etude de la turbulence dans TS (fin contrat septembre 2001)
Ecole Polytechnique/ CPT CNRS UMR 7633	#V2939.004 avenant 6	X. Garbet	J.F. Luciani	1.45		1T	Modes tearing: dynamique non linéaire dans un plasma tokamak avec pression
Univ. St Etienne/- LTSI CNRS UMR5516	#V2939.002 avenant 6	W. Hess	M. Druetta	1.0			Spectroscopie visible et infrarouge
Ecole Normale Superieure ENS-Ulm/LMD	#V3258.001	P. Devynck	M. Farge	0.45			Traitement du signal dans TS
Univ. Provence Aix-Marseille III/CP2M	#V3257.001	R. Reichle	A. Charai	0.7		1T	Corrélation entre propriétés emissive et état de surface du carbone

TOTAL	**25.35**	**6T 5P**	**4T 3P**

Tableau VII-2 : COLLABORATIONS INTERNATIONALES (hors JET et ITER) : 2000-2001

PAYS		LABO	NOUS	EUX	AUTRES LABOS		SUJET
Allemagne	1.1	IPP-Garching	Chappuis	Bolt		E	Caracterisation depôt B4C neutraliseur DE TS
	1.2	IPP-Garching	Imbeaux	Ryter		E,S	Transport electrons (modulation ECRH, simulations ASTRA)
	1.3	IPP-Garching	Zou	Conway	Lisbonne, Univ. Nancy et Marseille	E,S	Reflectometrie et fluctuations dans la transition L-H; comparaison avec le code 'advanced full-wave'
	1.4	IPP-Garching	Hemsworth	Speth		E	Développement source HF ions negatifs
	1.5	KFA-Juelich	Gauthier	Lyssoivan		E	Décharges nettoyage par ondes ECR et ICR
	1.6	KFA-Juelich	Gunn, Loarer	Finken, Lehnen	Univ. Gent (B)	E	Etude polarisation limiteur toroidal
	1.7	KFA-Juelich	Tsitrone	Reiter		S	B2-Eirene
	1.8	KFA-Juelich	Guirlet	Pospieszcziek		E	Spectres moleculaires avec DE
Angleterre	2.1	Culham	Eriksson	Helander	Chalmers Univ.	S	Code ARENA (Avalanche Runaway Electrons, Analysis)
Autriche	3.1	Ass. EUR-OAW	Litaudon	Kamelander		Th	Modélisations scenarios avancés
	3.2	Ass. EUR-OAW	Gunn	Kuhn		S	Interaction electrons energetiques antenne LH avec gaine
Belgique	4.1	Ass. EUR-Belgique	Misguish	Balescu		Th	Physique statistique transport turbulent
Grece	5.1	Univ. Athènes	Nguyen,Colas	Lazaros		Th	Stabilisation dents de scie durant chauffage FCI
Finlande	6.1	Assoc. EUR-TEKES	Litaudon	Kartunen		Th	Modélisation interaction onde LH au bord du plasma
Irlande	7.1	City Univ., Dublin	Hemsworth	Ellingboe		E	Développement source ions négatifs
Italie	8.1	ENEA-Frascati	Giruzzi	Pericoli		E,Th	Generation de courant ECCD et LHCD
	8.2	INFM, Torino	Ottaviani	Porcelli		Th	Stabilité modes de dechirement
	8.3	ENEA-Frascati	Peysson	Pericoli		E,S	Camera X-durs, analyse ECCD et LH à haute densité
Portugal	9.1	Ass. EUR-IST	Zou	Manso	IPP,Nancy,Marseille	E,S	Reflectometrie et fluctuations dans la transition L-H
Suede	10.1	RIT, Stockholm	Eriksson	Hellsten	Culham	Th,S	Effets largeur finie d'orbite et transport spatiale sur dépôt FCI
Suisse	11.1	EPFL-TCV	Sarazin	Villard	Univ. Nancy	S	Code gyrocinétique
	11.2	EPFL-TCV	Giruzzi	Alberti		S	Code F-P 3D pour ECRH sur TCV
	11.3	EPFL-TCV	Peysson	Coda		E,S	Camera X-durs, analyse electrons suprathermiques ECCD
	11.4	EPFL	Magne	Alberti	TED	E	Développement gyrotron 118 GHz
Rep. Tcheque	12.1	IPP-CASTOR	Devynck	Stokel	RFX, Univ. Nancy	E,S	Contrôle turbulence bord
	12.2	IPP-CASTOR	Gunn, Gauthier	Zacek	Univ. Nancy	E,Th	Ecoulements par polarisation electrode. Sondes Gunderstrup, RFA
	12.3	IPP-CASTOR	Goniche	Petrzilka	Univ. Innsbrück	E,S	Dynamique des particules au voisinage des antennes LH
Roumanie	13.1	Ass. EUR-Nasti	Misguish	Costantinescu		Th	Transport turbulent anormal
	13.2	Ass. EUR-Nasti	Misguish	Spineau		Th	Transport turbulent anormal

Russie	14.1	Moscow Eng. Phys.	Gunn	Begrambekov		E	Interaction carbone-deuterium
	14.2	PELIN, St. Petersb.	Geraud	Viniar	SBT Grenoble	E	Développement injecteur glaçons
	14.3	TRINITI	Basiuk	Katchouk		E	Mesure profil Ti par neutrons
Canada	15.1	INRS	Gunn	Boucher	Juelich	Th,S	Modélisation ecoulements bord
Chine	16.1	Heifei	Peysson	Shi	MIT, Madison	S	Code de calcul rayonnement X-durs
Corée	17.1	KSTAR					Discussions possibilité collaboration
Japon	18.1	JAERI	Goniche	Maebara		E	Module LH 4 guides d'onde
	18.2	JAERI	Reichle	Nishitani	IPP, FOM, CIEMAT	E	Test de bolometres sous irradiation
USA	19.1	Univ. Texas	Hoang	Horton		Th,S	Modélisation du transport electronique
	19.2	PPPL	Hoang	Budny		S	Analyse du transport avec le code TRANSP
	19.3	UCSD	Garbet	Diamond	Univ. Marseille	Th	Transport turbulent
	19.4	ORNL	De Michelis	Hogan		S	Modélisation bord, code BBQ, comparaison avec spectro visible
	19.5	MIT	Eriksson	Porcelli		Th	Rotation plasma induite par FCI
	19.6	MIT	Peysson	Bers		E,S	Rayonnement X-dur
	19.7	MST	Peysson	Forrest		S	Codes rayonnement X-dur pour RFP

E : expérience ; Th : théorie ; S : simulation

VIII. COMMUNICATION

VIII.1. Organisation of conferences/workshops

The DRFC organised 9 workshops or scientific meetings in 2000 and 14 in 2001. The subjects covered all the activities of the department :

- Plasma theory (2)
- Activities on JET (4)
- Technical IAEA meetings (3)
- ITER / EFDA technical meetings (6)
- Tore Supra meetings (2)
- Hot plasmas school (2)
- Miscellaneous (SFEN, University,..) (4)

Several of these meetings took on an added dimension, particularly the « Theory Festival » (3 weeks in Aix en Provence in July 2001) and the TCM / IAEA meeting on divertor designs (75 participants in September 2001).

VIII.2. Communication with the public at large

The Tore Supra site is one of the first CEA sites to open to the public and arouses great interest. To ensure a better welcome of the public, a video system was installed in the entrance hall of the tokamak building, to show pictures of Tore Supra plasmas and illustrate the basic operation of a tokamak. A set of public information documents – booklets, CD ROMs, presentation of fusion and of Tore Supra – has been updated and is now widely distributed. Over 20 DRFC agents have been designated as « communicating scientists »; in collaboration with the service for the promotion of the Cadarache Centre, several thousand visitors per year have been received. The DRFC also continues to welcome junior high school students within the framework of the CEA-Youth operation and the Tore Supra site is still very much visited during open house days.

The DRFC has been present each year for every public event : Sciences en fête in Marseilles (except in September 2001) , Physics Fair (Paris) on the CEA booth.

The « visitors » statistics are as follows:

	1999 (reminder)	**2000**	**2001**
open t	2441	4443	3195
open house days	500	0	1760
students	10	45	75
CD ROM distributed (not including exhibited)	0	156	1716 (of which 900 to other labs and institutions)

The effect of the anti-terrorist watch, Vigipirate, (starting on 11th September 2001) on the number of visitors can be seen in the very sharp drop in the 4th quarter of 2001 (1116 in 2000, 577 in 2001).

A virtual visit of the Tore Supra facility was developed and distributed on the CEA Internet site by the Communication Direction.

VIII.3. Edition and documentation

The management procedures for publications, applying the CEA general rules, are now well established, thanks to the implementation of publishing tools on the Intranet network of the Association.

The actual implementation of the nomenclature decided in May 1999 has been finalised and nearly all the internal documents follow now a common procedure, thus allowing electronic archiving and subsequently consultation on the web.

The computer system set up at DRFC now allows the on line access to all the reports written since 1958, the references of all the scientific publications and all internal documents written since 1986.

VIII.4. Expo Fusion

The EFDA FU contract, signed on 29th November 2000, covers the management of Expo Fusion for 2000, 2001 and 2002 ; it contains two main items:

- A certain number of expositions per year (5 in 2000, 6 in 2001 and 6 in 2002, for a total of 17 expositions). For each exposition, the organisers will be provided with 2000 CDs and 2000 booklets (64 A5 pages, quadrichrome) translated into the local language, and explaining each poster in the exposition ;
- The upkeep and material improvement of the exposition, with the inclusion of a 3D movie «Star makers », produced by the Swiss EURATOM Association and made in 3D computer images based on ITER draughts.

After Expo Fusion was re-modelled (to 30 posters in 1999), the exposition was duplicated and can even be modular.

For the first time, the CD ROM produced for Expo Fusion, presenting the research on fusion, was widely distributed by a magazine on sciences for the public at large (Natuur & Techniek, January 2000, the Netherlands).

Despite the delay in signing the contract, the number of expositions is nearly equal to that foreseen in the contract (9 instead of 11) at the end of 2001 :

- *Sorrente (Italy, September 2000)* : This exposition was reduced to the presentation of the 3D movie « Star Makers » during the IAEA conference on fusion. Over 300 people saw the film.
- *Seoul (Korea, November 2000)* : The exposition in Seoul lasted 2 weeks, was installed in the hall of the POSCO company headquarters (1st world steel producer). Having taken place within the framework of reinforcing the ties between Korea and the European Union in the area of controlled fusion, Expo Fusion included presentations of European laboratories and industrialists. The exposition was in English, but the written documents were in Korean. The CD ROM was provided by the Association .
- *Taejon (Korea, December 2000)* : The exposition lasted 3 weeks on the site of KSTAR, the korean supraconducting tokamak under construction. This exposition was after the one in Seoul.
- *Lisbon (Portugal, December 2000)* : The exposition lasted 4 weeks, in the buildings of the Institut Supérieur de Technologie (IST). 4500 visitors were counted and attended the 3D film on ITER, each having been given a booklet and a CD (3000 additional booklets have been asked for by the organisers).
- *Madrid (Spain, May to November 2001)* : The first part of the Expo Fusion (11 posters out of 30) has been integrated into a permanent exposition organised by CIEMAT in its offices for its 50th anniversary.
- *Ecole d'Ingénieur, Yverdon (Switzerland, June 2001)* : Roughly 1000 visitors ; 1000 brochures and 500 CDs were distributed.
- *CERN, Geneva (Switzerland, July 2001).*
- *Deutsches Technikmuseum, Berlin (Germany, September 2001).*
- *URANIA, Berlin (Germany, September, October 2001).*

The total number of booklets and CDs distributed during the expositions of 2000-2001 is of 25 000 and 10 000, respectively.

The renovation of Expo Fusion was started by the EFDA Committee for Public Information. The proposals made by the Association during summer of 2001 were accepted by the CPI and will soon be carried out.

The numerical video material scheduled for the multimedia workshop was delivered in 2001 ; it will allow the preparation of the mock-ups of all the multimedia objects likely to be developed for Expo Fusion, particularly information sequences on other European associations.

VIII.5. External Web site

The WEB site of the Association has been on line since June 2001 (http://www-fusion-magnetique.cea.fr). The aim is to present magnetic fusion research to a large public. The site describes the activities of the Association and is directed towards «fusion energy ». The directly accessed information is aimed for the public at large but it is however possible to access more specialised documents if the visitor so desires. Particular care has been given to the sections on the main principles and advantages of fusion in terms of safety. A chapter on fusion plasma physics is being written. Its level will be between a simplified introduction to the main principles of fusion and a document for a fusion specialist. The site is now in French but an English version is scheduled when the French one is final.

Figure VIII-1 : Welcome page of Euratom-CEA Association
(http://www-fusion-magnetique.cea.fr)

VIII.6. Internal Web site

The DRFC Intranet has been in operation for several years as an internal communication tool; it is not accessible from the outside. It allows easy access to information on departmental activity. This evolving site is now made of a welcome page with 8 sections on the department, its activities, life, documents and different practical services, without forgetting to mention some useful links to the outside world. This welcome page, under the responsibility of the webmaster, now contains 60 links to other pages downstream, managed by designated people. An editorial committee proposes changes

in the site depending on the needs of the department, which are then validated by the head of the department before being implemented.

Figure VIII-2 : Welcome page of Intranet site of EURATOM-CEA Association

IX. APPENDICES

IX.1. Budget of EURATOM - CEA Association

(Fiscal year 2000-2001 underway)

En thousands of francs	2000	2001 (Forecast)
A - Breakdown by type of expense		
Manpower (including support manpower) ……..	162 648	163 436
Overheads, rents, miscellaneous ……..	43 472	44 454
Investments ……..	30 598	26 211
Operating costs (not including engineering costs) ……	55 217	68 377
Total ……..	291 935	302 478
B - Breakdown by type of activity		
(according to the definitions in the Association contract)		
Général budget……..	251 446	249 764
Priority large equipment ……	18 125	11 438
EFDA support teams ……..	2 815	3 062
EFDA contracts……	6 835	25 778
Fusion technology (research group) ……	11 313	10 681
Research fellow ……	508	681
Secondment contract……	893	1 074
Total ……..	291 935	302 478
C - Fusion technology program		
(Not including research group)……..	110 679	132 837

IX.2. Organisation and personnel

IX.2.1. Management committee of the EURATOM-CEA Association

CEA representatives :	EURATOM representatives :
F. GOUNAND	U. FINZI
P. LIVANOS	H. BRUHNS
H. BERNARD	J. SPOOR

IX.2.2. Organisation chart of the EURATOM-CEA Association

ASSOCIATION EURATOM-CEA
DEPARTEMENT DE RECHERCHE SUR LA FUSION CONTROLEE
(DRFC)

Chef du Département : J. JACQUINOT

Adjoints : M. CHATELIER, G. MARBACH

SERVICE TOKAMAK EXPLOITATION ET PILOTAGE (STEP)

Chef de Service : D. VAN HOUTTE

Adjoint : C. GRISOLIA

SERVICE DE CHAUFFAGE ET CONFINEMENT DU PLASMA (SCCP)

Chef de Service : B. SAOUTIC

Adjoint : C. LAVIRON

SERVICE INTEGRATION PLASMA - PAROI (SIPP)

Chef de Service : A. GROSMAN

Adjoint : G. REY

Euratom CEA

CEA/DSM/DRFC
CEA/Cadarache
13108 SAINT PAUL LEZ DURANCE CEDEX - FRANCE

Téléphone : 04 42 25 70 01
Télécopie : 04 42 25 64 21
e-mail (SMTP) : dirdrfc@drfc.cad.cea.fr
Site Web DRFC : Http://www-drfc.cea.fr

TORE SUPRA

ORGANIGRAMME DU DEPARTEMENT DE RECHERCHES SUR LA FUSION CONTROLEE

Chef du Département	*JACQUINOT Jean*
Adjoints	*CHATELIER Michel*
	MARBACH Gabriel
Assistant Administratif	*FRANEL Bertrand*

Chefs de projet :

* EISS-Cadarache	*GARIN Pascal*
* CIMES	*BEAUMONT Bertrand*
* CIEL	*CORDIER J-Jacques*
* JET-Divertor	*CHAPPUIS Philippe*
* Infrarouge	*GUILHEM Dominique*

SERVICE CHAUFFAGE ET CONFINEMENT DU PLASMA

Chef de Service *SAOUTIC Bernard*
Adjoint *LAVIRON Clément*

* Chauffage et Génération de Courant (GCGC)	*PEYSSON Yves*
* Chauffage FCE (GFCE)	*MAGNE Roland*
* Diagnotics d'Ensemble (GDE)	*GIANNELLA Ruggero*
* Injection de Neutres (GIDN)	*HEMSWORTH Ronald*
* Laboratoire HF (GLHF)	*GONICHE Marc*
* Support aux Chauffages (GSAC)	*AGARICI Gilbert*
* Systèmes Hybride et Ion Cyclotron (GSHIC)	*BEAUMONT Bertrand*
* Théorie des Plasmas Chauds (GTPC)	*OTTAVIANI Maurizio*
* Transport et Confinement (GTC)	*GIRUZZI Gerardo*

SERVICE INTEGRATION PLASMA PAROI

Chef de Service *GROSMAN André*
Adjoint *REY Guy*

* Communication Edition Documentation (CED)	*DE GENTILE Benoît*
* Bureau d'Etudes Mécaniques (BEM)	*DOCEUL Louis*
* Préparation et Contrôle Qualité (PCQ)	*DUROCHER Alain*
* Suivi et Fabrication dans l'Industrie (SFI)	*BERTRAND Bernard*
* Ingénierie des Composants Internes (ICI)	*SCHLOSSER Jacques*
* Contrôle de l'Extraction de Chaleur (CEC)	*GUILHEM Dominique*
* Contrôle des Flux de Matière (CFM)	*LOARER Thierry*
* Contrôle des Impuretés & Physique Atomique (CIPA)	*DE MICHELIS Claudio*
* Théorie : Configuration Magnétique & Physique du Plasma de Bord (TCMP2)	*GHENDRIH Philippe*

SERVICE TOKAMAK EXPLOITATION ET PILOTAGE

Chef de Service *VAN HOUTTE Didier*
Adjoint *GRISOLIA Christian*

* Acquisitions et Contrôle-Commande (GACC)	*CHATELIER Elisabeth*
* Aimants (GAIM)	*LIBEYRE Paul*
* Alimentations Aimants et Distribution Electrique (GAADE)	*ZUNINO Karine*
* Cryogénie (GCRYO)	*GRAVIL Bernard*
* Machine et Vide (GMV)	*SAMAILLE Franck*
* Pilotage (GPILE)	*MARTIN Gilles*
* Réfrigération (GREF)	*CHANTANT Michel*
* Gestion des Données (GEDO)	*BALME Stéphane*

Euratom CEA

Direction des Sciences de la Matière
Département de Recherches sur la Fusion Contrôlée
CEA/Cadarache
F-13108 SAINT PAUL LEZ DURANCE CEDEX

ORGANIGRAMME DE LA DIRECTION

TORE SUPRA

Chef du Département	Jacquinot Jean
Adjoints	Chatelier Michel Marbach Gabriel
Chargés de Mission	Bottereau Jean-Michel Moreau Didier
Secrétariat	Bertin-Maghit Anne Di Martino Maura Polo Filisan Nathalie

Téléphone : **04 42 25 70 01**

Télécopie : **04 42 25 64 21**

e-mail (MS) : **dirdrfc@drfc.cad.cea.fr**
Site Web DRFC : http://www-drfc.cad.cea.fr:8002

GROUPE ADMINISTRATIF

Assistant Administratif Franel Bertrand

Tableaux de bord - Formation
François Philippe

Gestion des Contrats Européens
Le Bris Alain

Gestion Budgétaire et Commerciale
Benoit Eric — Lageste Lucette
Fortin Gérard — Volpe Brigitte

Gestion du Personnel
Le Bohec Annie — Salvador Joël

Magasin
Escop Jean-Paul — Pasquier Guy

SECURITE

Ingénieur Sécurité Jaunet Marc

COORDINATION ACTIONS DE TECHNOLOGIES

Responsable Marbach Gabriel

Magaud Philippe
Le Vaguerès Florence
Rodriguez Lina

PROJET CLES

Chef de Projet Garin Pascal

INSTALLATION

Chef d'Installation Journeaux J-Yves

Secrétariat Cousseau Josiane

Gestion des biens, Entretien des bâtiments
Malagoli Jacques — Thénot Alain

Agents mis à disposition :

CSU JET Culham :
Caminade J-pierre
Caminade Pascale
Paméla Jérôme

CSU Garching :
Le Marois Gilles

Total : 32

Service Tokamak Exploitation et Pilotage (S.T.E.P.)

COMMISSARIAT A L'ENERGIE ATOMIQUE

Association EURATOM-CEA

DSM/DRFC/STEP
CEA/Cadarache
13108 St Paul lez Durance Cedex - France

Télécopie	: 04.42.25.26.61
Tél. Secrétariat	: 04.42.25.62.25
	: 04.42.25.42.95
email (SMTP)	: dirstep@drfc.cad.cea.fr
email (MS)	: STEP@DRFCCAD.cea.fr

Effectifs :

AI :	41,0
AII :	58,0
Total CEA :	99,0
#Euratom :	2,0
*Contrat App. :	2,0
** Thèse :	1,0
†CTE :	1,0
Total Général :	105,0

Direction (DIR)

Chef du Service	***van Houtte Didier***
Adjoint	*Grisolia Christian*
Coordination Technique et planning	*Navarra Paul* Crest Ivan Fiet Patrice
Chef du Projet CIEL	*Cordier J. Jacques*
Chargé de mission	*Couturier Bruno*
Secrétaires	Bertrand M. Cécile Raulin Claire

Total AI : 5,0
Total AII : 4,0
Total CEA : 9,0 Total groupe : 9,0

Correspondant Informatique : J. Claude Alliez
Correspondant Formation : Alain Le Luyer

L'organigramme est accessible :
http://editex.cad.cea.fr/groupes/STEP

Cryogénie (GCRYO)

Balaguer David	*Henry Denis*
Bocquillon Anne	Maréchal J. Louis
Garbil Roger	Prochet Patrick
Girard Sylvain	*Reynaud Pascal*
Gravil Bernard	Roux Christophe
Huang Zhengmou†	

Total AI : 4,0
Total AII : 6,0 †CTE : 1,0
Total CEA : 10,0 Total groupe : 11,0

Machine & Vide (GMV)

Cantone Vincent	Le Goff Michel
Falchi Joseph	Moisan J. Claude (PRP)
Gargiulo Laurent	***Semeille Frank***
Hatchressian J. Cl	Soler Bernard
Le Roland	Zago Bertrand

Total AI : 2,0
Total AII : 7,5
Total CEA : 9,5 Total groupe : 9,5

Aimants (GAIM)

Bej Zygmunt	***Libeyre Paul(1)***
Ciazynski Daniel	*Nicollet Sylvie*
Cloez Hervé	Serries J. Paul
Decool Patrick	*Tena Manuel*
Duchateau J. Luc	*Zani Louis*
Hertout Patrick	

Total AI : 8,0
Total AII : 3,0
Total CEA : 11,0 Total groupe : 11,0

Réfrigération (GREF)

Chantant Michel	
Martinez André	Thos Bernard
Monbrun Daniel	Thouvenin Didier
Patier Patrick	Vigne Térence
Conturie Daniel*	

Total AI : 2,0 *Contrat apprent. 1,0
Total AII 5,0
Total CEA : 7,0 Total groupe 8,0

Alimentations Aimants et Distribution Electrique (GAADE)

Amédéo Michel	Louart André
Blanc J. Christophe	*Moustier Marcel*
Bruneth Jean (PRP)	Pelletier Thierry
Cara Philippe	Poquet Dominique
Chaix J. Pierre	***Zunino Karine***
Hourfoule Joël	Santagiustina Andréaff

Total AI : 3,0
Total AII : 7,5 #EUR 1,0
Total CEA : 10,5 Total groupe 11,5

Pilotage & Electronique (GPILE)

Alarcon Thierry	Marty Vincent
Barbuti Alain	Moreau Michel
Bucalossi Jérôme	Pastor Patrick
Garnier Daniel	Pirola Raymond
Géraud Alain	Russello Aldo
Gros Gilles	¤Sabathier Francis
How John†	*Saint-Laurent François*
Kirmaci Fatma*	*Spuig Pascal*
Le Luyer Alain	Villecroze Frédéric
Martin Gilles	Wisniewski Sylvain
	Sourd Frédéric**

Total AI : 5,0
Total AII : 12,0 #EUR : 1,0
Total CEA : 17,0 *Contrat apprent. 1,0
**Thèse 1,0 Total groupe : 20,0

Gestion des Données (GEDO)

Alba-Duran José	
Allez J. Claude	*Parrat Hélène*
Bahat Abbes	*Rothan Bernard*
Balme Stéphane	Signoret Jacqueline
Buravand Yves	*Signoret Jean*
Lamoureux J.M.	*Thois J. Marie*
Maini Patrick	*Utzel Nadine*

Total AI : 8,0
Total AII : 5,0
Total CEA : 13,0 Total groupe : 13,0

Acquisition et Contrôle-Commande (GACC)

Baudet Jacques	Hodasava Pascal
Caulier Gilles	Lebourg Philippe
Chatelier Elisabeth	Le Luyer Mireille
Ducobu Lionel	*Leroux Fabrice*
Fejoz Pascal	Mahieu J. François
Guillerminet Bernard	*Moulin Danièle*

Total AI : 4,0
Total AII : 8,0
Total CEA : 12,0 Total groupe : 12,0

Légende : *Contrat d'Apprentissage, ** Thèse, ***Post-Doc, #Euratom, ¤Détaché JET, ¤¤Scientif.Contingent, †CTE
Départ :
Arrivées : Térence Vigne : 19/11/01 (GREF), Frédéric Sourd : 1/10/01 (GPILE), Daniel Conturie : 15/10/01 (GREF), Zhengrong Ouyang : 30/10/01 (GCRYO)
Mouvements internes :
Pour mémoire : (1)Chef de Groupe, P. Libeyre intérim de J.L. Duchateau au 1/4/01

Diffusion : DRFC/DIR (3 ex), CI, INST/A. Thénot, IS, GA (3 ex), Magasin DRFC, SIPP (3 ex), SIPP/SFI/AM, SCCP (3 ex), RQ STEP/CdG, Affichage STEP, SMT/M. Giulianotto 35ex

Mise à jour : 04/12/2001

amcb/Personnel/Trombinoscope/Trombi12_01

SERVICE CHAUFFAGE ET CONFINEMENT DU PLASMA

DSM/DRFC/SCCP — **ASSOCIATION EURATOM-CEA**

Chauffage et Génération de Courant (GCGC)

BASIUK Vincent
BECOULET Alain
COLAS Laurent
DEFRASNE Pascal
DELPECH Léna*
ERIKSSON Lars-Göran
JOFFRIN Emmanuel**
JOUVE Michel
LITAUDON Xavier
MAZON Didier
MOREAU Philippe
NGUYEN Frédéric
PECQUET Annie-Laure
PEYSSON Yves
RIMINI Fernanda

ASSAS Stéphane
JU Myunghee
TRESSET Guillaume

Transport et Confinement (GTC)

ANIEL Thierry
ARTAUD Jean-François
FENZI Christel**
GIRUZZI Gerardo
HOANG Gia Tuong
HUTTER Thierry
IMBEAUX Frédéric
MASSET Régis
PASSERON Chantal
ZOU Xiao Lan

FOURMENT Claude
KRIVENSKI Vladimir

Théorie des Plasmas Chauds (GTPC)

GARBET Xavier**
HUYSMANS Gérardus
JOHNER Jean
MAGET Patrick
MISGUICH Jacques
OTTAVIANI Maurizio
REUSS Jean-Daniel
SARAZIN Yannick
ZWINGMANN Wolfgang

FLEURENCE Emmanuel
LABIT Benoît

Effectifs
Annexe 1 : 57 - Annexe 2 : 33 - Euratom : 14

Mise à jour : Décembre 2001

Direction

Chef du SCCP — SAOUTIC Bernard
Adjoint — LAVIRON Clément
Chargé de Mission — STOTT Peter, BAYETTI Pascal**
Secrétaires — DEPREZ Marie-Christine, AUDISIO Danielle

Diagnostics d'ensemble (GDE)

CHAU Stéphane
ECHARD Benjamin
ELBEZE Didier
GIANNELLA Ruggero
GIL Christophe
LASALLE Jean
LOTTE Philippe
PHILIP Joël
TOULOUSE Lionel
TRAVERE Jean-Marcel

Labo HF (GLHF)

ACHARD Joëlle
BERGER-BY Gilles
BOTTEREAU Christine
CHAREAU Jean-Marc
CLAIRET Frédéric
GONICHE Marc
MOLINA Diego
SABOT Roland
SEGUI Jean-Luc

Support aux Chauffages (GSAC)

AGARICI Gilbert
BOSIA Giuseppe
BRUGNETTI Robert
DELAPLANCHE Jean-Marc
DOUGNAC Hubert
GARIBALDI Pascal
PAGANO Marc
PIGNOLY Eric
POLI Serge
VOLPE Robert

Chauffage FCE (GFCE)

BOUQUEY Francis
CLARY Jacques
DARBOS Caroline
JUNG Marc
LENNHOLM Morten
MAGNE Roland
PAIN Mario*
PETIT Thomas
ROUX Daniel

CLAPIT Martial

Systèmes Hybride et Ion Cyclotron (GSHIC)

BEAUMONT Bertrand
BERTRAND Emmanuel
BIBET Philippe
BREMOND Sylvain
DUTHEIL Sophie
EKEDAHL Annika
KAZARIAN Fabienne
LOMBARD Gilles
MILLON Laurent
MOLLARD Patrick
PROU Marc
TANASKOVIC Lazar
VOLPE Daniel
VULLIEZ Karl

Injection de Neutres (GIDN)

ARMITANO Arthur
BOURG Joël
CANO Vincent
DE ESCH Hubert
FARJON Jean-Luc
GRAND Christian
HEISTER Peter
HEMSWORTH Ronald
MASSMANN Peter
SIMONIN Alain
SVENSSON Lennart

BOILSON Deirdre
KRYLOV Alexander

LEGENDE :
Italique : Collaborateurs, Doctorants, Stagiaires, Apprentis
**** Coopération/Détachement à JET**
*** Détaché, Mission, Congé, Formation longue durée**

Cadarache
13108 Saint Paul Lez Durance Cedex
FRANCE

CEA/DSM/DRFC

SERVICE INTEGRATION PLASMA PAROI
(SIPP)

Association EURATOM-CEA

Téléphone secrétariat 04 42 25 63 40
Télécopie 04 42 25 49 90
e-mail (SMTP) dirsipp@drfc.cad.cea.fr
e- mail (MS) SIPP@drfccad.cea.fr

DIRECTION (DIR)

506/3ème

Chef de Service **Grosman André**
Adjoint Rey Guy

Secrétariat Barbu Yvonne
Junique Colette

Total : 4 (AI:2-AII:2)

PROJETS ETUDES FABRICATION CONTROLE (PEFC)

506/3ème

Communication Edition Documentation (CED)

506/1er, 3ème

Brieu Marie-Claude Desmedt Hugues
Champin Gérard Poli Véronique
De Gentile Benoît

Total : 5 (AI:1-AII:3-EUR :1)

Contrôle de l'Extraction de Chaleur (CEC)

507/2ème

Balorin Colette **Pocheau Christine**
Desgranges Corinne **Reichle Roger**
Guilhem Dominique **Roche Hélène**
Messina Patricia **Vallet Jean-Claude**
Mitteau Raphaël
Delchambre Elise#

Total : 10 (AI:4-AII:4-EUR:1-CT :1)

Bureau d'Etudes Mécaniques (BEM)

Cantone Bruno Faisse Frédéric
Cappiello Françis Guérrin Jean-Louis
Chenevois Pierre Lucas Jean-Pierre
De Montgolfier Alban Patterlini Jean-Claude
Doceul Louis Raulin Dominique
Saille Alain

Masana Céline¤

Total : 12 (AI:1-AII:10-CT:1)

Théorie : Configuration Magnétique & Physique du Plasma de Bord (TCMP2)

513/1er

Ané Jean Marc Grandgirard Virginie
Bécoulet Marina Pégourié Bernard
Capes Hubert Tsitrone Emmanuelle
Ghendrih Philippe
Clément Caroline# Thomas Paul¤
Dejarnac Renaud#
Waller Vincent#

Contrôle des Flux de Matière (CFM)

508/2ème

Brosset Christophe Monier-Garbet Pascale**
Devynck Pascal Oddon Patricia
Gunn James Pascal Jean-Yves
Loarer Thierry Vartanian Stéphane

Lehnen Michael¤

Ingénierie des Composants Internes (ICI)

506/3ème

Béraud Alain Lipa Manfred
Chappuis Philippe Missirlian Marc
Escourbiac Frédéric Portafaix Christophe
Gauthier Eric **Schlosser Jacques**

Cambe Arnaud# Hurd Frederick¤
Roupillard Gabriel# Jaubert Carole¤

Total : 13 (AI:6-AII:1-EUR:1-CT:4)

Préparation et Contrôle Qualité (PCQ)

Durocher Alain Mayerhoeffer Jean-Louis
Gallay Philippe Paulus-Martin Valérie
Grand Monique Vignal Nicolas
Lisanti Marc

Total : 7 (AI:1-AII:6)

Suivi et Fabrication dans l'Industrie (SFI)

Bertrand Bernard Lallier Yves
Bondil Jean-Louis Verger Jean-Marc

Total : 4 (AI:1-AII:3)

Atelier Mécanique (AM)

Maillet Philippe

Total : 1(AII:1)

Contrôle des Impuretés et Physique Atomique (CIPA)

507/1er

Beauté Alain Lowry Chritopher
Chareyre Estelle* Maas Akko
De Michelis Claudio Meyer Olivier
Guirlet Rémi Schunke Beatrix
Hess Wulf

Corre Yann# Schwob Jean Louis¤

Total : 11 (AI:1-AII:3-EUR:5-CT:2)

Thésard
¤ Collaborateur extérieur
* Détaché/Mission/Congé longue durée

Total CEA AI 29
CEA AII 36

X.3. Quality

The Quality approach at DRFC is a long-term approach based on a structure consisting of a Quality correspondent and a group of Quality representatives in a number of clearly identified areas (Tore Supra operation, fabrication follow-up). This Quality approach concerns the entire department, both in the scientific and technical areas and the administration or safety areas. The main objective during 2000-2001 was focused on the appropriation of Quality by the executive level and all the members of the department. The Quality reference book of the DSM being used as a reference, this means the following important actions :

- The internal DRFC organisation was clarified by the distribution of organisation notes on projects or specific missions; the organisation charts of the services and department are kept up to date,
- For the projects, the people in charge are designated, the objectives, means and deadlines made clear and many training courses (project management, analysis of value, tools, etc.) have been organised,
- The generalisation of the use of the unified nomenclature for the internal working documents, in order to allow for a better follow-up, a long lasting archiving system and electronic recording and diffusion,
- The generalisation of the use of standardised laboratory notebooks, for a better traceability, and in the long run controlled archiving of all the departmental activities,
- The implementation of a monitoring and analysis system for Tore Supra incidents and the creation of a chart for the follow-up of the state of the Tore Supra systems to increase efficiency,
- The updating and gathering of several procedures, for example the control of Tore Supra systems, the quality control of mechanical components, or intervention “en astreinte”,
- The implementation of a welcoming procedure for new arrivals, with the designation of a counselor, distribution of a welcome booklet and yearly organisation of an open day describing our organisation and activities,
- A quality audit for outside suppliers.

IX.4. Safety

In terms of personnel safety, the following actions have been carried out over the period under consideration:

- The main action was the efficient management of safety during the CIEL project. It included both a work of co-ordination among the different people involved (safety inspections, prevention plans) and of on site control to reduce as much as possible, or prevent, the risks linked to the co-activity generated by the simultaneity of the different operations on the work site ;
- The effort on preventing electric risks was continued. Before the machine was started up, all the installed systems were checked. Also, during 2000 and 2001, over 60 DRFC workers were trained or re-trained in electricity. Lastly, all the work accidents due to electricity were rigorously analysed to find the technical and human causes of the accident, as well as to obtain a feedback which was largely distributed within the department;
- The control on the safety level of the department is maintained by means of safety visits : to be noted for 2000, a safety visit led by members of the CHSCT and in 2001 a visit made by the DSM Direction. No significant abnormality was noted. This control is also guaranteed by the repairing of abnormalities coming from the reports on the regular visits led by the regulatory committees (electricity, lifting machines, pressure and vapour machines, and lasers). An evaluation of the yearly D_2 consumption will nevertheless be made based on our experimental measurements to confirm that noted on the stock. The installation of a measurement of the quantity of tritium produced during plasma experimentation has been set up, so as to overlap the theoretical evaluations deduced from the measurement of the neutrons produced during plasma experiments;
- A specific effort on the elimination of pyralene components stored in the facility was conducted in 2001, in relation with the de-storage process underway on the Cadarache Centre.

IX.5. Bibliography

IX.5.1. Articles

[1] A high speed fibre communication link for measurement & I/O (M&IO-Net)
Fusion Engineering and Design, vol.56-57 (2001) p.999-1004
P. Spuig, B. Couturier

[2] A new internal matching impedance concept for ICRF antennas
Fusion Engineering and Design, vol.56-57 (2001) p.563-567
S. Bremond, G. Agarici, B. Beaumont, J.P. Chenevois

[3] Active cooling, calorimetry and energy balance in Tore Supra
Journal of Nuclear Materials, vol.290-293 (2001) p.1023-1029
J.C. Vallet, R. Reichle, M. Chantant, V. Basiuk, R. Mitteau

[4] Actively cooled plasma facing components in Tore Supra
Fusion Engineering and Design, vol.56-57 (2001) p.117-123
P. Garin, X. Tore supra team

[5] Alternative Schemes of power deposition with the Ergodic Divertor on Tore Supra
Journal of Nuclear Materials, vol.290-293 (2001) p.910-914
G. Mank, Ph. Ghendrih, C. Grisolia, J. Gunn, T. Loarer, P. Monier-Garbet, L. Costanzo, K. Finken, C. De Michelis, R. Reichle

[6] An H minority heating regime in Tore Supra showing improved L mode confinement
Nuclear Fusion, vol.40 n°5 (2000) p.913-921
G.T. Hoang, P. Monier-Garbet, T. Aniel, C. Bourdelle, R. Budny, F. Clairet, L.G. Eriksson, X. Garbet, C. Grisolia, P. Platz, J.C. Vallet

[7] Analysis of an in-service rupture of the inner first wall of Tore Supra
Fusion Engineering and Design, vol.56-57 (2001) p.445-449
R. Mitteau, Ph. Chappuis, G. Martin, S. Rosanvallon

[8] Analysis of energy flux deposition and sheath transmission factors during ergodic divertor operation on Tore Supra
Journal of Nuclear Materials, vol.290-293 (2001) p.840-844
L. Costanzo, J. Gunn, T. Loarer, L. Colas, Y. Corre, Ph. Ghendrih, C. Grisolia, A. Grosman, D. Guilhem, P. Monier-Garbet, R. Reichle, H. Roche, J.C. Vallet

[9] Anomalous particle pinch in tokamaks
Physics of Plasmas, vol.7 n°10 (2000) p.4197-4207
F. Miskane, X. Garbet, A. Dezairi, D. Saifaoui

[10] Atomic and molecular deuterium edge density evaluation from spectral analysis of the D? line shape
Plasma Physics and Controlled Fusion, vol.43 (2001) p.1733-1746
A. Escarguel, B. Pegourie, J.T. Hogan, C. De Michelis, Y. Corre, A. Azeroual, J.M. Ané, R. Guirlet, J. Gunn, H. Capes, L. Godbert-mouret, M. Koubiti, R. Stamm

[11] Bursty transport in tokamaks turbulence : role of zonal flows and internal transport barriers
Nuclear Fusion, vol.41 n°8 (2001) p.995-1001
S. Benkadda, P. Beyer, N. Bian, C. Figarella, O. Garcia, X. Garbet, Ph. Ghendrih, Y. Sarazin, P. Diamond

[12] Characterisation of radiation and flux measurements on a neutraliser plate of the Tore Supra ergodic divertor
Journal of Nuclear Materials, vol.290-293 (2001) p.250-254
Y. Corre, R. Giannella, C. De Michelis, R. Guirlet, A. Azeroual, E. Chareyre, L. Costanzo, A. Escarguel, E. Gauthier, Ph. Ghendrih, J. Gunn, J.T. Hogan, P. Monier-Garbet, B. Pegourie, A. Pospieszczyk, E. Tsitrone

[13] Characterisation of the separatrix position in the ergodic divertor discharges of the Tore Supra tokamak
Journal of Nuclear Materials, vol. 290-293 (2001) p.985-989
M. Zabiego, Ph. Ghendrih, M. Becoulet, L. Costanzo, C. De Michelis, C. Friant, J. Gunn

[14] Characterization of the ECRH system electromagnetic field : determination of the electromagnetic modes at high and low power
Fusion Engineering and Design, vol. 53 (2001) p.443-449
L. Courtois, A. Becoulet, G. Berger-By, J.P. Crenn, S. Tedjini

[15] CIEL in Tore Supra : how to master power and particles on very long discharges
Journal of Plasma and Fusion Research Series, vol.3 (2000) p.10-15
P. Garin, X. Tore supra team

[16] CIEL: Tore Supra's new power and particle extraction environment
Fusion Engineering and Design, vol. 49-50 (2000) p.89-95
P. Garin

[17] Collisional effects on diffusion scaling laws in electrostatic turbulence
Physical Review E, vol.61 n°3 (2000) p.3023-3032
M. Vlad, F. Spineanu, J.H. Misguich, R. Balescu

[18] Combined kinetic and transport modeling of radiofrequency current drive
Physics of Plasmas, vol.7 n°12 (2000) p.4972-4982
R. Dumont, G. Giruzzi, E. Barbato

[19] Comparison of impurity generation and penetration models with spectroscopy for the Tore Supra ergodic divertor
Plasma Physics and Controlled Fusion, vol.43 (2001) p.271-280
R. Giannella, Y. Corre, J.T. Hogan, Ph. Ghendrih, R. Guirlet, J. Gunn

[20] Complete suppression of neoclassical tearing modes with current drive at the electron-cyclotron resonance frequency in ASDEX Upgrade tokamak
Physical Review Letters, vol.85, n°6 (2000) p.1242-1245
G. Gantenbeim, H. Zohm, G. Giruzzi, S. Günter, F. Leuterer, M. Maraschek, J. Meskat, Q. Yu

[21] Completion of the ITER toroïdal field model coil (TFMC)
Fusion Engineering and Design, vol.58-59 (2001) p.159-164
R. Maix, H. Fillunger, F. Hurd, E. Salpietro, N. Mitchell, P. Libeyre, P. Decool, A. Ulbricht, G. Zahn, D. Bresson, A. Bourquard, B. Schellong, E. Theisen, N. Valle, F. Baudet

[22] Conditioning procedures in Tokamak : Tore Supra application
Vacuum, vol.60 (2001) p.147-152
A. Grisolia, J. Bucalossi, T. Loarer, S. Vartanian, A. Grosman, G. Martin

[23] Consistency check of Zeff measurements in ergodic divertor plasmas on Tore Supra
Journal of Nuclear Materials, vol.290-293 (2001) p.715-719
B. Schunke, C. De Michelis, R. Guirlet, P. Monier-Garbet, M. Mattioli, E. Chareyre, O. Meyer

[24] Control of divertor geometry and performance of the Ergodic Divertor of Tore Sup
Journal of Nuclear Materials, vol.290-293 (2001) p.798-804
Ph. Ghendrih, M. Becoulet, L. Costanzo, Y. Corre, C. Grisolia, A. Grosman, R. Guirlet, J. Gunn, T. Loarer, P. Monier-Garbet, G. Mank, R. Reichle, J.C. Vallet, M. Zabiego, A. Azeroual, J. Bucalossi, P. Devynck, C. De Michelis, K. Finken, J.T. Hogan, F. Laugier, F. Nguyen, B. Pegourie, F. Saint-Laurent, B. Schunke, X. Tore supra team

[25] Coupled full-wave and ray-tracing numerical treatment of mode conversion in a tokamak plasma
Physics of Plasmas, vol.7, n°3 (2000) p.911-922
Y. Petrov, A. Becoulet, I. Monakhov

[26] Coupling and power handling of the new Tore Supra LHCD launcher
Fusion Engineering and Design, vol.56-57 (2001) p.679-684
Ph. Bibet, A. Ekedahl, Ph. Froissard, F. Kazarian, E. Bertrand, S. Dutheil-hertout, L. Tanaskovic

[27] Damping of relativistic electron beams by synchrotron radiation
Physics of Plasmas, vol.8 n°12 (2001) p.5221-5229
F. Andersson, P. Helander, L.G. Eriksson

[28] Density fluctuations at high density in the Ergodic Divertor configuration of Tore Supra
Journal of Nuclear Materials, vol.290-293 (2001) p.584-587
P. Devynck, J. Gunn, Ph. Ghendrih, X. Garbet, G. Antar, P. Beyer, C. Boucher, C. Honoré, F. Gervais, P. Hennequin, A. Quéméneur, A. Truc

[29] Design criteria for Tore Supra high heat flux components
Fusion Engineering and Design, vol.56-57 (2001) p.457-463
M. Missirlian, J. Schlosser, M. Lipa, R. Mitteau, Ph. Chappuis, C. Portafaix

[30] Design of an improved vacuum vessel protection for very long pulse operation in Tore Supra
Fusion Engineering and Design, vol.56-57 (2001) p.855-859
M. Lipa, B. Cantone, P. Garin, R. Mitteau, C. Portafaix

[31] Design of the infrared monitoring system for CIEL project
Fusion Engineering and Design, vol.51-52 (2000) p.1065-1069
C. Portafaix, V. Basiuk, A. Beraud, M. Chantant, Ph. Chappuis, J.J. Cordier, R. Dahmani, L. Doceul, F. Faisse, P. Garin, X. Et al.

[32] Determination of non-inductive current profiles in Tore Supra
Plasma Physics and Controlled Fusion, vol.42 (2000) p.1227-1239
E. Joffrin, V. Basiuk, R. Bregeon, X. Litaudon

[33] Development of actively cooled components for the Tore Supra toroidal pump limiter
Physica Scripta, vol.T91 (2001) p.94-97
J. Schlosser, Ph. Chappuis, A. Durocher, L. Moncel, P. Garin

[34] Development of the IR interfero-polarimeter for long pulse operation at Tore Supra
Fusion Engineering and Design, vol.56-57 (2001) p.969-973
C. Gil, D. Elbeze, C. Portafaix

[35] Development of tungsten coating for fusion applications
Fusion Engineering and Design, vol.56-57 (2001) p.331-336
A. Cambe, E. Gauthier, J. Layet, S. Bentivegna

[36] Diagnostic development for steady-state high power operation
Journal of Plasma and Fusion Research SERIES, vol.3 (2000) p.393-396
C. Laviron

[37] Diffusion in biased turbulence
Physical Review E, vol.63 (2001) p.066304-1/10
M. Vlad, F. Spineanu, J. Misguich, R. Balescu

[38] Dust characterization and analysis in Tore Supra
Journal of Nuclear Materials, vol.290-293 (2001) p.245-249
Ph. Chappuis, E. Tsitrone, M. Mayne, X. Armand, J. Linke, H. Bolt, D. Petti, J. Sharpe

[39] Dynamics of chaotic magnetic lines : intermittency and noble internal transport barriers in the Tokamap
Physics of Plasmas, vol. 8 n°5 (2001) p.2132-2138
J.H. Misguich

[40] Dynamics of energetic ion orbits in magnetically confined plasmas
Plasma Physics and Controlled Fusion, vol.43 (2001) p.R145-R182
L.G. Eriksson, F. Porcelli

[41] Dynamics of fast electrons driven by the lower hybrid wave in giant sawtoothing plasmas
Physical Review Letters, vol.84 n°13 (2000) p.2873-2876
F. Imbeaux, Y. Peysson

[42] Edge cooling experiments and non-local transport phenomena in Tore Supra
Plasma Physics and Controlled Fusion, vol.42 (2000) p.1067-1076
X.L. Zou, A. Geraud, P. Gomez, M. Mattioli, J.L. Segui, F. Clairet, C. De Michelis, P. Devynck, T. Dudok de Wit, M. Erba, C. Fenzi, X. Garbet, C. Gil, P. Hennequin, F. Imbeaux, E. Joffrin, G. Leclert, A.L. Pecquet, Y. Peysson, R. Sabot, T.F. Seak

[43] Edge denstity profile measurements by X-mode reflectometry on Tore Supra
Plasma Physics and Controlled Fusion, vol.43 (2001) p.429-441
F. Clairet, C. Bottereau, J.M. Chareau, M. Paume, R. Sabot

[44] Edge flow measurements with Gundestrup probes
Physics of Plasmas, vol.8 n°5 (2001) p.1995-2001
J. Gunn, C. Boucher, P. Devynck, K. Dyabilin, J. Horacek, M. Hron, J. Stöckel, G. Van oost, H. Van goubergen, F. Zacek

[45] Effect of limiter recycling on measured poloidal impurity emission profiles in Tore Supra
Journal of Nuclear Materials, vol.290-293 (2001) p.628-632
J.T. Hogan, C. De Michelis, P. Monier-Garbet, M. Becoulet, Charles E. Bush, Ph. Ghendrih, R. Guirlet, W.R. Hess, M. Mattioli, J.C. Vallet

[46] Effect of q-profile modification by LHCD on internal transport barriers in JET
Plasma Physics and Controlled Fusion, vol.43 (2001) p.861-879
C. Challis, E. Joffrin, D. Mazon, F. Rimini, X. Et al.

[47] Electron cyclotron radiation, related power loss, and passive current drive in tokamaks: a review
Fusion Technology, vol.39 (2001) p.33-44
I. Fidone, G. Giruzzi, G. Granata

[48] Electron Transport in Tore Supra with Fast Wave Electron Heating
Physics of Plasmas, vol.7 n°5 (2000) p.1494-1510
W. Horton, P. Zhu, G.T. Hoang, T. Aniel, M. Ottaviani, X. Garbet

[49] Energetic particle physics in JET
Nuclear Fusion, vol.40 n°7 (2000) p.1363-1381
S. Sharapov, B. Alper, D. Borba, L.G. Eriksson, G. Huysmans, J. Jacquinot, X. Et al.

[50] Equilibrium analysis of tokamak discharges with anisotropic pressure
Plasma Physics and Controlled Fusion, vol.43 (2001) p.1441-1456
W. Zwingmann, L.G. Eriksson, P. Stubberfield

[51] Ergodic divertor experiments on the route to steady state operation of Tore Supra
Nuclear Fusion, vol.41 n°10 (2001) p.1401-1412
Ph. Ghendrih, M. Becoulet, L. Costanzo, Y. Corre, C. Grisolia, A. Grosman, R. Guirlet, J. Gunn, T. Loarer, P. Monier-Garbet, P. Thomas, M. Zabiego, J. Bucalossi, P. Devynck, G. Martin, C. De Michelis, F. Nguyen, B. Pegourie, R. Reichle, F. Saint-Laurent, J.C. Vallet, X. Tore Supra team

[52] Estimation of heat loads on the wall structures in parasitic absorption of lower hybrid power
Nuclear Fusion, vol.40 n°8 (2000) P.1477-1490
K. Rantamäki, T. Pättikangas, S. Karttunen, P. Bibet, X. Litaudon, D. Moreau

[53] European contributions to the beam source design and R&D of the ITER neutral beam injectors
Nuclear Fusion, vol.40 n° 3Y (2000) p.589-597
P. Massmann, P. Bayetti, J. Bucalossi, C. Desgranges, E. Di pietro, P. Frank, M. Fumelli, Y. Fujiwara, M. Hanada, B. Heinemann, R. Hemsworth, T. Inoue, C. Jacquot, W. Kraus, Y. Okumura, F. Probst, A. Simonin, E. Speth, R. Trainham, O. Vollmer

[54] Evaluations and prospects for the next steps in the low power RF systems of the Tore Supra transmitters
Fusion Engineering and Design, vol.56-57 (2001) p.673-677
G. Berger-By, J. Achard, B. Beaumont, Ph. Bibet, S. Dutheil-hertout, M. Goniche, G. Lombard, L. Millon, C. Mollard, K. Vulliez

[55] Experience feedback from high heat flux component manufacturing for Tore Supra
Fusion Engineering and design, vol.56-57 (2001) p.309-313
J. Schlosser, A. Durocher, T. Huber, P. Garin, B. Schedler, G. Agarici

[56] Experimental and theoretical evaluation of the He II 6560.1 A line contribution to the deuterium D? spectral line shape in Tore Supra ergodic divertor plasmas
Plasma Physics and Controlled Fusion, vol.43 (2001) p.177-194
R. Guirlet, M. Koubiti, A. Escarguel, C. De Michelis, M. Mattioli, M. O'mullane, H. Capes, L. Godbert-mouret, R. Stamm

[57] Experimental characterization of the electron heat transport in low-density ASDEX Upgrade plasmas
Physical Review Letters, vol.86 n°24 (2001) p.5498-5501
F. Ryter, F. Imbeaux, F. Leuterer, U. Fahrbach, W. Suttrop, X. Asdex upgrade team

[58] Experimental determination of critical threshold in electron transport on Tore Supra
Physical Review Letters, vol.87 n°12 (2001) p.125001/1-4
G.T. Hoang, C. Bourdelle, X. Garbet, G. Giruzzi, T. Aniel, M. Ottaviani, W. Horton, P. Zhu, R. Budny

[59] Experimental studies of electron transport
Plasma Physics and Controlled Fusion, vol.43 (2001) p.A323-A338
F. Ryter, G.T. Hoang, F. Imbeaux, X. Et al.

[60] Experiments and 3D non-linear modelling of heat transport in ergodic zone on Tore Supra
Contribution to Plasma Physics, vol.40 n°3-4 (2000) p.251-255
M. Becoulet, H. Capes, Ph. Ghendrih, A. Grosman, J. Gunn, G.T. Hoang, J.L. Segui, M. Zabiego

[61] Feedback control achievements and endeavours in Tore Supra plasma wall interactions control
Journal of Plasma and Fusion Research Series, vol.3 (2000) p.206-210
A. Grosman, Ph. Ghendrih, C. Grisolia, J. Gunn, T. Loarer, P. Monier-Garbet, X. Tore Supra team

[62] Feedback control on edge plasma parameters with ergodic divertor in Tore Supra
Journal of Nuclear Materials, vol.290-293 (2001) p.566-570
J. Bucalossi, J. Gunn, A. Geraud, Ph. Ghendrih, C. Grisolia, A. Grosman, G. Martin, D. Moulin, J.Y. Pascal, F. Saint-Laurent

[63] First observation of pT fusion in JET tritium plasmas with ICRF heating of protons
Nuclear Fusion, vol.41 n°12 (2001) p.1815-1822
M. Mantsinen, O. Jarvis, V. Kiptily, S. Sharapov, B. Alper, L.G. Eriksson, A. Gondhalekar, R. Heeter, D. Mcdonald

[64] First plasma experiments in Tore Supra with a new generation of high heat flux limiters for RF antennas
Fusion Engineering and Design, vol.49-50 (2000) p.145-150
G. Agarici, B. Beaumont, Ph. Bibet, S. Bremond, J. Bucalossi, L. Colas, A. Durocher, L. Gargiulo, L. Ladurelle, G. Lombard, X. Et al.

[65] First principles based transport theroy
Nuclear Fusion, vol.40 n°4 (2000) p.873-878
D. Biskamp, P. Diamond, X. Garbet, Z. Lin, J. Nührenberg, R. Rogers

[66] From 10 years experience with the Tore Supra ergodic divertor towards its implementation in a next step device
Fusion Engineering and Design, vol.56-57 (2001) p.795-800
A. Grosman, X. Tore supra team

[67] Fusion Thermonucléaire
Les Techniques de l'Ingénieur, vol. BN 3 013 (2000) p.1-21
J. Weisse

[68] Hard x-ray CdTe tomography of tokamak fusion plasmas
Nuclear Instruments and Methods in Physics Research, A 458 (2001) p. 269-274
Y. Peysson, S. Coda, F. Imbeaux

[69] Heating and current drive system for Tore Supra steady-state operation
Journal of Plasma and Fusion Research Series, vol.3 (2000) p.51-57
A. Becoulet, X. Tore supra team

[70] Helium transport in advanced tokamak scenarios with internal transport barrier
Fusion Technology, vol.39 (MAR.2001) p.119-126
G. Kamelander, X. Litaudon, D. Moreau, I. Voitsekhovitch

[71] High heat flux behavior of damaged plasma facing components
Fusion Engineering and Design, vol.56-57 (2001) p.285-290
F. Escourbiac, Ph. Chappuis, J. Schlosser, M. Merola, I. Vastra, M. Febvre

[72] High power lower hybrid current drive experiments in the Tore Supra tokamak
Nuclear Fusion, vol.41 n°11 (2001) p.1703-1713
Y. Peysson, X. Tore supra team

[73] High radiation from intrinsic and injected impurities in Tore Supra ergodic divertor plasmas.
Journal of Nuclear Materials, vol.290-293 (2001) p.925-929
P. Monier-Garbet, C. De Michelis, Ph. Ghendrih, C. Grisolia, A. Grosman, R. Guirlet, J. Gunn, T. Loarer, Charles E. Bush, C. Clement, Y. Corre, L. Costanzo, B. Schunke, J.C. Vallet

[74] Ignition conditions for magnetized target fusion in cylindrical geometry
Nuclear Fusion, vol.40 n°1 (2000) p.59-68
M. Basko, A. Kemp, J. Meyer-ter-vehn

[75] Impact of charge exchange neutrals on plasma facing components of Tore Supra
Fusion Engineering and Design, vol.56-57 (2001) p.439-443
E. Tsitrone, Ph. Chappuis, E. Gauthier, M. Lipa, D. Reiter

[76] Improved calculation of synchrotron radiation losses in realistic tokamak plasmas
Nuclear Fusion, vol.41 n°6 (2001) p.665-678
F. Albajar, J. Johner, G. Granata

[77] Improvement of density control by feedback on Langmuir probe signals in Tore Supra ergodic divertor experiments
Plasma Physics and Controlled Fusion, vol.42 (2000) p.557-568
J. Gunn, J. Bucalossi, L. Costanzo, C. Grisolia, Ph. Ghendrih, A. Grosman, T. Loarer, G. Martin, P. Monier-Garbet, D. Moulin, J.Y. Pascal, F. Saint-Laurent

[78] Impurity radiation modulations in an ergodic divertor
Journal of Nuclear Materials, vol.290-293 (2001) p.892-895
F. Laugier, M. Becoulet, C. De Michelis, Ph. Ghendrih, J. Gunn, P. Monier-Garbet, R. Reichle, J.C. Vallet

[79] Interaction of ICRF power and edge plasma in Tore Supra ergodic divertor configuration
Journal of Nuclear Materials, vol.278 (2000) p.117-122
F. Nguyen, A. Grosman, V. Basiuk, D. Fraboulet, B. Beaumont, A. Becoulet, Ph. Ghendrih, L. Ladurelle, B. Meslin

[80] Internal transport barrier with ion-cyclotron-resonance minority heating on Tore Supra
Physical Review Letters, vol.84 n°20 (2000) p.4593-4596
G.T. Hoang, C. Bourdelle, X. Garbet, G. Antar, R. Budny, T. Aniel, V. Basiuk, A. Becoulet, P. Devynck, J. Lasalle, G. Martin, F. Saint-Laurent, X. Tore supra team

[81] Interplay between edge and outer core fluctuations in the tokamak Tore Supra
Nuclear Fusion (Letters), vol.40 n°9 (2000) p.1621-1626
C. Fenzi, X. Garbet, A. Truc, H. Capes, P. Devynck, F. Gervais, P. Hennequin, C. Laviron, A. Quéméneur

[82] Intrinsic impurity radiation in attached divertor plasmas
Plasma Physics and Controlled Fusion, vol.42 (2000) p.317-326
F. Laugier, Ph. Ghendrih

[83] Investigation of electron-distribution function and dynamo mechanisms in a reversed-field pinch by analysis of hydrogen-pellet deflection
Physical Review Letters, vol.84 n°24 (2000) p.5532-5535
L. Garzotti, B. Pegourie, R. Bartiromo, P. Innocente, S. Martini

[84] ITER relevant ICRF heating scenarios with large ion heating fraction
Nuclear Fusion, vol.40 n°1 (2000) p.35-51
V. Bergeaud, L.G. Eriksson, D. Start

[85] JET progress towards an advanced mode of ITER operation with current profile control
Plasma Physics and Controlled Fusion, vol.43 (2001) p.A395-A406
A. Becoulet, X. The jet-efda team

[86] Joints for large superconducting conductors
Fusion Engineering and Design, vol.58-59 (2001) p.123-127
P. Decool, D. Ciazynski, A. Nobili, S. Parodi, P. Pesenti, A. Bourquard, F. Beaudet

[87] Large superconductors and joints for fusion magnets : from conceptual design to test at full scale
Nuclear Fusion, vol.41 n°2 (2001) p.223-226
D. Ciazynski, J.L. Duchateau, P. Decool, P. Libeyre, B. Turck

[88] Linear stability and mode struture of drift tearing modes
Physics of Plasmas, vol. 8 n°10 (2001) p.4306-4317
D. Grasso, M. Ottaviani, F. Porcelli

[89] Lower hybrid dynamics by ECE Spectra in Tore Supra
Fusion Engineering and Design, vol.53 (2001) p.169-175
P. Gomez, J. Segui, G. Giruzzi, Ph. Froissard, Y. Peysson, D. Thouvenin

[90] Magnetized plasma flow through a small orifice
Physics of Plasmas, vol. 8 n°3 (2001) p.1040-1047
J. Gunn

[91] Magnetohydrodynamics in type II superconductors : application to force free configurations
Physical Review B, vol.64 (2001) p.094517.1-094517.11
J.F. Artaud, D. Ciazynski, A. Samain

[92] Material activation observation on the Tore Supra Tokamak
Fusion Engineering and Design, vol.58-59 (2001) p.973-977
G. Martin, A. Le luyer, F. Saint Laurent

[93] Measurement and simulation of edge flows induced by ergodization in Tore Supra
Journal of Nuclear Materials, vol.290-293 (2001) p.877-881
J. Gunn, C. Boucher, Y. Corre, P. Devynck, Ph. Ghendrih, J.Y. Pascal

[94] Measurement of central toroidal rotation in ohmic Tore Supra plasmas
Nuclear Fusion, Vol.40, n°3 (2000) p.319-324
A. Romannikov, C. Bourdelle, J. Bucalossi, T. Hutter, P. Platz, F. Saint-Laurent

[95] Measurements of heat transfer coefficients at low contact pressures for actively cooled bolted armour concepts in Tore Supra
Fusion Engineering and Design, vol.49-50 (2000) p.243-248
M. Lipa, Ph. Chappuis, A. Dufayet

[96] MHD stability of lower hybrid enhanced performance discharges on the Tore Supra tokamak
Plasma Physics and Controlled Fusion, vol.43 (2001) p.1625-1639
M. Zabiego, G. Huysmans, Y. Peysson, J.F. Artaud, F. Imbeaux, X. Litaudon

[97] Modeling of the stabilization of neoclassical tearing modes by localized radio frequency current drive
Physics of Plasmas, vol.7, n°1 (2000) p.312-322
Q. Yu, S. Günter, G. Giruzzi, K. Lackner, M. Zabiego

[98] Modelling of "advanced tokamak" scenarios with radiofrequency heating and current drive for Tore Supra
Nuclear Fusion, vol.41 n°7 (2001) p.845-864
I. Voitsekhovitch, D. Moreau

[99] Modelling of ECH modulation experiments in ASDEX Upgrade with an empirical critical temperature gradient length transport model
Plasma Physics and Controlled Fusion, vol.43 (2001) p.1503-1524
F. Imbeaux, F. Ryter, X. Garbet

[100] Modelling of macroscopic magnetic islands in tokamaks
Nuclear Fusion, vol.41 n°9 (2001) p.1207-1218
F. Porcelli, M. Ottaviani, X. Et al.

[101] Modelling of Ripple Losses in Tokamak Plasmas Heated by ICRF Waves
Plasma Physics and Controlled Fusion, vol.43 (2001) p.1291-1302
L.G. Eriksson, V. Bergeaud, V. Basiuk, T. Hellsten

[102] NbTi superconducting busbars for the ITER TFMC
Fusion Engineering and Design, vol.58-59 (2001) p.117-
P. Libeyre, P. Decool, J.L. Duchateau, H. Cloez, A. Kienzler, A. Lingor, H. Fillunger, R. Maix, A. Bourquard, F. Beaudet

[103] Neoclassical tearing mode stabilization by ECCD in ITER
Fusion Engineering and Design, vol.53 (2001) p.43-46
G. Giruzzi, M. Zabiego

[104] Net erosion measurements on plasma facing components of Tore Supra
Journal of Nuclear Materials, vol.290-293 (2001) p.331-335
E. Tsitrone, Ph. Chappuis, Y. Corre, E. Gauthier, A. Grosman, J.Y. Pascal

[105] New advanced launcher for lower hybrid current drive on Tore Supra
Fusion Engineering and Design, vol. 51-52 (2000) p.741-746
Ph. Bibet, G. Agarici , M. Chantant, J.J. Cordier, C. Deck, L. Doceul, A. Durocher, A. Ekedahl, Ph. Froissard, L. Gargiulo, L. Garampon, M. Goniche, P. Hertout, F. Kazarian, D. Lafon, C. Portafaix, G. Rey, F. Samaille, F. Surle, G. Tonon

[106] New developments of the Tore Supra acquisition system
Fusion Engineering and Design, vol.56-57 (2001) p.1029-1031
Y. Buravand, S. Balme, B. Guillerminet, T. Hutter, J.Y. Pascal, B. Rothan

[107] Numerical assessment of the ion turbulent thermal transport scaling laws
Nuclear Fusion, vol.41 n°5 (2001) p.637-643
M. Ottaviani, G. Manfredi

[108] Observation of zero current density in the core of JET discharges with lower hybrid heating and current drive
Physical Review Letters, vol.87 n°11 (2001) p.115001-1/115001-4
N. Hawkes, C. Giroud, E. Joffrin, Ph. Lotte, D. Mazon, X. Et al.

[109] On the role of different phasings of the ICRF antennas in optimized shear discharges in JET
Nuclear Fusion, vol.40 n°10 (2000) p.1773-1789
M. Mantsinen, L.G. Eriksson, C. Gormezano, N. Hawkes, T. Hellsten, X. Litaudon, F. Rimini, S. Sharapov, B. Stratton

[110] On the Role of Ion Heating in ICRF heated Discharges in Tore Supra
Nuclear Fusion, vol.41 n°1 (2001) p.91-97
L.G. Eriksson, G.T. Hoang, V. Bergeaud

[111] Particle collection and exhaust in ergodic divertor experiments on Tore Supra
Journal of Nuclear Materials, vol.290-293 (2001) p.900-904
T. Loarer, Ph. Ghendrih, J. Gunn, A. Azeroual, L. Costanzo, C. Grisolia, R. Guirlet, G. Mank, P. Monier-Garbet, B. Pegourie

[112] Particle collection with the ergodic divertor of Tore Supra
Nuclear Fusion, vol.40, n°9 (2000) p.1651-1668
A. Azeroual, B. Pegourie, E. Chareyre, Y. Corre, A. Escarguel, G. Granata, R. Guirlet, J. Gunn, T. Loarer, E. Tsitrone, S. Vartanian

[113] Particle trapping in Carbon walls during ICRH heating in Tore Supra
Journal of Nuclear Materials, vol. 290-293 (2001) p.402-406
C. Grisolia, J.T. Hogan, Ph. Ghendrih, T. Loarer, J. Gunn, P. Monier-Garbet, M. Becoulet, T. Hutter

[114] Pellet injectors developed at the PELIN laboratory for international projects
Fusion Engineering and Design, vol.58-59 (2001) p.295-299
I. Viniar, S. Sudo, A. Geraud, J. Perin, J. Manzagol, P. Ladd, G. Saksaganskii, S. Skoblikov, A. Lukin, A. Umov, P. Reznichenko, K. Khlopenkov, I. Krasilnikov, I. Rukhlenko

[115] Performance and control of optimized shear discharges in JET
Nuclear Fusion, vol.40 n°6 (2000) p.1113-1123
A. Becoulet, L.G. Eriksson, Y. Baranov, D. Borba, C. Challis, G. Conway, V. Fuchs, C. Gormezano, C. Gowers, N. Hawkes, T. Hender, G. Huysmans, E. Joffrin, X. Litaudon, P. Lomas, A. Maas, M. Mayoral, V.V. Parail, F. Rimini, F. Rochard, Y. Sarazin, A. Sips, F. Söldner, K. Zastrow, W. Zwingmann

[116] Physics and design interplay phenomena in an actively cooled tokamak : Tore Supra
Physics of Plasmas, vol.8 n°5 (2001) p.2148-2152
M. Chatelier, X. Tore supra team

[117] Plasma Control at JET
Fusion Engineering and Design, vol.48 (2000) p.37-45
M. Lennholm, T. Budd, R. Felton, M. Gadeberg, A. Goodyear, F. Milani, R. Sartori

[118] Plasma control in advanced steady state operation of tokamaks
Journal of Plasma and Fusion Research Series, vol.3 (2000) p.502-508
D. Moreau, G. Kamelander, X. Litaudon, I. Voitsekhovitch

[119] Plasma-material interactions in current tokamaks and their implications for next step fusion reactors
Nuclear Fusion, vol.41 n°12R (2001) p.1967-2137
G. Federici, C. Skinner, J. Brooks, J. Coad, C. Grisolia, A. Haasz, A. Hassanein, V. Philipps, C. Pitcher, J. Roth, W. Wampler, D. Whyte

[120] Power deposition and margins on the Tore Supra pump limiter and fabrication of the high heat flux components
Fusion Engineering and Design, vol.49-50 (2000) p.337-342
J. Schlosser, R. Mitteau, L. Plöchl, C. Depit, E. Tsitrone

[121] Progress towards high-power lower hybrid current drive in Tore Supra
Plasma Physics and Controlled Fusion, vol.42, suppl.12B (2000) p.B87-B114
Y. Peysson, X. Tore supra team

[122] Proper orthogonal decomposition and Galerkin projection for a three-dimensional plasma dynamical system
Physical Review E, vol.61, n°1 (2000) p.813-823
P. Beyer, S. Benkadda, X. Garbet

[123] q-profile evolution and improved core electron confinement in the full current drive operation on Tore Supra
Plasma Physics and Controlled Fusion, vol.43 (2001) p.677-693
X. Litaudon, Y. Peysson, T. Aniel, G. Huysmans, F. Imbeaux, E. Joffrin, J. Lasalle, Ph. Lotte, B. Schunke, J. Segui, G. Tresset, M. Zabiego

[124] Real time determination and control of the plasma localisation and internal inductance in Tore Supra
Fusion Engineering and Design, vol.56-57 (2001) p.761-765
F. Saint-Laurent, G. Martin

[125] Remote participation at JET from DRFC Cadarache
Fusion Engineering and Design, vol.56-57 (2001) p.1057-1061
J. How, A. Maas, J.M. Theis, Y. Buravand, X. Litaudon

[126] Report on the 7th European Fusion Physics Workshop, Kloster Seeon, Germany, 8-10 December 1999
Plasma Physics and Controlled Fusion, vol. 43 (2001) p.603-628
D. Campbell, R. Buttery, C. Challis, S. Günter, F. Nguyen

[127] Response to "comment on the hurst exponent and long time correlation" [Phys. Plasmas 7, 5267 (2000)
Physics of Plasmas, vol.7 n°12 (2000) p.5269-5271
G. Antar, P. Devynck, Guiding Wang

[128] RF current drive by electron cyclotron waves in the presence of magnetic islands
Plasma Physics and Controlled Fusion, vol.42 (2000) p.755-769
P. Da Silva Rosa, G. Giruzzi

[129] Risks and benefits of incoloy 908
Fusion Engineering and Design, vol.58-59 (2001) p.129-134
P. Libeyre, C. Brosset, P. Decool, M. Rubino, G. Bevilacqua, A. Laurenti, P. Pesenti, M. Ursuleac, N. Valle, A. Nyilas

[130] Self-shadowing, gaps and leading edges on Tore Supra's inner first wall
Journal of Nuclear Materials, vol.290-293 (2001) p.1036-1039
R. Mitteau, Ph. Chappuis, Ph. Ghendrih, A. Grosman, D. Guilhem, J. Gunn, J.T. Hogan, M. Lipa, G. Martin, J. Schlosser, E. Tsitrone

[131] Shear effect on the radial profile of fluctuations measured by a reciprocating Langmuir probe in Tore Supra
Plasma Physics and Controlled Fusion, vol.42 (2000) p.327-335
P. Devynck, G. Antar, Guiding Wang, X. Garbet, J. Gunn, J.Y. Pascal

[132] Spectral profile analysis of the Dalpha line in the divertor region of Tore Supra
Journal of Nuclear Materials, vol.290-293 (2001) p.854-858
Escarguel, R. Guirlet, A. Azeroual, B. Pegourie, J. Gunn, T. Loarer, H. Capes, Y. Corre, C. De Michelis, L. Godbert-mouret, M. Koubiti, M. Mattioli, R. Stamm

[133] Spectroscopic study of neon emission and retention in the Tore Supra ergodic divertor
Journal of Nuclear Materials, vol.290-293 (2001) p.872-876
R. Guirlet, J.T. Hogan, Y. Corre, C. De Michelis, A. Escarguel, W.R. Hess, P. Monier-Garbet, B. Schunke

[134] Spectrum of coherent structures in a turbulent environment
Physical Review Letters, vol.84 n°21 (2000) p.4854-4857
F. Spineanu, M. Vlad

[135] Steady state operation and control experiments on Tore Supra
Nuclear Fusion, vol.40, n°6 (2000) p.1047-1055
X. Tore supra team, F. Saint-Laurent

[136] Studies of suprathermal electron loss in the magnetic ripple of Tore Supra
Nuclear Fusion, vol.41 n°5 (2001) p.477-485
V. Basiuk, Y. Peysson, M. Lipa, G. Martin, M. Chantant, D. Guilhem, F. Imbeaux, R. Mitteau, F. Surle

[137] Superadiabatic behavior of fast particles accelerated by ion cyclotron resonance heating
Physics of Plasmas, vol.8 n°1 (2001) p.139-145
V. Bergeaud, F. Nguyen, A. Becoulet, L.G. Eriksson

[138] Suppression of runaway electron avalanches by radial diffusion
Physics of Plasmas, vol.7 n°10 (2000) p.4106-4111
P. Helander, L.G. Eriksson, F. Andersson

[139] Sustained fully non-inductive scenarios using pressure and current profile control with ECCD
Fusion Engineering and Design, vol. 53 (2001) p.289-299
O. Sauter, T. Goodman, S. Coda, M. Henderson, F. Hofmann, J. Hogge, Y. Peysson, Z. Pietrzyk, R. Pitts, H. Reimerdes, H. Weisen

[140] Synchrotron radiation loss in tokamaks of arbitrary geometry
Nuclear Fusion, vol.41 n°12 (2001) p.1755-1758
I. Fidone, G. Giruzzi, G. Granata

[141] Technical issues associated with the control of steady state tokamaks
Nuclear Fusion, vol. 40, n°6 (2000) p.1167-1181
J. Lister, P. Bruzzone, A. Costley, T. Fukuda, Y. Gribov, V. Mertens, D. Moreau, T. Oikawa, R. Pitts, A. Portone, G. Vayakis, J. Wesley, R. Yoshino

[142] Ten years of maintenance on Tore Supra actively cooled components
Fusion Engineering and Design, vol.51-52 (2000) p.949-954
J.J. Cordier, M. Chantant, Ph. Chappuis, A. Durocher

[143] Test of an extruder feed system on the Tore Supra centrifugal pellet injector
Fusion Engineering and Design, vol.58-59 (2001) p.337-341
A. Geraud, J.F. Artaud, G. Gros, C. Pocheau, S. Combs, C. Foust

[144] Test program preparations of the ITER toroïdal field model coil (TFMC)
Fusion Engineering and Design, vol.58-59 (2001) p.147-151
J.L. Duchateau, H. Fillunger, S. Fink, R. Heller, P. Hertout, P. Libeyre, R. Maix, C. Marinucci, A. Martinez, R. Meyder, S. Nicollet, S. Raff, M. Ricci, L. Savoldi, A. Ulbricht, F. Wüchner, G. Zahn, R. Zanino

[145] The 118 GHz ECRH experiment on Tore Supra
Fusion Engineering and Design, vol.56-57 (2001) p.605-609
C. Darbos, R. Magne, S. Alberti, A. Barbuti, G. Berger-By, F. Bouquey, P. Cara, J. Clary, L. Courtois, R. Dumont, E. Giguet, D. Gil, G. Giruzzi, M. Jung, Y. Le Goff, F. Legrand, M. Lennholm, C. Liévin, Y. Peysson, D. Roux, M. Thumm, T. Wagner, M. Tran, X.L. Zou

[146] The acquisition system for Tore Supra 1000 s discharges
Fusion Engineering and Design, vol.48 (2000) p.155-161
J. How, B. Guillerminet, X. Tore supra team

[147] The Cadarache 1 MV porcelain SINGAP bushing
Fusion Engineering and Design, vol.56-57 (2001) p.539-544
P. Massmann, H. De esch, R. Hemsworth, T. Inoue, L. Svensson

[148] The Hurst exponent and long-time correlation
Physics of Plasmas, vol.7 n°4 (2000) p.1181-1183
Guiding Wang, G. Antar, P. Devynck

[149] The influence of non-standard orbits on the ICRH power deposition in tokamaks
Nuclear Fusion, vol.40 n°11 (2000) p.1819-1824
J. Hedin, T. Hellsten, L.G. Eriksson

[150] The international multi-tokamak profile database
Nuclear Fusion, vol.40 n°12 (2000) p.1955-1981
D. Boucher, J. Connor, W.A. Houlberg, M. Turner, G. Bracco, A. Chudnovskiy, G. Cordey, M. Greenwald, G.T. Hoang, X. Et al.

[151] The Tore Supra cryoplant control system upgrade
Fusion Engineering and Design, vol.58-59 (2001) p.217-223
R. Garbil, J.L. Marechal, B. Gravil, D. Henry, J.Y. Journeaux, D. Balaguer, J. Baudet, A. Bocquillon, P. Fejoz, P. Prochet, C. Roux, J.P. Serries

[152] The Tore Supra LHCD control system : new improvements using PLCs and state machines
Fusion Engineering and Design, vol.56-57 (2001) p.767-771
J.Y. Journeaux, Ph. Froissard, F. Kazarian, P. Pastor, J. Baudet

[153] Thermography of target plates with near-infrared optical fibres at Tore Supra
Journal of Nuclear Materials, vol.290-293 (2001) p.701-705
R. Reichle, V. Basiuk, V. Bergeaud, A. Cambe, M. Chantant, E. Delchambre, M. Druetta, E. Gauthier, W.R. Hess, C. Pocheau

[154] Tore Supra divertor screening efficiency during density regime experiments
Journal of Nuclear Materials, vol. 290-293 (2001) p.863-866
C. Grisolia, Ph. Ghendrih, J. Gunn, T. Loarer, P. Monier-Garbet, C. De Michelis, L. Costanzo, J.Y. Pascal

[155] Tore Supra steady state power and particles injection : the "CIMES" project
Fusion Engineering and Design, vol.56-57 (2001) p.667-672
B. Beaumont, A. Becoulet, Ph. Bibet, C. Darbos, P. Garin, A. Geraud, G. Giruzzi, A. Grosman, G. Martin, M. Ottaviani, Y. Peysson, B. Saoutic, P. Stott, M. Zabiego

[156] Toward steady-state operation of a large tokamak: the Tore Supra experience
Fusion Engineering and Design, vol.51-52 (2000) p.1007-1013
G. Martin

[157] Transport due to front propagation in tokamaks
Physics of Plasmas, vol.7 n°4 (2000) p.1085-1088
Y. Sarazin, X. Garbet, Ph. Ghendrih, S. Benkadda

[158] Trapped-ion driven turbulence in tokamak plasmas
Plasma Physics and Controlled Fusion, vol.42 (2000) p.949-971
G. Dépret, X. Garbet, P. Bertrand, A. Ghizzo

[159] Turbulence in Fusion Plasmas: Key Issues and Impact on Transport Modelling
Plasma Physics and Controlled Fusion, vol.43 (2001) p.A251-A266
X. Garbet

[160] Turbulence intermittency and bursts properties in tokamak scrape-off layer
Physics of Plasmas, vol.8 n°5 (2001) p.1612-1624
G. Antar, P. Devynck, X. Garbet, S. Luckhardt

[161] Turbulence reduction and poloidal shear steepening in reversed shear plasmas investigated by light scattering on Tore Supra
Physics of Plasmas, vol.8 n°1 (2001) p.186-192
G. Antar, G.T. Hoang, P. Devynck, X. Garbet, C. Laviron, M. Goniche

[162] Ultrafast frequency sweep heterodyne reflectometer on the Tore Supra tokamak
Review of Scientific Instruments, vol.71 n°1 (2000) p.74-81
P. Moreau, F. Clairet, J.M. Chareau, M. Paume, C. Laviron

[163] X-mode heterodyne reflectometer for edge density profile measurements on Tore Supra
Review of Scientific Instruments, vol.72 n°1 (2001) p.340-343
F. Clairet, R. Sabot, C. Bottereau, J.M. Chareau, M. Paume, S. Heuraux, M. Colin, S. Hacquin, G. Leclert

IX.5.2. Conference communications

[164] 1D simulations of current profile control in purely non-inductive discharges for the Tore Supra CIEL project
27th EPS Conf. on Controlled Fusion and Plasma Physics
F. Imbeaux, I. Voitsekhovitch, V. Basiuk, A. Becoulet, G. Giruzzi, Y. Peysson

[165] A 70 keV neutral hydrogen beam injector with energy recovery for an MSE diagnostic application in fusion research
2001 Particle Accelerator Conference
A. Simonin, A. Armitano, R. Brugnetti, V. Cano, H. Dougnac, Ph. Fazilleau

[166] A high speed fibre communication link for measurement & I/O (M&IO-Net)
21st Symposium On Fusion Technology
P. Spuig, B. Couturier

[167] A hybrid edge-core (3D / 1D) model for impurity transport in Tore Supra ergodic divertor discharges
28th EPS Conference on Controlled Fusion and Plasma Physics
B. Schunke, J.T. Hogan, C. De Michelis, W.R. Hess, M. Mattioli, J.C. Vallet

[168] A new internal matching impedance concept for ICRF antennas
21st Symposium On Fusion Technology
S. Bremond, G. Agarici, B. Beaumont, J.P. Chenevois

[169] Acceleration of energetic ions during reconnection in MAST
7th IAEA TCM on Energetic Particles in Magnetic Confinement Systems
P. Helander, R. Akers, C. Byrom, L.G. Eriksson, C. Gimblett, M. Tournianski

[170] Active cooling, calorimetry and energy balance in Tore Supra
14th Int. Conf. on Plasma Surface Interaction in Controlled Fusion Devices
J.C. Vallet, R. Reichle, M. Chantant, V. Basiuk, R. Mitteau, X. Tore supra team

[171] Actively cooled plasma facing components in Tore Supra
21st Symposium On Fusion Technology
P. Garin, X. Tore supra team

[172] Advances in thermal imaging
Int. Conf. on Advanced Diagnostics for Magnetic and Inertial Fusion
R. Reichle, D. Guilhem, C. Balorin, E. Delchambre, C. Desgranges, L. Ducobu, M. Jouve, M. Lipa, P. Messina, R. Mitteau, D. Moulin, C. Pocheau, H. Roche, A. Saille, Z. Wang, G. Zhuang

[173] Alpha particle physics studies on JET with ICRH-accelerated 4He beams ions
7th IAEA TCM on Energetic Particles in Magnetic Confinement Systems
M. Mantsinen, L.G. Eriksson, F. Nguyen, X. Et al.

[174] Alternative Schemes of power deposition with the Ergodic Divertor on Tore Supra
14th Int. Conf. on Plasma Surface Interaction in Controlled Fusion Devices
G. Mank, Ph. Ghendrih, C. Grisolia, J. Gunn, T. Loarer, P. Monier-Garbet, L. Costanzo, K. Finken, C. De Michelis, R. Reichle

[175] Analysis of an in-service rupture of the inner first wall of Tore Supra
21st Symposium On Fusion Technology
R. Mitteau, Ph. Chappuis, G. Martin, S. Rosanvallon

[176] Analysis of energy flux deposition during ergodic divertor operation on Tore Supra
14th Int. Conf. on Plasma Surface Interaction in Controlled Fusion Devices
L. Costanzo, J. Gunn, T. Loarer, L. Colas, Y. Corre, Ph. Ghendrih, C. Grisolia, A. Grosman, D. Guilhem, P. Monier-Garbet, R. Reichle, H. Roche, J.C. Vallet

[177] Analysis of ion cyclotron current drive at **~2**cH for sawtooth control in JET plasmas
28th EPS Conference on Controlled Fusion and Plasma Physics
M. Mantsinen, M. Mayoral, L.G. Eriksson, F. Nguyen, X. Et al.

[178] Analysis of plasma edge profiles at JET
28th EPS Conference on Controlled Fusion and Plasma Physics
M. Beurskens, J. Gunn, J.M. Chareau, X. Et al.

[179] Analytical Calculation of Current Drive Synergy between LH and EC Waves
14th Topical Conference on Radio Frequency Power in Plasmas
R. Dumont, G. Giruzzi

[180] Assembly in the Test Facility, Acceptance and First Test Results of the ITER TF Model Coil
17th International Conference on Magnet Technology
R. Maix, H. Fillunger, F. Hurd, E. Salpietro, D. Ciazynski, J.L. Duchateau, P. Libeyre, A. Martinez, E. Bobrov, W. Herz, V. Marchese, M. Süsser, A. Ulbricht, F. Wüchner, G. Zahn, A. Della corte, M. Ricci, E. Theisen, G. Kraft, A. Bourquard, F. Beaudet, B. Schellong, R. Zanino, L. Savoldi

[181] Assessment of impurity control by the ergodic divertor on Tore Supra
28th EPS Conference on Controlled Fusion and Plasma Physics
P. Monier-Garbet, C. Clement, Y. Corre, C. De Michelis, A. Escarguel, Ph. Ghendrih, A. Grosman, C. Grisolia, R. Guirlet, J. Gunn, T. Loarer, B. Pegourie

[182] Assessment of impurity control by the ergodic divertor on Tore Supra
IAEA/TCM on Divertor Concepts
P. Monier-Garbet, C. Clement, Y. Corre, C. De Michelis, A. Escarguel, Ph. Ghendrih, A. Grosman, C. Grisolia, R. Guirlet, J. Gunn, T. Loarer, B. Pegourie

[183] Beam afterglow scenario for TAE excitation in optimised shear JET plasmas
28th EPS Conference on Controlled Fusion and Plasma Physics
S. Sharapov, C. Giroud, X. Et al.

[184] Biasing experiments on TEXTOR-94
4th Electric Workshop on Role of Electric Field in Plasma Confinement and Exhaus
T. Loarer, J. Gunn, J. Lachambre, G. Mank, C. Boucher, K. Finken, S. Jachmich, M. Lehnen, H. Van goubergen, G. Van oost

[185] Bursty transport in tokamaks with internal transport barriers
18th IAEA Fusion Energy Conference
S. Benkadda, O. Agullo, P. Beyer, N. Bian, P. Diamond, C. Figarella, X. Garbet, Ph. Ghendrih, V. Grandgirard, Y. Sarazin

[186] Calculations of NTM stabilization in ITER-FEAT by ECCD with realistic antenna geometry
14th Topical Conference on Radio Frequency Power in Plasmas
G. Ramponi, G. Giruzzi, S. Nowak, E. Lazzaro, G. Bosia

[187] Calculations of pressure drop and mass flow repartition related to the Toroidal Field Moddel Coil of the ITER project
Wks on Computation of Thermo-Hydraulic Transients in Superconductors
S. Nicollet, J.L. Duchateau, H. Fillunger, A. Martinez

[188] Characterisation of internal transport barriers in JET and simulations of control algorithms
28th EPS Conference on Controlled Fusion and Plasma Physics
G. Tresset, D. Moreau, X. Litaudon, C. Challis, X. Garbet, E. Joffrin, D. Mazon, X. The jet-efda team

[189] Characterisation of the separatrix position in the ergodic divertor discharges of the Tore Supra tokamak
14th Int. Conf. on Plasma Surface Interaction in Controlled Fusion Devices
M. Zabiego, Ph. Ghendrih, M. Becoulet, L. Costanzo, C. De Michelis, C. Friant, J. Gunn

[190] Characterization of radiation and flux measurements on a neutraliser plate of the Tore Supra ergodic divertor
14th Int. Conf. on Plasma Surface Interaction in Controlled Fusion Devices
Y. Corre, R. Giannella, R. Guirlet, A. Azeroual, E. Chareyre, L. Costanzo, C. De Michelis, A. Escarguel, E. Gauthier, Ph. Ghendrih, J. Gunn, J.T. Hogan, P. Monier-Garbet, B. Pegourie, E. Tsitrone

[191] Characterization of the 118 GHz ECRH output beam on Tore Supra
SPIE's 45th Annual Meeting : the International Symposium on Optical Science and
L. Courtois, R. Magne, A. Becoulet, S. Tedjini, D. Roux, C. Desgranges, C. Liévin, J. Achard, A. Barbuti, G. Berger-By, F. Bouquey, J. Clary, C. Darbos, F. Legrand, M. Lennholm, P. Messina, H. Roche

[192] Characterization of transport properties variations with magnetic field and temperature of ITER-candidate NbTi strands
5th European Conference of Applied Superconductivity
L. Zani, J.P. Serries, H. Cloez, Z. Bej, E. Mossang

[193] CIEL in Tore Supra : how to master power and particles on very long discharges
10th International Toki Conference on Plasma Physics and Controlled Nuclear Fusi
P. Garin, X. Tore supra team

[194] Cold pulse propagation experiments in ITB plasmas of JET
28th EPS Conference on Controlled Fusion and Plasma Physics
P. Mantica, Y. Sarazin, X. Et al

[195] Comparison of FWCD scenarios on ASDEX-Upgrade, JET, and DIII-D Tokamaks
14th Topical Conference on Radio Frequency Power in Plasmas
F. Meo, M. Brambilla, R. Bilato, J. Noterdaeme, C. Petty, F. Nguyen

[196] Comparison of L-mode regimes with enhanced confinement by impurity seeding in JET and DIII-D
28th EPS Conference on Controlled Fusion and Plasma Physics
G. Jackson, E. Joffrin, P. Monier-Garbet, X. Et al.

[197] Comparison of theory with rotation measurements in JET ICRH plasmas
28th EPS Conference on Controlled Fusion and Plasma Physics
R. Budny, C. Giroud, X. Et al.

[198] Completion of the ITER toroïdal field model coil (TFMC)
21st Symposium On Fusion Technology
R. Maix, H. Fillunger, F. Hurd, E. Salpietro, N. Mitchell, P. Libeyre, P. Decool, A. Ulbricht, G. Zahn, D. Bresson, A. Bourquard, J. Baudet, B. Schellong, E. Theisen, N. Valle

[199] Conductor Analysis of the ITER FEAT Poloidal Field Coils during a Plasma Scenario
2001 Cryogenic Engineering Conf. & Intern. Cryogenic Materials Conference
S. Nicollet, P. Hertout, J.L. Duchateau, A. Bleyer, D. Bessette

[200] Confinement and transport studies of conventional scenarios in ASDEX Upgrade
18th IAEA Fusion Energy Conference
F. Ryter, J. Stober, A. Stäbler, G. Tardini, U. Fahrbach, O. Gruber, A. Herrmann, F. Imbeaux, A. Kallenbach, M. Kaufmann, B. Kurzan, F. Leuterer, M. Maraschek, H. Meister, A. Peeters, G. Pereverzev, A. Sips, W. Suttrop, W. Treutterer, H. Zohm, X. Asdex upgrade team

[201] Confinement properties of high density impurity seeded ELMY H-mode discharges at low and high triangularity on JET
28th EPS Conference on Controlled Fusion and Plasma Physics
P. Dumortier, P. Monier-Garbet, X. Et al.

[202] Consistency check of Zeff measurements in ergodic divertor plasmas on Tore Supra
14th Int. Conf. on Plasma Surface Interaction in Controlled Fusion Devices
B. Schunke, C. De Michelis, R. Guirlet, P. Monier-Garbet, M. Mattioli, E. Chareyre, O. Meyer

[203] Control of divertor geometry and performance with the Ergodic Divertor of Tore Supra
14th Int. Conf. on Plasma Surface Interaction in Controlled Fusion Devices
Ph. Ghendrih, M. Becoulet, L. Costanzo, C. Grisolia, A. Grosman, R. Guirlet, J. Gunn, T. Loarer, P. Monier-Garbet, G. Mank, B. Pegourie, R. Reichle, J.C. Vallet, M. Zabiego, C. De Michelis, K. Finken, J.T. Hogan, F. Laugier, F. Nguyen, F. Saint-Laurent, B. Schunke, X. Tore supra team

[204] Control of edge electric field and flows in the CASTOR tokamak
ICCP2000_Int. Congress on Plasma Physics/42nd APS
J. Stöckel, J. Gunn, M. Hron, K. Dyabilin, J. Horacek, S. Nanobashvili, G. Van oost, F. Zacek

[205] Core and edge confinement studies with different heating methods in JET
18th IAEA Fusion Energy Conference
The JET team, F. Rimini, G. Saibene

[206] Correlation between magnetic shear and ExB flow shearing rate in JET ITB discharges
28th EPS Conference on Controlled Fusion and Plasma Physics
B. Esposito, P. Maget, A. Becoulet, C. Giroud, X. Et al

[207] Coupling and power handling of the new Tore Supra LHCD launcher
21st Symposium On Fusion Technology
Ph. Bibet, A. Ekedahl, Ph. Froissard, F. Kazarian, E. Bertrand, S. Dutheil-hertout, L. Tanaskovic

[208] Current distribution and strain influence on the electromagnetic performance of the CS insert
ASC2000 Applied Superconductivity Conference
V. Galindo, D. Ciazynski, J.L. Duchateau, G. Nishijima, N. Koizumi, Y. Takahashi, T. Ando

[209] Density fluctuations at high density in the Ergodic Divertor configuration of Tore Supra
14th Int. Conf. on Plasma Surface Interaction in Controlled Fusion Devices
P. Devynck, J. Gunn, Ph. Ghendrih, X. Garbet, G. Antar, P. Beyer, C. Boucher, C. Honoré, F. Gervais, P. Hennequin, A. Quéméneur, A. Truc

[210] Dependence of divertor helium pressure on power, geometry and confinement mode in JET
ICCP2000_Int. Congress on Plasma Physics/42nd APS
C. Grisolia, D. Hillis, J.T. Hogan, W. Fundamenski, J. Spence, G. Corrigan, P. Morgan, G. Matthews, V. Philipps

[211] Design criteria for Tore Supra high heat flux components
21st Symposium On Fusion Technology
M. Missirlian, J. Schlosser, M. Lipa, R. Mitteau, Ph. Chappuis, C. Portafaix

[212] Design of an improved vacuum vessel protection for very long pulse operation in Tore Supra
21st Symposium On Fusion Technology
M. Lipa, B. Cantone, P. Garin, R. Mitteau, C. Portafaix

[213] Design of next step tokamak : consistent analysis of plasma flux consumption and poloidal field system
18th IAEA Fusion Energy Conference
J.M. Ané, V. Grandgirard, F. Albajar, J. Johner

[214] Detachment control by heat flux analysis on Tore Supra
28th EPS Conference on Controlled Fusion and Plasma Physics
L. Costanzo, T. Loarer, B. Pegourie, E. Gauthier, Ph. Ghendrih, D. Guilhem, J. Gunn, P. Monier-Garbet, H. Roche

[215] Development and application of European high power CW gyrotrons for ECRH experiments
1st IEEE Internat. Vacuum Electronics Conference
R. Magne, C. Darbos, S. Alberti, A. Barbuti, F. Blanchard, P. Cara, J. Clary, C. Dubrovin, E. Giguet, D. Gil, J. Hogge, G. Le cloarec, Y. Le Goff, F. Legrand, C. Liévin, D. Roux, M. Thumm, M. Tran

[216] Development of actively cooled components for theTore Supra toroidal pump limiter
9th International Workshop on CARBON MATERIALS
J. Schlosser, Ph. Chappuis, A. Durocher, L. Moncel, P. Garin

[217] Development of the IR interfero-polarimeter for long pulse operation at Tore Supra
21st Symposium On Fusion Technology
C. Gil, D. Elbeze, C. Portafaix

[218] Development of tungsten coating for fusion applications
21st Symposium On Fusion Technology
A. Cambe, E. Gauthier, J. Layet, S. Bentivegna

[219] Diagnostic development for steady-state high power operation
10th International Toki Conference on Plasma Physics and Controlled Nuclear Fusi
C. Laviron

[220] Direct measurements of E X B flow and its impact on edge turbulence in the CASTOR Tokamak using an optimized gundestrup probe
4th Electric Workshop on Role of Electric Field in Plasma Confinement and Exhaus
J. Gunn, J. Stöckel, J. Adamek, I. Duran, J. Horacek, M. Hron, K. Jakubka, L. Kryska, F. Zacek, G. Van oost

[221] Direct measurements of EXB flow and its impact on edge turbulence in the Castor tokamak
28th EPS Conference on Controlled Fusion and Plasma Physics
G. Van oost, J. Stöckel, J. Gunn, J. Adamek, I. Duran, J. Horacek, M. Hron, K. Jakubka, L. Kryska, F. Zacek

[222] Dual Channel Cable in Conduit Thermohydraulics : Analysis of the European Full Size Joint Samples Test Results
18th International Cryogenic Engineering Conference
A. Martinez, J.L. Duchateau, P. Decool, S. Nicollet

[223] Dust characterization and analysis in Tore Supra
14th Int. Conf. on Plasma Surface Interaction in Controlled Fusion Devices
Ph. Chappuis, E. Tsitrone, M. Mayne, X. Armand, J. Linke, H. Bolt, D. Petti, J. Sharpe

[224] Dynamics of chaotic magnetic lines : intermittency and "noble" internal transport barriers in the Tokamap
7th EU-US Transport Task Force Workshop
J.H. Misguich, J.D. Reuss, B. Weyssow, R. Balescu, D. Constantinescu, G. Steinbrecher, F. Spineanu, M. Vlad

[225] Dynamics of chaotic magnetic lines : intermittency and noble ITB's in the Tokamap
ICCP2000_Int. Congress on Plasma Physics/42nd APS
J.H. Misguich

[226] Dynamics of ITB perturbation due to large ELMs in JET
27th EPS Conf. on Controlled Fusion and Plasma Physics
Y. Sarazin, P. Beyer, C. Challis, X. Garbet, Ph. Ghendrih, E. Joffrin, P. Lomas, V.V. Parail, G. Saibene, R. Sartori

[227] ECR and ICRF conditioning discharges comparison in TEXTOR-94
28th EPS Conference on Controlled Fusion and Plasma Physics
E. Gauthier, A. Lyssoivan, H. Esser, M. Freisinger, F. Hoekzema, P. Hettemann, J. Ihde, R. Koch, V. Philipps, H. Reimer, M. Vervier, E. Westerhof, R. Weynants

[228] ECRH experiments and developments for long pulse in Tore Supra
18th IAEA Fusion Energy Conference
G. Giruzzi, C. Darbos, R. Dumont, R. Magne, Y. Peysson, X.L. Zou, F. Bouquey, L. Courtois, G.T. Hoang, F. Imbeaux, X. Litaudon, P. Moreau, A. Pecquet, J.L. Segui, M. Zabiego, X. Tore supra team

[229] Eddy current and thermal analysis of the TF Model Coil during safety discharges
ASC2000 Applied Superconductivity Conference
P. Hertout, J.L. Duchateau, A. Martinez

[230] Edge fast magnetic measurements during ELMs of different types on JET
IAEA/TCM on Divertor Concepts
M. Becoulet, A. Loarte, G. Saibene, R. Sartori, B. Alper, G. Matthews, S. Sharapov, P. Hennequin, Ph. Ghendrih, G. Huysmans

[231] Edge flow measurements with gundestrup probes
ICCP2000_Int. Congress on Plasma Physics/42nd APS
J. Gunn, C. Boucher, P. Devynck, K. Dyabilin, J. Horacek, M. Hron, J. Stöckel, G. Van oost, H. Van goubergen, F. Zacek

[232] Edge operational space for high density/high coninement ELMY H-modes in JET
28th EPS Conference on Controlled Fusion and Plasma Physics
R. Sartori, M. Becoulet, X. Et al.

[233] Effect of internal flux shaping in JET transport barrier
28th EPS Conference on Controlled Fusion and Plasma Physics
O. Tudisco, E. Joffrin, F. Rimini, A. Becoulet, C. Giroud, X. Et al.

[234] Effect of limiter recycling on measured poloidal impurity emission profiles in Tore Supra
14th Int. Conf. on Plasma Surface Interaction in Controlled Fusion Devices
J.T. Hogan, C. De Michelis, P. Monier-Garbet, M. Becoulet, Charles E. Bush, Ph. Ghendrih, R. Guirlet, W.R. Hess, M. Mattioli, J.C. Vallet

[235] Effect of toroidicity and temperature profiles on synchrotron losses in a tokamak plasma
27th EPS Conf. on Controlled Fusion and Plasma Physics
F. Albajar, J. Johner, G. Granata, J. Villar colome, J. Dies

[236] Effects of finite drift orbit width and RF-induced spatial transport on plasmas heated by ICRH
14th Topical Conference on Radio Frequency Power in Plasmas
T. Hellsten, J. Hedin, J. Carlsson, L.G. Eriksson, T. Johnson, M. Laxaback, M. Mantsinen

[237] Electrical and thermal designs and analyses of joints of the ITER PF coils.
17th International Conference on Magnet Technology
D. Ciazynski, A. Martinez

[238] Electromagnetic evaluation of the collective behaviour of 720 twisted strands for the TF model coil experiment
ASC2000 Applied Superconductivity Conference
J.L. Duchateau, D. Ciazynski, P. Hertout, M. Spadoni, W. Specking

[239] Electron heated internal transport barriers in JET
28th EPS Conference on Controlled Fusion and Plasma Physics
G. Hogeweij, X. Litaudon, X. Et al.

[240] Electron transport analysis using a wide database of hot electron plsmas on Tore Supra
7th EU-US Transport Task Force Workshop
T. Aniel, G.T. Hoang, Y. Peysson, F. Imbeaux, M. Ottaviani, W. Horton, P. Zhu

[241] Electron transport and improved confinement on Tore Supra
18th IAEA Fusion Energy Conference
G.T. Hoang, C. Bourdelle, X. Garbet, T. Aniel, G. Giruzzi, M. Ottaviani, W. Horton, P. Zhu, R. Budny

[242] Electron transport in Tore Supra with Lower Hybrid Current Drive
43rd APS Conference
F. Imbeaux, G.T. Hoang, M. Ottaviani, Y. Peysson, X. Garbet, W. Horton, C. Crabtree, P. Zhu

[243] Electrostatic turbulence with finite parallel correlation length and radial electric field generation
18th IAEA Fusion Energy Conference
M. Vlad, F. Spineanu, J.H. Misguich, R. Balescu

[244] ELM moderation in high density H-modes on JET and Alcator C-Mod
28th EPS Conference on Controlled Fusion and Plasma Physics
G. Maddison, J.M. Chareau, X. Et al.

[245] ELMs Behaviour and edge plasma stability in JET
8th IAEA Technical Committee Meeting on H-Mode Physics and Transport Barriers
M. Becoulet, G. Huysmans, E. Joffrin, Y. Sarazin, X. Litaudon, A. Becoulet, Ph. Ghendrih, X. The jet-efda Team

[246] Equilibrium reconstruction of Tokamak discharges with anisotropic pressure
27th EPS Conf. on Controlled Fusion and Plasma Physics
W. Zwingmann, P. Stubberfield

[247] Ergodic divertor effect on low Z impurity transport for inner wall limited plasmas in Tore Supra
IAEA/TCM on Divertor Concepts
J.T. Hogan, C. De Michelis, P. Monier-Garbet, Y. Corre, R. Guirlet

[248] Ergodic divertor experiments in Tore Supra above the Greenwald density limit with ICRF power at low magnetic field
27th EPS Conf. on Controlled Fusion and Plasma Physics
F. Nguyen, Ph. Ghendrih, V. Basiuk, L. Colas, T. Aniel, P. Monier-Garbet, C. De Michelis

[249] Ergodic divertor experiments on the route to steady state operation of Tore Supra
18th IAEA Fusion Energy Conference
Ph. Ghendrih, X. Tore supra team

[250] Etude de l'érosion des composants face au plasma dans Tore Supra, par interférométrie de speckle
Colloque : "Méthodes et Techniques Optiques pour l'Industrie"
G. Roupillard, E. Gauthier, V. Chalvidan

[251] Evaluations and prospects for the next steps in the low power RF systems of the Tore Supra transmitters
21st Symposium On Fusion Technology
G. Berger-By, J. Achard, B. Beaumont, Ph. Bibet, S. Dutheil-hertout, M. Goniche, G. Lombard, L. Millon, C. Mollard, K. Vulliez

[252] Evolution of turbulent transport during the formation of internal transport barrier in tokamak
27th EPS Conf. on Controlled Fusion and Plasma Physics
P. Beyer, C. Figarella, I. Voitsekhovitch, S. Benkadda

[253] Experience feedback from high heat flux component manufacturing for Tore Supra
21st Symposium On Fusion Technology
J. Schlosser, A. Durocher, T. Huber, P. Garin, B. Schedler, G. Agarici

[254] Experimental evidence for RF-induced transport of resonant 3He ions in JET
7th IAEA TCM on Energetic Particles in Magnetic Confinement Systems
T. Johnson, F. Nguyen, X. Et al.

[255] Experimental studies of electron transport
28th EPS Conference on Controlled Fusion and Plasma Physics
F. Ryter, F. Imbeaux, G.T. Hoang, X. Et al.

[256] Experiments on helium enrichment and removal at JET
28th EPS Conference on Controlled Fusion and Plasma Physics
K. Finken, T. Loarer, X. Et al.

[257] Extrapolation of the Ergodic Divertor to a Next Step tokamak
28th EPS Conference on Controlled Fusion and Plasma Physics
A. Grosman, J.M. Ané, P. Barabaschi, K. Finken, Ph. Ghendrih, M. Lipa, P. Thomas

[258] Extreme shear reversal in JET discharges
28th EPS Conference on Controlled Fusion and Plasma Physics
N. Hawkes, C. Giroud, E. Joffrin, Ph. Lotte, D. Mazon, G. Tresset, X. Et al.

[259] Fast electron dynamics in the Tore Supra plasma edge
27th EPS Conf. on Controlled Fusion and Plasma Physics
G. Martin, R. Mitteau, Y. Peysson

[260] Feedback control achievements and endeavours in Tore Supra plasma wall interactions control
10th International Toki Conference on Plasma Physics and Controlled Nuclear Fusi
A. Grosman, Ph. Ghendrih, C. Grisolia, J. Gunn, T. Loarer, P. Monier-Garbet, X. Tore supra team,

[261] Feedback control of drift waves turbulence and chaos
27th EPS Conf. on Controlled Fusion and Plasma Physics
C. Figarella, S. Benkadda, P. Beyer, P. Gabbai, A. Sen, X. Garbet

[262] Feedback control on edge plasma parameters with ergodic divertor in Tore Supra
14th Int. Conf. on Plasma Surface Interaction in Controlled Fusion Devices
J. Bucalossi, J. Gunn, A. Geraud, Ph. Ghendrih, C. Grisolia, A. Grosman, G. Martin, D. Moulin, J.Y. Pascal, F. Saint-Laurent

[263] First core poloidal flow velocity measurements in JET
28th EPS Conference on Controlled Fusion and Plasma Physics
F. Sattin, C. Giroud, X. Et al.

[264] First ECRH experiments in Tore Supra
27th EPS Conf. on Controlled Fusion and Plasma Physics
X.L. Zou, C. Darbos, R. Dumont, G. Giruzzi, R. Magne, Y. Peysson, G.T. Hoang, F. Imbeaux, X. Litaudon, P. Moreau, A. Pecquet, J.L. Segui, M. Zabiego

[265] First results of coupling and edge plasma interaction experiments with the new advanced LHCD launcher in Tore Supra
27th EPS Conf. on Controlled Fusion and Plasma Physics
A. Ekedahl, Ph. Bibet, B. Beaumont, E. Bertrand, S. Dutheil-hertout, Ph. Froissard, F. Kazarian, X. Litaudon, Y. Peysson, M. Goniche, R. Guirlet

[266] First Test Results for the ITER Central Solenoid Model Coil
18th IAEA Fusion Energy Conference
T. Kato, H. Tsuji, K. Arai, T. Ishigouoka, K. Okuno, N. Martovetsky, M. Ricci, R. Zanino, A. Martinez, G. Zahn, X. Et al.

[267] Formation condition of internal transport barrier
28th EPS Conference on Controlled Fusion and Plasma Physics
T. Fukuda, A. Becoulet, L.G. Eriksson, F. Imbeaux, P. Maget, T. Aniel, X. Garbet, G.T. Hoang, X. Litaudon, X. Et al.

[268] From 10 years experience with the Tore Supra ergodic divertor towards its implementation in a next step device
21st Symposium On Fusion Technology
A. Grosman, X. Tore supra team

[269] Global Simulations of Ion Turbulence with Magnetic Shear Reversal
Theory of Fusion Plasmas, Joint Varenna-Lausanne Int. Workshop
X. Garbet, C. Bourdelle, G.T. Hoang, P. Maget, S. Benkadda, P. Beyer, C. Figarella, I. Voitsekhovitch, O. Agullo

[270] Heat Deposition in the ITER FEAT Poloidal Field Coils during a Plasma Scenario.
17th International Conference on Magnet Technology
P. Hertout, D. Bessette, A. Bleyer, J.L. Duchateau, S. Nicollet

[271] Heat load patterns on Tore Supra ICRH antennas
27th EPS Conf. on Controlled Fusion and Plasma Physics
L. Colas, M. Becoulet, L. Costanzo, S. Pecoul, S. Heuraux, S. Bremond, C. Desgranges, A. Becoulet, Ph. Ghendrih

[272] High fusion performance in JET plasmas with highly negative central magnetic shear
28th EPS Conference on Controlled Fusion and Plasma Physics
C. Challis, A. Becoulet, C. Giroud, E. Joffrin, X. Litaudon, P. Maget, G. Tresset, X. Et al.

[273] High heat flux behaviour of damaged plasma facing components
21st Symposium On Fusion Technology
F. Escourbiac, Ph. Chappuis, J. Schlosser, M. Merola, I. Vastra, M. Febvre

[274] High power lower hybrid current drive experiments in Tore Supra tokamak
18th IAEA Fusion Energy Conference
Y. Peysson, X. Tore supra team

[275] High radiation from intrinsic and injected impurities in Tore Supra ergodic divertor plasmas
14th Int. Conf. on Plasma Surface Interaction in Controlled Fusion Devices
P. Monier-Garbet, C. De Michelis, Ph. Ghendrih, C. Grisolia, R. Guirlet, J. Gunn, T. Loarer, Charles E. Bush, C. Clement, Y. Corre, L. Costanzo, J.T. Hogan, B. Schunke, J.C. Vallet

[276] High-power CW gyrotron developments for ECRH systems
2nd IEEE International Vacuum Electronics Conference
E. Giguet, F. Bouquey, C. Darbos, M. Lennholm, R. Magne

[277] ICANT code : a tool to compute the characteristics of ICRH realistic antennae and their near fields
27th EPS Conf. on Controlled Fusion and Plasma Physics
S. Pecoul, S. Heuraux, R. Koch, G. Leclert, M. Becoulet, L. Colas

[278] ICRF current drive experiments on JET
28th EPS Conference on Controlled Fusion and Plasma Physics
F. Nguyen, J. Noterdaeme, M. Mayoral, L.G. Eriksson, Ph. Lotte, A.L. Pecquet, Y. Sarazin, M. Zabiego, X. Et al.

[279] ICRF heating scenarios in JET with emphasis on 4He plasmas for the non-activated phase of ITER
14th Topical Conference on Radio Frequency Power in Plasmas
M. Mantsinen, M. Mayoral, F. Rimini, J. Bucalossi, J.M. Chareau, L.G. Eriksson, F. Nguyen, X. Et al.

[280] ICRF mode conversion experiments on JET
28th EPS Conference on Controlled Fusion and Plasma Physics
M. Mantsinen, M. Mayoral, J. Bucalossi, F. Nguyen, F. Rimini, X. Et al.

[281] Impact of charge exchange neutrals on plasma facing components of Tore Supra
21st Symposium On Fusion Technology
E. Tsitrone, Ph. Chappuis, E. Gauthier, M. Lipa, D. Reiter

[282] Impact of different preheating methods on q-profile evolution in JET
28th EPS Conference on Controlled Fusion and Plasma Physics
T. Tala, A. Becoulet, X. Et al.

[283] Improvment of LH-power coupling on JET
28th EPS Conference on Controlled Fusion and Plasma Physics
Y. Sarazin, A. Ekedahl, F. Imbeaux, E. Joffrin, X. Litaudon, F. Rimini, X. Et al.

[284] Impurity behaviour in ITB discharges with reversed shear on JET
28th EPS Conference on Controlled Fusion and Plasma Physics
R. Dux, C. Giroud, X. Et al.

[285] Impurity penetration and contamination in Tore Supra ergodic divertor experiments
18th IAEA Fusion Energy Conference
R. Guirlet, J.T. Hogan, P. Monier-Garbet, Y. Corre, C. De Michelis, Ph. Ghendrih, R. Giannella, C. Grisolia, A. Grosman, J. Gunn, B. Schunke, X. Tore supra team

[286] Impurity radiation modulations in an ergodic divertor
14th Int. Conf. on Plasma Surface Interaction in Controlled Fusion Devices
F. Laugier, M. Becoulet, C. De Michelis, Ph. Ghendrih, J. Gunn, P. Monier-Garbet, R. Reichle, J.C. Vallet

[287] Influence of edge current profile on type III-type I ELMs transition in optimised shear discharges on JET
28th EPS Conference on Controlled Fusion and Plasma Physics
M. Becoulet, E. Joffrin, R. Sartori, P. Lomas, G. Saibene, V.V. Parail, Y. Sarazin, C. Challis, X. Litaudon, A. Becoulet, G. Matthews, Ph. Ghendrih, X. The jet-efda team

[288] Influence of electron heating on confinement in JET and ASDEX Upgrade internal transport barrier plasmas
28th EPS Conference on Controlled Fusion and Plasma Physics
R. Wolf, C. Giroud, D. Mazon, F. Rimini, X. Et al.

[289] Influence of minority ion concentration on the plasma rotation and the plasma performance in ICRH discharges on Tore Supra
14th Topical Conference on Radio Frequency Power in Plasmas
G.T. Hoang, L.G. Eriksson, V. Bergeaud, K. Strom sthal

[290] Interaction of ion cyclotron range of frequencies wave with energetic particles
27th EPS Conf. on Controlled Fusion and Plasma Physics
V. Bergeaud, L.G. Eriksson, A. Becoulet, F. Nguyen

[291] Interface quality control by infrared thermography measurement
15th World Conference on Non-Destructive Testing
A. Durocher, R. Mitteau, V. Paulus-martin, J. Schlosser

[292] Interplay of Kinetic and Transport Effects on RF Current Drive
14th Topical Conference on Radio Frequency Power in Plasmas
G. Giruzzi, R. Dumont

[293] Investigation of particle flows by limiter biasing on Textor-94
ICCP2000_Int. Congress on Plasma Physics/42nd APS
G. Mank, C. Boucher, E. Gravier, J. Gunn, T. Loarer, K. Finken, S. Jachmich, J. Lachambre, M. Lehnen, H. Van goubergen, G. Van oost

[294] Ion fluxes in the ergodic divertor of Tore Supra
28th EPS Conference on Controlled Fusion and Plasma Physics
J. Gunn, T. Loarer, P. Monier-Garbet, C. Boucher, C. Clement, Y. Corre, L. Costanzo, P. Devynck, C. De Michelis, A. Escarguel, Ph. Ghendrih, A. Grosman, R. Guirlet, J.Y. Pascal, B. Pegourie, B. Schunke, P. Thomas, J.C. Vallet

[295] IR reflectivity measurements depending on carbon film thickness
QIRT 2000 (5th Quantitative Infrared Thermography)
C. Desgranges, C. Balorin, J. Bucalossi, D. Garnier, D. Guilhem, P. Messina

[296] Issues related to current profile control and internal transport barriers in tokamaks
7th EU-US Transport Task Force Workshop
D. Moreau, I. Voitsekhovitch, X. Litaudon, G. Tresset, X. Garbet

[297] ITER TF Model Coil Assembly, Commissioning and Instrumentation
21st Symposium On Fusion Technology
F. Hurd, H. Fillunger, G. Zahn, A. Ulbricht, P. Libeyre, E. Theisen, F. Beaudet

[298] JAVA graphical User Interface for the supervision of Tore Supra
3rd IAEA TCM on Control, Data Acquisition, and Remote Participation for Fusion R
N. Utzel, B. Guillerminet, M. Le Luyer, D. Moulin

[299] JET and ASDEX Upgrade divertor modelling
28th EPS Conference on Controlled Fusion and Plasma Physics
D. Coster, E. Tsitrone, X. Et al.

[300] JET progress towards an advanced mode of ITER operation with current profile control
28th EPS Conference on Controlled Fusion and Plasma Physics
A. Becoulet, X. The jet-efda team

[301] JET-EP ICRF antenna electrical features assessment
14th Topical Conference on Radio Frequency Power in Plasmas
S. Bremond, K. Vulliez, G. Agarici, B. Beaumont, F. Durodié

[302] Joints for large superconducting conductors
21st Symposium On Fusion Technology
P. Decool, D. Ciazynski, A. Nobili, S. Parodi, P. Pesenti, A. Bourquard, F. Beaudet

[303] La Fusion par Confinement magnétique et la Supraconductivité.
Sixièmes Journées de Cryogénie et Supraconductivité
J.L. Duchateau

[304] Large superconducting conductors and joints for fusion magnets : from conceptual design to test at full size scale
18th IAEA Fusion Energy Conference
D. Ciazynski, J.L. Duchateau, P. Decool, P. Libeyre, B. Turck

[305] Le point sur la fusion thermonucléaire contrôlée
Les Réacteurs de Recherche
J. Johner

[306] LHCD coupling during H-mode and ITB in JET plasmas
14th Topical Conference on Radio Frequency Power in Plasmas
V. Pericoli ridolfini, S. Podda, J. Mailloux, Y. Sarazin, Y. Baranov, S. Bernabei, R. Cesario, V. Cocilovo, A. Ekedahl, K. Erents, G. Granucci, F. Imbeaux, F. Rimini, X. Et al.

[307] LHCD Effects on Pellet Ablation in a Tokamak Plasma
14th Topical Conference on Radio Frequency Power in Plasmas
R. Dumont, V. Waller, B. Pegourie

[308] Linear analysis and nonlinear behavior of drift-tearing modes
28th EPS Conference on Controlled Fusion and Plasma Physics
D. Grasso, M. Ottaviani, F. Porcelli

[309] Long pulse tokamak research with Tore Supra
14th Topical Conference on Radio Frequency Power in Plasmas
J. Jacquinot, X. Tore supra team

[310] Lower hybrid current drive efficiency and power deposition profile during MHD activity in Tore Supra
14th Topical Conference on Radio Frequency Power in Plasmas
Y. Peysson, R. Dumont, G. Giruzzi, G. Huysmans, F. Imbeaux, M. Ju, X. Litaudon, G. Martin, R. Mitteau, F. Rimini, M. Zabiego, T. Aniel, V. Basiuk, Ph. Bibet, C. Bourdelle, A. Ekedahl, X. Garbet, B. Schunke

[311] Material activation observation on the Tore Supra Tokamak
21st Symposium On Fusion Technology
G. Martin, A. Le luyer, F. Saint Laurent

[312] Material properties and consequences on the quality of Tore Supra plasma facing components
10th International Conference on Fusion Reactor Materials
J. Schlosser, A. Durocher, T. Huber, Ph. Chappuis, P. Garin, W. Knabl, B. Schedler

[313] Measurement and simulation of edge flows induced by ergodization in Tore Supra
14th Int. Conf. on Plasma Surface Interaction in Controlled Fusion Devices
J. Gunn, C. Boucher, Y. Corre, P. Devynck, Ph. Ghendrih, J.Y. Pascal

[314] Measurement of impurity profile modifications with a modulated diagnostic beam on Tore Supra
27th EPS Conf. on Controlled Fusion and Plasma Physics
W.R. Hess, C. De Michelis, J.T. Hogan, J.L. Farjon, M. Druetta, Charles E. Bush

[315] Measurement of The Runaway Electron Energy during Disruptions
7th IAEA TCM on Energetic Particles in Magnetic Confinement Systems
G. Martin, F. Sourd

[316] Mechanical design and analysis of joints for the ITER PF Coils
17th International Conference on Magnet Technology
P. Libeyre, P. Decool

[317] Method for determination of the conductor current sharing temperature using travelling heat slug in the ITER TFMC
17th International Conference on Magnet Technology
A. Martinez, J.L. Duchateau

[318] MHD in advanced scenarios in the large Tokamaks
7th EU-US Transport Task Force Workshop
G. Huysmans

[319] MHD performance limits in JET optimised shear discharges
28th EPS Conference on Controlled Fusion and Plasma Physics
P. Hennequin, T. Hender, B. Alper, C. Challis, N. Hawkes, T. Hellsten, D. Howell, G. Huysmans, X. Litaudon, Ph. Lotte, J. Manickam, M. Maraschek, D. Mazon, F. Nave, A. Pochelon, S. Sharapov

[320] Microinstability and flow shear analysis in high-performance JET ITB plasma
43rd APS Conference
R. Budny, A. Becoulet, X. Et al.

[321] Model of Heat Deposition during fast Discharge Tests of the ITER Toroidal Field Model Coil
17th International Conference on Magnet Technology
P. Hertout, A. Bleyer, J.L. Duchateau, A. Martinez, S. Nicollet

[322] Modeling of recycling coefficients and wall equilibration in Tore Supra
28th EPS Conference on Controlled Fusion and Plasma Physics
P. Mioduszewski, L. Owen, B. Pegourie

[323] Modelling of ECH modulation experiments in ASDEX Upgrade : a test of the critical temperature gradient length assumption
28th EPS Conference on Controlled Fusion and Plasma Physics
F. Imbeaux, F. Ryter, X. Garbet

[324] Modelling of ion-diamagnetic effects on ideal MHD modes in tokamak plasmas
27th EPS Conf. on Controlled Fusion and Plasma Physics
G. Huysmans, S. Sharapov, A. Mikhailovskii, V.V. Parail

[325] Modelling of particle flows in a scrape off layer with limiter biasing
3rd Europhysics Workshop on Role of Electric Fields in Plas
T. Loarer, E. Gravier, J. Gunn, J. Lachambre, K. Finken, S. Jachmich, M. Lehnen, G. Mank, H. Van goubergen, G. Van oost

[326] Molecular contribution to the Deuterium influx in Tore Supra ergodic divertor experiments
28th EPS Conference on Controlled Fusion and Plasma Physics
R. Guirlet, A. Escarguel, S. Brezinsek, J.T. Hogan, A. Pospieszczyk, C. De Michelis

[327] Monte Carlo solution of the orbit averaged Fokker-Planck equation including ripple losses
27th EPS Conf. on Controlled Fusion and Plasma Physics
L.G. Eriksson, V. Bergeaud, V. Basiuk, T. Hellsten

[328] NbTi superconducting busbars for the ITER TFMC
21st Symposium On Fusion Technology
P. Libeyre, P. Decool, J.L. Duchateau, H. Cloez, A. Kienzler, A. Lingor, H. Fillunger, R. Maix, A. Bourquard, F. Beaudet

[329] Near infrared emission of carbonaceous surfaces under impact of plasma, high energy ions and high energy electrons
28th EPS Conference on Controlled Fusion and Plasma Physics
R. Reichle, E. Delchambre, F. Escourbiac, M. Febvre, C. Pocheau

[330] Neoclassical tearing mode seed island control with ICRH in JET
28th EPS Conference on Controlled Fusion and Plasma Physics
O. Sauter, M. Mayoral, F. Nguyen, A.L. Pecquet, X. Et al.

[331] Neon transport in JET plasmas close to ITB formation with monotonic and reversed q-profiles
28th EPS Conference on Controlled Fusion and Plasma Physics
C. Giroud, G. Tresset, X. Et al.

[332] Net erosion measurements on plasma facing components of Tore Supra
14th Int. Conf. on Plasma Surface Interaction in Controlled Fusion Devices
E. Tsitrone, Ph. Chappuis, Y. Corre, E. Gauthier, A. Grosman, J.Y. Pascal

[333] New 80k cryo-mechanical-pump project
21st Symposium On Fusion Technology
J. Manzagol, J. Perin, J.J. Cordier, P. Garin, F. Samaille

[334] New developments of the Tore Supra acquisition system
21st Symposium On Fusion Technology
Y. Buravand, S. Balme, B. Guillerminet, T. Hutter, J.Y. Pascal, B. Rothan

[335] New insights into MHD dynamics of magnetically confined plasmas from experiments in RFX
18th IAEA Fusion Energy Conference
P. Martin, B. Pegourie, X. Et al.

[336] New magnetic diagnostic for the CIEL project on Tore Supra
21st Symposium On Fusion Technology
P. Moreau, P. Defrasne, E. Joffrin, F. Saint-Laurent

[337] Non-inductive tokamak : advanced scenario with radio frequency heating and current drive
27th EPS Conf. on Controlled Fusion and Plasma Physics
I. Voitsekhovitch, D. Moreau

[338] Nonlinear diamagnetic effects on the evolution and the saturation of drift- tearing modes
Theory of Fusion Plasmas, Joint Varenna-Lausanne Int. Workshop
D. Grasso, M. Ottaviani, F. Porcelli

[339] Novel method to study SOL-response to ELMs by divertor target probes in JET
28th EPS Conference on Controlled Fusion and Plasma Physics
S. Jachmich, M. Becoulet, X. Et al.

[340] Numerical assessment of the ion turbulent thermal transport scaling laws
7th EU-US Transport Task Force Workshop
M. Ottaviani, G. Manfredi

[341] Numerical assessment of the ion turbulent thermal transport scaling laws
18th IAEA Fusion Energy Conference
M. Ottaviani, G. Manfredi

[342] Numerical simulations and error analysis for the far-infrared polarimeter measurements on Tore Supra
28th EPS Conference on Controlled Fusion and Plasma Physics
D. Elbeze, C. Gil, R. Giannella

[343] Oblique ECE measurements during stron ECH at 140 GHZ in FTU
28th EPS Conference on Controlled Fusion and Plasma Physics
O. Tudisco, E. De la luna, V. Krivenski, G. Giruzzi, P. Amadeo, A. Bruschi, F. Gandini, G. Granucci, V. Muzzini, A. Simonetto

[344] On sustaining low or reversed magnetic shear equilibria with non-inductive current drive on JET
27th EPS Conf. on Controlled Fusion and Plasma Physics
V. Fuchs, M. Becoulet, L.G. Eriksson, C. Giroud, X. Garbet, E. Joffrin, W. Horton, P. Maget, X. Litaudon, D. Mazon, G. Tresset, P. Zhu

[345] On the dynamics of runaway electrons
Theory of Fusion Plasmas, Joint Varenna-Lausanne Int. Workshop
P. Helander, F. Andersson, L.G. Eriksson

[346] Operating Experience of the Tore Supra Cryogenic System
Satellite Workshop on Cryogenics for Large Systems
B. Gravil, R. Garbil, D. Henry, Tore supra cryogenic team

[347] Optimization of gundestrup probe for ion flow measurements in magnetized plasmas
28th EPS Conference on Controlled Fusion and Plasma Physics
J. Stöckel, J. Gunn, G. Van oost, I. Duran, M. Hron, J. Adamek, J. Horacek, R. Hrach, K. Jakubka, L. Kryska, M. Vicher, F. Zacek

[348] Particle and energy transport analysis by means of pellet injection in the RFX reversed field pinch
27th EPS Conf. on Controlled Fusion and Plasma Physics
R. Lorenzini, L. Garzotti, P. Innocente, S. Martini, B. Pegourie

[349] Particle balance studies in JET
28th EPS Conference on Controlled Fusion and Plasma Physics
J. Bucalossi, T. Loarer, V. Philipps, D. Brennan, P. Coad, C. Grisolia, R. Stagg, X. The jet-efda team

[350] Particle collection and exhaust in ergodic divertor experiments on Tore Supra
14th Int. Conf. on Plasma Surface Interaction in Controlled Fusion Devices
T. Loarer, Ph. Ghendrih, J. Gunn, A. Azeroual, L. Costanzo, C. Grisolia, R. Guirlet, G. Mank, P. Monier-Garbet, B. Pegourie

[351] Particle recirculation studies in JET
IAEA/TCM on Divertor Concepts
E. Tsitrone, J. Bucalossi, T. Loarer, Ph. Ghendrih, A. Loarte, P. Andrew, J. Coad, W. Fundamenski, M. Stamp, D. Coster, X. The jet-efda team

[352] Particle transport analysis of L-mode pellet fuelled plasmas in JET
27th EPS Conf. on Controlled Fusion and Plasma Physics
L. Garzotti, G. Corrigan, D. Heading, T. Jones, V.V. Parail, B. Pegourie, J. Spence

[353] Particle trapping in Carbon walls during ICRH heating in Tore Supra
14th Int. Conf. on Plasma Surface Interaction in Controlled Fusion Devices
C. Grisolia, J.T. Hogan, Ph. Ghendrih, T. Loarer, J. Gunn, P. Monier-Garbet, M. Becoulet, T. Hutter

[354] Pellet ablation in plasmas with a high level of additional power
28th EPS Conference on Controlled Fusion and Plasma Physics
V. Waller, B. Pegourie, A. Geraud, G. Granata, V. Bergeaud, R. Dumont, F. Imbeaux, V. Basiuk, L.G. Eriksson, L. Garzotti

[355] Pellet injectors developed at the PELIN laboratory for international projects
21st Symposium On Fusion Technology
I. Viniar, S. Sudo, A. Geraud, J. Perin, J. Manzagol, P. Ladd, G. Saksaganskii, S. Skoblikov, A. Lukin, A. Umov, P. Reznichenko, K. Khlopenkov, I. Krasilnikov, I. Rukhlenko

[356] Peripheral plasma perturbations and transient improved confinement in JET optimised shear discharges
28th EPS Conference on Controlled Fusion and Plasma Physics
G. Gorini, E. Joffrin, Y. Sarazin, X. Litaudon, X. Et al.

[357] Physics and design interplay phenomena in an actively cooled tokamak :Tore Supra
ICCP2000_Int. Congress on Plasma Physics/42nd APS
M. Chatelier, X. Tore supra team

[358] Plasma control in advanced steady state operation of tokamaks
10th International Toki Conference on Plasma Physics and Controlled Nuclear Fusi
D. Moreau, G. Kamelander, X. Litaudon, I. Voitsekhovitch

[359] Plasma particle trapping and release by the graphite first wall during different Tore Supra plasmas
14th Int. Conf. on Plasma Surface Interaction in Controlled Fusion Devices
C. L Begrambekov, C. Grisolia, J. Bucalossi, D. Garnier, J. Gunn, T. Loarer, S. Vergazov, A. Zakharov

[360] Potential structures and flow measurements with separatrix biasing in the CASTOR tokamak
11th Int. Toki Conference on Potential and Structure in Plasmas
G. Van oost, J. Stöckel, M. Hron, P. Devynck, K. Dyabilin, J. Gunn, J. Horacek, E. Martines, M. Tendler

[361] Predictive modelling of JET plasmas with edge and core transport barriers
28th EPS Conference on Controlled Fusion and Plasma Physics
V.V. Parail, A. Becoulet, M. Becoulet, P. Maget, X. Et al.

[362] Present status and future plans for Tore Supra
8th Ukrainian Conference and School on Plasma Phsics and Controlled Fusion
P. Stott, B. Beaumont, A. Becoulet, Ph. Bibet, C. Darbos, P. Garin, A. Geraud, G. Giruzzi, A. Grosman, G. Martin, M. Ottaviani, Y. Peysson, B. Saoutic, M. Zabiego

[363] Probabilistic approach to plasma diagnostic measurements : an application to Tore Supra's Thomson Scattering data
28th EPS Conference on Controlled Fusion and Plasma Physics
R. Giannella, J. Lasalle, M. Fois

[364] Progress in internal transport barrier plasmas with lower hybrid current drive and heating in JET
43rd APS Conference
J. Mailloux, A. Becoulet, A. Ekedahl, F. Imbeaux, E. Joffrin, X. Litaudon, D. Mazon, F. Rimini, Y. Sarazin, X. Et al.,

[365] Progress of the ITER Central Solenoid Model Coil Program
18th IAEA Fusion Energy Conference
H. Tsuji, K. Okuno, R. Thome, E. Salpietro, S. Egorov, N. Martovetsky, M. Ricci, R. Zanino, G. Zahn, A. Martinez, X. Et al.

[366] Progress towards high power lower hybrid current drive in Tore Supra
27th EPS Conf. on Controlled Fusion and Plasma Physics
Y. Peysson, X. Tore supra team

[367] Q-profile evolution and improved core electron confinement in the full current drive operation on Tore Supra
27th EPS Conf. on Controlled Fusion and Plasma Physics
X. Litaudon, Y. Peysson, T. Aniel, G. Huysmans, F. Imbeaux, E. Joffrin, J. Lasalle, Ph. Lotte, B. Schunke, J.L. Segui, G. Tresset, M. Zabiego

[368] Radiation hardness test of mica bolometers for ITER in JMTR
28th EPS Conference on Controlled Fusion and Plasma Physics
R. Reichle, T. Nishitani, E. Hodgson, L. Ingesson, E. Ishitsuka, S. Kasai, K. Mast, T. Shikama, J.C. Vallet, S. Yamamoto

[369] Radiation hardness test of mica bolometers for ITER in JMTR
Int. Conf. on Advanced Diagnostics for Magnetic and Inertial Fusion
R. Reichle, T. Nishitani, E. Hodgson, L. Ingesson, E. Ishitsuka, S. Kasai, K. Mast, T. Shikama, J.C. Vallet, S. Yamamoto

[370] Radiation pattern and impurity transport in impurity seeded ELMy H-mode discharges in JET
28th EPS Conference on Controlled Fusion and Plasma Physics
M.E. Puiatti, P. Monier-Garbet, C. Giroud, X. Et al.

[371] Real time determination and control of the plasma localisation and internal inductance in Tore Supra
21st Symposium On Fusion Technology
F. Saint-Laurent, G. Martin

[372] Real time plasma feed-back control : an overview of Tore Supra achievements
18th IAEA Fusion Energy Conference
G. Martin, J. Bucalossi, A. Ekedahl, C. Gil, C. Grisolia, D. Guilhem, J. Gunn, F. Kazarian, D. Moulin, J.Y. Pascal, F. Saint-Laurent

[373] Real-time plasma control of internal transport barriers in JET
28th EPS Conference on Controlled Fusion and Plasma Physics
D. Mazon, X. Litaudon, M. Riva, G. Tresset, A. Becoulet, T. Bolzonella, J.M. Chareau, S. Dalley, S. Dorling, R. Felton, A. Goodyear, E. Joffrin, D. Moreau, R. Prentice, X. The jet-efda team

[374] Recent advances on the phys ics of the wave plasma interaction in the ion cyclotron range of frequency
Theory of Fusion Plasmas, Joint Varenna-Lausanne Int. Workshop
F. Nguyen, D. Fraboulet, V. Bergeaud, A. Becoulet

[375] Recent heating and current drive result on JET
14th Topical Conference on Radio Frequency Power in Plasmas
Tuccillo, Ph. Bibet, F. Nguyen, A. Ekedahl, F. Rimini, F. Imbeaux, Y. Sarazin, X. Litaudon, P. Maget, M. Mayoral, F. Nguyen, F. Rimini, Y. Sarazin, X. Et al.

[376] Recent heating and current drive results on JET
14th Topical Conference on Radio Frequency Power in Plasmas
A. Tucillo, Ph. Bibet, A. Ekedahl, F. Imbeaux, X. Litaudon, P. Maget, M. Mayoral, F. Nguyen, F. Rimini, Y. Sarazin, X. Et al.

[377] Récentes avancées dans le domaine de la cryoélectricité des forts courants : Les programmes de la fusion par confinement magnétique
Electrotechnique du futur 2001
J.L. Duchateau, D. Ciazynski, P. Decool

[378] Relation between low Z impurity poloidal emission profiles and transport in Tore Supra ergodic divertor plasmas
28th EPS Conference on Controlled Fusion and Plasma Physics
C. De Michelis, J.T. Hogan, P. Monier-Garbet, Y. Corre, Ph. Ghendrih, R. Guirlet, J. Gunn

[379] Relationship between self-similarity properties and hurst exponents in plasma turbulence
ICCP2000_Int. Congress on Plasma Physics/42nd APS
G. Bonhomme, J.H. Chatenet, P. Devynck

[380] Remote participation at JET from DRFC Cadarache
21st Symposium On Fusion Technology
J. How, A. Maas, J.M. Theis, Y. Buravand, X. Litaudon

[381] Remote participation at JET Task Force work : user's experience
3rd IAEA TCM on Control, Data Acquisition, and Remote Participation for Fusion R
W. Suttrop, D. Kinna, J. Farthing, O. Hemming, J. How, V. Schmidt, X. Efda-jet team

[382] Remote participation infrastructure in the European Fusion Laboratories
12th IEEE NPSS Real Time Conference
V. Schmidt, J. How

[383] Remote Participation Technical Infrastructure for the JET Facilities under EFDA
21st Symposium On Fusion Technology
V. Schmidt, J. How

[384] Resistances of electrical joints in the TF model coil of ITER: comparisons of first test results with samples results
17th International Conference on Magnet Technology
D. Ciazynski, M. Ricci, J.L. Duchateau, A. Ulbricht, F. Wuechner, G. Zahn, H. Fillunger, R. Maix

[385] RF-induced pinch of resonant 3He minority ions in JET
14th Topical Conference on Radio Frequency Power in Plasmas
T. Johnson, M. Mayoral, F. Nguyen, X. Et al.

[386] RF-sheath physics assessment of Tore Supra ICRF antenna designs
14th Topical Conference on Radio Frequency Power in Plasmas
L. Colas, S. Heuraux, S. Pecoul, S. Bremond, M. Becoulet

[387] Ripple loss studies during ICRF heating on Tore Supra
27th EPS Conf. on Controlled Fusion and Plasma Physics
V. Basiuk, V. Bergeaud, M. Chantant, G. Martin, F. Nguyen, R. Reichle, J.C. Vallet, L.G. Eriksson, L. Delpech, F. Surle

[388] Risks and benefits of incoloy 908
21st Symposium On Fusion Technology
P. Libeyre, C. Brosset, P. Decool, M. Rubino, G. Bevilacqua, A. Laurenti, P. Pesenti, M. Ursuleac, N. Valle, A. Nyilas

[389] Role of MHD in the triggering and destruction of ITBs in JET
27th EPS Conf. on Controlled Fusion and Plasma Physics
E. Joffrin, B. Alper, C. Challis, T. Hender, D. Howell, G. Huysmans, K. Zastrow

[390] Rotation and Particle Loss in Tore Supra
27th EPS Conf. on Controlled Fusion and Plasma Physics
R. White, F. Perkins, X. Garbet, C. Bourdelle, V. Basiuk, L.G. Eriksson

[391] Rotation and shape dependence of neoclassical tearing mode thresholds on JET
28th EPS Conference on Controlled Fusion and Plasma Physics
R. Buttery, G. Huysmans, M. Zabiego, X. Et al.

[392] Runaway current damping by synchrotron radiation
7th IAEA TCM on Energetic Particles in Magnetic Confinement Systems
F. Andersson, P. Helander, L.G. Eriksson

[393] Runaway Electron during Disruptions impact on the First Wall Components
9th European Fusion Physics Workshop
G. Martin

[394] Sawtooth and impurity accumulation control in JET radiative mantle discharges
28th EPS Conference on Controlled Fusion and Plasma Physics
F. Nave, Ph. Lotte, X. Et al.

[395] Sawtooth and neoclassical tearing mode seed island control by ICRF current drive on JET
14th Topical Conference on Radio Frequency Power in Plasmas
M. Mayoral, F. Nguyen, X. Et al.

[396] Sawtoothing in reversed shear plasmas
28th EPS Conference on Controlled Fusion and Plasma Physics
T. Hellsten, A. Becoulet, E. Joffrin, D. Mazon, X. Et al.

[397] Scaling laws for the ICRF coupling resistance on Tore Supra
14th Topical Conference on Radio Frequency Power in Plasmas
M. Goniche, S. Bremond, L. Colas

[398] Screening of hydrocarbon sources in JET
28th EPS Conference on Controlled Fusion and Plasma Physics
J. Strachan, C. Giroud, X. Et al.

[399] Self consistent calculations of the velocity distribution and wavefield during ICRH
Theory of Fusion Plasmas, Joint Varenna-Lausanne Int. Workshop
J. Hedin, T. Hellsten, T. Johnson, L.G. Eriksson

[400] Self shadowing, gaps and leading edges on Tore Supra's inner first wall
14th Int. Conf. on Plasma Surface Interaction in Controlled Fusion Devices
R. Mitteau, Ph. Chappuis, Ph. Ghendrih, A. Grosman, D. Guilhem, J. Gunn, J.T. Hogan, M. Lipa, G. Martin, J. Schlosser, E. Tsitrone

[401] Self-consistent modelling of profile control by rf current drive in advanced tokamak regimes
28th EPS Conference on Controlled Fusion and Plasma Physics
G. Giruzzi, R. Dumont

[402] Similar advanced tokamak experiments in JET and ASDEX-Upgrade
28th EPS Conference on Controlled Fusion and Plasma Physics
E. Joffrin, A. Becoulet, C. Giroud, D. Mazon, X. Et al.

[403] Simulation of alpha particle plasma self-heating using ICRH under real-time control
28th EPS Conference on Controlled Fusion and Plasma Physics
T. Jones, Y. Sarazin, X. Et al.

[404] SINGAP : the European concept for negative ion acceleration in the ITER neutral injectors
9th International Conference on Ion Sources
H. De esch, R. Hemsworth, P. Massmann

[405] Spectral profile analysis of the Dalpha line in the divertor region of Tore Supra
14th Int. Conf. on Plasma Surface Interaction in Controlled Fusion Devices
A. Escarguel, R. Guirlet, A. Azeroual, B. Pegourie, J. Gunn, T. Loarer, H. Capes, Y. Corre, C. De Michelis, L. Godbert-mouret, M. Koubiti, M. Mattioli, R. Stamm

[406] Spectroscopic study of neon emission and retention in the Tore Supra ergodic divertor
14th Int. Conf. on Plasma Surface Interaction in Controlled Fusion Devices
R. Guirlet, J.T. Hogan, Y. Corre, C. De Michelis, A. Escarguel, W.R. Hess, P. Monier-Garbet, B. Schunke

[407] Stability analysis of internal transport barrier on Tore Supra
27th EPS Conf. on Controlled Fusion and Plasma Physics
C. Bourdelle, X. Garbet, G.T. Hoang

[408] Strategy of the Tore Supra diagnostic set for steady-state high power operation
Int. Conf. on Advanced Diagnostics for Magnetic and Inertial Fusion
C. Laviron

[409] Suppression of runaway electron avalanches by radial diffusion
27th EPS Conf. on Controlled Fusion and Plasma Physics
P. Helander, L.G. Eriksson, F. Andersson

[410] Synergy between LH and ECH waves in the FTU tokamak
14th Topical Conference on Radio Frequency Power in Plasmas
V. Pericoli ridolfini, E. Barbato, A. Bruschi, R. Dumont, F. Gandini, G. Giruzzi, C. Gormezano, G. Granucci, L. Panaccione, Y. Peysson, S. Podda, A. Saveliev

[411] Techniques for measuring the plasma radial electric field using the motional Stark effect diagnostic at JET
4th Europhysics Wks on Role of Electric Field in Plasma Confinement and Exhaust
S. Reyes cortes, N. Hawkes, Ph. Lotte, C. Giroud, B. Stratton, X. Efda-jet team

[412] Test of an extruder feed system on the Tore Supra centrifugal pellet injector
21st Symposium On Fusion Technology
A. Geraud, J.F. Artaud, G. Gros, C. Pocheau, S. Combs, C. Foust

[413] Test of electron heat diffusivity against the electron temperature gradient turbulence model & investigation of critical temperature gradient on Tore Supra
27th EPS Conf. on Controlled Fusion and Plasma Physics
G.T. Hoang, C. Bourdelle, X. Garbet, T. Aniel, M. Ottaviani, W. Horton, P. Zhu

[414] Test program preparations of the ITER toroïdal field model coil (TFMC)
21st Symposium On Fusion Technology
A. Ulbricht, J.L. Duchateau, H. Fillunger, S. Fink, R. Heller, P. Hertout, P. Libeyre, R. Maix, C. Marinucci, A. Martinez, R. Meyder, S. Nicollet, S. Raff, M. Ricci, L. Savoldi, F. Wüchner, G. Zahn, R. Zanino

[415] The 118 GHz ECRH experiment on Tore Supra
21st Symposium On Fusion Technology
C. Darbos, R. Magne, S. Alberti, A. Barbuti, G. Berger-By, F. Bouquey, P. Cara, J. Clary, L. Courtois, R. Dumont, E. Giguet, D. Gil, G. Giruzzi, M. Jung, Y. Le Goff, F. Legrand, M. Lennholm, C. Liévin, Y. Peysson, D. Roux, M. Thumm, T. Wagner, M. Tran, X.L. Zou

[416] The Cadarache 1 MV porcelain SINGAP bushing
21st Symposium On Fusion Technology
P. Massmann, H. De esch, R. Hemsworth, T. Inoue, L. Svensson

[417] The Data Acquisition System for the Infrared Cameras on Tore Supra
12th IEEE NPSS Real Time Conference
D. Moulin, C. Balorin, Y. Buravand, G. Caulier, L. Ducobu, D. Guilhem, M. Jouve, H. Roche

[418] The data management at Tore Supra : links with data validation process
W7-X Data Validation Workshop
T. Hutter, J.F. Artaud, S. Balme, G. Martin, R. Masset, R. Reichle

[419] The effect of inhomogeneity of toroidal magnetic field on the solution of bounce-averaged Fokker-Planck equation on Tore Supra
14th Topical Conference on Radio Frequency Power in Plasmas
M. Ju, Y. Peysson, V. Basiuk

[420] The effect of plasma shape on density and confinement of ELMY H-modes in JET
28th EPS Conference on Controlled Fusion and Plasma Physics
G. Saibene, M. Becoulet, X. Et al

[421] The effects of target density, plasma shaping and divertor configuration on the H-mode pedestal in ITB experiments on JET
28th EPS Conference on Controlled Fusion and Plasma Physics
P. Lomas, E. Joffrin, F. Rimini, A. Becoulet, M. Becoulet, C. Giroud, P. Maget, Y. Sarazin, X. Et al

[422] The hurst exponent and long-time correlation
27th EPS Conf. on Controlled Fusion and Plasma Physics
P. Devynck, Guiding Wang, G. Antar, G. Bonhomme

[423] The role of radial electric fields in edge transport barriers in tokamaks
4th Symposium on Current Trends in International Fusion Research
G. Van oost, J. Gunn, A. Melnikov, J. Stöckel, M. Tendler

[424] The Technical Infrastructure to Remote Participation in European Fusion Programme
3rd IAEA TCM on Control, Data Acquisition, and Remote Participation for Fusion R
J. How, V. Schmidt

[425] The Tore Supra cryoplant control system upgrade
21st Symposium On Fusion Technology
R. Garbil, J.L. Marechal, B. Gravil, D. Henry, J.Y. Journeaux, D. Balaguer, J. Baudet, A. Bocquillon, P. Fejoz, P. Prochet, C. Roux, J.P. Serries

[426] The Tore Supra LHCD control system : new improvements using PLCs and state machines
21st Symposium On Fusion Technology
J.Y. Journeaux, Ph. Froissard, F. Kazarian, J. Baudet, P. Pastor, J. Simoncini

[427] Theoretical and experimental analysis of the LHCD power coupling in JET optimised shear plasmas
14th Topical Conference on Radio Frequency Power in Plasmas
A. Ekedahl, Ph. Bibet, M. Lennholm, X. Litaudon, J. Mailloux, V. Pericoli ridolfini, Y. Sarazin, A. Tucillo

[428] Theoretical issues in tokamak confinement : (i) internal/edge transport barriers and (ii) runaway avalanche confinement
18th IAEA Fusion Energy Conference
J. Connor, P. Helander, A. Thyagaraja, F. Andersson, T. Fülöp, L.G. Eriksson, M. Romanelli

[429] Thermography of target plates with near infrared optical fibers at Tore Supra
14th Int. Conf. on Plasma Surface Interaction in Controlled Fusion Devices
R. Reichle, V. Basiuk, V. Bergeaud, A. Cambe, M. Chantant, E. Delchambre, M. Druetta, E. Gauthier, W.R. Hess, C. Pocheau

[430] Tore Supra continuous acquisition system
3rd IAEA TCM on Control, Data Acquisition, and Remote Participation for Fusion R
B. Guillerminet, Y. Buravand, M. Le Luyer, F. Leroux, D. Moulin, Ja. Signoret, P. Spuig

[431] Tore Supra Divertor screening efficiency during density regime
14th Int. Conf. on Plasma Surface Interaction in Controlled Fusion Devices
C. Grisolia, Ph. Ghendrih, J. Gunn, T. Loarer, P. Monier-Garbet, C. De Michelis, L. Costanzo, J.Y. Pascal

[432] Tore Supra experience of copper chromium zirconium electron beam welding
10th International Conference on Fusion Reactor Materials
A. Durocher, M. Lipa, Ph. Chappuis, J. Schlosser, T. Huber, B. Schedler

[433] Tore Supra steady state power and particles injection : the "CIMES" project
21st Symposium On Fusion Technology
B. Beaumont, A. Becoulet, Ph. Bibet, C. Darbos, P. Garin, A. Geraud, G. Giruzzi, A. Grosman, G. Martin, M. Ottaviani, Y. Peysson, B. Saoutic, P. Stott, M. Zabiego

[434] Toroidal plasma rotation with ICRF on JET
28th EPS Conference on Controlled Fusion and Plasma Physics
J. Noterdaeme, F. Nguyen, X. Et al

[435] Towards full current drive operation in JET
28th EPS Conference on Controlled Fusion and Plasma Physics
X. Litaudon, V. Basiuk, A. Becoulet, M. Becoulet, L.G. Eriksson, C. Giroud, G. Huysmans, F. Imbeaux, E. Joffrin, Ph. Lotte, P. Maget, D. Mazon, D. Moreau, F. Rimini, Y. Sarazin, G. Tresset, X. The jet-efda team

[436] Towards Realistic Simulations of Runaway Electrons in Tokamaks
7th IAEA TCM on Energetic Particles in Magnetic Confinement Systems
L.G. Eriksson, P. Helander, F. Andersson

[437] Transport mechanisms and enhanced confinement studies in RFX
18th IAEA Fusion Energy Conference
V. Antoni, B. Pegourie, X. Et al

[438] Turbulence behaviour during electron heated reversed shear discharges in JET
28th EPS Conference on Controlled Fusion and Plasma Physics
G. Conway, J.M. Chareau, X. Litaudon, R. Sabot, Y. Sarazin, X. Et al

[439] Turbulence in Fusion Plasmas: Key Issues and Impact on Transport Modelling
28th EPS Conference on Controlled Fusion and Plasma Physics
X. Garbet

[440] Turbulence Simulations of Transport Barriers
7th EU-US Transport Task Force Workshop
X. Garbet, C. Bourdelle, G.T. Hoang, P. Maget, S. Benkadda, P. Beyer, N. Bian, C. Figarella, I. Voitsekhovitch, O. Agullo

[441] Type 1 ELM energy and particle losses in JET ELMy H-modes
28th EPS Conference on Controlled Fusion and Plasma Physics
A. Loarte, M. Becoulet, X. Et al

[442] Use of lower hybrid current drive and heating in optimised shear plasmas in JET
28th EPS Conference on Controlled Fusion and Plasma Physics
J. Mailloux, A. Becoulet, F. Imbeaux, E. Joffrin, X. Litaudon, D. Mazon, Y. Sarazin, X. Et al.

[443] Validation of the CEA Electrical Network Model for the ITER Coils
ASC2000 Applied Superconductivity Conference
D. Ciazynski, J.L. Duchateau

[444] Very long pulse testing of the 1506 B 118 GHz gyrotron
14th Topical Conference on Radio Frequency Power in Plasmas
R. Magne, S. Alberti, A. Barbuti, F. Bouquey, J. Clary, C. Darbos, E. Giguet, J. Hogge, M. Jung, Y. Legoff, M. Lennholm, C. Liévin, C. Portafaix, D. Roux, B. Saoutic, M. Thumm

[445] Very long pulse testing of the TH 1506B 118 GHz Gyrotron for the ECRH experiment on Tore Supra
26th Int. Conference on Infrared and millimeter waves
R. Magne, C. Darbos, S. Alberti, F. Bouquey, E. Giguet, J. Hogge, Y. Legoff, M. Lennholm, C. Liévin, C. Portafaix, M. Thumm

[446] X mode heterodyne reflectometer for edge density profile measurements on Tore Supra
13th Topical Conference on High-Temperature Plasma Diagnostics
R. Sabot, F. Clairet, C. Bottereau, J.M. Chareau, M. Paume, S. Heuraux, M. Colin, S. Hacquin, G. Leclert

[447] X mode heterodyne reflectometry measurements on Tore Supra
27th EPS Conf. on Controlled Fusion and Plasma Physics
F. Clairet, R. Sabot, C. Bottereau, J.M. Chareau, S. Heuraux, M. Colin, S. Hacquin

IX.5.3. Books

[448] Density control and plasma wall interaction in Tore Supra
Hydrogen Recycling at Plasma Facing Materials, [C.H. Wu (ed.) 2000 Kluwer Acad.
C. Grisolia

[449] Ergodic divertor experiments in Tore Supra above the Greenwald density limit with ICRF power at low magnetic field
Europhysics Conference Abstracts, vol. 24B [K. Szegö, T.N. Todd, S. Zoletnik]
F. Nguyen, Ph. Ghendrih, V. Basiuk, L. Colas, T. Aniel, P. Monier-Garbet, C. De Michelis

[450] Interaction of ion cyclotron range of frequencies wave with energetic particles
Europhysics Conference Abstracts, vol.24B [K. Szegö, T.N. Todd, S. Zoletnik], (2
V. Bergeaud, L.G. Eriksson, A. Becoulet, F. Nguyen

[451] Plasma-material interactions in current tokamaks and their implications for next-step fusion reactors
Rapport IPP 9/128 (PPPL-3531) [Max-Planck Institut für Plasmaphysik], 2001
G. Federici, C. Skinner, J. Brooks, J. Coad, C. Grisolia, A. Haasz, A. Hassanein, V. Philipps, C. Pitcher, J. Roth, W. Wampler, D. Whyte

[452] Recent advances on the physics of the wave plasma interaction in the ion cyclotron range of frequency
Theory of Fusion Plasmas (Proc. of the Joint Varenna-Lausanne Int. Workshop)
F. Nguyen, D. Fraboulet, V. Bergeaud, A. Becoulet

[453] Ripple loss studies during ICRF heating on Tore Supra
Europhysics Conference Abstracts, vol. 24B [K. Szegö, T.N. Todd, S. Zoletnik], (
V. Basiuk, V. Bergeaud, M. Chantant, G. Martin, F. Nguyen, R. Reichle, J.C. Vallet, L.G. Eriksson, L. Delpech, F. Surle

IX.5.4. EURATOM-CEA Association reports

[454] A dimensionless criterion for characterising internal transport barriers in tokamaks
EUR-CEA-FC-1700
G. Tresset, X. Litaudon, D. Moreau

[455] A sensitivity analysis for fire and ITER-FEAT performances
EUR-CEA-FC-1698
J. Johner, F. Albajar

[456] Analyse de stabilité de plasmas de tokamak
EUR-CEA-FC-1706
C. Bourdelle

[457] Anomalous particle pinch in tokamaks
EUR-CEA-FC-1696
F. Miskane, X. Garbet, A. Dezairi, D. Saifaoui

[458] Bounce-averaged fokker-planck solver in non-axisymmetric toroidal geometry
EUR-CEA-FC-1712
M. Ju, V. Basiuk, Y. Peysson

[459] Combined kinetic and transport modeling of radiofrequency current drive
EUR-CEA-FC-1697
R. Dumont, G. Giruzzi, E. Barbato

[460] Comparison of impurity generation and penetration models with spectroscopy for the Tore Supra ergodic divertor
EUR-CEA-FC-1699
R. Giannella, Y. Corre, J.T. Hogan, Ph. Ghendrih, R. Guirlet, J. Gunn

[461] Contribution to the study of superconducting magnetic systems in the frame of fusion projects
EUR-CEA-FC-1692
J.L. Duchateau, H. Artiguelongue, Z. Bej, D. Ciazynski, H. Cloez, P. Decool, P. Hertout, P. Libeyre, A. Martinez, S. Nicollet, M. Rubino, T. Schild, J.M. Verger

[462] Contrôle du profil de courant par ondes cyclotroniques électroniques dans les tokamaks
EUR-CEA-FC-1716
R. Dumont

[463] Edge denstiy profile measurements by X-mode reflectometry on Tore Supra
EUR-CEA-FC-1707
F. Clairet, C. Bottereau, J.M. Chareau, M. Paume, R. Sabot

[464] Edge plasma density convection during ICRH on Tore Supra
EUR-CEA-FC-1721
M. Becoulet, L. Colas, S. Pecoul, J. Gunn, Ph. Ghendrih, A. Becoulet, S. Heuraux

[465] Equilibrium analysis of tokamak discharges with anisotropic pressure
EUR-CEA-FC-1715
W. Zwingmann, L.G. Eriksson, P. Stubberfield

[466] Etude de la production, du transport et du rayonnement de l'impureté carbone dans le tokamak Tore Supra à proximité du Divertor Ergodique
EUR-CEA-FC-1722
Y. Corre

[467] Etude des phénomènes d'interaction plasma/paroi dans Tore Supra
EUR-CEA-FC-1690
R. Ruggieri

[468] Etude du rayonnement dans les plasmas de divertor
EUR-CEA-FC-1711
F. Laugier

[469] Etude expérimentale des aspects topologiques du divertor ergodique de Tore Supra
EUR-CEA-FC-1718
L. Costanzo

[470] EURATOM-CEA Association Contributions to the 14th Int. Conf. on Plasma Surface Interactions in Controlled Fusion Devices, Rosenheim (Germany) May 22-26, 2000
EUR-CEA-FC-1701
X. Tore supra team

[471] EURATOM-CEA Association Contributions to the 18th IAEA Fusion Energy Conference Sorrento (Italy), October 4-10, 2000
EUR-CEA-FC-1709
X. Tore supra team

[472] EURATOM-CEA Association Contributions to the 21st Symposium on Fusion Technology, Madrid (Spain) September 11-15, 2000
EUR-CEA-FC-1708
X. Tore supra team

[473] EURATOM-CEA Association Contributions to the 27th EPS Conference on Controlled Fusion and Plasma Physics, Budapest (Hungary) June 12-16, 2000
EUR-CEA-FC-1703
X. Tore supra team

[474] High harmonics radiation, related power loss and passive current drive in tokamaks
EUR-CEA-FC-1688
I. Fidone, G. Giruzzi, G. Granata

[475] Interaction des ions rapides avec les ondes à la fréquence cyclotronique ionique dans un plasma de tokamak
EUR-CEA-FC-1720
V. Bergeaud

[476] Internal transport barrier with ICRH minority heating on Tore Supra
EUR-CEA-FC-1691
G.T. Hoang, C. Bourdelle, X. Garbet, G. Antar, R. Budny, T. Aniel, V. Basiuk, A. Becoulet, P. Devynck, J. Lasalle, G. Martin, F. Saint-Laurent, X. Tore supra team

[477] MHD stability of advanced tokamak scenarios with reversed central current : an explanation of the "current hole"
EUR-CEA-FC-1717
G. Huysmans, T. Hender, N. Hawkes, X. Litaudon

[478] Modelisation of synchrotron radiation losses in realistic tokamak plasmas
EUR-CEA-FC-1702
F. Albajar, J. Johner, G. Granata

[479] Modelling of ECH modulation experiments in ASDEX Upgrade with an empirical critical temperature gradient length transport model
EUR-CEA-FC-1714
F. Imbeaux, F. Ryter, X. Garbet

[480] Momentum and heat transfer from lower hybrid antennas to the tokamak edge plasma
EUR-CEA-FC-1713
V. Fuchs, M. Goniche, J. Gunn, V. Petrzilka

[481] Numerical methods for finding periodic points in discrete maps. High order islands chains and noble barriers in a toroidal magnetic configuration
EUR-CEA-FC-1719
G. Steinbrecher, J.D. Reuss, J.H. Misguich

[482] On the Role of Ion Heating in ICRF-heated Discharges in Tore Supra
EUR-CEA-FC-1705
L.G. Eriksson, G.T. Hoang, V. Bergeaud

[483] Pompage des particules au moyen de structures à évents dans les tokamaks. Application au divertor ergodique de Tore Supra
EUR-CEA-FC-1695
A. Azeroual

[484] Preliminary Assessment of Ignitor Performances
EUR-CEA-FC-1694
J. Johner

[485] Profile control studies for JET optimised shear regime
EUR-CEA-FC-1693
X. Litaudon, P. Bayetti, A. Becoulet, L.G. Eriksson, V. Fuchs, G. Huysmans, J. How, E. Joffrin, P. Maget, M. Mayoral, D. Mazon, D. Moreau, F. Rochard, Y. Sarazin, G. Tresset, I. Voitsekhovitch, W. Zwingmann

[486] Q-profile evolution and improved core electron confinement in the full current drive operation on Tore Supra
EUR-CEA-FC-1710
X. Litaudon, Y. Peysson, T. Aniel, G. Huysmans, F. Imbeaux, E. Joffrin, J. Lasalle, Ph. Lotte, B. Schunke, J. Segui, G. Tresset, M. Zabiego

[487] Transport des particules-test dans le potentiel électrique généré par un modèle de turbulence de bord. Cas d'un forçage par le flux.
EUR-CEA-FC-1704
V. Grandgirard, O. Agullo, S. Benkadda, X. Garbet, Ph. Ghendrih, Y. Sarazin

IX.5.5. Thesis, memoirs

[488] Adaptation du système de champ magnétique de Tore Supra aux régimes de décharges longues.
Mémoire, CNAM Aix-en-Provence
P. Reynaud

[489] Analyse de stabilité de plasmas de tokamak
Thèse Doctorat, Université de Grenoble I
C. Bourdelle

[490] Base INV II : base d'inventaire du matériel informatique du DRFC
Mémoire Fin d'Etudes, ITII Marseille
J.L. Jimenez

[491] Contrôle du profil de courant par ondes cyclotroniques électroniques dans les tokamaks
Thèse Doctorat, Université Henri Poincaré - Nancy I
R. Dumont

[492] Détermination de modes électromagnétiques de guides d'ondes corrugués surdimen- sionnés sur l'installation de chauffage des électrons du tokamak Tore Supra
Thèse Doctorat, Institut National Polytechnique de Grenoble
L. Courtois

[493] Etude de la production, du transport et du rayonnement de l'impureté carbone dans le tokamak Tore Supra à proximité du Divertor Ergodique
Thèse Université Pierre et Marie Curie, Paris , Novembre 2001
Y. Corre

[494] Etude du rayonnement dans les plasmas de divertor
Thèse Doctorat, Université de Paris IX
F. Laugier

[495] Etude ergonomique d'un espace "remote participation" du Département de Recherches sur la Fusion Contrôlée
Mémoire, CNAM Aix-en-Provence
V. Paulus-martin

[496] Etude et modification du circuit de coupure du courant continu du système de champ poloïdal de Tore Supra
Mémoire CNAM, Aix-en-Provence
P. Cara

[497] Etude expérimentale des aspects topologiques du divertor ergodique de Tore Supra
Thèse Université de Provence, Aix-Marseille 1
L. Costanzo

[498] Instabilités, turbulence et transport dans un plasma magnétisé
Thèse Directeur de Recherches, Université de Provence - Marseille 1
X. Garbet

[499] Intégration du système de chauffage FCI au sein du réseau de contrôle commande du Tokamak Tore Supra
Mémoire CNAM, Aix-en-Provence
S. Wisniewski

[500] Interaction des ions rapides avec les ondes à la fréquence cyclotronique ionique dans un plasma de tokamak
Thèse Doctorat, Université de Parix XI
V. Bergeaud

[501] Pompage des particules au moyen de structures à évents dans les tokamaks. Application au divertor ergodique de Tore Supra
Thèse Doctorat, Université d'Aix-Marseille 1
A. Azeroual

[502] Traitement numérique du signal
Mémoire Institut des Techniques d'Ingénieur de l'Industrie, Juin 2000
E. Denicolai

IX.5.6. Probation reports

[503] Analyse du rayonnement thermique de la plaquette ripple
Mémoire de stage
E. Delchambre

[504] Analyse linéaire et simulation numérique de la turbulence de bord dans un plasma de tokamak
Mémoire de stage
B. Biehler

[505] Automatisation de la régulation de puissance des nouveaux klystrons 750 kW du chauffage additionnel hybride
Mémoire de stage DESS, Université de Provence
C. Jimenez

[506] Calcul hydraulique pour le système hybride d'ITER-FEAT
Mémoire de stage IUT St.Jérôme-Marseille
M. Garibaldi

[507] Composition du rayonnement dans Tore Supra.
Mémoire de stage
C. Clement

[508] Etude de l'asymétrie des pertes "ripple" ioniques sur le tokamak Tore Supra en présence de chauffage radiofréquence
Mémoire de stage DEA, Aix-Marseille I
S. Assas
[509] Etude de la réponse thermique des aimants supraconducteurs à refroidissement forcé à des régimes transitoires électromagnétiques
Mémoire de stage DESS, ESM2-Marseille
A. Bleyer
[510] Etude du fonctionnement d'un groupe de recherche à travers les étapes de la démarche de projet technologique
Mémoire de stage 2001
F. Lasalle
[511] Méthode de détermination de la pureté d'un faisceau gaussien à la sortie d'un gyrotron sur l'installation de chauffage des électrons du tokamak Tore Supra
Mémoire de stage DESS, Université de Besançon
V. Vargas
[512] Polarisation du limiteur pompé de Tore Supra, dans le cadre du projet CIEL. Modélisation des flux de particules dans la section dans l'ombre du limiteur
Mémoire de stage 2000
E. Gravier
[513] Propagation et absorption de l'onde hybride dans un tokamak
Mémoire de stage DESS, Université de Besançon
J. Ecarnot
[514] Qualification des cartes électroniques intégrateur de Tore Supra
Mémoire de stage Juin 2001
J. Malpas
[515] Sortie du réflectomètre de l'antenne hybride
Mémoire de stage IUT-Aix-en-Provence
S. Lokocki
[516] Validation d'un composant d'accord radiofréquence
Mémoire de stage IUT-Marseille
M. Dembinski

IX.6. List of abbreviations

ABBREVIATION	Meaning
AMC	Active Metal Casting
AP	Action Programmatique
API	Automate Programmable Industriel
BEL	Bâti d'Essais en Ligne
CCD	Camera Coupled Device
CCE-FU	Comité Consultatif Européen de la Fusion
CD	Current Drive
CEA	Commissariat à l'Énergie Atomique
CFC	Carbon Fiber Composite
CFP	Composants face au plasma
CIC	Compression Isostatique à Chaud
CIEL	Composants Internes Et Limiteurs
CIMES	Chauffage Injection de Matière Etat Stationnaire
CS(MC)	Central Solenoid (Model Coil)
CSU	Close Support Unit
CXR(S)	Charge Exchange Recombination (Spectroscopy)
DA	Divertor Axisymetrique
DAC	Décret d'Autorisation de Création
DARPE	Décret d'Autorisation de Rejets et de Prélèvements d'Eau
DE	Divertor Ergodique
DEN	Direction de l'Énergie Nucléaire
DER	Département d'Etudes des Réacteurs
DoD	Degré de Détachement
DOS	Dossier d'Options de Sûreté

DRT	Direction de Recherche Technologique
ECE	Emission Cyclotronique Electronique
ECR(H)	Electron Cyclotron Resonant (Heating)
EDA	Engineering Design Activities (ITER)
EDF	Électricité De France
EFDA	European Fusion Development Agreement
EISS	European ITER Site Study
ELD	Electron Landau Damping
ELM	Edge Localised Mode
EM	Électromagnétique
EPFL	École Polytechnique Fédérale de Lausanne
EPS	European Physical Society
ES	Électrostatique
ETG	Electron Temperature Gradient
FCE	Fréquence Cyclotronique Electronique
FCI	Fréquence Cyclotronique Ionique
FWCD	Fast Wave Current Drive
FWEH	Fasr Wave Electron Heating
HF	Haute fréquence
HT	Haute tension
IBW	Ion Bernstein Wave
ICR(F)	Ion Cyclotron Resonant (Frequency)
ICR(H)	Ion Cyclotron Resonant (Heating)
ICS	Inter-Coil Structure
IDN	Injection De Neutres
ILE	ITER Legal Entity
INB	Installation Nucléaire de Base
IR	InfraRouge
IRIFA	InfraRed Irradiation FAcility
ISPI	Injection Supersonique Par Impulsion
ITB	Internal Transport Barrier
ITER	International Thermonuclear Experimental Reactor
ITER-EDA	ITER Engineering Design Activities
ITER-FEAT	ITER-Fusion Energy Advanced Tokamak
ITER-IAM	ITER-Intermediate Aspect-ratio Machine
ITER-LAM	ITER-Intermediate Aspect-ratio Machine
ITG	Ion Temperature Gradient
JAERI	Japan Atomic Energy Research Institute
JAL	JET Associate Leader
JCT	Joint Central Team (ITER)
JET	Joint European Torus
JET-EP	JET Enhanced Performances
JIA	JET Implementing Agreement
JOC	JET Operation Contract
LCR	Laser Cavity Ringdown
LDC	Limiteur de démarrage CIEL
LH	Lower Hybrid
LHCD	Lower Hybrid Current Drive
LHEP	Lower Hybrid Enhanced Performance
LPA	Limiteur de Protection d'Antenne
LPT	Limiteur Pompé Toroïdal
LRC	Laboratoire de Recherche Conventionné
MARFE	Multifacetted Asymmetric Radiation From the Edge
MHD	MagnetoHydroDynamique

MSE	Motional Stark Effect
NBCD	Neutral Beam Current Drive
NB(I)	Neutral Beam (Injection)
NTM	Neoclassical Tearing Modes
PAM	Passif Actif Multijonction
PCM	Pompe CryoMécanique
PEI	Protection de l'Enceinte Interne
PF	Poloidal Field
PMS	Permanences pour Motif de Sécurité
PPI	Première Paroi Interne
RBM	Resistive Ballooning Modes
RCA	Remote Computer Access
RDA	Remote Data Access
RF	RadioFréquence
RFP	Reversed Field Pinch
RLW	Rebut-Lallia-Watkins (model)
RPRS	Rapport Préliminaire de Sûreté
SATIR	Station d'Acquisition et de Traitement Infra-Rouge
SOL	Scrape off layer
SPR	Sécurité de Puissance Réfléchie
TFA	Très Faible Activité
TFFT	Task Force Fusion Technology
TF(MC)	Toroidal Field (Model Coil)
TIG	Tungsten Inert Gas
TNL	Transport Non Local
TTMP	Transit Time Magnetic Pumping
TS	Tore Supra
UKAEA	United Kingdom Atomic Energy Authority
VME	type de bus
YAG	Yttrium Aluminium Garnet